HIDING IN PLAIN SIGHT: UNVEILING CRYPTIC DIVERSITY AND PATTERNS IN BUMBLE BEES

BY

MICHELLE A. DUENNES

DISSERTATION

Submitted in partial fulfillment of the requirements
for the degree of Doctor of Philosophy in Entomology
in the Graduate College of the
University of Illinois at Urbana-Champaign, 2015

Urbana, Illinois

Doctoral Committee:

Professor Sydney A. Cameron, Chair, Director of Research
Assistant Professor Zachary Cheviron
Ornithologist Kevin Johnson
Associate Professor Ripan Malhi
Associate Professor Zoi Rapti

ABSTRACT

Bumble bee research has a rich history that spans more than three centuries. The distributions and the vibrant color patterns of nearly all species of bumble bees are well mapped and described. In addition, the natural history, colony structure and social behavior of bumble bees are well documented and a well-supported phylogeny of the ~250 species currently recognized within the genus has been constructed. Yet despite the breadth of research that has been conducted on bumble bees, there is still much that is unknown about this charismatic group of social insects. My dissertation focuses on three areas: phylogenetics, population genetics and evolutionary development.

In Chapter One I explore the population genetics of the *Bombus ephippiatus-Bombus wilmattae* species group. The color pattern diversity within this group across a variety of habitats in Mexico and Central America has brought their taxonomic status into question for over 150 years. To resolve the uncertain species status of this group, I collected extensive genetic data from twelve microsatellite loci and a fragment of the *cytochrome oxidase I* gene to conduct an in-depth population genetic and phylogenetic study of the group across its widespread distribution. I also explore the use of wing geometric morphometrics to delineate species within this taxon. This group exhibits extensive genetic structure across its range, with major barriers to gene flow at the Isthmus of Tehuantepec in southern Mexico and the Nicaraguan Depression in southern Nicaragua. Wing morphometric data support these genetic divisions within the species complex. The differences in wing shape are not sufficiently divergent to be useful as species diagnostic characters, but they provide another line of evidence to support species boundaries.

These extensive genetic and morphometric data provide a wealth of evidence for revising the taxonomic status of the *B. ephippiatus-B. wilmattae* complex. In Chapter Two, I describe two genetically distinct, sympatric species with limited gene flow in Mexico south of the Isthmus of Tehuantepec through Honduras. I revise the species *B. wilmattae* within this region to include previously unknown queen and worker polymorphisms and describe a new species sympatric with *B. wilmattae*, *B. maya* sp. nov. I recognize a single species in Mexico north of the Isthmus of Tehuantepec, with extensive population structure corresponding to the four main mountain ranges of the Mexican highlands. I consider the species *B. ephippiatus* to extend only from northwest Mexico to the southern state of Oaxaca, just north of the Isthmus of Tehuantepec.

There is also a distinct species in Costa Rica, to which I assign the resurrected name *B. schneideri*.

In Chapter Three, I explore trends in variation among the color patterns of *Bombus* worldwide. The white, yellow, orange, and black contrasting stripes of color on bumble bees have long served as classic examples of aposematic coloration and their convergence upon common patterns across their extensive distribution has served as a classic example of Müllerian mimicry. Yet nothing is known about the developmental regulation of these color patterns. As a first step in exploring the developmental regulation of color, I mapped the color patterns across the body of individual species with high resolution using a grid map. My collaborators and I use this system to look for common elements of pattern across ~95% of the known species of bumble bees. This novel method revealed twelve primary pattern elements across the dorsal thorax and abdomen, with six on the thorax and six on the abdomen. It also revealed five smaller secondary pattern elements that lie medially and laterally on the abdomen. With the exception of three elements on the scutum, these primary elements correspond to segmental boundaries across the body, which suggests that the developmental regulation of color pattern might involve Hox genes, the same genes that control the development of segmental boundaries early in development.

This meticulous exploration of color pattern also revealed common trends in the occurrence of certain colors across the body. Black hairs occur in the center of the thorax in up to 77% of the species included in the analysis, and yellow hairs are found predominantly anteriorly and posteriorly along the edges of the thorax and the first two segments of the abdomen. Orange hairs predominate throughout the last segments of the abdomen. The differential patterns of color expression across species suggest that certain colors occur in specific positions on the body to maximize contrast and aposematic signal to predators. My study of the genotypic and phenotypic diversity of the *B. ephippiatus*-*B. wilmattae* species group and investigation of the core elements of pattern responsible for generating the diversity of color patterns across *Bombus* worldwide explore historically well-characterized systems, providing novel insights into long-standing questions within each system using new methods and approaches.

ACKNOWLEDGMENTS

First and foremost I would like to thank my advisor, Sydney Cameron, for her mentorship, guidance and friendship these past five years as I completed my PhD. I am also grateful to her for instilling in me a sincere love, respect and awe of bumble bees. Our many discussions over the years have taught me how to rigorously address scientific questions and to let my passion drive my pursuit of understanding the natural world. I am also thankful to all of my committee members for their comments and helpful discussion of my dissertation. I am greatly indebted to Chris Petranek for removing and mounting all of the bee wings analyzed in Chapter One and to Zoi Rapti for summarizing and analyzing the color pattern data in Chapter Three. None of the research in Chapters One and Two would have been possible without my excellent collaborators and friends at ECOSUR who collected thousands of bees for the project throughout Mexico and Guatemala: Rémy Vandame, Oscar Martinez, Jorge Mérida, Esteban Pineda and Philippe Sagot. Many other collaborators provided the Cameron Lab with specimens or accompanied me on collecting trips: R. Ayala, M. Guzman, P. Hanson, H. Hines, L. Masner, M. Metz, A. Picado, D. Sanchez, M. Sharkey, J. Torres.

I would also like to thank my fellow entomology graduate students at the University of Illinois, particularly Heather Hines, Annie Ray and Josephine Rodriguez who taught me very early on how to be a successful and productive graduate student. None of my graduate work would have been possible without the support of my friends and family, especially Kyle Parks who provided me with emotional and intellectual support as I finished my degree and my teammates of the Twin City Derby Girls who provided me with an outlet to stay active and a life outside of graduate school.

During my PhD, I was lucky enough to receive a scholarship from the Illinois Chapter of the Achievement Rewards for College Scientists (ARCS) Foundation, Inc. that funded a substantial portion of my dissertation research. I am grateful to ARCS not only because of the funding I received, but also for giving me the opportunity to meet the inspiring women who are their members. I also received funding from the Society of Systematic Biologists, the Illinois Natural History Survey, the School of Integrative Biology and the Department of Entomology and the United States Department of Agriculture.

TABLE OF CONTENTS

CHAPTER 1: PHYLOGENETICS, POPULATION GENETICS AND GEOMETRIC MORPHOMETRICS OF THE *BOMBUS EPHIPPIATUS-BOMBUS WILMATTAE* SPECIES GROUP IN MEXICO AND CENTRAL AMERICA

Abstract

Mexico and Central America are among the most biodiverse regions on Earth, harboring many species with high levels of interpopulation morphological diversity and genetic divergence. The mountainous topography of this region contains numerous isolated sky island habitats that have the potential to promote speciation, yet few studies have examined the phylogeographic and genetic structure of insect species encompassing this region. Here I investigate geographic patterns of genetic and morphological divergence and speciation among widespread populations of the highly polymorphic bumble bee *Bombus ephippiatus* and its closest relative *B. wilmattae*. I used DNA sequences from a fragment of *cytochrome oxidase I* (COI), genotypes for twelve microsatellite markers, and morphometric data from wings to construct a well-supported inference of the divergences among these taxa. I have found complex patterns of genetic isolation and morphological divergence within *B. ephippiatus* across its geographic range and evidence that *B. ephippiatus* comprises multiple independent evolutionary lineages. The pattern of their diversification corresponds to geographic and environmental isolating mechanisms, including the Mexican highlands, the lowlands of the Isthmus of Tehuantepec in southern Mexico, the Nicaraguan Depression, the patchily distributed volcanic ranges in Nuclear Central America and Pleistocene glacial cycles.

Introduction

Mexico and Central America are well known for their biological complexity (Mittermeier *et al*., 2000). The great biodiversity in this area is frequently attributed to its location between two large continents, arising from biotic interchange between North and South America. This region is also a transition zone between the northern Nearctic and southern Neotropical biogeographic regions (Heilprin, 1887). Its volcanic topography has led to isolation and speciation in birds (Cracraft & Prum, 1988; Roy *et al.,* 1997; García-Moreno *et al*., 2006), mammals (Vrba, 1993; Sullivan *et al*., 2000; León-Paniagua *et al*., 2007), and herptofauna

(Mulcahy *et al*., 2006; Castoe *et al*., 2009; Daza *et al*., 2010). Many endemic forms have been restricted within the last few million to particular ecosystems, such as montane pine-oak or cloud forests years (Escalante et al., 1993, León-Paniagua *et al*., 2007, Kerhoulas & Arbogast, 2010, Barber & Klicka, 2010). For example, many bird species restricted by ecological limits exist as a series of isolated populations in islands of suitable habitat (García-Moreno *et al*., 2004).

There are two particularly notable lowland regions within Mexico and Central America that have served as geographic barriers between these montane sky island habitats, preventing species movement. One of these barriers, the Isthmus of Tehuantepec (IT) (Fig. 1.1), is a large, narrow area of low elevation that separates the Sierra Madre del Sur of southern Mexico from the highland regions of the Sierra Madre de Chiapas in southern Mexico and northern Guatemala. The IT is proposed to be a major barrier to dispersal in toads (Mulcahy *et al*., 2006), snakes (Castoe *et al*., 2009; Daza *et al*., 2010), birds (Barber & Klicka, 2010), and rodents (Sullivan *et al*., 2000). The other significant barrier is the Nicaraguan Depression (Fig. 1.1), a lowland expanse separating the Chortis Block highlands of Honduras and Nicaragua from the highlands of Costa Rica. The Nicaraguan Depression is an important isolating mechanism in snakes (Castoe *et al*., 2009; Daza *et al*., 2010).

The highlands of Mexico are also important geographic barriers for many plant and animal taxa, both during their uprising and origin, and in more recent Pleistocene glacial cycles (Ornelas *et al.,* 2013; Mastretta-Yanes *et al*., 2015). Within Mexico, there are four distinct mountain ranges that have shaped the genetic structure of the organisms that live within them: the Sierra Madre Occidental, the Sierra Madre Oriental, the Trans-Mexican Volcanic Belt and the Sierra Madre del Sur (Fig. 1.1). South of the IT in Mexico, there are two mountain ranges: the Central American highlands that extend into Guatemala and Honduras and the Sierra Madre de Chiapas that extends into Guatemala (Fig. 1.1). These ranges are partially separated in Mexico by a lowland region called the Central Depression (CD) (Fig. 1.1), a barrier that has been shown as important to hummingbirds and passerines (Ornelas *et al*., 2013).

This pattern of high endemism and recent diversification across Mexico and Central America via geological isolation has likely affected insect diversity in the region as well. Biogeographic patterns of some groups of beetles, for instance, support that the uplift of montane regions in Central America allowed the southerly movement of Nearctic beetles into the region, while the tropical lowlands allowed South American beetles to move northward after the

Panamanian land bridge connection ~3 mya (Halffter, 1987; Liebherr, 1994; Lobo & Halffter, 2000; Marshall & Liebherr, 2000; Morrone, 2006). These studies have generated numerous hypotheses to explain the diversification of Mexican and Central American beetles, but their conclusions about how geological barriers may have shaped this diversification are limited because of their reliance on species distribution data alone. Multi-locus phylogenetic and population genetic analyses can clarify how evolutionary divergence is shaped by historical events. Furthermore, to understand whether communities respond similarly to the same historical events and shared barriers, it is important to compare patterns across different groups of taxa. To date, few molecular data (Morse & Farrell, 2005; Anducho-Reyes *et al*., 2008; Dorn *et al*., 2009; de Jesús May-Itzá *et al*., 2010; Ruiz *et al*., 2010; Baselga *et al*., 2011; Sánchez-Sánchez *et al*., 2012) are available for insect species that have been studied in this region.

Bumble bees (*Bombus*) represent one insect group that has been well studied taxonomically (Williams, 1998) and phylogenetically (Cameron *et al*., 2007) throughout the New World. Although mostly a northern temperate group, several *Bombus* clades are suggested to have dispersed from North America and undergone recent divergence (2-3 mya) in Central and South America (Hines, 2008). The phylogenetic patterns and known biogeographic distributions of these taxa provide the background for investigating the structuring of inter- and intraspecific genetic diversity and for examining whether bumble bee diversification in Mexico and Central America correlates with the same historical events that have shaped the speciation of vertebrate taxa. *Bombus ephippiatus* and *B. wilmattae* comprise a species complex especially relevant for the study of Mexican and Central American biodiversity. First, its estimated divergence from the northern bumble bee *B. impatiens* (~ 1 mya, Duennes *et al*., 2012) fits within the pertinent timescale of geological and climatic events in this region.

Second, *B. ephippiatus*, is distributed widely throughout Mexico and Central America and is found in diverse montane habitats, while *B. wilmattae*, of uncertain species status (Williams, 1998), is restricted within a much smaller geographic range. This pattern lends itself to comparative studies of genetic diversity in widespread and contracted populations. Lastly, *B. ephippiatus* is highly polymorphic across its broad range. It exhibits a gradation in color pattern from north to south and is also genetically diverse (Duennes *et al*., 2012). Preliminary studies of the genetic diversity of this group (Duennes *et al*., 2012) revealed five main lineages within *B. ephippiatus* and *B. wilmattae*: one lineage of *B. ephippiatus* in Mexico north of the IT, two

sympatric lineages of *B. ephippiatus* in Mexico south of the IT through Honduras, one lineage of *B. ephippiatus* in Costa Rica and the fifth lineage of *B. wilmattae* nested within *B. ephippiatus* (Fig. 1.2). Together its widespread geographic distribution over a topologically complex region, its highly polymorphic color pattern, and its genetic diversity suggest the possibility of additional cryptic diversity within the *B. ephippiatus-B. wilmattae* species group.

Here, I advance the Duennes *et al.* (2012) study by adding four additional microsatellite loci and over a thousand more specimens from across the range of this species complex, particularly northern Mexico. I also add wing morphometric data from over 600 specimens to explore whether morphological variation corresponds to genetic variation and isolation. I provide an in-depth comparison of the efficacy of the Bayesian assignment programs STRUCTURE (Pritchard *et al*., 2000) and GENELAND (Guillot *et al*., 2012) and discuss possible geographic barriers and climatic events that could have caused the observed patterns of diversification within this group.

Materials and Methods

Taxa examined

Phylogenetic analysis. To resolve the more basal relationships between the lineages in the *B. ephippiatus-B. wilmattae* species complex, I collected sequence fragment data from *cytochrome oxidase I* for 254 specimens spanning the group's broad geographic distribution. One hundred fifty two specimens from Mexico and Guatemala were added to the 92 specimens previously analyzed in Duennes *et al.* (2012). In total, 71 specimens of *B. wilmattae* and 171 specimens of *B. ephippiatus* were included in the analysis. Ten specimens of *B. impatiens* and one specimen each of *B. huntii* and *B. vosnesenskii* were selected as outgroup taxa. A list of all samples used for phylogenetic analyses can be found in Table 1.1.

Microsatellite analysis. To delimit distinct genetic groups within the *B. ephippiatus-B. wilmattae* complex, extensive sampling was conducted by collaborators at El Colegio de la Frontera Sur (ECOSUR) throughout Mexico and Guatemala. Samples were collected from one to three sites approximately five kilometers apart within a single population. A maximum of twenty samples was collected from each population, and each population sampled was at least ten kilometers apart. Samples previously genotyped in Duennes *et al.* (2012) were also included and

genotyped at an additional 4 loci. In total, 1917 female samples of *B. ephippiatus* and *B. wilmattae* were genotyped at 12 microsatellite loci (Table 1.1).

Geometric morphometric analysis. To test whether genetic structure has shaped morphology in this group, I also collected geometric morphometric data from the left forewings of *B. ephippiatus* and *B. wilmattae* with my undergraduate research assistant, Christopher Petranek. The wings were removed from 606 female specimens (Table 1.1) across the distribution of the species complex. Following Aytekin *et al.* (2007) twenty landmarks on the forewing were mapped and analyzed (Fig. 1.3, see details below).

Phylogenetic inference

Cytochrome oxidase I. An 811 base pair fragment of the *cytochrome oxidase I* (COI) gene was amplified from 254 specimens (Table 1.1) using the primers RevmtR and FormtR from Duennes *et al.* (2012). These highly specific primers were designed by Heather Hines to minimize amplification of mitochondrial insertions into the nuclear genome and span a region of the gene more variable in *Bombus* than the typical COI barcoding region. Other mitochondrial genes were explored for use within this bumble bee group, but lacked informative nucleotide variation (data not shown).

PCR and DNA sequencing. I obtained tissue from the specimens by removing one of the forelegs. All samples housed at the University of Illinois are stored in 95-100% ethanol at 4°C; all samples collected and stored at ECOSUR are pinned and dried (Table 1.1). Tissue was digested and DNA extracted in 150µL of 5% Chelex® 100 resin (Bio-Rad, Hercules, CA) and 3µL of Proteinase K (20mg/µL) for 60 mins at 55°C, 15 mins at 99°C, 1 min at 37°C, and then 15 mins at 99°C using a PCR thermocyler.

Standard conditions for PCR amplification included an initial denaturation step of 95°C for 3 min; 35 cycles of denaturation for 60 s at 94°C, annealing for 60 s at 48–57°C, and elongation for 60 s at 72°C, and a final extension of 3 min at 72°C, 25µL. PCR reactions were conducted in 5 µL of 5X GoTaq® reaction buffer (Promega, Fitchburg, WI), 1.875 mM $MgCl_2$, 0.2 mM each dNTP, 10µL of each primer and 0.4 U of GoTaq® DNA polymerase (Promega) with 2.5µL of genomic DNA. I purified PCR products using ExoSAP-IT® (Affymetrix, Santa Clara, CA). BigDye® Terminator v3.1 Cycle Sequencing Kit (Applied Biosystems, Foster City, CA) was used for sequencing sense and anti-sense strands of PCR products with the

corresponding primers. Sequencing was performed at the W.M. Keck Center for Comparative and Functional Genomics at the University of Illinois using an ABI 3730XL (Applied Biosystems) capillary sequencer.

Alignment and phylogenetic analysis. DNA sequences were edited in Geneious 8.1.7 (Biomatters Ltd) and aligned using MUSCLE (Edgar, 2004). An evolutionary substitution model of HKY+I was selected for Bayesian phylogenetic inference based on correct Akaike and Bayesian information criteria calculated by jModelTest 2.1.7 (Darriba *et al.,* 2012). For phylogenetic inference, I analyzed the aligned COI sequence data using MrBayes 3.2.5 (Ronquist *et al*., 2012) with 10,000,000 generations, four chains, flat priors and sampling trees every 1,000 generations. I compared the log likelihood plots of the two parallel runs from one MrBayes analysis using Tracer 1.6.0 (Rambaut *et al*., 2014) and selected a discarded burnin of the first 2,500,000 generations (2500 trees). The two runs were summarized and the posterior probability support for each node in the consensus tree was calculated. Pairwise F_{ST} between clades and average number of nucleotide differences within and between clades from the Bayesian phylogeny were calculated with DnaSPv5.10.1 (Librado & Rozas 2009). In addition to using Bayesian methods to reconstruct relationships, I generated a parsimony haplotype network with TCS1.21 (Clement *et al.* 2000) using the default parsimony connection limit of the program.

Microsatellite analysis

Microsatellite genotyping. To identify areas of restricted gene flow and genetic structure within this widespread species group, I genotyped 1917 female specimens at twelve microsatellite loci using the following published PCR primers: B10, B124, B126 (Estoup *et al*., 1995); B96, B100, B131, B132 (Estoup *et al*., 1996); BT10, BL13, BT30, BT28 (Reber-Funk *et al*., 2006); BTMS0125 (Stolle *et al*., 2009). A total of twenty microsatellite loci were tested for use with *B. ephippiatus* and *B.wilmattae*, but these twelve markers were selected for their consistent amplification across multiple *Bombus* species and the lack of evidence for null alleles or other scoring errors that could complicate analyses. See Lozier and Cameron (2009) for PCR reaction protocols and thermal cycling conditions. Final PCR products were genotyped at the high throughput DNA facility at the W.M. Keck Center at the University of Illinois using ABI 3730xl capillary DNA sequencers (Applied Biosystems). Genotypes were scored manually with

the Geneious Microsatellite Plugin 1.4 in Geneious 8.1.7 (Biomatters Ltd) using the same allele bin-set for all species. A random subset of samples was genotyped a second time to check the accuracy of allele identification and no inconsistencies were observed. For consistency between datasets, all of the microsatellite genotypes for *B. ephippiatus* and *B. wilmattae* taken from Duennes *et al.* (2012) were re-scored with the Geneious Microsatellite Plugin 1.4 in Geneious 8.1.7 (Biomatters Ltd) for this study (Table 1.1).

Population differentiation. All microsatellite data were tested for population differentiation using STRUCTURE 2.3.4 (Pritchard *et al*., 2000). I ran multiple analyses with different groups of samples because it is known that the assignment of individuals to genetic groups by STRUCTURE can be strongly influenced by sample size (Kalinowski, 2011). The following groups of samples were assessed for the following K values: all samples (N=1917; K=2-7), only the samples that have also been sequenced for the COI fragment (N=225; K=2-7), equal sample sizes for each region (Sierra Madre Occidental, Sierra Madre Oriental, Trans-Mexican Volcanic Belt, Sierra Madre del Sur, 2 for the sympatric groups in Mexico south of the IT through Honduras, Costa Rica; N=119; N=2-7); only the samples from the Mexican state of Chiapas, Guatemala, and Honduras (N=664). All analyses were run with the model parameter defaults (admixture model with allele frequencies correlated among populations and no prior sample information) with a burnin of 150,000 generations followed by an additional 150,000 generations. Between three to six independent runs were conducted for each value of K tested. While the ΔK method (implemented in STUCTURE HARVESTER; Earl & vonHoldt, 2011) was used to assess the optimal K value (Evanno *et al*., 2005) for each dataset, other values of K that corresponded to potential geographic barriers or biologically relevant factors were also considered and are reported below.

The Bayesian assignment program GENELAND 4.0.5 was also used to assess population structure (Guillot *et al*., 2012). All six analyses (Table 1.2) were run with the following parameters for 1,000,000 iterations with every 1,000th iteration saved: maximum rate of Poisson process at 100; uncertainty on spatial coordinates of 1; uncorrelated allele frequency, null allele and spatial models. 10 independent runs were computed for each analysis for K values from one to ten. I chose the iteration with the highest log likelihood after successive burnin values of 100, 200, 300, 400 and 500 as the best fit to the data and independently examined the MCMC plot for that iteration to determine stationarity and the ultimate burnin for the results.

Geometric morphometric analysis

Imaging and landmark mapping. The left forewing was removed and mounted in glycerol on glass slides with glass slipcovers. All slide-mounted wings were imaged at 10X with a Leica microscope camera (DFC425) in Leica Application Suite 3.8.0. After the order of specimen images was randomized using tpsUtil 1.64 (Rohlf, 2015b), the coordinates of twenty landmarks on the forewing (Fig. 1.3) were mapped on the images using tpsDIG2.22 (Rohlf, 2015a). Christopher Petranek removed, mounted and imaged all wings and mapped all landmark coordinates to ensure that landmarks were placed in the same location and to avoid researcher bias in the mapping of the landmarks.

MorphoJ analyses. I used the program MorphoJ1.06d (Klingenberg, 2011) for all post-processing analyses of the landmark coordinate dataset. Procrustes superimposition was performed to rotate and scale landmark data across specimens. A regression was then conducted with the Procrustes coordinates (shape) as the dependent variable and the log centroid size (an approximation of size) as the independent variable. To control for any size-based shape variation (allometry), I used the residuals of the regression for further analysis of the data. To test whether morphometric variation corresponded to genetic differentiation, I performed a canonical analysis of variance (CVA). Haplotype groups were assigned to each specimen based on their genotypic assignment in the STRUCTURE analysis (>50% assignment to a STRUCTURE-determined K group using the K=6 result from the analysis of the entire population genetic dataset [N=1917]) and these assignments were used as the classifier variables for the CVA. I also ran a permutation test for 1000 iterations to test the significance of the difference between the haplotype groups tested. Because the sample size of the Costa Rican lineage (N=17) was much smaller than the sample size for all other haplotype groups, I also ran all analyses on a dataset where each haplotype group had an equal sample size of N=17 to control for the effect of sample size on the results.

Results

COI phylogenetic relationships and concordance with genotypic divergences

A polytomy of three clades are present in the Bayesian phylogenetic analysis of the COI sequence data (Fig. 1.4). A large, strongly supported (poster probability, PP=0.9457) clade (**a)**

contains all *B. ephippiatus* samples collected in Mexico north of the IT, as well as a subset of the *B. ephippiatus* samples from Mexico south of the IT through to Honduras (Fig. 1.4). Within this clade (**a**), all *B. ephippiatus* samples collected in Honduras appear most basally outside of a moderately supported clade (PP= 0.7899, **b**) containing *B. ephippiatus* samples collected in Mexico both south and north of the IT. But within this Mexican clade (**b**) is a highly supported (PP=0.9993) node (**c**) containing *B. ephippiatus* from Mexico south of the IT (Fig. 1.4).

At the base of the phylogenetic tree there is a polytomy of clades (**d**) with low support (PP=0.6789) containing *B. ephippiatus* and *B. wilmattae* samples from Mexico south of the IT through Costa Rica (Fig. 1.4) in addition to a well-supported clade (PP=1.00, **e**) of *B. wilmattae* from Mexico south of the IT and Guatemala. Within the polytomous clade (**d**), are four geographically structured nodes: a group of *B. wilmattae* from Chiapas, Mexico (PP=0.9947, **f**), a group of *B. ephippiatus* from Honduras (PP=0.9974, **g**) and a group of *B. ephippiatus* from Costa Rica (PP=1.00, **h**) that is weakly (PP=0.6165) placed as sister to a small group of *B. ephippiatus* from Chiapas, Mexico (PP=0.9988, **i**).

The parsimony haplotype network of the COI sequence fragment data (Fig. 1.5) is highly congruent with the Bayesian phylogeny. All strongly supported clades from the phylogeny comprise distinct haplotype groups in the network (Fig. 1.5). The most divergent lineage in the network is the group from Costa Rica, with 4 steps separating it from a haplotype of *B. wilmattae* (Fig. 1.5). Clade (**e**), (**f**) and (**g**) from the phylogeny are also distinct in the haplotype network (Fig. 1.5). Differences between groups in the network are also reflected in the pairwise F_{ST} (Table 1.3) between clades and the average number of nucleotide differences between and among clades in the phylogeny (Table 1.4). Both distance measures demonstrate the high divergence of the individuals from Costa Rica as well as between the different sympatric clades from Mexico South of the IT through Honduras (Table 1.3; Table 1.4).

I conducted a STRUCTURE analysis of microsatellite genotype data for only the samples that were also sequenced for COI for a direct comparison of the COI phylogeny (Fig. 1.6A) to the genetic groups discerned from the microsatellite genotypes (Fig. 1.6B). Using ΔK criteria, K=4 was the best fit to the genotype data (Fig. 1.7). This comparison (Fig. 1.6) demonstrates that the resulting genetic groups are largely congruent with the results of the Bayesian phylogeny and the haplotype network. The individuals that belong to the green K cluster can largely be found within clade (**a**) and all of the individuals assigned to the orange K clusters are present in clade

(**d**) and (**e**) in the phylogeny (Fig. 1.6). All samples from Mexico north of the IT belong to the same K cluster and are also grouped together in a polytomy at the base of clade (**b**) in the phylogenetic tree (Fig. 1.6). The samples placed into the light and dark orange K clusters are also structured phylogenetically, with most of the light orange individuals belonging to clade (**f**) and the dark orange individuals belonging largely to clades (**e**), (**g**), and (**i**) (Fig. 1.6). The only strong incongruence between the datasets is the mixed assignment of the Costa Rican individuals in the STRUCTURE analysis. While STRUCTURE cannot assign the Costa Rican samples to a single K cluster, they all belong to the well-supported clade (**h**) in the phylogeny (Fig. 1.6).

Genetic groups inferred from STRUCTURE analyses of the microsatellite genotype data

In accordance with ΔK criteria, K=5 was the best fit to the large genotype dataset of 1917 samples (Fig. 1.8). The K values assigned are highly congruent with geographic location. The blue cluster (Fig. 1.9) predominates throughout the Sierra Madre Occidental, but also occurs in high frequency in samples from the western region of the Trans-Mexican Volcanic Belt where these two mountain ranges overlap with each other (Fig. 1.9). The pink cluster (Fig. 1.9) is found throughout the eastern side of Mexico in the Sierra Madre Oriental, the Sierra Madre del Sur, as well as the eastern region of the Trans-Mexican Volcanic Belt. While the samples from the Trans-Mexican Volcanic Belt share genotypes with mountain ranges in the far western and eastern portions of the region, a distinct purple cluster (Fig. 1.9) occurs in the middle of the range. The genetic structure presented in this analysis corresponds to the mountains of Mexico, but there are signatures of gene flow in samples where these mountain chains connect and overlap (Fig. 1.9).

In Mexico south of the IT through Honduras a genotypic composition very different from that north of the IT exists (Fig. 1.9). Within this region, also called Nuclear Central America (Nuc CA), there are two distinct sympatric clusters. Within the green cluster (Fig. 1.9) are individuals of *B. ephippiatus* from Mexico south of the IT, Guatemala and Honduras and within the orange cluster (Fig. 1.9) are specimens of *B. ephippiatus* from Mexico south of the IT and Honduras and all samples of *B. wilmattae* from Mexico south of the IT and Guatemala. While the orange cluster in this analysis is separated into two groups in the smaller STRUCTURE analysis of samples with COI data (Fig. 1.6B) and it is placed in multiple lineages in the COI phylogeny (Fig. 1.6A), this larger analysis of all samples identifies one panmictic cluster (Fig.

1.9); this panmictic group is also identified at higher values of K for this large dataset. While ΔK criteria select K=5 for this dataset, K=6 demonstrates further genetic structure corresponding to the mountain ranges of Mexico (Fig. 1.10). When K is increased from 5 to 6, a new cluster (red) is revealed that corresponds to the Sierra Madre Oriental and the eastern sides of the Trans-Mexican Volcanic Belt and the Sierra Madre del Sur.

The net nucleotide distances between the clusters at K=6 (Table 1.5) demonstrates that the orange cluster (*B. wilmattae* and *B. ephippiatus* from Nuc CA) and the green cluster (*B. ephippiatus* from Nuc CA) are most divergent from the populations in Mexico north of the IT. After this, the northwestern blue cluster (Sierra Madre Oriental) and the southern pink cluster (Sierra Madre del Sur) exhibit fairly high differentiation in addition to the two sympatric lineages in Nuc CA (orange and green; Nuc CA *B. wilmattae* and Nuclear Central America) (Table 1.5).

Both this large analysis and the smaller analysis using only samples with COI sequence data (Fig. 1.6B) did not always assign Costa Rican individuals to a single cluster, so I ran a separate analysis with all samples sizes equal to that of Costa Rica (N=17 for each of the seven main regions; see Methods; Fig. 1.11). At K=2, Costa Rica is clustered with the two sympatric lineages from Nuclear Central America, while all samples north of the IT are a second cluster (Fig. 1.11). At K=3, the samples from the Sierra Madre Occidental separate from the rest of the samples north of the IT (Fig. 1.11). At K=4, the sympatric lineage of *B. ephippiatus* samples from Nuclear Central America separates from the rest of the samples south of the IT (Fig. 1.11). At K=5, the *B. ephippiatus*/*B. wilmattae* lineage from Nuclear Central America separates from the Costa Rican samples (Fig. 1.11). At K=6, the Sierra Madre del Sur samples separate from the Sierra Madre Oriental and the Trans-Mexican Volcanic Belt and at K=7, the Sierra Madre Oriental separates from the Trans-Mexican Volcanic Belt (Fig. 1.11).

I also ran a separate analysis with the samples from Nuc CA (N=664; Fig. 1.12). Across K values, the green cluster from the larger analysis remains the same, but the orange cluster separates into smaller groups (Fig. 1.12). The results from K=2 mirror those of the analysis with all (N=1917) samples; the samples are separated into the same two clusters from the larger dataset. At K=3, the orange cluster is separated into one group of *B. ephippiatus* and *B. wilmattae* from Chiapas, Mexico and a second group of *B. wilmattae* from Chiapas, Mexico and Guatemala and *B. ephippiatus* from Honduras (Fig. 1.12). At K=4, the orange cluster splits into one group of *B. ephippiatus* from Chiapas, Mexico, a group of *B. wilmattae* from Chiapas,

Mexico and a third group of *B. wilmattae* from Chiapas, Mexico and Guatemala and *B. ephippiatus* from Honduras (Fig. 1.12). At K=5, the orange cluster is split into four groups: a group of *B. ephippiatus* from Chiapas, Mexico, a group of *B. wilmattae* from Chiapas, Mexico, a group of *B. wilmattae* from Chiapas, Mexico and Guatemala and a fourth group of *B. ephippiatus* from Honduras (Fig. 1.12; Fig. 1.13).

Genetic groups inferred from the GENELAND analyses of the microsatellite genotype data

The first analysis of all samples with wing morphometric data and genotype data (scenario 1 in Table 1.2) revealed eight distinct genetic clusters (Fig. 1.14). Two groups were differentiated in Mexico north of the IT; the samples from the Sierra Madre Occidental separated into a cluster (8) distinct from the rest of Mexico north of the IT (4; Fig. 1.14). A single distinct group was assigned to the individuals from Costa Rica (7; Fig. 1.14). In Nuc CA, five groups were assigned to the samples (1, 2, 3, 5, 6; Fig. 1.14). These five groups largely correspond to their assignment by STRUCTURE in the analysis of all samples (Table 1.6). Of the samples assigned to the green cluster in the STRUCTURE analysis (Fig. 1.10), 51% were assigned to group 1, 18% were assigned to group 2, 22% were assigned to group 5 and 9% were assigned to group 6 (Table 1.6). The samples assigned to the orange cluster by STRUCTURE (Fig. 1.10) were more evenly split between groups 1, 2, 3, 5 and 6 (Table 1.6): 3% were assigned to group 1, 37% were assigned to group 2, 8% were assigned to group 3, 21% were assigned to group 5 and 31% were assigned to group 6.

When the morphometric data are excluded from this analysis (scenario 2 in Table 1.2; Fig 1.15), the results are largely congruent with those including morphometric data (scenario 1 in Table 1.2). These analyses differ in two ways (Table 1.7): 26 samples placed into group 5 from scenario 1 are placed into group 1 in scenario 2 and 8 samples placed into group 6 in scenario 1 are placed into group 2 in scenario 2. Because of this, the assignments of each GENELAND group to the two sympatric lineages discerned by STRUCTURE change (Table 1.8). For the individuals assigned to the green STRUCTURE cluster (Fig. 1.10), 67% are assigned to group 1, 23% are assigned to group 2, 6% are assigned to group 5 and 4% are assigned to group 6 (Table 1.8). For the individuals assigned to the orange STRUCTURE cluster (Fig. 1.10), 6% are assigned to group 1, 38% are assigned to group 2, 8% are assigned to group 3, 18% are assigned to group 5 and 30% are assigned to group 6 (Table 1.8).

GENELAND analyses of the samples from Mexico north of the IT with morphometric data (scenario 3) and without morphometric data (scenario 4) reveal three and five groups, respectively (Table 1.2), which correspond to geography. In scenario 3 (Fig. 1.16), group 1 occurs in the Sierra Madre Oriental, the Trans-Mexican Volcanic Belt and the eastern edge of the Sierra Madre del Sur, group 2 occurs in the Sierra Madre Occidental and group 3 occurs in the Sierra Madre del Sur and southeastern Trans-Mexican Volcanic Belt. These groups also correspond to the same regions identified by STRUCTURE (Table 1.9). When morphometric data are excluded (scenario 4) five genetic groups are identified by GENELAND (Fig. 1.17). Group 1 occurs in the Sierra Madre del Sur, group 2 occurs in the Sierra Madre Oriental through to the eastern Sierra Madre del Sur, group 3 occurs in the Sierra Madre Occidental, group 4 occurs in the western Trans-Mexican Volcanic Belt and southern Sierra Madre Occidental and group 5 occurs in the Trans-Mexican Volcanic Belt (Fig. 1.17). These groups are also highly congruent with the STRUCTURE clusters assigned to these samples (Table 1.10).

When the samples from Nuc CA are analyzed separately, five groups are identified with morphometric data (scenario 5; Fig. 1.18) and 6 groups are identified without morphometric data (scenario 6; Fig. 1.19). With the exception of a few outlier samples, the five groups identified with morphometric data largely correspond to the five STRUCTURE groups identified in the analysis of only the Nuc CA samples (Table 1.11; Fig. 1.12). Group 1 comprises *B. ephippiatus* samples from Chiapas, Mexico and Guatemala and Honduras and corresponds mainly to the green STRUCTURE cluster (Fig. 1.18). Group 2 consists mostly of *B. ephippiatus* in Honduras; group 3 contains *B. ephippiatus* from Chiapas, Mexico; group 4 is mainly composed of *B. wilmattae* samples from Chiapas, Mexico and group 5 consists mostly of *B. wilmattae* samples from Chiapas, Mexico and Guatemala (Fig. 1.18). When morphometric data are excluded (scenario 6; Fig. 1.19), a sixth group is added (61% *B. ephippiatus* from Guatemala and Honduras and 39% *B. wilmattae* from Guatemala) and the distribution of samples among groups corresponds less so to the STRUCTURE results (Table 1.12).

Morphological divergence inferred from wing morphometric data

A CVA of all morphometric data (N=606) with samples classified by their genotype assignment revealed that each pairwise comparison of haplotype groups was statistically significant (Table 1.13) and 67.36% of the variation in the data is explained in the first two

canonical variates (Fig. 1.20). Costa Rica was most divergent in wing shape from all other haplotype groups (Table 1.13; Fig. 1.20). The Nuc CA lineage with both *B. ephippiatus* and *B. wilmattae* (orange) was the second most different from all groups (Table 1.13; Fig. 1.20). Of the three haplotype groups south of the IT, the Nuc CA group (green) containing *B. ephippiatus* is the least different in wing shape from the samples north of the IT (Table 1.13; Fig. 1.20), which also reflects its close relationship to Mexico north of the IT group, as shown in the COI phylogeny (Fig. 1.6A). The Sierra Madre Oriental and the Sierra Madre del Sur are the least different in wing shape (Table 1.13). This close relationship is also reflected in the STRUCTURE analyses (Table 1.5).

The CVA with equal samples sizes (N=17 for each haplotype group; N=119 total) demonstrates the same patterns seen in the larger dataset, with 72.55% of the variation in the data explained by the first two canonical variates (Table 1.14; Fig. 1.21). The only substantial difference between the analyses is that no pairwise comparison between haplotypes north of the IT has a greater Mahalanobis distance than the comparisons between haplotypes south of the IT (Table 1.14). In the larger analysis, the Mahalanobis distance between the most northern (Sierra Madre Occidental) and the most southern (Sierra Madre del Sur) haplotypes in Mexico north of the IT is greater than any comparison of the Nuc CA group (green) containing *B. ephippiatus* to any haplotype group north of the IT (Table 1.14).

Discussion

Phylogenetic relationships between *B. ephippiatus* and *B. wilmattae*

The Bayesian phylogenetic analysis and parsimony haplotype network of the COI sequence data support many of the relationships discerned in Duennes *et al.* (2012). Increased sampling from Mexico and Guatemala, however, reveals previously unknown genetic diversity (Fig. 1.6A). Adding specimens from Mexico north of the IT did not reveal greater genetic diversity in Mexico at the COI locus; all of these samples still group together as an unresolved polytomy within clade (**b**) (Fig. 1.6A). The *B. ephippiatus* samples from Chiapas, Mexico continue to form a well-supported sub-clade (**c**) within clade (**b**), despite the inclusion of many more samples from this region. In addition, a novel clade (**i**) comprising a small subset (N=4) of these specimens appears in the phylogeny (Fig. 1.6A). The separation of clade (**c**) Chiapas

samples from the Honduras samples at the base of clade (**a**), despite being placed into the same K cluster in the STRUCTURE analysis of the microsatellite genotype data (Fig. 1.6B), suggests that this might be a case of secondary contact, where the ancestral distribution was south of the IT, dispersed from there into northern Mexico and then dispersed back south of the IT, having complete introgression with the ancestral population. Complete gene flow in the STRUCTURE analysis (Fig. 1.6B) and divergent placement in the COI tree (Fig. 1.6A) also suggests that the orange clusters have been present in Nuc CA longer than the green cluster. Divergence estimates from Duennes *et al.* (2012) indicate that both of these possible events could have occurred during Pleistocene glacial cycles; studies across animal and plant taxa inhabiting montane regions of Mexico and Central America suggest multiple dispersal events across the IT have occurred during the late Pliocene and Pleistocene (Ornelas *et al*., 2013).

In previous analyses (Duennes *et al*., 2012), *B. wilmattae* was placed as sister to the *B. ephippiatus* from Costa Rica with moderate support (Fig. 1.2); but with additional sampling, the Costa Rican *B. ephippiatus* are now placed as sister to a small clade of *B. ephippiatus* from Chiapas (Fig. 1.6A). Targeted sampling of Nuc CA added specimens of *B. wilmattae* from southern Chiapas and northern Guatemala to the previously identified clade (**e**) of this putative species, but also revealed an additional, separate clade (**f)** of *B. wilmattae* from northern Chiapas (Fig. 1.6A). The large amount of genetic diversity at COI for these orange groups that is also present in the microsatellite data provides further support to the hypothesis that these groups have been in Nuc CA much longer than the green clusters, and suggests that these lineages might even represent the ancestral range of the group with a retention of ancestral polymorphism. These orange groups also show that the Central Depression (CD; Fig. 1) might restrict gene flow between populations of the orange cluster, with distinct genotypes on either side of the depression (Fig. 1.18; Fig. 1.13), a result that could not have been discerned from the smaller sampling of Duennes *et al.* (2012).

Population structure inferred from STRUCTURE and GENELAND

For this study I tested different groups of samples of varying sample sizes, which uncovered some of the limitations of and differences between STRUCTURE and GENELAND. Different groups of samples produced different K clusters in both STRUCTURE and GENELAND. All analyses of the microsatellite genotype data with STRUCTURE failed to

assign the Costa Rica samples to a single cluster, except when samples from all regions were pared down to equal that of Costa Rica (Fig. 1.11). This illustrates the difficulty of using the STRUCTURE algorithm to assign unequal population samples to genetic groups (Kalinowski, 2011). However, GENELAND, which incorporates geospatial data, readily identified Costa Rica as a unique genetic group in an analysis of all samples with morphometric data included (Fig. 1.14) and excluded (Fig 1.15).

In an analysis of all samples (N=1917), STRUCTURE identified five distinct clusters: two corresponding to the sympatric lineages south of the IT through Honduras and three corresponding to the mountain ranges of northern Mexico (Fig. 1.9). When a sixth cluster is added to STRUCTURE, it identifies an additional lineage corresponding to the Sierra Madre Oriental in northeastern Mexico (Fig. 1.10). GENELAND also identifies these three lineages in northern Mexico when morphometric data are included (Fig. 1.16). When these morphometric data are excluded from GENELAND, the analysis identifies a distinct Sierra Madre Oriental population (Fig. 1.17) corresponding to the same sixth population identified by STRUCTURE (Fig. 1.10), but also separates the western Trans-Mexican Volcanic Belt into a unique population. In general, fewer populations are identified by GENELAND when morphometric data are included in the analysis, but the results from GENELAND do not appear to change notably when sample sizes are changed or samples are excluded.

Regardless of sample size, GENELAND consistently separates the samples from Nuc CA into at least five lineages (Figs. 1.14, 1.15, 1.18, 1.19). Five distinct lineages within this region are also delineated by STRUCTURE, but not unless Nuc CA is analyzed separately (Fig. 1.12). The analyses of this region show where STRUCTURE and GENELAND differ the most in their assignment. STRUCTURE consistently identifies the green cluster as distinct from all other samples from Nuc CA, regardless of the K value being tested (Fig. 1.12); this suggests that there is little to no gene flow between these lineages. In contrast to this, GENELAND does not separate these same samples into a single cluster; this program instead assigns only 57-71% of these samples to the green cluster and places the remaining samples into genetic groups within the orange cluster (Table 1.11; Table 1.12). Comparing a map of the groups assigned by GENELAND (Fig. 1.18; Fig. 1.19) to a map of the STRUCTURE assignments (Fig. 1.13), it is clear that GENELAND is prioritizing placing these samples into groups based on their geographic proximity rather than their genotype. Therefore, GENELAND provides more robust

results with unequal samples sizes than STRUCTURE, and its ability to include spatial and phenotypic information suggests it provides a more holistic picture of evolutionary history, but it appears to prioritize geospatial data over genetic data when multiple cryptic, sympatric lineages are included from a single population (i.e. populations deviate from Hardy-Weinberg equilibrium).

Geometric morphometric differences corresponding to genetic divergences

In the morphometric analysis, bees grouped together based on variations in the shape in the venation of the left forewing of *B. ephippiatus* and *B. wilmattae.* These morphometric groups are remarkably similar to the genetic groups I recovered in my mitochondrial COI analysis. Costa Rican specimens in particular have highly divergent wing shapes, (Table 1.13; Table 1.14) which supports that *B. ephippiatus* from Costa Rica are a distinct lineage. This also supports that STRUCTURE's inability to place this group into a single genetic cluster is due to unequal samples sizes. These landmark-based wing morphometric data also demonstrate that there is morphological evidence supporting two distinct sympatric lineages within Nuc CA, despite the fact that these groups share identical color pattern polymorphisms (Fig. 1.22).

In addition to identifying unique populations, morphometric data can provide insight into the evolutionary relationships between the lineages of the *B. ephippiatus-B. wilmattae* complex. Of the three lineages south of the IT, the green Nuc CA lineage is most similar to those samples north of the IT (Table 1.13; Table 1.14), reflecting its close relationship to Mexico north of the IT in the COI phylogeny (Fig. 1.6A). While the morphometric comparisons among the populations north of the IT are among the lowest Mahalanobis values (Table 1.13; Table 1.14), the most northern (Sierra Madre Occidental) and the most southern (Sierra Madre del Sur) populations in Mexico north of the IT have large differences in wing shape, demonstrating that there are even morphometric differences at the broad population level within this group.

These results support previous wing geometric morphometric studies in Apidae that show not only species and subgeneric differences in wing shape (Aytekin *et al*., 2007; Francoy *et al*., 2012), but that morphometric techniques can also distinguish divisions below the species level (Francoy *et al*., 2008). While the morphometric results presented here provide further data towards robustly defining species boundaries within this complex, a pairwise comparison of groups via discriminant function analysis (data not shown) could not identify large enough

differences to use as diagnostic characters for species delimitation. Future research on this complex could use discriminant function analyses of these data to identify groups of additional samples to each lineage even though there do not appear to be any easily recognizable, diagnostic characters on the wing.

Conservation implications

Within Mexico alone, twelve independent companies across five different states are rearing *B. ephippiatus* for commercial pollination of greenhouse crops (personal comm. Asociación Mexicana de Criadores de Abejorros Nativos, A.C.). Although raising *B. ephippiatus* as a native species is a more sustainable alternative to the non-native *B. impatiens* currently used for commercial pollination in Mexico and Central America, the inter-regional movement of *B. ephippiatus* colonies with unique population structure could be detrimental to the other species in this complex as well as to native population diversity within northern Mexico. Not only does their movement pose the threat of facilitating the spread of potential diseases, but commercial *B. ephippiatus* could outcompete native populations for resources and even cause genetic pollution of the native populations through interbreeding (Goulson, 2010; Kraus *et al*., 2011). The results presented here show that *B. ephippiatus* exhibits substantial population structure across its range and I suggest that bombiculture companies restrict the trade of colonies within the distinct mountain ranges of Mexico and do not move colonies between, thereby preserving the native diversity across the species' range.

Consequences for species delimitation

The genetic and phenotypic evidence presented here strongly suggests that the *B. ephippiatus*-*B. wilmattae* species group is in need of taxonomic revision. Based equally on the genetic and morphometric results, I will divide *B. ephippiatus* and *B. wilmattae* into four new species (Fig. 1.22). "*Bombus* sp. A" resides in Mexico north of the IT with a diversity of color polymorphism present in the species (Fig. 1.22). "*Bombus* sp. B" and *"Bombus* sp. C" are sympatric through Mexico south of the IT, Guatemala, and Honduras, with "*Bombus sp.* C" containing the previously recognized *B. wilmattae* (Fig. 1.22). "*Bombus* sp. D" inhabits Costa Rica, and presumably also Panama based on the consistent color pattern phenotype present

through these regions (Fig. 1.22). A formal taxonomic revision of this group is presented in Chapter Two.

References

Anducho-Reyes MA, Cognato AI, Hayes JL, Zúñiga G. 2008. Phylogeography of the bark beetle *Dendroctonus mexicanus* Hopkins (Coleoptera: Curculionidae: Scolytinae). *Molecular Phylogenetics and Evolution* 49: 930–940.

Aytekin MA, Terzo M, Rasmont P, Çağatay N. 2007. Landmark based geometric morphometric analysis of wing shape in *Sibiricobombus* Vogt (Hymenoptera: Apidae: *Bombus* Latreille). *Annales de la Société entomologique de France (N.S.)* 43: 95-102.

Barber BR, Klicka J. 2010. Two pulses of diversification across the Isthmus of Tehuantepec in a montane Mexican bird fauna. *Proceedings of the Royal Society of London (B)* 277: 2675-2681.

Baselga A, Recuero E, Parra-Olea G, García-París M. 2011. Phylogenetic patterns in zopherine beetles are related to ecological niche width and dispersal limitation. *Molecular Ecology* 20: 5060–5073.

Cameron SA, Hines HM, Williams PH. 2007. A comprehensive phylogeny of the bumble bees (*Bombus*). *Biological Journal of the Linnean Society* 91: 161-188.

Castoe TA, Daza JM, Smith EN, Sasa MM, Kuch U, Campbell JA, Chippindale PT, Parkinson CL. 2009. Comparative phylogeography of pitvipers suggests a consensus of ancient Middle American highland biogeography. *Journal of Biogeography* 36: 88-103.

Clement M, Posada D, Crandall K. 2000. TCS: A computer program to estimate gene genealogies. *Molecular Ecology* 10: 1657-1660.

Cracraft J, Prum RO. 1988. Patterns and processes of diversification: speciation and historical congruence in some Neotropical birds. *Evolution* 42: 603-620.

Darriba D, Taboada GL, Doallo R, Posada D. 2012. jModelTest 2: more models, new heuristics and parallel computing. *Nature Methods* 9: 772.

Daza JM, Castoe TA, Parkinson CL. 2010. Using regional comparative phylogeographic data from snake lineage to infer historical processes in Middle America. *Ecography* 33: 343-354.

Duennes MA, JD Lozier, HM Hines, SA Cameron. 2012. Geographical patterns of genetic divergence in the widespread Mesoamerican bumble bee *Bombus ephippiatus* (Hymenoptera: Apidae). *Molecular Phylogenetics and Evolution* 64: 219-231.

de Jesús May-Itzá W, Quezada-Euán JJG, Medina Medina LA, Enríquez E, De la Rúa P. 2010. Morphometric and genetic differentiation in isolated populations of the endangered Mesoamerican stingless bee *Melipona yucatanica* (Hymenoptera: Apoidea) suggest the existence of a two species complex. *Conservation Genetics* 11: 2079-2084.

Dorn PL, Calderon C, Melgar S, Moguel B, Solorzano E, Dumonteil E, Rodas A, de la Rua N, Garnica R, Monroy C. 2009. Two distinct *Triatoma dimidiata* (Latreille, 1811) taxa are found in sympatry in Guatemala and Mexico. *PLoS Neglected Tropical Diseases* 3: e393.

Edgar RC. 2004. MUSCLE: multiple sequence alignment with high accuracy and high throughput. *Nucleic Acids Research* 32: 1792–1797.

Escalante P, Navarro-Sigüenza AG, Peterson AT. 1993. A geographic, ecological and historical analysis of land bird diversity in Mexico. In: *Biological Diversity in Mexico: Origins and Distributions* (eds Ramamoorthy TP, Bye R, Lot A, Fa J) 281-307. New York, NY: Oxford University Press.

Estoup A, Scholl A, Pouvreau A, Solignac M. 1995. Monoandry and polyandry in bumble bees (Hymenoptera — Bombinae) as evidenced by highly variable microsatellites. *Molecular Ecology* 4: 89–93.

Estoup A, Solignac M, Cornuet JM, Goudet J, Scholl A. 1996. Genetic differentiation of continental and island populations of *Bombus terrestris* (Hymenoptera: Apidae) in Europe. *Molecular Ecology* 5: 19–31.

Francoy TM, Wittmann D, Drauschke M, Müller S, Steinhage V, Bezerra-Laure MAF, De Jong D, Gonçalves LS. 2008. Identification of Africanized honey bees through wing morphometrics: two fast and efficient procedures. *Apidologie* 39: 488-494.

Francoy TM, Faria Franco F, Roubik DW. 2012. Integrated landmark and outline-based morphometric methods efficiently distinguish species of *Euglossa* (Hymenoptera, Apidae, Euglossini). *Apidologie* 43: 609-617.

García-Moreno J, Navarro-Sigüenza AG, Peterson AT, Sánchez-González LA. 2004. Genetic variation coincides with geographic structure in the common bush-tanager (*Chlorospingus ophthalmicus*) complex from Mexico. *Molecular Phylogenetics and Evolution* 33: 186-196.

García-Moreno J, Cortés N, García-Deras G, Hernández-Baños B. 2006. Local origin and diversification among *Lampornis* hummingbirds: A Mesoamerican taxon. *Molecular Phylogenetics and Evolution* 38: 488-498.

Goulson D. 2010. Impacts of non-native bumblebees in Western Europse and North America. *Applied Entomology and Zoology* 45: 7-12.

Guillot G, Renaud S, Ledevin R, Michaux J, Claude J. 2012. A unifying model for the analysis of phenotypic, genetic and geographic data. *Systematic Biology* 61: 897-911.

Halffter G. 1987. Biogeography of the montane entomofauna of Mexico and Central America. *Annual Review of Entomology* 32: 95-114.

Heilprin A. 1887. *The geographical and geological distribution of animals*. London, UK: Kegan Paul, Trench & Co.

Hines HM. 2008. Historical biogeography, divergence times, and diversification patterns of bumble bees (Hymenoptera: Apidae: *Bombus*). *Systematic Biology* 57: 58–75.

Huth-Schwarz A, León A, Vandame R, Moritz RFA, Kraus FB. 2011. Mating frequency and genetic colony structure of the neotropical bumble bee *Bombus wilmattae*. *Apidologie* 42: 519-525.

Kalinowski ST. 2011. The computer program STRUCTURE does not reliably identify the main genetic clusters within species: simulations and implications for human population structure. *Heredity* 106: 625-632.

Kerhoulas NJ, Arbogast BS. 2010. Molecular systematics and Pleistocene biogeography of Mesoamerican flying squirrels. *Journal of Mammalogy* 91: 654-667.

Klingenberg CP. 2011. MorphoJ: an integrated software package for geometric morphometrics. *Molecular Ecology Resources* 11: 353-357.

Kraus FB, Szentgyörgyi H, Rożej E, Rhode M, Moroń D, Woyciechowski M, Moritz RFA. 2011. Greenhouse bumblebees (*Bombus terrestris*) spread their genes into the wild. *Conservation Genetics* 12: 187-192.

León-Paniagua L, Navarro-Sigüenza AG, Hernández-Baños BE, Morales JC. 2007. Diversification of the arboreal mice of the genus *Habromys* (Rodentia: Cricetidae: Neotominae) in the Mesoamerican highlands. *Molecular Phylogenetics and Evolution* 42: 653-664.

Librado P, Rozas J. 2009. DnaSP v5: A software for comprehensive analysis of DNA polymorphism data. *Bioinformatics* 25: 1451-1452.

Liebherr JK. 1994. Biogeographic patterns of montane Mexican and Central American carabidae (Coleoptera). *Canadian Entomologist* 126: 841-860.

Lobo JM, Halffter G. 2000. Biogeographical and ecological factors affecting the altitudinal variation of mountainous communities of coprophagous beetles (Coleoptera: Scarabaeoidea): a comparative study. *Annals of the Entomological Society of America* 93: 115-126.

Lozier JD, Cameron SA. 2009. Comparative genetic analyses of historical and contemporary collections highlight contrasting demographic histories for the bumble bee *Bombus pensylvanicus* and *B. impatiens* in Illinois. *Molecular Ecology* 18: 1875–1886.

Mastretta-Yanes A, Moreno-Letelier A, Piñero D, Jorgensen TH, Emerson BC. 2015. Biodiversity in the Mexican highlands and the interaction of geology, geography and climate within the Trans-Mexican Volcanic Belt. *Journal of Biogeography* 42: 1586-1600.

Marshall CJ, Liehberr JK. 2000. Cladistic biogeography of the Mexican transition zone. *Journal of Biogeography* 27: 203-216.

Mittermeier R, Myers N, Goettsch Mittermeier C. 2000. *Hotspots: Earth's Biologically Richest and Most Endangered Terrestrial Ecoregions.* Washington, DC: Conservation International.

Morrone JJ. 2006. Biogeographic areas and transition zones of Latin America and the Caribbean Islands, based on panbiogeographic and cladistic analyses of the entomofauna. *Annual Review of Entomology* 51: 467-494.

Morse GE, Farrell BD. 2005. Interspecific phylogeography of the *Stator limbatus* species complex: the geographic context of speciation and specialization. *Molecular Phylogenetics and Evolution* 36: 201-213.

Mulcahy DG, Morrill BH, Mendelson JR. 2006. Historical biogeography of lowland species of toads (*Bufo*) across the Trans-Mexican Neovolcanic Belt and the Isthmus of Tehuantepec. *Journal of Biogeography* 33: 1889-1904.

Ornelas JF, Sosa V, Soltis DE, Daza JM, González C, Soltis PS, Gutiérrez-Rodríguez C, de los Monteros AE, Castoe TA, Bell C, Ruiz-Sanchez E. 2013. Comparative phylogeographic analyses illustrate the complex evolutionary history of threatened cloud forests of northern Mesoamerica. *PLOS One* DOI: 10.1371/journal.pone.0056283.

Pritchard JK, Stephens M, Donnelly P. 2000. Inference of population structure using multilocus genotype data. *Genetics* 155: 949–959.

Rambaut A, Suchard MA, Xie D & Drummond AJ. 2014. Tracer v1.6, Available from http://beast.bio.ed.ac.uk/Tracer.

Reber-Funk CR, Schmid-Hempel R, Schmid-Hempel P. 2006. Microsatellite loci for *Bombus spp*. *Molecular Ecology Resources* 6: 83–86.

Rohlf FJ. 2015. tpsDIG2: a program for digitizing landmarks and outlines from image files, scanner or video. *Department of Ecology and Evolution, State University of New York at Stony Brook*. Available at https://life.bio.sunysb.edu/morph/.

Rohlf FJ. 2015. tpsUtil: a tps file utility program. *Department of Ecology and Evolution, State University of New York at Stony Brook*. Available at https://life.bio.sunysb.edu/morph/.

Ronquist F, Teslenko M, van der Mark P, Ayres DL, Darling A, Höhna S, Larget B, Liu L, Suchard MA, Huelsenbeck JP. 2012. MrBayes 3.2: Efficient Bayesian phylogenetic inference and model choice across a large model space. *Systematic Biology* 61: 539-542.

Roy MS, da Silva JMC, Arctander P, García-Moreno J, Fjeldså J. 1997. The speciation of South American and African birds in montane regions. In: *Avian molecular evolution and systematics* (ed Mindell D) 325-343. San Diego, CA: Academic Press.

Ruiz EA, Rinehart JE, Hayes JL, Zuñiga G. 2010. Historical demography and phylogeography of a specialist bark beetle, *Dendroctonus pseudotsugae* Hopkins (Curculionidae: Scolytinae). *Environmental Entomology* 39: 1685–1697.

Sánchez-Sánchez H, López-Barrera G, Peñaloza-Ramírez JM, Rocha-Ramírez V, Oyama K. 2012. Phylogeography reveals routes of colonization of the bark beetle *Dendroctonus approximatus* Dietz in Mexico. *Journal of Heredity*103: 638-650.

Stolle E, Rohde M, Vautrin D, Solignac M, Schmid-Hempel P, Schmid-Hempel R, Moritz RFA. 2009. Novel microsatellite DNA loci for *Bombus terrestris*. *Molecular Ecology Resources* 9: 1345-1352.

Sullivan J, Arellano E, Rogers DS. 2000. Comparative phylogeography of Mesoamerican highland rodents: concerted versus independent response to past climate fluctuations. *American Naturalist* 155: 755–768.

Vrba E. 1993. Mammal evolution in the African Neogene and a new look at the Great American Interchange. In *Biological Relationships between Africa and South America* (ed Goldblatt, P) 393-434. New Haven, CT: Yale University Press.

Williams PH. 1998. An annotated checklist of bumble bees with an analysis of patterns of description (Hymenoptera: Apidae, Bombini). *Bulletin of the Natural History Museum, Entomology Series* 67: 79-152.

Table 1.1. Information on all samples used for analysis. Phenotype indicates the original species designation of the specimen. MSAT= microsatellite data collected; COI= COI gene fragment data collected; WING= wing geometric morphometric data collected.

Voucher Name	Phenotype	Country	Population	Latitude	Longitude	Altitude	MSAT	COI	WING
2417	*B. ephippiatus*	Mexico	BBDUR772	23.71	-105.05	2595	+		
2418	*B. ephippiatus*	Mexico	BBDUR772	23.71	-105.05	2595	+		
2420	*B. ephippiatus*	Mexico	BBDUR772	23.71	-105.05	2595	+		
2421	*B. ephippiatus*	Mexico	BBDUR772	23.71	-105.05	2595	+		
2422	*B. ephippiatus*	Mexico	BBDUR772	23.71	-105.05	2595	+		
2423	*B. ephippiatus*	Mexico	BBDUR773	23.7	-105.15	2585	+		
2424	*B. ephippiatus*	Mexico	BBDUR773	23.7	-105.15	2585	+		
2425	*B. ephippiatus*	Mexico	BBDUR773	23.7	-105.15	2585	+		
2426	*B. ephippiatus*	Mexico	BBDUR772	23.71	-105.05	2595	+		
2427	*B. ephippiatus*	Mexico	BBDUR772	23.71	-105.05	2595	+		
2428	*B. ephippiatus*	Mexico	BBDUR772	23.71	-105.05	2595	+		
2429	*B. ephippiatus*	Mexico	BBDUR773	23.7	-105.15	2585	+		
2430	*B. ephippiatus*	Mexico	BBDUR773	23.7	-105.15	2585	+		
2431	*B. ephippiatus*	Mexico	BBDUR773	23.7	-105.15	2585	+		
2432	*B. ephippiatus*	Mexico	BBDUR773	23.7	-105.15	2585	+		
2433	*B. ephippiatus*	Mexico	BBDUR773	23.7	-105.15	2585	+		
2434	*B. ephippiatus*	Mexico	BBDUR773	23.7	-105.15	2585	+		
2435	*B. ephippiatus*	Mexico	BBDUR773	23.7	-105.15	2585	+		
2436	*B. ephippiatus*	Mexico	BBDUR772	23.71	-105.05	2595	+		
2442	*B. ephippiatus*	Mexico	BBDUR423	24.22	-105.44	2370	+		
2443	*B. ephippiatus*	Mexico	BBDUR423	24.22	-105.44	2370	+		
2444	*B. ephippiatus*	Mexico	BBDUR423	24.22	-105.44	2370	+		
2445	*B. ephippiatus*	Mexico	BBDUR423	24.22	-105.44	2370	+		
2446	*B. ephippiatus*	Mexico	BBDUR382	24.54	-105.83	1504	+		

Table 1.1 (cont.)

Voucher Name	Phenotype	Country	Population	Latitude	Longitude	Altitude	MSAT	COI	WING
2447	*B. ephippiatus*	Mexico	BBDUR383	24.51	-105.8	2257	+		
2448	*B. ephippiatus*	Mexico	BBDUR441	23.89	-105.43	2485	+	+	
2449	*B. ephippiatus*	Mexico	BBDUR442	23.86	-105.41	2557	+		
2450	*B. ephippiatus*	Mexico	BBDUR442	23.86	-105.41	2557	+		
2451	*B. ephippiatus*	Mexico	BBDUR441	23.89	-105.43	2485	+		
2452	*B. ephippiatus*	Mexico	BBDUR441	23.89	-105.43	2485	+		
2453	*B. ephippiatus*	Mexico	BBDUR441	23.89	-105.43	2485	+		
2454	*B. ephippiatus*	Mexico	BBDUR442	23.86	-105.41	2557	+		
2455	*B. ephippiatus*	Mexico	BBDUR442	23.86	-105.41	2557	+		
2456	*B. ephippiatus*	Mexico	BBDUR442	23.86	-105.41	2557	+		
2457	*B. ephippiatus*	Mexico	BBDUR443	23.84	-105.39	2569	+		
2458	*B. ephippiatus*	Mexico	BBDUR443	23.84	-105.39	2569	+		
2464	*B. ephippiatus*	Mexico	BBDUR462	23.63	-105.84	2288	+		
2465	*B. ephippiatus*	Mexico	BBDUR463	23.65	-105.79	2394	+		
2466	*B. ephippiatus*	Mexico	BBDUR463	23.65	-105.79	2394	+		
2467	*B. ephippiatus*	Mexico	BBDUR464	23.65	-105.76	2470	+		
2468	*B. ephippiatus*	Mexico	BBDUR464	23.65	-105.76	2470	+		
2469	*B. ephippiatus*	Mexico	BBDUR464	23.65	-105.76	2470	+		
2470	*B. ephippiatus*	Mexico	BBDUR461	23.64	-105.81	2351	+		
2474	*B. ephippiatus*	Mexico	BBDUR466	23.58	-105.84	2071	+		
2475	*B. ephippiatus*	Mexico	BBDUR465	23.6	-105.85	2042	+		
2476	*B. ephippiatus*	Mexico	BBDUR465	23.6	-105.85	2042	+		
2487	*B. ephippiatus*	Mexico	BBDUR461	23.64	-105.81	2351	+		
2488	*B. ephippiatus*	Mexico	BBDUR461	23.64	-105.81	2351	+		
2489	*B. ephippiatus*	Mexico	BBDUR462	23.63	-105.84	2288	+		
2493	*B. ephippiatus*	Mexico	BBDUR231	25.19	-106.55	1768	+	+	
2494	*B. ephippiatus*	Mexico	BBDUR231	25.19	-106.55	1768	+		

Table 1.1 (cont.)

Voucher Name	Phenotype	Country	Population	Latitude	Longitude	Altitude	MSAT	COI	WING
2495	*B. ephippiatus*	Mexico	BBDUR232	25.16	-106.55	1717	+		
2496	*B. ephippiatus*	Mexico	BBDUR232	25.16	-106.55	1717	+		
2497	*B. ephippiatus*	Mexico	BBDUR235	25.13	-106.5	2172	+		
2498	*B. ephippiatus*	Mexico	BBDUR235	25.13	-106.5	2172	+		
2499	*B. ephippiatus*	Mexico	BBDUR235	25.13	-106.5	2172	+		
2500	*B. ephippiatus*	Mexico	BBDUR301	25.07	-106.2	2405	+		
2501	*B. ephippiatus*	Mexico	BBDUR301	25.07	-106.2	2405	+		
2502	*B. ephippiatus*	Mexico	BBDUR301	25.07	-106.2	2405	+		
2503	*B. ephippiatus*	Mexico	BBDUR301	25.07	-106.2	2405	+		
2504	*B. ephippiatus*	Mexico	BBDUR301	25.07	-106.2	2405	+		
2505	*B. ephippiatus*	Mexico	BBDUR301	25.07	-106.2	2405	+		
2508	*B. ephippiatus*	Mexico	BBDUR234	25.13	-106.52	1854	+		
2509	*B. ephippiatus*	Mexico	BBDUR235	25.13	-106.5	2172	+		
2510	*B. ephippiatus*	Mexico	BBDUR235	25.13	-106.5	2172	+		
2511	*B. ephippiatus*	Mexico	BBDUR235	25.13	-106.5	2172	+		
2513	*B. ephippiatus*	Mexico	BBDUR551	22.96	-104.29	2678	+		
2514	*B. ephippiatus*	Mexico	BBDUR551	22.96	-104.29	2678	+		
2515	*B. ephippiatus*	Mexico	BBDUR551	22.96	-104.29	2678	+		
2516	*B. ephippiatus*	Mexico	BBDUR551	22.96	-104.29	2678	+		
2517	*B. ephippiatus*	Mexico	BBDUR551	22.96	-104.29	2678	+		
2518	*B. ephippiatus*	Mexico	BBDUR551	22.96	-104.29	2678	+		
2519	*B. ephippiatus*	Mexico	BBDUR552	22.98	-104.29	2717	+		
2520	*B. ephippiatus*	Mexico	BBDUR471	23.59	-105.39	2774	+	+	+
2522	*B. ephippiatus*	Mexico	BBDUR472	23.55	-105.36	2721	+		
2523	*B. ephippiatus*	Mexico	BBDUR472	23.55	-105.36	2721	+		
2524	*B. ephippiatus*	Mexico	BBDUR472	23.55	-105.36	2721	+		
2539	*B. ephippiatus*	Mexico	BBDUR462	23.63	-105.84	2288	+		

Table 1.1 (cont.)

Voucher Name	Phenotype	Country	Population	Latitude	Longitude	Altitude	MSAT	COI	WING
2546	*B. ephippiatus*	Mexico	BBDUR464	23.65	-105.76	2470	+		
2547	*B. ephippiatus*	Mexico	BBDUR312	25.01	-105.75	2567	+		
2548	*B. ephippiatus*	Mexico	BBDUR312	25.01	-105.75	2567	+		
2549	*B. ephippiatus*	Mexico	BBDUR312	25.01	-105.75	2567	+		
2551	*B. ephippiatus*	Mexico	BBDUR313	25.03	-105.73	2454	+		
2552	*B. ephippiatus*	Mexico	BBDUR312	25.01	-105.75	2567	+		
2553	*B. ephippiatus*	Mexico	BBDUR231	25.19	-106.55	1768	+		
2554	*B. ephippiatus*	Mexico	BBDUR312	25.01	-105.75	2567	+		
2556	*B. ephippiatus*	Mexico	BBDUR312	25.01	-105.75	2567	+		
2608	*B. ephippiatus*	Mexico	BBDUR231	25.19	-106.55	1768	+		
2811	*B. ephippiatus*	Mexico	BBSLP392	21.17	-101.24	2466	+		
2812	*B. ephippiatus*	Mexico	BBSLP393	21.14	-101.24	2715	+		
2813	*B. ephippiatus*	Mexico	BBSLP393	21.14	-101.24	2715	+		
2814	*B. ephippiatus*	Mexico	BBSLP393	21.14	-101.24	2715	+		
2815	*B. ephippiatus*	Mexico	BBSLP393	21.14	-101.24	2715	+		
2816	*B. ephippiatus*	Mexico	BBSLP393	21.14	-101.24	2715	+		
2817	*B. ephippiatus*	Mexico	BBSLP393	21.14	-101.24	2715	+		
2818	*B. ephippiatus*	Mexico	BBSLP393	21.14	-101.24	2715	+		
2819	*B. ephippiatus*	Mexico	BBSLP393	21.14	-101.24	2715	+		
2820	*B. ephippiatus*	Mexico	BBSLP393	21.14	-101.24	2715	+		
3280	*B. ephippiatus*	Mexico	BBJAL252	19.33	-103.27	2019	+		
3281	*B. ephippiatus*	Mexico	BBJAL252	19.33	-103.27	2019	+		
3282	*B. ephippiatus*	Mexico	BBJAL252	19.33	-103.27	2019	+		
3283	*B. ephippiatus*	Mexico	BBJAL251	19.28	-103.25	1987	+		
3284	*B. ephippiatus*	Mexico	BBJAL251	19.28	-103.25	1987	+		
3285	*B. ephippiatus*	Mexico	BBJAL251	19.28	-103.25	1987	+		
3286	*B. ephippiatus*	Mexico	BBJAL253	19.37	-103.28	1833	+		

Table 1.1 (cont.)

Voucher Name	Phenotype	Country	Population	Latitude	Longitude	Altitude	MSAT	COI	WING
3287	*B. ephippiatus*	Mexico	BBJAL253	19.37	-103.28	1833	+		
3288	*B. ephippiatus*	Mexico	BBJAL251	19.28	-103.25	1987	+		
3289	*B. ephippiatus*	Mexico	BBJAL251	19.28	-103.25	1987	+		
3290	*B. ephippiatus*	Mexico	BBJAL251	19.28	-103.25	1987	+		
3291	*B. ephippiatus*	Mexico	BBJAL251	19.28	-103.25	1987	+		
3300	*B. ephippiatus*	Mexico	BBJAL252	19.33	-103.27	2019	+		
3301	*B. ephippiatus*	Mexico	BBJAL252	19.33	-103.27	2019	+		
3302	*B. ephippiatus*	Mexico	BBJAL252	19.33	-103.27	2019	+		
3315	*B. ephippiatus*	Mexico	BBJAL253	19.37	-103.28	1833	+		
3316	*B. ephippiatus*	Mexico	BBJAL253	19.37	-103.28	1833	+		
3317	*B. ephippiatus*	Mexico	BBJAL253	19.37	-103.28	1833	+		
3325	*B. ephippiatus*	Mexico	BBSLP372	21.29	-101.66	2333	+		
3326	*B. ephippiatus*	Mexico	BBJAL271	22.02	-103.89	2399	+		
3327	*B. ephippiatus*	Mexico	BBJAL271	22.02	-103.89	2399	+		
3328	*B. ephippiatus*	Mexico	BBJAL271	22.02	-103.89	2399	+		
3329	*B. ephippiatus*	Mexico	BBJAL272	22.07	-103.9	2547	+		
3330	*B. ephippiatus*	Mexico	BBJAL272	22.07	-103.9	2547	+		
3331	*B. ephippiatus*	Mexico	BBJAL272	22.07	-103.9	2547	+		
3332	*B. ephippiatus*	Mexico	BBJAL273	22.1	-103.88	2793	+		
3333	*B. ephippiatus*	Mexico	BBJAL273	22.1	-103.88	2793	+		
3334	*B. ephippiatus*	Mexico	BBJAL273	22.1	-103.88	2793	+		
3335	*B. ephippiatus*	Mexico	BBJAL271	22.02	-103.89	2399	+		
3336	*B. ephippiatus*	Mexico	BBJAL271	22.02	-103.89	2399	+		
3337	*B. ephippiatus*	Mexico	BBJAL271	22.02	-103.89	2399	+		
3338	*B. ephippiatus*	Mexico	BBJAL271	22.02	-103.89	2399	+		
3354	*B. ephippiatus*	Mexico	BBJAL272	22.07	-103.9	2547	+		
3355	*B. ephippiatus*	Mexico	BBJAL272	22.07	-103.9	2547	+		

Table 1.1 (cont.)

Voucher Name	Phenotype	Country	Population	Latitude	Longitude	Altitude	MSAT	COI	WING
3356	*B. ephippiatus*	Mexico	BBJAL272	22.07	-103.9	2547	+		
3357	*B. ephippiatus*	Mexico	BBJAL272	22.07	-103.9	2547	+		
3367	*B. ephippiatus*	Mexico	BBJAL273	22.1	-103.88	2793	+		
3368	*B. ephippiatus*	Mexico	BBJAL273	22.1	-103.88	2793	+		
3376	*B. ephippiatus*	Mexico	BBDUR101	22.61	-104.27	2670	+		
3377	*B. ephippiatus*	Mexico	BBDUR101	22.61	-104.27	2670	+		
3378	*B. ephippiatus*	Mexico	BBDUR101	22.61	-104.27	2670	+		
3379	*B. ephippiatus*	Mexico	BBDUR101	22.61	-104.27	2670	+		
3380	*B. ephippiatus*	Mexico	BBDUR101	22.61	-104.27	2670	+		
3381	*B. ephippiatus*	Mexico	BBDUR101	22.61	-104.27	2670	+		
3382	*B. ephippiatus*	Mexico	BBDUR101	22.61	-104.27	2670	+		
3385	*B. ephippiatus*	Mexico	BBDUR102	22.62	-104.24	2639	+		
3386	*B. ephippiatus*	Mexico	BBDUR102	22.62	-104.24	2639	+		
3387	*B. ephippiatus*	Mexico	BBDUR102	22.62	-104.24	2639	+		
3388	*B. ephippiatus*	Mexico	BBDUR102	22.62	-104.24	2639	+		
3389	*B. ephippiatus*	Mexico	BBDUR102	22.62	-104.24	2639	+		
3396	*B. ephippiatus*	Mexico	BBDUR103	22.63	-104.22	2511	+		
3397	*B. ephippiatus*	Mexico	BBDUR103	22.63	-104.22	2511	+		
3398	*B. ephippiatus*	Mexico	BBDUR103	22.63	-104.22	2511	+		
4233	*B. ephippiatus*	Mexico	BBNAY151	22.72	-105.19	1745	+		
4234	*B. ephippiatus*	Mexico	BBNAY151	22.72	-105.19	1745	+		
4236	*B. ephippiatus*	Mexico	BBNAY152	22.79	-105.18	2112	+		
4237	*B. ephippiatus*	Mexico	BBNAY152	22.79	-105.18	2112	+		
4238	*B. ephippiatus*	Mexico	BBNAY152	22.79	-105.18	2112	+		
4239	*B. ephippiatus*	Mexico	BBNAY152	22.79	-105.18	2112	+		
4240	*B. ephippiatus*	Mexico	BBNAY152	22.79	-105.18	2112	+		
4243	*B. ephippiatus*	Mexico	BBNAY161	22.26	-104.72	2044	+		

Table 1.1 (cont.)

Voucher Name	Phenotype	Country	Population	Latitude	Longitude	Altitude	MSAT	COI	WING
4244	*B. ephippiatus*	Mexico	BBNAY161	22.26	-104.72	2044	+		
4245	*B. ephippiatus*	Mexico	BBNAY161	22.26	-104.72	2044	+		
4246	*B. ephippiatus*	Mexico	BBNAY161	22.26	-104.72	2044	+		
4247	*B. ephippiatus*	Mexico	BBNAY161	22.26	-104.72	2044	+		
4248	*B. ephippiatus*	Mexico	BBNAY161	22.26	-104.72	2044	+		
4249	*B. ephippiatus*	Mexico	BBNAY161	22.26	-104.72	2044	+		
4250	*B. ephippiatus*	Mexico	BBNAY162	22.23	-104.71	2088	+		
4251	*B. ephippiatus*	Mexico	BBNAY162	22.23	-104.71	2088	+		
4252	*B. ephippiatus*	Mexico	BBNAY162	22.23	-104.71	2088	+		
4253	*B. ephippiatus*	Mexico	BBNAY162	22.23	-104.71	2088	+		
4254	*B. ephippiatus*	Mexico	BBNAY162	22.23	-104.71	2088	+		
4255	*B. ephippiatus*	Mexico	BBNAY162	22.23	-104.71	2088	+		
5342	*B. ephippiatus*	Mexico	BBDUR122	21.42	-103.21	2387	+		
5343	*B. ephippiatus*	Mexico	BBDUR122	21.42	-103.21	2387	+		
5344	*B. ephippiatus*	Mexico	BBJAL261	21.28	-103.05	2112	+		
5345	*B. ephippiatus*	Mexico	BBDUR122	21.42	-103.21	2387	+		
5346	*B. ephippiatus*	Mexico	BBDUR122	21.42	-103.21	2387	+		
5347	*B. ephippiatus*	Mexico	BBDUR123	21.38	-103.23	2595	+		
5348	*B. ephippiatus*	Mexico	BBDUR123	21.38	-103.23	2595	+		
5349	*B. ephippiatus*	Mexico	BBDUR122	21.42	-103.21	2387	+		
77511	*B. ephippiatus*	Mexico	BBCHI153	16.738	-92.7184	2459	+		
77512	*B. ephippiatus*	Mexico	BBCHI151	16.768	-92.736	2139	+		+
77527	*B. ephippiatus*	Mexico	BBCHI153	16.738	-92.718	2459	+		+
77531	*B. ephippiatus*	Mexico	BBCHI011	16.639	-92.397	2327	+		+
77532	*B. ephippiatus*	Mexico	BBCHI011	16.6386	-92.3973	2327	+		
77533	*B. ephippiatus*	Mexico	BBCHI011	16.6386	-92.3973	2327	+		
77534	*B. ephippiatus*	Mexico	BBCHI011	16.6386	-92.3973	2327	+		

Table 1.1 (cont.)

Voucher Name	Phenotype	Country	Population	Latitude	Longitude	Altitude	MSAT	COI	WING
77553	*B. ephippiatus*	Mexico	BBCHI013	16.6597	-92.449	2332	+		
77554	*B. ephippiatus*	Mexico	BBCHI013	16.6597	-92.449	2332	+		
77563	*B. ephippiatus*	Mexico	BBCHI153	16.738	-92.7184	2459	+		
77564	*B. ephippiatus*	Mexico	BBCHI153	16.738	-92.7184	2459	+		
77565	*B. ephippiatus*	Mexico	BBCHI151	16.7684	-92.7355	2139	+		
77566	*B. ephippiatus*	Mexico	BBCHI151	16.768	-92.736	2139	+		+
77567	*B. ephippiatus*	Mexico	BBCHI151	16.7684	-92.7355	2139	+		
77568	*B. ephippiatus*	Mexico	BBCHI151	16.768	-92.736	2139	+		+
77569	*B. ephippiatus*	Mexico	BBCHI151	16.7684	-92.7355	2139	+		
77570	*B. ephippiatus*	Mexico	BBCHI151	16.7684	-92.7355	2139	+		
77664	*B. ephippiatus*	Mexico	BBCHI012	16.637	-92.331	2087	+		+
77665	*B. ephippiatus*	Mexico	BBCHI012	16.637	-92.331	2087	+		+
77777	*B. ephippiatus*	Mexico	BBCHI092	17.1737	-92.9162	1792	+		
77800	*B. ephippiatus*	Mexico	BBCHI041	17.1885	-93.1416	1859	+		
77801	*B. ephippiatus*	Mexico	BBCHI041	17.1885	-93.1416	1859	+		
77802	*B. ephippiatus*	Mexico	BBCHI041	17.1885	-93.1416	1859	+		
77803	*B. ephippiatus*	Mexico	BBCHI041	17.1885	-93.1416	1859	+		
77804	*B. ephippiatus*	Mexico	BBCHI041	17.1885	-93.1416	1859	+		
77805	*B. ephippiatus*	Mexico	BBCHI042	17.1885	-93.1416	1859	+		
77806	*B. ephippiatus*	Mexico	BBCHI042	17.1885	-93.1416	1859	+		
77807	*B. ephippiatus*	Mexico	BBCHI042	17.1885	-93.1416	1859	+		
77808	*B. ephippiatus*	Mexico	BBCHI042	17.1885	-93.1416	1859	+		
77809	*B. ephippiatus*	Mexico	BBCHI042	17.1885	-93.1416	1859	+		
77810	*B. ephippiatus*	Mexico	BBCHI042	17.1885	-93.1416	1859	+		
77811	*B. ephippiatus*	Mexico	BBCHI042	17.1885	-93.1416	1859	+		
77812	*B. ephippiatus*	Mexico	BBCHI042	17.1885	-93.1416	1859	+		
77813	*B. ephippiatus*	Mexico	BBCHI042	17.1885	-93.1416	1859	+		

Table 1.1 (cont.)

Voucher Name	Phenotype	Country	Population	Latitude	Longitude	Altitude	MSAT	COI	WING
77814	*B. ephippiatus*	Mexico	BBCHI042	17.1885	-93.1416	1859	+		
77815	*B. ephippiatus*	Mexico	BBCHI042	17.1885	-93.1416	1859	+		
77816	*B. ephippiatus*	Mexico	BBCHI042	17.1885	-93.1416	1859	+		
77817	*B. ephippiatus*	Mexico	BBCHI042	17.1885	-93.1416	1859	+		
77818	*B. ephippiatus*	Mexico	BBCHI042	17.1885	-93.1416	1859	+		
77819	*B. ephippiatus*	Mexico	BBCHI042	17.1885	-93.1416	1859	+		
77820	*B. ephippiatus*	Mexico	BBCHI042	17.1885	-93.1416	1859	+		
77821	*B. ephippiatus*	Mexico	BBCHI042	17.1885	-93.1416	1859	+		
77822	*B. ephippiatus*	Mexico	BBCHI042	17.1885	-93.1416	1859	+		
77823	*B. ephippiatus*	Mexico	BBCHI042	17.1885	-93.1416	1859	+		
77824	*B. ephippiatus*	Mexico	BBCHI042	17.1885	-93.1416	1859	+		
77825	*B. ephippiatus*	Mexico	BBCHI042	17.1885	-93.1416	1859	+		
77826	*B. ephippiatus*	Mexico	BBCHI042	17.1885	-93.1416	1859	+		
77827	*B. ephippiatus*	Mexico	BBCHI042	17.1885	-93.1416	1859	+		
77828	*B. ephippiatus*	Mexico	BBCHI042	17.1885	-93.1416	1859	+		
77829	*B. ephippiatus*	Mexico	BBCHI042	17.1885	-93.1416	1859	+		
77830	*B. ephippiatus*	Mexico	BBCHI042	17.1885	-93.1416	1859	+		
77831	*B. ephippiatus*	Mexico	BBCHI043	17.1463	-93.1474	1709	+		
77832	*B. ephippiatus*	Mexico	BBCHI043	17.1463	-93.1474	1709	+		
77833	*B. ephippiatus*	Mexico	BBCHI044	17.1338	-93.1684	1586	+		
77834	*B. ephippiatus*	Mexico	BBCHI044	17.1338	-93.1684	1586	+		
77835	*B. ephippiatus*	Mexico	BBCHI091	17.174	-92.897	1725	+		
77836	*B. ephippiatus*	Mexico	BBCHI091	17.174	-92.897	1725	+		
77852	*B. ephippiatus*	Mexico	BBCHI091	17.174	-92.897	1725	+		+
77853	*B. ephippiatus*	Mexico	BBCHI091	17.174	-92.897	1725	+		
77858	*B. ephippiatus*	Mexico	BBCHI092	17.1737	-92.9162	1792	+		
77859	*B. ephippiatus*	Mexico	BBCHI092	17.1737	-92.9162	1792	+		

Table 1.1 (cont.)

Voucher Name	Phenotype	Country	Population	Latitude	Longitude	Altitude	MSAT	COI	WING
77861	*B. ephippiatus*	Mexico	BBCHI092	17.1737	-92.9162	1792	+		
77862	*B. ephippiatus*	Mexico	BBCHI092	17.174	-92.916	1792	+		+
77863	*B. ephippiatus*	Mexico	BBCHI093	17.2139	-92.9608	1911	+		
77864	*B. ephippiatus*	Mexico	BBCHI093	17.2139	-92.9608	1911	+		
77889	*B. ephippiatus*	Mexico	BBCHI082		-92.291	1620	+		+
77890	*B. ephippiatus*	Mexico	BBCHI082		-92.291	1620	+		+
77891	*B. ephippiatus*	Mexico	BBCHI082		-92.2908	1620	+		
77892	*B. ephippiatus*	Mexico	BBCHI082		-92.2908	1620	+		
77895	*B. ephippiatus*	Mexico	BBCHI082		-92.2908	1620	+		
77901	*B. ephippiatus*	Mexico	BBCHI083	16.788	-92.353	2128	+		+
77903	*B. ephippiatus*	Mexico	BBCHI083	16.788	-92.353	2128	+		+
77904	*B. ephippiatus*	Mexico	BBCHI083	16.7881	-92.3534	2128	+		
77905	*B. ephippiatus*	Mexico	BBCHI083	16.7881	-92.3534	2128	+		
77906	*B. ephippiatus*	Mexico	BBCHI081	16.7993	-92.3222	1958	+		
77907	*B. ephippiatus*	Mexico	BBCHI083	16.7881	-92.3534	2128	+		
77909	*B. ephippiatus*	Mexico	BBCHI082		-92.2908	1620	+		
77911	*B. ephippiatus*	Mexico	BBCHI083	16.7881	-92.3534	2128	+		
77912	*B. ephippiatus*	Mexico	BBCHI081	16.7993	-92.3222	1958	+		
77913	*B. ephippiatus*	Mexico	BBCHI082		-92.2908	1620	+		
77914	*B. ephippiatus*	Mexico	BBCHI081	16.7993	-92.3222	1958	+		
77918	*B. ephippiatus*	Mexico	BBCHI081	16.7993	-92.3222	1958	+		
79450	*B. ephippiatus*	Mexico	BBCHI011	16.6386	-92.3973	2327	+		
79451	*B. ephippiatus*	Mexico	BBCHI011	16.6386	-92.3973	2327	+		
79452	*B. ephippiatus*	Mexico	BBCHI011	16.639	-92.397	2327	+		+
79453	*B. ephippiatus*	Mexico	BBCHI012	16.6369	-92.3314	2087	+		
79458	*B. ephippiatus*	Mexico	BBCHI013	16.6597	-92.449	2332	+		
79460	*B. ephippiatus*	Mexico	BBCHI013	16.6597	-92.449	2332	+		

Table 1.1 (cont.)

Voucher Name	Phenotype	Country	Population	Latitude	Longitude	Altitude	MSAT	COI	WING
79461	*B. ephippiatus*	Mexico	BBCHI013	16.66	-92.449	2332	+		+
79462	*B. ephippiatus*	Mexico	BBCHI013	16.6597	-92.449	2332	+		
79463	*B. ephippiatus*	Mexico	BBCHI013	16.6597	-92.449	2332	+		
79465	*B. ephippiatus*	Mexico	BBCHI013	16.6597	-92.449	2332	+		
79487	*B. ephippiatus*	Mexico	BBCHI013	16.6597	-92.449	2332	+		
79489	*B. ephippiatus*	Mexico	BBCHI152	16.7579	-92.7622	2007	+		
79490	*B. ephippiatus*	Mexico	BBCHI152	16.7579	-92.7622	2007	+		
79500	*B. ephippiatus*	Mexico	BBCHI153	16.738	-92.7184	2459	+		
79501	*B. ephippiatus*	Mexico	BBCHI153	16.738	-92.718	2459	+		+
79504	*B. ephippiatus*	Mexico	BBCHI151	16.7684	-92.7355	2139	+		
79562	*B. ephippiatus*	Mexico	BBCHI081	16.799	-92.322	1958	+		+
79564	*B. ephippiatus*	Mexico	BBCHI081	16.7993	-92.3222	1958	+		
79565	*B. ephippiatus*	Mexico	BBCHI081	16.7993	-92.3222	1958	+		
79741	*B. ephippiatus*	Mexico	BBCHI091	17.174	-92.897	1725	+		
79745	*B. ephippiatus*	Mexico	BBCHI093	17.2139	-92.9608	1911	+		
79746	*B. ephippiatus*	Mexico	BBCHI093	17.214	-92.961	1911	+		+
79750	*B. ephippiatus*	Mexico	BBCHI093	17.214	-92.961	1911	+		+
79755	*B. ephippiatus*	Mexico	BBCHI091	17.174	-92.897	1725	+		
79756	*B. ephippiatus*	Mexico	BBCHI091	17.174	-92.897	1725	+		
79769	*B. ephippiatus*	Mexico	BBCHI092	17.1737	-92.9162	1792	+		
79773	*B. ephippiatus*	Mexico	BBCHI092	17.1737	-92.9162	1792	+		
79797	*B. ephippiatus*	Mexico	BBCHI093	17.2139	-92.9608	1911	+		
79808	*B. ephippiatus*	Mexico	BBCHI121	16.51014	-92.3286	1585	+		
79809	*B. ephippiatus*	Mexico	BBCHI121	16.51014	-92.3286	1585	+		
79810	*B. ephippiatus*	Mexico	BBCHI122	16.50867	-92.06382	1589	+		
79811	*B. ephippiatus*	Mexico	BBCHI122	16.50867	-92.06382	1589	+		
79812	*B. ephippiatus*	Mexico	BBCHI122	16.509	-92.064	1589	+		+

Table 1.1 (cont.)

Voucher Name	Phenotype	Country	Population	Latitude	Longitude	Altitude	MSAT	COI	WING
79813	*B. ephippiatus*	Mexico	BBCHI122	16.50867	-92.06382	1589	+		
79814	*B. ephippiatus*	Mexico	BBCHI122	16.50867	-92.06382	1589	+		
79815	*B. ephippiatus*	Mexico	BBCHI122	16.509	-92.064	1589	+		+
79816	*B. ephippiatus*	Mexico	BBCHI122	16.50867	-92.06382	1589	+		
79817	*B. ephippiatus*	Mexico	BBCHI122	16.50867	-92.06382	1589	+		
79818	*B. ephippiatus*	Mexico	BBCHI122	16.50867	-92.06382	1589	+		
79819	*B. ephippiatus*	Mexico	BBCHI122	16.50867	-92.06382	1589	+		
79820	*B. ephippiatus*	Mexico	BBCHI122	16.509	-92.064	1589	+		+
79821	*B. ephippiatus*	Mexico	BBCHI122	16.50867	-92.06382	1589	+		
79822	*B. ephippiatus*	Mexico	BBCHI122	16.50867	-92.06382	1589	+		
79823	*B. ephippiatus*	Mexico	BBCHI122	16.509	-92.064	1589	+		+
79836	*B. ephippiatus*	Mexico	BBCHI123	16.5224	-92.0612	1537	+		
79888	*B. ephippiatus*	Mexico	BBCHI123	16.5224	-92.0612	1537	+		
79889	*B. ephippiatus*	Mexico	BBCHI123	16.5224	-92.0612	1537	+		
79890	*B. ephippiatus*	Mexico	BBCHI123	16.522	-92.061	1537	+		+
79917	*B. ephippiatus*	Mexico	BBCHI141	15.6197	-92.2099	1785	+		
92196	*B. ephippiatus*	Mexico	BBCHI113	15.2958	-92.2413	2460	+		
92197	*B. ephippiatus*	Mexico	BBCHI113	15.2958	-92.2413	2460	+		
92198	*B. ephippiatus*	Mexico	BBCHI113	15.2958	-92.2413	2460	+		
92199	*B. ephippiatus*	Mexico	BBCHI113	15.296	-92.241	2460	+		+
92203	*B. ephippiatus*	Mexico	BBCHI113	15.296	-92.241	2460	+		+
92205	*B. ephippiatus*	Mexico	BBCHI113	15.296	-92.241	2460	+		+
92208	*B. ephippiatus*	Mexico	BBCHI113	15.2958	-92.2413	2460	+		
92209	*B. ephippiatus*	Mexico	BBCHI113	15.2958	-92.2413	2460	+		
92211	*B. ephippiatus*	Mexico	BBCHI113	15.296	-92.241	2460	+		+
92213	*B. ephippiatus*	Mexico	BBCHI113	15.2958	-92.2413	2460	+		
92216	*B. ephippiatus*	Mexico	BBCHI113	15.296	-92.241	2460	+		+

Table 1.1 (cont.)

Voucher Name	Phenotype	Country	Population	Latitude	Longitude	Altitude	MSAT	COI	WING
92312	*B. ephippiatus*	Mexico	BBCHI051	17.12897	-92.36132	1538	+		
92313	*B. ephippiatus*	Mexico	BBCHI051	17.12897	-92.36132	1538	+		
92314	*B. ephippiatus*	Mexico	BBCHI052	17.15326	-92.37399	1810	+		
92315	*B. ephippiatus*	Mexico	BBCHI052	17.15326	-92.37399	1810	+		
92316	*B. ephippiatus*	Mexico	BBCHI052	17.15326	-92.37399	1810	+		
92317	*B. ephippiatus*	Mexico	BBCHI052	17.153	-92.374	1810	+		+
92318	*B. ephippiatus*	Mexico	BBCHI052	17.15326	-92.37399	1810	+		
92319	*B. ephippiatus*	Mexico	BBCHI052	17.15326	-92.37399	1810	+		
92320	*B. ephippiatus*	Mexico	BBCHI052	17.15326	-92.37399	1810	+		
92321	*B. ephippiatus*	Mexico	BBCHI052	17.153	-92.374	1810	+		+
92322	*B. ephippiatus*	Mexico	BBCHI052	17.153	-92.374	1810	+		+
92323	*B. ephippiatus*	Mexico	BBCHI052	17.15326	-92.37399	1810	+		
92324	*B. ephippiatus*	Mexico	BBCHI052	17.15326	-92.37399	1810	+		
92325	*B. ephippiatus*	Mexico	BBCHI052	17.15326	-92.37399	1810	+		
92326	*B. ephippiatus*	Mexico	BBCHI052	17.153	-92.374	1810	+		+
92327	*B. ephippiatus*	Mexico	BBCHI052	17.15326	-92.37399	1810	+		
92339	*B. ephippiatus*	Mexico	BBCHI053	17.14926	-92.34991	1598	+		
92340	*B. ephippiatus*	Mexico	BBCHI053	17.14926	-92.34991	1598	+		
92341	*B. ephippiatus*	Mexico	BBCHI053	17.14926	-92.34991	1598	+		
92346	*B. ephippiatus*	Mexico	BBCHI071	16.0832	-91.65746	1490	+		
92347	*B. ephippiatus*	Mexico	BBCHI071	16.0832	-91.65746	1490	+		
92348	*B. ephippiatus*	Mexico	BBCHI071	16.083	-91.657	1490	+		+
92349	*B. ephippiatus*	Mexico	BBCHI071	16.0832	-91.65746	1490	+		
92350	*B. ephippiatus*	Mexico	BBCHI071	16.0832	-91.65746	1490	+		
92351	*B. ephippiatus*	Mexico	BBCHI071	16.083	-91.657	1490	+		+
92352	*B. ephippiatus*	Mexico	BBCHI071	16.0832	-91.65746	1490	+		
92353	*B. ephippiatus*	Mexico	BBCHI071	16.0832	-91.65746	1490	+		

Table 1.1 (cont.)

Voucher Name	Phenotype	Country	Population	Latitude	Longitude	Altitude	MSAT	COI	WING
92354	*B. ephippiatus*	Mexico	BBCHI071	16.0832	-91.65746	1490	+		
92356	*B. ephippiatus*	Mexico	BBCHI071	16.0832	-91.65746	1490	+		
92357	*B. ephippiatus*	Mexico	BBCHI071	16.083	-91.657	1490	+		+
92358	*B. ephippiatus*	Mexico	BBCHI071	16.0832	-91.65746	1490	+		
92359	*B. ephippiatus*	Mexico	BBCHI072	16.1117	-91.62929	1451	+		
92360	*B. ephippiatus*	Mexico	BBCHI072	16.112	-91.629	1451	+		+
92361	*B. ephippiatus*	Mexico	BBCHI072	16.1117	-91.62929	1451	+		
92362	*B. ephippiatus*	Mexico	BBCHI072	16.112	-91.629	1451	+		+
92394	*B. ephippiatus*	Mexico	BBCHI053	17.149	-92.35	1598	+		+
92420	*B. ephippiatus*	Mexico	BBPUE021	18.66921	-97.02053	1006	+		
92421	*B. ephippiatus*	Mexico	BBPUE021	18.66921	-97.02053	1006	+		
92422	*B. ephippiatus*	Mexico	BBPUE021	18.66921	-97.02053	1006	+		
92423	*B. ephippiatus*	Mexico	BBPUE022	18.68139	-97.05264	1854	+		
92424	*B. ephippiatus*	Mexico	BBPUE022	18.68139	-97.05264	1854	+		
92425	*B. ephippiatus*	Mexico	BBPUE022	18.68139	-97.05264	1854	+		
92427	*B. ephippiatus*	Mexico	BBPUE022	18.681	-97.053	1854	+		+
92428	*B. ephippiatus*	Mexico	BBPUE022	18.68139	-97.05264	1854	+		
92429	*B. ephippiatus*	Mexico	BBPUE022	18.68139	-97.05264	1854	+		
92431	*B. ephippiatus*	Mexico	BBPUE022	18.681	-97.053	1854	+		+
92433	*B. ephippiatus*	Mexico	BBPUE023	18.7072	-97.06669	1869	+		
92434	*B. ephippiatus*	Mexico	BBPUE023	18.7072	-97.06669	1869	+		
92435	*B. ephippiatus*	Mexico	BBPUE023	18.7072	-97.06669	1869	+		
92436	*B. ephippiatus*	Mexico	BBPUE023	18.707	-97.067	1869	+		+
92438	*B. ephippiatus*	Mexico	BBPUE023	18.7072	-97.06669	1869	+		
92439	*B. ephippiatus*	Mexico	BBPUE023	18.7072	-97.06669	1869	+		
92440	*B. ephippiatus*	Mexico	BBPUE023	18.707	-97.067	1869	+		+
92447	*B. ephippiatus*	Mexico	BBPUE023	18.7072	-97.06669	1869	+		

Table 1.1 (cont.)

Voucher Name	Phenotype	Country	Population	Latitude	Longitude	Altitude	MSAT	COI	WING
92448	*B. ephippiatus*	Mexico	BBPUE023	18.7072	-97.06669	1869	+		
92449	*B. ephippiatus*	Mexico	BBPUE023	18.707	-97.067	1869	+		+
92603	*B. ephippiatus*	Mexico	BBPUE011	18.49961	-97.16229	2458	+		
92604	*B. ephippiatus*	Mexico	BBPUE011	18.49961	-97.16229	2458	+		
92605	*B. ephippiatus*	Mexico	BBPUE011	18.49961	-97.16229	2458	+		
92606	*B. ephippiatus*	Mexico	BBPUE011	18.5	-97.162	2458	+		+
92615	*B. ephippiatus*	Mexico	BBPUE011	18.5	-97.162	2458	+		+
92618	*B. ephippiatus*	Mexico	BBPUE011	18.5	-97.162	2458	+		+
92621	*B. ephippiatus*	Mexico	BBPUE012	18.47984	-97.13905	2499	+		
92622	*B. ephippiatus*	Mexico	BBPUE012	18.47984	-97.13905	2499	+		
92623	*B. ephippiatus*	Mexico	BBPUE013	18.45465	-97.11639	2563	+		
92624	*B. ephippiatus*	Mexico	BBPUE013	18.45465	-97.11639	2563	+		
92629	*B. ephippiatus*	Mexico	BBPUE013	18.45465	-97.11639	2563	+		
92842	*B. ephippiatus*	Mexico	BBPUE062	19.26712	-97.20188	2439	+		
92843	*B. ephippiatus*	Mexico	BBPUE062	19.26712	-97.20188	2439	+		
92844	*B. ephippiatus*	Mexico	BBPUE062	19.26712	-97.20188	2439	+		
92845	*B. ephippiatus*	Mexico	BBPUE062	19.267	-97.202	2439	+		+
92847	*B. ephippiatus*	Mexico	BBPUE062	19.267	-97.202	2439	+		+
92848	*B. ephippiatus*	Mexico	BBPUE062	19.267	-97.202	2439	+		+
92849	*B. ephippiatus*	Mexico	BBPUE062	19.26712	-97.20188	2439	+		
92850	*B. ephippiatus*	Mexico	BBPUE062	19.26712	-97.20188	2439	+		
92851	*B. ephippiatus*	Mexico	BBPUE062	19.26712	-97.20188	2439	+		
92852	*B. ephippiatus*	Mexico	BBPUE062	19.26712	-97.20188	2439	+		
92853	*B. ephippiatus*	Mexico	BBPUE062	19.26712	-97.20188	2439	+		
92854	*B. ephippiatus*	Mexico	BBPUE062	19.26712	-97.20188	2439	+		
92855	*B. ephippiatus*	Mexico	BBPUE062	19.267	-97.202	2439	+		+
92856	*B. ephippiatus*	Mexico	BBPUE062	19.267	-97.202	2439	+		+

Table 1.1 (cont.)

Voucher Name	Phenotype	Country	Population	Latitude	Longitude	Altitude	MSAT	COI	WING
92857	*B. ephippiatus*	Mexico	BBPUE062	19.26712	-97.20188	2439	+		
92858	*B. ephippiatus*	Mexico	BBPUE062	19.26712	-97.20188	2439	+		
92859	*B. ephippiatus*	Mexico	BBPUE062	19.26712	-97.20188	2439	+		
92860	*B. ephippiatus*	Mexico	BBPUE062	19.26712	-97.20188	2439	+		
92872	*B. ephippiatus*	Mexico	BBPUE062	19.26712	-97.20188	2439	+		
92881	*B. ephippiatus*	Mexico	BBPUE063	19.29478	-97.22847	2746	+		
92957	*B. ephippiatus*	Mexico	BBPUE041	19.49667	-96.99029	1547	+		
92958	*B. ephippiatus*	Mexico	BBPUE041	19.49667	-96.99029	1547	+		
92959	*B. ephippiatus*	Mexico	BBPUE041	19.49667	-96.99029	1547	+		
92960	*B. ephippiatus*	Mexico	BBPUE041	19.497	-96.99	1547	+	+	+
92961	*B. ephippiatus*	Mexico	BBPUE041	19.49667	-96.99029	1547	+		
92967	*B. ephippiatus*	Mexico	BBPUE041	19.49667	-96.99029	1547	+		
92969	*B. ephippiatus*	Mexico	BBPUE041	19.49667	-96.99029	1547	+		
92970	*B. ephippiatus*	Mexico	BBPUE042	19.51	-97.015	1786	+		+
92971	*B. ephippiatus*	Mexico	BBPUE042	19.51026	-97.01456	1786	+		
92972	*B. ephippiatus*	Mexico	BBPUE042	19.51026	-97.01456	1786	+		
92973	*B. ephippiatus*	Mexico	BBPUE042	19.51026	-97.01456	1786	+		
92975	*B. ephippiatus*	Mexico	BBPUE042	19.51026	-97.01456	1786	+		
92977	*B. ephippiatus*	Mexico	BBPUE042	19.51026	-97.01456	1786	+		
92981	*B. ephippiatus*	Mexico	BBPUE042	19.51026	-97.01456	1786	+		
92982	*B. ephippiatus*	Mexico	BBPUE042	19.51026	-97.01456	1786	+		
92983	*B. ephippiatus*	Mexico	BBPUE042	19.51	-97.015	1786	+		+
92984	*B. ephippiatus*	Mexico	BBPUE042	19.51026	-97.01456	1786	+		
92996	*B. ephippiatus*	Mexico	BBPUE043	19.51903	-97.05841	2617	+		
92997	*B. ephippiatus*	Mexico	BBPUE043	19.519	-97.058	2617	+		+
92998	*B. ephippiatus*	Mexico	BBPUE043	19.519	-97.058	2617	+		+
93061	*B. ephippiatus*	Mexico	BBPUE101	19.731245	-96.87531	1930	+		

Table 1.1 (cont.)

Voucher Name	Phenotype	Country	Population	Latitude	Longitude	Altitude	MSAT	COI	WING
93064	*B. ephippiatus*	Mexico	BBPUE101	19.731	-96.875	1930	+		+
93066	*B. ephippiatus*	Mexico	BBPUE101	19.731245	-96.87531	1930	+		
93068	*B. ephippiatus*	Mexico	BBPUE101	19.731245	-96.87531	1930	+		
93069	*B. ephippiatus*	Mexico	BBPUE101	19.731245	-96.87531	1930	+		
93074	*B. ephippiatus*	Mexico	BBPUE101	19.731245	-96.87531	1930	+		
93076	*B. ephippiatus*	Mexico	BBPUE101	19.731245	-96.87531	1930	+		
93077	*B. ephippiatus*	Mexico	BBPUE101	19.731245	-96.87531	1930	+		
93083	*B. ephippiatus*	Mexico	BBPUE101	19.731245	-96.87531	1930	+		
93085	*B. ephippiatus*	Mexico	BBPUE101	19.731245	-96.87531	1930	+		
93087	*B. ephippiatus*	Mexico	BBPUE101	19.731245	-96.87531	1930	+		
93088	*B. ephippiatus*	Mexico	BBPUE101	19.731245	-96.87531	1930	+		
93089	*B. ephippiatus*	Mexico	BBPUE101	19.731245	-96.87531	1930	+		
93092	*B. ephippiatus*	Mexico	BBPUE101	19.731245	-96.87531	1930	+		
93094	*B. ephippiatus*	Mexico	BBPUE101	19.731245	-96.87531	1930	+		
93095	*B. ephippiatus*	Mexico	BBPUE101	19.731245	-96.87531	1930	+		
93096	*B. ephippiatus*	Mexico	BBPUE102	19.731	-96.904	2011	+		+
93098	*B. ephippiatus*	Mexico	BBPUE102	19.731	-96.904	2011	+		+
93104	*B. ephippiatus*	Mexico	BBPUE103	19.735	-96.93	2241	+		+
93105	*B. ephippiatus*	Mexico	BBPUE103	19.735	-96.93	2241	+		+
93165	*B. ephippiatus*	Mexico	BBPUE091	19.78709	-97.24866	1729	+		
93166	*B. ephippiatus*	Mexico	BBPUE091	19.78709	-97.24866	1729	+		
93167	*B. ephippiatus*	Mexico	BBPUE091	19.78709	-97.24866	1729	+		
93179	*B. ephippiatus*	Mexico	BBPUE092	19.78465	-97.27666	1914	+		
93180	*B. ephippiatus*	Mexico	BBPUE092	19.78465	-97.27666	1914	+		
93181	*B. ephippiatus*	Mexico	BBPUE092	19.78465	-97.27666	1914	+		
93193	*B. ephippiatus*	Mexico	BBPUE093	19.78995	-97.35296	2111	+		
93194	*B. ephippiatus*	Mexico	BBPUE093	19.78995	-97.35296	2111	+		

Table 1.1 (cont.)

Voucher Name	Phenotype	Country	Population	Latitude	Longitude	Altitude	MSAT	COI	WING
93195	*B. ephippiatus*	Mexico	BBPUE093	19.78995	-97.35296	2111	+		
93330	*B. ephippiatus*	Mexico	BBPUE192	19.28935	-98.04553	2979	+		
93331	*B. ephippiatus*	Mexico	BBPUE192	19.28935	-98.04553	2979	+		
93335	*B. ephippiatus*	Mexico	BBPUE192	19.28935	-98.04553	2979	+		
93337	*B. ephippiatus*	Mexico	BBPUE193	19.27065	-98.07847	2987	+		
93338	*B. ephippiatus*	Mexico	BBPUE193	19.27065	-98.07847	2987	+		
93339	*B. ephippiatus*	Mexico	BBPUE193	19.27065	-98.07847	2987	+		
93341	*B. ephippiatus*	Mexico	BBPUE193	19.271	-98.078	2987	+		+
93342	*B. ephippiatus*	Mexico	BBPUE193	19.27065	-98.07847	2987	+		
93343	*B. ephippiatus*	Mexico	BBPUE193	19.27065	-98.07847	2987	+		
93345	*B. ephippiatus*	Mexico	BBPUE193	19.27065	-98.07847	2987	+		
93346	*B. ephippiatus*	Mexico	BBPUE193	19.271	-98.078	2987	+		+
93347	*B. ephippiatus*	Mexico	BBPUE193	19.271	-98.078	2987	+		+
93348	*B. ephippiatus*	Mexico	BBPUE193	19.271	-98.078	2987	+		+
93350	*B. ephippiatus*	Mexico	BBPUE193	19.27065	-98.07847	2987	+		
93353	*B. ephippiatus*	Mexico	BBPUE193	19.27065	-98.07847	2987	+		
93354	*B. ephippiatus*	Mexico	BBPUE193	19.271	-98.078	2987	+		+
93356	*B. ephippiatus*	Mexico	BBPUE193	19.27065	-98.07847	2987	+		
93358	*B. ephippiatus*	Mexico	BBPUE193	19.27065	-98.07847	2987	+		
93362	*B. ephippiatus*	Mexico	BBPUE193	19.27065	-98.07847	2987	+		
93363	*B. ephippiatus*	Mexico	BBPUE193	19.27065	-98.07847	2987	+		
93452	*B. ephippiatus*	Mexico	BBPUE214	19.07832	-98.57484	3065	+		
93457	*B. ephippiatus*	Mexico	BBPUE214	19.078	-98.575	3065	+		+
93458	*B. ephippiatus*	Mexico	BBPUE214	19.078	-98.575	3065	+		+
93460	*B. ephippiatus*	Mexico	BBPUE214	19.07832	-98.57484	3065	+		
93462	*B. ephippiatus*	Mexico	BBPUE214	19.07832	-98.57484	3065	+		
93464	*B. ephippiatus*	Mexico	BBPUE214	19.07832	-98.57484	3065	+		

Table 1.1 (cont.)

Voucher Name	Phenotype	Country	Population	Latitude	Longitude	Altitude	MSAT	COI	WING
93465	*B. ephippiatus*	Mexico	BBPUE214	19.078	-98.575	3065	+		+
93467	*B. ephippiatus*	Mexico	BBPUE214	19.078	-98.575	3065	+		+
93469	*B. ephippiatus*	Mexico	BBPUE214	19.07832	-98.57484	3065	+		
93470	*B. ephippiatus*	Mexico	BBPUE214	19.07832	-98.57484	3065	+		
93471	*B. ephippiatus*	Mexico	BBPUE214	19.07832	-98.57484	3065	+		
93472	*B. ephippiatus*	Mexico	BBPUE214	19.07832	-98.57484	3065	+		
93473	*B. ephippiatus*	Mexico	BBPUE214	19.078	-98.575	3065	+		+
93474	*B. ephippiatus*	Mexico	BBPUE214	19.07832	-98.57484	3065	+		
93475	*B. ephippiatus*	Mexico	BBPUE214	19.07832	-98.57484	3065	+		
93476	*B. ephippiatus*	Mexico	BBPUE214	19.07832	-98.57484	3065	+		
93478	*B. ephippiatus*	Mexico	BBPUE214	19.07832	-98.57484	3065	+		
93479	*B. ephippiatus*	Mexico	BBPUE214	19.07832	-98.57484	3065	+		
93480	*B. ephippiatus*	Mexico	BBPUE214	19.07832	-98.57484	3065	+		
93635	*B. ephippiatus*	Mexico	BBPUE081	19.85492	-97.58496	1836	+		
93638	*B. ephippiatus*	Mexico	BBPUE081	19.855	-97.585	1836	+		+
93640	*B. ephippiatus*	Mexico	BBPUE081	19.85492	-97.58496	1836	+		
93641	*B. ephippiatus*	Mexico	BBPUE081	19.85492	-97.58496	1836	+		
93642	*B. ephippiatus*	Mexico	BBPUE081	19.85492	-97.58496	1836	+		
93643	*B. ephippiatus*	Mexico	BBPUE081	19.85492	-97.58496	1836	+		
93644	*B. ephippiatus*	Mexico	BBPUE081	19.855	-97.585	1836	+		+
93646	*B. ephippiatus*	Mexico	BBPUE081	19.855	-97.585	1836	+		+
93647	*B. ephippiatus*	Mexico	BBPUE082	19.83285	-97.57095	2103	+		
93648	*B. ephippiatus*	Mexico	BBPUE082	19.83285	-97.57095	2103	+		
93649	*B. ephippiatus*	Mexico	BBPUE082	19.83285	-97.57095	2103	+		
93650	*B. ephippiatus*	Mexico	BBPUE082	19.83285	-97.57095	2103	+		
93651	*B. ephippiatus*	Mexico	BBPUE082	19.83285	-97.57095	2103	+		
93652	*B. ephippiatus*	Mexico	BBPUE082	19.83285	-97.57095	2103	+		

Table 1.1 (cont.)

Voucher Name	Phenotype	Country	Population	Latitude	Longitude	Altitude	MSAT	COI	WING
93653	*B. ephippiatus*	Mexico	BBPUE082	19.83285	-97.57095	2103	+		
93654	*B. ephippiatus*	Mexico	BBPUE082	19.833	-97.571	2103	+		+
93655	*B. ephippiatus*	Mexico	BBPUE082	19.83285	-97.57095	2103	+		
93656	*B. ephippiatus*	Mexico	BBPUE082	19.83285	-97.57095	2103	+		
93657	*B. ephippiatus*	Mexico	BBPUE082	19.833	-97.571	2103	+		+
93658	*B. ephippiatus*	Mexico	BBPUE082	19.83285	-97.57095	2103	+		
93706	*B. ephippiatus*	Mexico	BBPUE111	19.81491	-97.76472	2043	+		
93708	*B. ephippiatus*	Mexico	BBPUE112	19.80473	-97.79343	2051	+		
93709	*B. ephippiatus*	Mexico	BBPUE112	19.80473	-97.79343	2051	+		
93710	*B. ephippiatus*	Mexico	BBPUE112	19.80473	-97.79343	2051	+		
93711	*B. ephippiatus*	Mexico	BBPUE112	19.80473	-97.79343	2051	+		
93712	*B. ephippiatus*	Mexico	BBPUE112	19.80473	-97.79343	2051	+		
93713	*B. ephippiatus*	Mexico	BBPUE112	19.80473	-97.79343	2051	+		
93714	*B. ephippiatus*	Mexico	BBPUE112	19.805	-97.793	2051	+		+
93715	*B. ephippiatus*	Mexico	BBPUE112	19.805	-97.793	2051	+		+
93716	*B. ephippiatus*	Mexico	BBPUE112	19.805	-97.793	2051	+		+
93717	*B. ephippiatus*	Mexico	BBPUE112	19.80473	-97.79343	2051	+		
93720	*B. ephippiatus*	Mexico	BBPUE112	19.80473	-97.79343	2051	+		
93721	*B. ephippiatus*	Mexico	BBPUE112	19.80473	-97.79343	2051	+		
93722	*B. ephippiatus*	Mexico	BBPUE112	19.80473	-97.79343	2051	+		
93724	*B. ephippiatus*	Mexico	BBPUE112	19.80473	-97.79343	2051	+		
93725	*B. ephippiatus*	Mexico	BBPUE112	19.80473	-97.79343	2051	+		
93726	*B. ephippiatus*	Mexico	BBPUE112	19.805	-97.793	2051	+		+
93727	*B. ephippiatus*	Mexico	BBPUE112	19.805	-97.793	2051	+		+
93728	*B. ephippiatus*	Mexico	BBPUE112	19.80473	-97.79343	2051	+		
93731	*B. ephippiatus*	Mexico	BBPUE112	19.80473	-97.79343	2051	+		
93872	*B. ephippiatus*	Mexico	BBPUE141	20.36246	-98.39787	2226	+		

Table 1.1 (cont.)

Voucher Name	Phenotype	Country	Population	Latitude	Longitude	Altitude	MSAT	COI	WING
93873	*B. ephippiatus*	Mexico	BBPUE141	20.36246	-98.39787	2226	+		
93874	*B. ephippiatus*	Mexico	BBPUE141	20.36246	-98.39787	2226	+		
93875	*B. ephippiatus*	Mexico	BBPUE141	20.36246	-98.39787	2226	+		
93876	*B. ephippiatus*	Mexico	BBPUE141	20.36246	-98.39787	2226	+		
93877	*B. ephippiatus*	Mexico	BBPUE141	20.36246	-98.39787	2226	+		
93878	*B. ephippiatus*	Mexico	BBPUE141	20.36246	-98.39787	2226	+		
93879	*B. ephippiatus*	Mexico	BBPUE141	20.362	-98.398	2226	+		+
93881	*B. ephippiatus*	Mexico	BBPUE141	20.362	-98.398	2226	+		+
93882	*B. ephippiatus*	Mexico	BBPUE141	20.36246	-98.39787	2226	+		
93889	*B. ephippiatus*	Mexico	BBPUE142	20.33596	-98.40122	2155	+		
93890	*B. ephippiatus*	Mexico	BBPUE142	20.33596	-98.40122	2155	+		
93893	*B. ephippiatus*	Mexico	BBPUE143	20.38706	-98.37212	2067	+		
93894	*B. ephippiatus*	Mexico	BBPUE143	20.38706	-98.37212	2067	+		
93895	*B. ephippiatus*	Mexico	BBPUE143	20.38706	-98.37212	2067	+		
93896	*B. ephippiatus*	Mexico	BBPUE143	20.387	-98.372	2067	+		+
93897	*B. ephippiatus*	Mexico	BBPUE143	20.387	-98.372	2067	+		+
93898	*B. ephippiatus*	Mexico	BBPUE143	20.38706	-98.37212	2067	+		
93899	*B. ephippiatus*	Mexico	BBPUE143	20.38706	-98.37212	2067	+		
93902	*B. ephippiatus*	Mexico	BBPUE143	20.387	-98.372	2067	+		+
94089	*B. ephippiatus*	Mexico	BBPUE201	20.21245	-98.69215	2551	+		
94090	*B. ephippiatus*	Mexico	BBPUE201	20.21245	-98.69215	2551	+		
94091	*B. ephippiatus*	Mexico	BBPUE201	20.21245	-98.69215	2551	+		
94101	*B. ephippiatus*	Mexico	BBPUE201	20.212	-98.692	2551	+		+
94102	*B. ephippiatus*	Mexico	BBPUE201	20.21245	-98.69215	2551	+		
94116	*B. ephippiatus*	Mexico	BBPUE201	20.21245	-98.69215	2551	+		
94117	*B. ephippiatus*	Mexico	BBPUE201	20.21245	-98.69215	2551	+		
94118	*B. ephippiatus*	Mexico	BBPUE201	20.21245	-98.69215	2551	+		

Table 1.1 (cont.)

Voucher Name	Phenotype	Country	Population	Latitude	Longitude	Altitude	MSAT	COI	WING
94121	*B. ephippiatus*	Mexico	BBPUE202	20.20469	-98.66502	2320	+		
94123	*B. ephippiatus*	Mexico	BBPUE202	20.20469	-98.66502	2320	+		
94125	*B. ephippiatus*	Mexico	BBPUE203	20.21854	-98.73955	2356	+		
94126	*B. ephippiatus*	Mexico	BBPUE203	20.21854	-98.73955	2356	+		
94127	*B. ephippiatus*	Mexico	BBPUE203	20.21854	-98.73955	2356	+		
94129	*B. ephippiatus*	Mexico	BBPUE203	20.219	-98.74	2356	+		+
94130	*B. ephippiatus*	Mexico	BBPUE203	20.21854	-98.73955	2356	+		
94131	*B. ephippiatus*	Mexico	BBPUE203	20.219	-98.74	2356	+		+
94134	*B. ephippiatus*	Mexico	BBPUE204	20.18645	-98.74992	2880	+		
94135	*B. ephippiatus*	Mexico	BBPUE204	20.18645	-98.74992	2880	+		
94174	*B. ephippiatus*	Mexico	BBPUE012	18.47984	-97.13905	2499	+		
94175	*B. ephippiatus*	Mexico	BBPUE012	18.47984	-97.13905	2499	+		
94176	*B. ephippiatus*	Mexico	BBPUE012	18.47984	-97.13905	2499	+		
94177	*B. ephippiatus*	Mexico	BBPUE012	18.48	-97.139	2499	+		+
94181	*B. ephippiatus*	Mexico	BBPUE013	18.45465	-97.11639	2563	+		
94183	*B. ephippiatus*	Mexico	BBPUE013	18.45465	-97.11639	2563	+		
94291	*B. ephippiatus*	Mexico	BBPUE013	18.45465	-97.11639	2563	+		
94292	*B. ephippiatus*	Mexico	BBPUE013	18.45465	-97.11639	2563	+		
94293	*B. ephippiatus*	Mexico	BBPUE013	18.45465	-97.11639	2563	+		
94949	*B. ephippiatus*	Mexico	BBJAL161	19.50125	101.83519	2137	+		
94950	*B. ephippiatus*	Mexico	BBJAL162	19.50682	101.8279	2300	+		
94951	*B. ephippiatus*	Mexico	BBJAL162	19.50682	101.8279	2300	+		
94952	*B. ephippiatus*	Mexico	BBJAL162	19.50682	101.8279	2300	+		
94953	*B. ephippiatus*	Mexico	BBJAL162	19.50682	-101.8279	2300	+		
94954	*B. ephippiatus*	Mexico	BBJAL162	19.50682	-101.8279	2300	+		
94955	*B. ephippiatus*	Mexico	BBJAL162	19.507	-101.828	2300	+		+
94956	*B. ephippiatus*	Mexico	BBJAL162	19.507	-101.828	2300	+		+

Table 1.1 (cont.)

Voucher Name	Phenotype	Country	Population	Latitude	Longitude	Altitude	MSAT	COI	WING
94965	*B. ephippiatus*	Mexico	BBJAL163	19.49071	101.79509	2365	+		
94966	*B. ephippiatus*	Mexico	BBJAL163	19.49071	101.79509	2365	+		
94967	*B. ephippiatus*	Mexico	BBJAL163	19.49071	101.79509	2365	+		
94968	*B. ephippiatus*	Mexico	BBJAL163	19.491	-101.795	2365	+		+
94969	*B. ephippiatus*	Mexico	BBJAL163	19.49071	-101.79509	2365	+		
94970	*B. ephippiatus*	Mexico	BBJAL163	19.49071	-101.79509	2365	+		
94979	*B. ephippiatus*	Mexico	BBJAL164	19.50963	101.81342	2416	+		
94980	*B. ephippiatus*	Mexico	BBJAL164	19.50963	101.81342	2416	+		
94981	*B. ephippiatus*	Mexico	BBJAL164	19.50963	101.81342	2416	+		
94982	*B. ephippiatus*	Mexico	BBJAL164	19.51	-101.813	2416	+		+
94983	*B. ephippiatus*	Mexico	BBJAL164	19.50963	-101.81342	2416	+		
94984	*B. ephippiatus*	Mexico	BBJAL164	19.51	101.813	2416	+		+
95114	*B. ephippiatus*	Mexico	BBJAL151	19.38259	102.33641	2619	+		
95115	*B. ephippiatus*	Mexico	BBJAL151	19.38259	102.33641	2619	+		
95116	*B. ephippiatus*	Mexico	BBJAL151	19.38259	102.33641	2619	+		
95118	*B. ephippiatus*	Mexico	BBJAL152	19.36362	102.34437	2358	+		
95120	*B. ephippiatus*	Mexico	BBJAL152	19.36362	102.34437	2358	+		
95122	*B. ephippiatus*	Mexico	BBJAL152	19.364	-102.344	2358	+		+
95123	*B. ephippiatus*	Mexico	BBJAL152	19.36362	-102.34437	2358	+		
95124	*B. ephippiatus*	Mexico	BBJAL152	19.364	-102.344	2358	+		+
95125	*B. ephippiatus*	Mexico	BBJAL152	19.36362	-102.34437	2358	+		
95133	*B. ephippiatus*	Mexico	BBJAL153	19.3681	102.36614	2207	+		
95134	*B. ephippiatus*	Mexico	BBJAL153	19.3681	102.36614	2207	+		
95135	*B. ephippiatus*	Mexico	BBJAL153	19.3681	102.36614	2207	+		
95137	*B. ephippiatus*	Mexico	BBJAL153	19.368	-102.366	2207	+		+
95138	*B. ephippiatus*	Mexico	BBJAL153	19.3681	-102.36614	2207	+		
95140	*B. ephippiatus*	Mexico	BBJAL153	19.368	-102.366	2207	+		+

Table 1.1 (cont.)

Voucher Name	Phenotype	Country	Population	Latitude	Longitude	Altitude	MSAT	COI	WING
95144	*B. ephippiatus*	Mexico	BBJAL154	19.38987	102.37088	2446	+		
95145	*B. ephippiatus*	Mexico	BBJAL154	19.38987	102.37088	2446	+		
95146	*B. ephippiatus*	Mexico	BBJAL154	19.38987	102.37088	2446	+		
95148	*B. ephippiatus*	Mexico	BBJAL154	19.38987	-102.37088	2446	+		
95225	*B. ephippiatus*	Mexico	BBJAL154	19.39	-102.371	2446	+		+
95392	*B. ephippiatus*	Mexico	BBJAL111	19.90008	103.0095	2341	+		
95393	*B. ephippiatus*	Mexico	BBJAL111	19.90008	103.0095	2341	+		
95394	*B. ephippiatus*	Mexico	BBJAL111	19.90008	103.0095	2341	+		
95395	*B. ephippiatus*	Mexico	BBJAL111	19.90008	-103.0095	2341	+		
95397	*B. ephippiatus*	Mexico	BBJAL111	19.9	-103.01	2341	+		+
95398	*B. ephippiatus*	Mexico	BBJAL111	19.90008	-103.0095	2341	+		
95399	*B. ephippiatus*	Mexico	BBJAL111	19.90008	-103.0095	2341	+		
95400	*B. ephippiatus*	Mexico	BBJAL111	19.90008	-103.0095	2341	+		
95403	*B. ephippiatus*	Mexico	BBJAL111	19.90008	-103.0095	2341	+		
95404	*B. ephippiatus*	Mexico	BBJAL111	19.9	-103.01	2341	+		+
95405	*B. ephippiatus*	Mexico	BBJAL111	19.90008	-103.0095	2341	+		
95414	*B. ephippiatus*	Mexico	BBJAL112	19.87192	103.00435	2448	+		
95415	*B. ephippiatus*	Mexico	BBJAL112	19.87192	103.00435	2448	+		
95416	*B. ephippiatus*	Mexico	BBJAL112	19.87192	103.00435	2448	+		
95417	*B. ephippiatus*	Mexico	BBJAL112	19.872	-103.004	2448	+		+
95426	*B. ephippiatus*	Mexico	BBJAL113	19.84026	103.00011	2181	+		
95427	*B. ephippiatus*	Mexico	BBJAL113	19.84026	103.00011	2181	+		
95428	*B. ephippiatus*	Mexico	BBJAL113	19.84026	103.00011	2181	+		
95429	*B. ephippiatus*	Mexico	BBJAL113	19.84	-103	2181	+		+
95493	*B. ephippiatus*	Mexico	BBJAL113	19.84026	-103.00011	2181	+		
95789	*B. ephippiatus*	Mexico	BBJAL022	19.611	-103.566	2524	+		+
95790	*B. ephippiatus*	Mexico	BBJAL022	19.61094	-103.56602	2524	+		

Table 1.1 (cont.)

Voucher Name	Phenotype	Country	Population	Latitude	Longitude	Altitude	MSAT	COI	WING
95791	*B. ephippiatus*	Mexico	BBJAL022	19.61094	-103.56602	2524	+		
95793	*B. ephippiatus*	Mexico	BBJAL022	19.611	-103.566	2524	+		+
95800	*B. ephippiatus*	Mexico	BBJAL022	19.61094	-103.56602	2524	+		
95803	*B. ephippiatus*	Mexico	BBJAL022	19.611	-103.566	2524	+		+
95805	*B. ephippiatus*	Mexico	BBJAL023	19.602	-103.579	3028	+		+
95817	*B. ephippiatus*	Mexico	BBJAL024	19.583	-103.605	3520	+		+
95978	*B. ephippiatus*	Mexico	BBJAL101	20.11764	103.59927	2287	+		
95979	*B. ephippiatus*	Mexico	BBJAL101	20.118	-103.599	2287	+		+
95980	*B. ephippiatus*	Mexico	BBJAL101	20.11764	103.59927	2287	+		
95981	*B. ephippiatus*	Mexico	BBJAL101	20.118	-103.599	2287	+		+
95982	*B. ephippiatus*	Mexico	BBJAL101	20.11764	103.59927	2287	+		
95983	*B. ephippiatus*	Mexico	BBJAL101	20.11764	103.59927	2287	+		
95986	*B. ephippiatus*	Mexico	BBJAL101	20.11764	103.59927	2287	+		
95999	*B. ephippiatus*	Mexico	BBJAL102	20.09508	103.61578	2597	+		
96000	*B. ephippiatus*	Mexico	BBJAL102	20.09508	-103.61578	2597	+		
96001	*B. ephippiatus*	Mexico	BBJAL102	20.09508	103.61578	2597	+		
96002	*B. ephippiatus*	Mexico	BBJAL102	20.095	-103.616	2597	+		+
96003	*B. ephippiatus*	Mexico	BBJAL102	20.09508	-103.61578	2597	+		
96004	*B. ephippiatus*	Mexico	BBJAL102	20.095	-103.616	2597	+		+
96005	*B. ephippiatus*	Mexico	BBJAL102	20.095	-103.616	2597	+		+
96008	*B. ephippiatus*	Mexico	BBJAL103	20.09732	103.6415	2668	+		
96013	*B. ephippiatus*	Mexico	BBJAL103	20.09732	103.6415	2668	+		
96014	*B. ephippiatus*	Mexico	BBJAL103	20.09732	103.6415	2668	+		
96015	*B. ephippiatus*	Mexico	BBJAL103	20.09732	103.6415	2668	+		
96022	*B. ephippiatus*	Mexico	BBJAL104	20.09843	103.6666	2533	+		
96023	*B. ephippiatus*	Mexico	BBJAL104	20.09843	103.6666	2533	+		
96254	*B. ephippiatus*	Mexico	BBJAL051	20.62531	104.72578	2004	+		

Table 1.1 (cont.)

Voucher Name	Phenotype	Country	Population	Latitude	Longitude	Altitude	MSAT	COI	WING
96255	*B. ephippiatus*	Mexico	BBJAL051	20.62531	104.72578	2004	+		
96256	*B. ephippiatus*	Mexico	BBJAL051	20.62531	104.72578	2004	+		
96258	*B. ephippiatus*	Mexico	BBJAL051	20.625	-104.726	2004	+		+
96259	*B. ephippiatus*	Mexico	BBJAL051	20.625	-104.726	2004	+		+
96263	*B. ephippiatus*	Mexico	BBJAL051	20.625	-104.726	2004	+		+
96267	*B. ephippiatus*	Mexico	BBJAL051	20.625	-104.726	2004	+		+
96268	*B. ephippiatus*	Mexico	BBJAL051	20.62531	-104.72578	2004	+		
96274	*B. ephippiatus*	Mexico	BBJAL052	20.60395	104.71072	2262	+		
96275	*B. ephippiatus*	Mexico	BBJAL052	20.60395	104.71072	2262	+		
96276	*B. ephippiatus*	Mexico	BBJAL052	20.60395	104.71072	2262	+		
96302	*B. ephippiatus*	Mexico	BBJAL053	20.65091	104.65725	2290	+		
96303	*B. ephippiatus*	Mexico	BBJAL053	20.65091	104.65725	2290	+		
96307	*B. ephippiatus*	Mexico	BBJAL054	20.5957	104.75322	1580	+		
96410	*B. ephippiatus*	Mexico	BBJAL041	20.69893	104.85777	2179	+		
96411	*B. ephippiatus*	Mexico	BBJAL041	20.69893	104.85777	2179	+		
96414	*B. ephippiatus*	Mexico	BBJAL042	20.7016	104.8381	2306	+		
96415	*B. ephippiatus*	Mexico	BBJAL042	20.7016	104.8381	2306	+		
96416	*B. ephippiatus*	Mexico	BBJAL042	20.7016	104.8381	2306	+		
96422	*B. ephippiatus*	Mexico	BBJAL042	20.7016	-104.8381	2306	+		+
96430	*B. ephippiatus*	Mexico	BBJAL043	20.73571	-104.81548	2244	+		
96431	*B. ephippiatus*	Mexico	BBJAL043	20.73571	104.81548	2244	+		
96432	*B. ephippiatus*	Mexico	BBJAL043	20.73571	104.81548	2244	+		
96433	*B. ephippiatus*	Mexico	BBJAL043	20.73571	-104.81548	2244	+		+
96435	*B. ephippiatus*	Mexico	BBJAL043	20.73571	-104.81548	2244	+		
96436	*B. ephippiatus*	Mexico	BBJAL043	20.73571	-104.81548	2244	+		
96456	*B. ephippiatus*	Mexico	BBJAL044	20.75388	104.83514	1568	+		
96457	*B. ephippiatus*	Mexico	BBJAL044	20.75388	104.83514	1568	+		

Table 1.1 (cont.)

Voucher Name	Phenotype	Country	Population	Latitude	Longitude	Altitude	MSAT	COI	WING
96458	*B. ephippiatus*	Mexico	BBJAL044	20.75388	104.83514	1568	+		
96459	*B. ephippiatus*	Mexico	BBJAL044	20.75388	-104.83514	1568	+		+
96460	*B. ephippiatus*	Mexico	BBJAL044	20.75388	-104.83514	1568	+		+
96461	*B. ephippiatus*	Mexico	BBJAL044	20.75388	-104.83514	1568	+		+
96462	*B. ephippiatus*	Mexico	BBJAL044	20.75388	-104.83514	1568	+		
96463	*B. ephippiatus*	Mexico	BBJAL044	20.75388	-104.83514	1568	+		
96465	*B. ephippiatus*	Mexico	BBJAL044	20.75388	-104.83514	1568	+		
96466	*B. ephippiatus*	Mexico	BBJAL044	20.75388	-104.83514	1568	+		
96527	*B. ephippiatus*	Mexico	BBJAL072	20.18601	104.71767	2179	+		
96547	*B. ephippiatus*	Mexico	BBJAL073	20.16791	104.71288	2119	+		
96548	*B. ephippiatus*	Mexico	BBJAL073	20.16791	104.71288	2119	+		
96549	*B. ephippiatus*	Mexico	BBJAL073	20.16791	104.71288	2119	+		
96550	*B. ephippiatus*	Mexico	BBJAL073	20.16791	-104.71288	2119	+		+
96553	*B. ephippiatus*	Mexico	BBJAL073	20.16791	104.71288	2119	+		
96554	*B. ephippiatus*	Mexico	BBJAL073	20.16791	-104.71288	2119	+		+
96555	*B. ephippiatus*	Mexico	BBJAL073	20.16791	-104.71288	2119	+		
96558	*B. ephippiatus*	Mexico	BBJAL073	20.16791	-104.71288	2119	+		
96560	*B. ephippiatus*	Mexico	BBJAL073	20.16791	-104.71288	2119	+		
96561	*B. ephippiatus*	Mexico	BBJAL073	20.16791	-104.71288	2119	+		
96562	*B. ephippiatus*	Mexico	BBJAL073	20.16791	-104.71288	2119	+		+
96564	*B. ephippiatus*	Mexico	BBJAL073	20.16791	-104.71288	2119	+		+
96565	*B. ephippiatus*	Mexico	BBJAL073	20.16791	-104.71288	2119	+		+
96569	*B. ephippiatus*	Mexico	BBJAL074	20.15719	104.67592	2313	+		
96572	*B. ephippiatus*	Mexico	BBJAL074	20.15719	104.67592	2313	+		
96653	*B. ephippiatus*	Mexico	BBJAL031	20.37491	104.97572	2036	+		
96654	*B. ephippiatus*	Mexico	BBJAL031	20.37491	104.97572	2036	+		
96655	*B. ephippiatus*	Mexico	BBJAL031	20.37491	104.97572	2036	+		

Table 1.1 (cont.)

Voucher Name	Phenotype	Country	Population	Latitude	Longitude	Altitude	MSAT	COI	WING
96656	*B. ephippiatus*	Mexico	BBJAL031	20.37491	-104.97572	2036	+		
96657	*B. ephippiatus*	Mexico	BBJAL031	20.37491	-104.97572	2036	+		
96658	*B. ephippiatus*	Mexico	BBJAL031	20.37491	-104.97572	2036	+		
96659	*B. ephippiatus*	Mexico	BBJAL031	20.37491	-104.97572	2036	+		
96660	*B. ephippiatus*	Mexico	BBJAL031	20.37491	-104.97572	2036	+		+
96661	*B. ephippiatus*	Mexico	BBJAL031	20.37491	-104.97572	2036	+		+
96662	*B. ephippiatus*	Mexico	BBJAL031	20.37491	-104.97572	2036	+		
96663	*B. ephippiatus*	Mexico	BBJAL031	20.37491	-104.97572	2036	+		+
96664	*B. ephippiatus*	Mexico	BBJAL031	20.37491	-104.97572	2036	+		
96665	*B. ephippiatus*	Mexico	BBJAL031	20.37491	-104.97572	2036	+		
96667	*B. ephippiatus*	Mexico	BBJAL031	20.37491	-104.97572	2036	+		
96668	*B. ephippiatus*	Mexico	BBJAL031	20.37491	-104.97572	2036	+		
96669	*B. ephippiatus*	Mexico	BBJAL031	20.37491	-104.97572	2036	+		+
96670	*B. ephippiatus*	Mexico	BBJAL031	20.37491	-104.97572	2036	+		
96674	*B. ephippiatus*	Mexico	BBJAL032	20.36005	-105	2483	+		
96675	*B. ephippiatus*	Mexico	BBJAL032	20.36005	-105	2483	+		
96676	*B. ephippiatus*	Mexico	BBJAL032	20.36005	-105	2483	+		
96907	*B. ephippiatus*	Mexico	BBJAL211	19.43785	-103.96143	2032	+		
96908	*B. ephippiatus*	Mexico	BBJAL211	19.43785	-103.96143	2032	+		
96909	*B. ephippiatus*	Mexico	BBJAL211	19.43785	-103.96143	2032	+		
96910	*B. ephippiatus*	Mexico	BBJAL211	19.43785	-103.96143	2032	+		+
96911	*B. ephippiatus*	Mexico	BBJAL211	19.43785	-103.96143	2032	+		+
96916	*B. ephippiatus*	Mexico	BBJAL212	19.43152	-103.93003	2148	+		
96917	*B. ephippiatus*	Mexico	BBJAL212	19.43152	-103.93003	2148	+		
96918	*B. ephippiatus*	Mexico	BBJAL212	19.43152	-103.93003	2148	+		
96920	*B. ephippiatus*	Mexico	BBJAL212	19.43152	-103.93003	2148	+		
96921	*B. ephippiatus*	Mexico	BBJAL212	19.43152	-103.93003	2148	+		+

Table 1.1 (cont.)

Voucher Name	Phenotype	Country	Population	Latitude	Longitude	Altitude	MSAT	COI	WING
96923	*B. ephippiatus*	Mexico	BBJAL213	19.43326	-103.89906		+		
96924	*B. ephippiatus*	Mexico	BBJAL213	19.43326	-103.89906		+		
96925	*B. ephippiatus*	Mexico	BBJAL213	19.43326	-103.89906		+		
96926	*B. ephippiatus*	Mexico	BBJAL213	19.43326	-103.89906		+		
96927	*B. ephippiatus*	Mexico	BBJAL213	19.43326	-103.89906		+		+
96933	*B. ephippiatus*	Mexico	BBJAL214	19.43984	-103.87894	2001	+		
96934	*B. ephippiatus*	Mexico	BBJAL214	19.43984	-103.87894	2001	+		
96935	*B. ephippiatus*	Mexico	BBJAL214	19.43984	-103.87894	2001	+		
96936	*B. ephippiatus*	Mexico	BBJAL214	19.43984	-103.87894	2001	+		
96937	*B. ephippiatus*	Mexico	BBJAL214	19.43984	-103.87894	2001	+		+
97183	*B. ephippiatus*	Mexico	BBOAX191	17.65104	-100.87428	1859	+		+
97184	*B. ephippiatus*	Mexico	BBOAX191	17.65104	-100.87428	1859	+		+
97185	*B. ephippiatus*	Mexico	BBOAX191	17.65104	-100.87428	1859	+		+
97189	*B. ephippiatus*	Mexico	BBOAX192	17.68741	-100.87179	2139	+		
97190	*B. ephippiatus*	Mexico	BBOAX192	17.68741	-100.87179	2139	+		+
97209	*B. ephippiatus*	Mexico	BBOAX194				+		+
97210	*B. ephippiatus*	Mexico	BBOAX194				+		
97275	*B. ephippiatus*	Mexico	BBOAX174	17.50831	-100.10748	2592	+		
97276	*B. ephippiatus*	Mexico	BBOAX174	17.50831	-100.10748	2592	+		
97277	*B. ephippiatus*	Mexico	BBOAX174	17.50831	-100.10748	2592	+		
97278	*B. ephippiatus*	Mexico	BBOAX174	17.50831	-100.10748	2592	+		
97532	*B. ephippiatus*	Mexico	BBOAX171	17.45474	-100.05516	2643	+		
97533	*B. ephippiatus*	Mexico	BBOAX172	17.46564	-100.08416	2889	+		
97534	*B. ephippiatus*	Mexico	BBOAX172	17.46564	-100.08416	2889	+		+
97535	*B. ephippiatus*	Mexico	BBOAX172	17.46564	-100.08416	2889	+		
97543	*B. ephippiatus*	Mexico	BBOAX173	17.48924	-100.09657	2589	+		
97544	*B. ephippiatus*	Mexico	BBOAX173	17.48924	-100.09657	2589	+		+

Table 1.1 (cont.)

Voucher Name	Phenotype	Country	Population	Latitude	Longitude	Altitude	MSAT	COI	WING
97545	*B. ephippiatus*	Mexico	BBOAX173	17.48924	-100.09657	2589	+		
97546	*B. ephippiatus*	Mexico	BBOAX173	17.48924	-100.09657	2589	+		+
97555	*B. ephippiatus*	Mexico	BBOAX173	17.48924	-100.09657	2589	+		
97556	*B. ephippiatus*	Mexico	BBOAX173	17.48924	-100.09657	2589	+		
97557	*B. ephippiatus*	Mexico	BBOAX173	17.48924	-100.09657	2589	+		
97564	*B. ephippiatus*	Mexico	BBOAX174	17.50831	-100.10748	2592	+		
97566	*B. ephippiatus*	Mexico	BBOAX174	17.50831	-100.10748	2592	+		
97567	*B. ephippiatus*	Mexico	BBOAX174	17.50831	-100.10748	2592	+		+
97727	*B. ephippiatus*	Mexico	BBOAX142	17.69348	-99.013445	2250	+		
97728	*B. ephippiatus*	Mexico	BBOAX142	17.69348	-99.013445	2250	+		
97729	*B. ephippiatus*	Mexico	BBOAX142	17.69348	-99.013445	2250	+		
97730	*B. ephippiatus*	Mexico	BBOAX142	17.69348	-99.013445	2250	+		+
97731	*B. ephippiatus*	Mexico	BBOAX142	17.69348	-99.013445	2250	+		
97732	*B. ephippiatus*	Mexico	BBOAX142	17.69348	-99.013445	2250	+		
97733	*B. ephippiatus*	Mexico	BBOAX142	17.69348	-99.013445	2250	+		
97735	*B. ephippiatus*	Mexico	BBOAX142	17.69348	-99.013445	2250	+		
97736	*B. ephippiatus*	Mexico	BBOAX142	17.69348	-99.013445	2250	+		
97737	*B. ephippiatus*	Mexico	BBOAX142	17.69348	-99.013445	2250	+		+
97738	*B. ephippiatus*	Mexico	BBOAX142	17.69348	-99.013445	2250	+		
97739	*B. ephippiatus*	Mexico	BBOAX142	17.69348	-99.013445	2250	+		+
97778	*B. ephippiatus*	Mexico	BBOAX121	17.50047	-98.78541	2237	+		
97779	*B. ephippiatus*	Mexico	BBOAX121	17.50047	-98.78541	2237	+		
97780	*B. ephippiatus*	Mexico	BBOAX121	17.50047	-98.78541	2237	+		
97782	*B. ephippiatus*	Mexico	BBOAX121	17.50047	-98.78541	2237	+	+	+
97783	*B. ephippiatus*	Mexico	BBOAX121	17.50047	-98.78541	2237	+		+
97784	*B. ephippiatus*	Mexico	BBOAX121	17.50047	-98.78541	2237	+		
97785	*B. ephippiatus*	Mexico	BBOAX121	17.50047	-98.78541	2237	+		

Table 1.1 (cont.)

Voucher Name	Phenotype	Country	Population	Latitude	Longitude	Altitude	MSAT	COI	WING
97786	*B. ephippiatus*	Mexico	BBOAX121	17.50047	-98.78541	2237	+		+
97787	*B. ephippiatus*	Mexico	BBOAX121	17.50047	-98.78541	2237	+		
97788	*B. ephippiatus*	Mexico	BBOAX121	17.50047	-98.78541	2237	+		
97789	*B. ephippiatus*	Mexico	BBOAX121	17.50047	-98.78541	2237	+		
97791	*B. ephippiatus*	Mexico	BBOAX121	17.50047	-98.78541	2237	+		
97792	*B. ephippiatus*	Mexico	BBOAX121	17.50047	-98.78541	2237	+		
97793	*B. ephippiatus*	Mexico	BBOAX121	17.50047	-98.78541	2237	+		
97816	*B. ephippiatus*	Mexico	BBOAX122	17.50172	-98.81459	2401	+		+
97817	*B. ephippiatus*	Mexico	BBOAX122	17.50172	-98.81459	2401	+		
97818	*B. ephippiatus*	Mexico	BBOAX122	17.50172	-98.81459	2401	+		+
97819	*B. ephippiatus*	Mexico	BBOAX122	17.50172	-98.81459	2401	+		
97838	*B. ephippiatus*	Mexico	BBOAX122	17.50172	-98.81459	2401	+		
97839	*B. ephippiatus*	Mexico	BBOAX122	17.50172	-98.81459	2401	+		
97868	*B. ephippiatus*	Mexico	BBOAX081	17.09341	-97.61556	2599	+		
97869	*B. ephippiatus*	Mexico	BBOAX081	17.09341	-97.61556	2599	+		
97870	*B. ephippiatus*	Mexico	BBOAX081	17.09341	-97.61556	2599	+	+	
97871	*B. ephippiatus*	Mexico	BBOAX081	17.09341	-97.61556	2599	+		+
97874	*B. ephippiatus*	Mexico	BBOAX081	17.09341	-97.61556	2599	+		
97886	*B. ephippiatus*	Mexico	BBOAX082	17.11315	-97.61062	2941	+		
97887	*B. ephippiatus*	Mexico	BBOAX082	17.11315	-97.61062	2941	+		
97888	*B. ephippiatus*	Mexico	BBOAX082	17.11315	-97.61062	2941	+		
97889	*B. ephippiatus*	Mexico	BBOAX082	17.11315	-97.61062	2941	+		+
97890	*B. ephippiatus*	Mexico	BBOAX082	17.11315	-97.61062	2941	+		
97903	*B. ephippiatus*	Mexico	BBOAX083	17.13285	-97.61788	3112	+		
97904	*B. ephippiatus*	Mexico	BBOAX083	17.13285	-97.61788	3112	+		+
97905	*B. ephippiatus*	Mexico	BBOAX083	17.13285	-97.61788	3112	+		
97906	*B. ephippiatus*	Mexico	BBOAX083	17.13285	-97.61788	3112	+		

Table 1.1 (cont.)

Voucher Name	Phenotype	Country	Population	Latitude	Longitude	Altitude	MSAT	COI	WING
97907	*B. ephippiatus*	Mexico	BBOAX083	17.13285	-97.61788	3112	+		+
97935	*B. ephippiatus*	Mexico	BBOAX084	17.15602	-97.625	2649	+		
97936	*B. ephippiatus*	Mexico	BBOAX084	17.15602	-97.625	2649	+		
97937	*B. ephippiatus*	Mexico	BBOAX084	17.15602	-97.625	2649	+		
97938	*B. ephippiatus*	Mexico	BBOAX084	17.15602	-97.625	2649	+		
97939	*B. ephippiatus*	Mexico	BBOAX084	17.15602	-97.625	2649	+		+
97971	*B. ephippiatus*	Mexico	BBOAX061	17.21384	-97.87483	2544	+		
97972	*B. ephippiatus*	Mexico	BBOAX061	17.21384	-97.87483	2544	+		
97973	*B. ephippiatus*	Mexico	BBOAX061	17.21384	-97.87483	2544	+		
97974	*B. ephippiatus*	Mexico	BBOAX061	17.21384	-97.87483	2544	+		+
97975	*B. ephippiatus*	Mexico	BBOAX061	17.21384	-97.87483	2544	+		+
97976	*B. ephippiatus*	Mexico	BBOAX061	17.21384	-97.87483	2544	+		
97977	*B. ephippiatus*	Mexico	BBOAX061	17.21384	-97.87483	2544	+		
98009	*B. ephippiatus*	Mexico	BBOAX062	17.19357	-97.86246	2419	+		
98010	*B. ephippiatus*	Mexico	BBOAX062	17.19357	-97.86246	2419	+		
98011	*B. ephippiatus*	Mexico	BBOAX062	17.19357	-97.86246	2419	+		
98012	*B. ephippiatus*	Mexico	BBOAX062	17.19357	-97.86246	2419	+		+
98013	*B. ephippiatus*	Mexico	BBOAX062	17.19357	-97.86246	2419	+		+
98020	*B. ephippiatus*	Mexico	BBOAX063	17.16852	-97.64682	2473	+		
98021	*B. ephippiatus*	Mexico	BBOAX063	17.16852	-97.64682	2473	+		
98022	*B. ephippiatus*	Mexico	BBOAX063	17.16852	-97.64682	2473	+		
98037	*B. ephippiatus*	Mexico	BBOAX064	17.18854	-97.80746	2439	+		
98038	*B. ephippiatus*	Mexico	BBOAX064	17.18854	-97.80746	2439	+		
98039	*B. ephippiatus*	Mexico	BBOAX064	17.18854	-97.80746	2439	+		
98040	*B. ephippiatus*	Mexico	BBOAX064	17.18854	-97.80746	2439	+		+
98041	*B. ephippiatus*	Mexico	BBOAX064	17.18854	-97.80746	2439	+		
98089	*B. ephippiatus*	Mexico	BBOAX101	16.15408	-96.49549	2438	+		

Table 1.1 (cont.)

Voucher Name	Phenotype	Country	Population	Latitude	Longitude	Altitude	MSAT	COI	WING
98090	*B. ephippiatus*	Mexico	BBOAX101	16.15408	-96.49549	2438	+		
98091	*B. ephippiatus*	Mexico	BBOAX101	16.15408	-96.49549	2438	+		
98092	*B. ephippiatus*	Mexico	BBOAX101	16.15408	-96.49549	2438	+		
98093	*B. ephippiatus*	Mexico	BBOAX101	16.15408	-96.49549	2438	+	+	+
98094	*B. ephippiatus*	Mexico	BBOAX101	16.15408	-96.49549	2438	+		
98095	*B. ephippiatus*	Mexico	BBOAX101	16.15408	-96.49549	2438	+		+
98098	*B. ephippiatus*	Mexico	BBOAX102	16.18904	-96.51511	2387	+		
98099	*B. ephippiatus*	Mexico	BBOAX102	16.18904	-96.51511	2387	+		
98100	*B. ephippiatus*	Mexico	BBOAX102	16.18904	-96.51511	2387	+		
98107	*B. ephippiatus*	Mexico	BBOAX102	16.18904	-96.51511	2387	+		+
98124	*B. ephippiatus*	Mexico	BBOAX102	16.18904	-96.51511	2387	+		
98125	*B. ephippiatus*	Mexico	BBOAX102	16.18904	-96.51511	2387	+		+
98126	*B. ephippiatus*	Mexico	BBOAX102	16.18904	-96.51511	2387	+		
98159	*B. ephippiatus*	Mexico	BBOAX103	16.21267	-96.52859	2420	+		
98160	*B. ephippiatus*	Mexico	BBOAX103	16.21267	-96.52859	2420	+		
98161	*B. ephippiatus*	Mexico	BBOAX103	16.21267	-96.52859	2420	+		
98171	*B. ephippiatus*	Mexico	BBOAX103	16.21267	-96.52859	2420	+		
98172	*B. ephippiatus*	Mexico	BBOAX103	16.21267	-96.52859	2420	+		+
98173	*B. ephippiatus*	Mexico	BBOAX103	16.21267	-96.52859	2420	+		
98225	*B. ephippiatus*	Mexico	BBOAX223	16.14865	-96.36588	2804	+		
98226	*B. ephippiatus*	Mexico	BBOAX223	16.14865	-96.36588	2804	+		
98227	*B. ephippiatus*	Mexico	BBOAX223	16.14865	-96.36588	2804	+		
98228	*B. ephippiatus*	Mexico	BBOAX223	16.14865	-96.36588	2804	+		+
98229	*B. ephippiatus*	Mexico	BBOAX223	16.14865	-96.36588	2804	+		
98270	*B. ephippiatus*	Mexico	BBOAX222	16.19076	-96.39581	2674	+		
98271	*B. ephippiatus*	Mexico	BBOAX222	16.19076	-96.39581	2674	+		+
98272	*B. ephippiatus*	Mexico	BBOAX222	16.19076	-96.39581	2674	+		+

Table 1.1 (cont.)

Voucher Name	Phenotype	Country	Population	Latitude	Longitude	Altitude	MSAT	COI	WING
98277	*B. ephippiatus*	Mexico	BBOAX222	16.19076	-96.39581	2674	+		+
102880	*B. ephippiatus*	Mexico	BBPUE204	20.18645	-98.74992	2880	+		+
102890	*B. ephippiatus*	Mexico	BBPUE201	20.21245	-98.69215	2551	+	+	+
103658	*B. ephippiatus*	Mexico	BBNLE211	24.89264	-100.18502	2059	+	+	
103659	*B. ephippiatus*	Mexico	BBNLE211	24.89264	-100.18502	2059	+		
103787	*B. ephippiatus*	Mexico	BBNLE231	24.45746	-99.97533	2302	+	+	
103788	*B. ephippiatus*	Mexico	BBNLE231	24.45746	-99.97533	2302	+		
103804	*B. ephippiatus*	Mexico	BBNLE231	24.45746	-99.97533	2302	+		
104211	*B. ephippiatus*	Mexico	BBNLE252	23.86574	-99.82588	2610	+		
104221	*B. ephippiatus*	Mexico	BBNLE253	23.84438	-99.84843	2685	+		
104222	*B. ephippiatus*	Mexico	BBNLE253	23.84438	-99.84843	2685	+		
104223	*B. ephippiatus*	Mexico	BBNLE253	23.84438	-99.84843	2685	+		
104224	*B. ephippiatus*	Mexico	BBNLE253	23.84438	-99.84843	2685	+		+
104388	*B. ephippiatus*	Mexico	BBNLE281	23.01414	-99.28081	1477	+		
104389	*B. ephippiatus*	Mexico	BBNLE281	23.01414	-99.28081	1477	+		
104390	*B. ephippiatus*	Mexico	BBNLE281	23.01414	-99.28081	1477	+		
104391	*B. ephippiatus*	Mexico	BBNLE281	23.01414	-99.28081	1477	+	+	+
104393	*B. ephippiatus*	Mexico	BBNLE281	23.01414	-99.28081	1477	+		
104394	*B. ephippiatus*	Mexico	BBNLE281	23.01414	-99.28081	1477	+		
104396	*B. ephippiatus*	Mexico	BBNLE281	23.01414	-99.28081	1477	+		+
104400	*B. ephippiatus*	Mexico	BBNLE281	23.01414	-99.28081	1477	+		
104402	*B. ephippiatus*	Mexico	BBNLE282	23.03392	-99.2766	1636	+		
104403	*B. ephippiatus*	Mexico	BBNLE282	23.03392	-99.2766	1636	+		
104404	*B. ephippiatus*	Mexico	BBNLE282	23.03392	-99.2766	1636	+		
104405	*B. ephippiatus*	Mexico	BBNLE283	23.0471	-99.25472	1651	+		
104406	*B. ephippiatus*	Mexico	BBNLE283	23.0471	-99.25472	1651	+		
104407	*B. ephippiatus*	Mexico	BBNLE283	23.0471	-99.25472	1651	+		+

Table 1.1 (cont.)

Voucher Name	Phenotype	Country	Population	Latitude	Longitude	Altitude	MSAT	COI	WING
104408	*B. ephippiatus*	Mexico	BBNLE283	23.0471	-99.25472	1651	+		
104409	*B. ephippiatus*	Mexico	BBNLE283	23.0471	-99.25472	1651	+		+
104410	*B. ephippiatus*	Mexico	BBNLE283	23.0471	-99.25472	1651	+		
104411	*B. ephippiatus*	Mexico	BBNLE283	23.0471	-99.25472	1651	+		
104412	*B. ephippiatus*	Mexico	BBNLE283	23.0471	-99.25472	1651	+		+
104414	*B. ephippiatus*	Mexico	BBNLE283	23.0471	-99.25472	1651	+		
104481	*B. ephippiatus*	Mexico	BBSLP321	21.98248	-99.47355	1305	+		
104482	*B. ephippiatus*	Mexico	BBSLP321	21.98248	-99.47355	1305	+		
104483	*B. ephippiatus*	Mexico	BBSLP321	21.98248	-99.47355	1305	+		
104484	*B. ephippiatus*	Mexico	BBSLP321	21.98248	-99.47355	1305	+		
104489	*B. ephippiatus*	Mexico	BBSLP321	21.98248	-99.47355	1305	+		
104490	*B. ephippiatus*	Mexico	BBSLP321	21.98248	-99.47355	1305	+		+
104499	*B. ephippiatus*	Mexico	BBSLP321	21.98248	-99.47355	1305	+		
104500	*B. ephippiatus*	Mexico	BBSLP321	21.98248	-99.47355	1305	+		+
104502	*B. ephippiatus*	Mexico	BBSLP321	21.98248	-99.47355	1305	+		+
104529	*B. ephippiatus*	Mexico	BBSLP322	22.00349	-99.49312	1353	+		
104537	*B. ephippiatus*	Mexico	BBSLP322	22.00349	-99.49312	1353	+		
104538	*B. ephippiatus*	Mexico	BBSLP322	22.00349	-99.49312	1353	+		
104539	*B. ephippiatus*	Mexico	BBSLP322	22.00349	-99.49312	1353	+		+
104540	*B. ephippiatus*	Mexico	BBSLP322	22.00349	-99.49312	1353	+		+
104541	*B. ephippiatus*	Mexico	BBSLP322	22.00349	-99.49312	1353	+		
104542	*B. ephippiatus*	Mexico	BBSLP322	22.00349	-99.49312	1353	+		
104548	*B. ephippiatus*	Mexico	BBSLP322	22.00349	-99.49312	1353	+		
104562	*B. ephippiatus*	Mexico	BBSLP323	22.0218	-99.5149	1331	+		
104563	*B. ephippiatus*	Mexico	BBSLP323	22.0218	-99.5149	1331	+		
104576	*B. ephippiatus*	Mexico	BBSLP325	22.0463	-99.50702	1436	+		
104759	*B. ephippiatus*	Mexico	BBSLP341	21.11976	-99.66409	2640	+		

Table 1.1 (cont.)

Voucher Name	Phenotype	Country	Population	Latitude	Longitude	Altitude	MSAT	COI	WING
104760	*B. ephippiatus*	Mexico	BBSLP341	21.11976	-99.66409	2640	+		
104761	*B. ephippiatus*	Mexico	BBSLP341	21.11976	-99.66409	2640	+		
104769	*B. ephippiatus*	Mexico	BBSLP342	21.12629	-99.63838	2594	+		
104770	*B. ephippiatus*	Mexico	BBSLP341	21.11976	-99.66409	2640	+		
104771	*B. ephippiatus*	Mexico	BBSLP341	21.11976	-99.66409	2640	+		
104786	*B. ephippiatus*	Mexico	BBSLP342	21.12629	-99.63838	2594	+		+
104792	*B. ephippiatus*	Mexico	BBSLP343	21.14558	-99.61848	2240	+		
104793	*B. ephippiatus*	Mexico	BBSLP343	21.14558	-99.61848	2240	+		
104795	*B. ephippiatus*	Mexico	BBSLP343	21.14558	-99.61848	2240	+		
104804	*B. ephippiatus*	Mexico	BBSLP343	21.14558	-99.61848	2240	+		
104805	*B. ephippiatus*	Mexico	BBSLP343	21.14558	-99.61848	2240	+		
104806	*B. ephippiatus*	Mexico	BBSLP343	21.14558	-99.61848	2240	+		
104867	*B. ephippiatus*	Mexico	BBSLP351	21.37403	-99.06444	1360	+		
104868	*B. ephippiatus*	Mexico	BBSLP351	21.37403	-99.06444	1360	+		
104869	*B. ephippiatus*	Mexico	BBSLP351	21.37403	-99.06444	1360	+		
104870	*B. ephippiatus*	Mexico	BBSLP351	21.37403	-99.06444	1360	+		
104871	*B. ephippiatus*	Mexico	BBSLP351	21.37403	-99.06444	1360	+		
104872	*B. ephippiatus*	Mexico	BBSLP351	21.37403	-99.06444	1360	+		
104873	*B. ephippiatus*	Mexico	BBSLP351	21.37403	-99.06444	1360	+		+
104884	*B. ephippiatus*	Mexico	BBSLP351	21.37403	-99.06444	1360	+		+
104885	*B. ephippiatus*	Mexico	BBSLP351	21.37403	-99.06444	1360	+		
104903	*B. ephippiatus*	Mexico	BBSLP352	21.33348	-99.08237	1356	+		
104904	*B. ephippiatus*	Mexico	BBSLP352	21.33348	-99.08237	1356	+		
104905	*B. ephippiatus*	Mexico	BBSLP352	21.33348	-99.08237	1356	+		
104910	*B. ephippiatus*	Mexico	BBSLP352	21.33348	-99.08237	1356	+		
104911	*B. ephippiatus*	Mexico	BBSLP352	21.33348	-99.08237	1356	+		
104912	*B. ephippiatus*	Mexico	BBSLP352	21.33348	-99.08237	1356	+		+

Table 1.1 (cont.)

Voucher Name	Phenotype	Country	Population	Latitude	Longitude	Altitude	MSAT	COI	WING
104913	*B. ephippiatus*	Mexico	BBSLP352	21.33348	-99.08237	1356	+		+
104923	*B. ephippiatus*	Mexico	BBSLP353	21.33774	-99.10539	1648	+		
104924	*B. ephippiatus*	Mexico	BBSLP353	21.33774	-99.10539	1648	+		
104927	*B. ephippiatus*	Mexico	BBSLP353	21.33774	-99.10539	1648	+		
104928	*B. ephippiatus*	Mexico	BBSLP353	21.33774	-99.10539	1648	+		+
104989	*B. ephippiatus*	Mexico	BBSLP361	21.05076	-99.11475	1678	+		
104990	*B. ephippiatus*	Mexico	BBSLP361	21.05076	-99.11475	1678	+		
104991	*B. ephippiatus*	Mexico	BBSLP361	21.05076	-99.11475	1678	+		
104993	*B. ephippiatus*	Mexico	BBSLP361	21.05076	-99.11475	1678	+		
104994	*B. ephippiatus*	Mexico	BBSLP361	21.05076	-99.11475	1678	+		
104995	*B. ephippiatus*	Mexico	BBSLP361	21.05076	-99.11475	1678	+		+
104996	*B. ephippiatus*	Mexico	BBSLP361	21.05076	-99.11475	1678	+		+
105001	*B. ephippiatus*	Mexico	BBSLP362	21.07676	-99.10389	1654	+		
105002	*B. ephippiatus*	Mexico	BBSLP362	21.07676	-99.10389	1654	+		
105003	*B. ephippiatus*	Mexico	BBSLP362	21.07676	-99.10389	1654	+		
105004	*B. ephippiatus*	Mexico	BBSLP362	21.07676	-99.10389	1654	+		+
105005	*B. ephippiatus*	Mexico	BBSLP362	21.07676	-99.10389	1654	+		+
105006	*B. ephippiatus*	Mexico	BBSLP362	21.07676	-99.10389	1654	+		
105007	*B. ephippiatus*	Mexico	BBSLP362	21.07676	-99.10389	1654	+		
105022	*B. ephippiatus*	Mexico	BBSLP363	21.09593	-99.08622	1298	+		
105023	*B. ephippiatus*	Mexico	BBSLP363	21.09593	-99.08622	1298	+		
105024	*B. ephippiatus*	Mexico	BBSLP363	21.09593	-99.08622	1298	+		
105025	*B. ephippiatus*	Mexico	BBSLP363	21.09593	-99.08622	1298	+		
105026	*B. ephippiatus*	Mexico	BBSLP363	21.09593	-99.08622	1298	+		+
105033	*B. ephippiatus*	Mexico	BBSLP363	21.09593	-99.08622	1298	+		
105326	*B. ephippiatus*	Mexico	BBEDM051	20.11168	-99.92153	2452	+		+
105586	*B. ephippiatus*	Mexico	BBMICH031	20.09873	-100.40507	2739	+		

Table 1.1 (cont.)

Voucher Name	Phenotype	Country	Population	Latitude	Longitude	Altitude	MSAT	COI	WING
105587	*B. ephippiatus*	Mexico	BBMICH031	20.09873	-100.40507	2739	+		+
105588	*B. ephippiatus*	Mexico	BBMICH031	20.09873	-100.40507	2739	+		+
105589	*B. ephippiatus*	Mexico	BBMICH031	20.09873	-100.40507	2739	+		
105590	*B. ephippiatus*	Mexico	BBMICH031	20.09873	-100.40507	2739	+		
105591	*B. ephippiatus*	Mexico	BBMICH031	20.09873	-100.40507	2739	+		
105592	*B. ephippiatus*	Mexico	BBMICH031	20.09873	-100.40507	2739	+		
105600	*B. ephippiatus*	Mexico	BBMICH031	20.09873	-100.40507	2739	+		
105601	*B. ephippiatus*	Mexico	BBMICH031	20.09873	-100.40507	2739	+		+
105602	*B. ephippiatus*	Mexico	BBMICH031	20.09873	-100.40507	2739	+		
105603	*B. ephippiatus*	Mexico	BBMICH031	20.09873	-100.40507	2739	+		
105604	*B. ephippiatus*	Mexico	BBMICH031	20.09873	-100.40507	2739	+		
105605	*B. ephippiatus*	Mexico	BBMICH031	20.09873	-100.40507	2739	+		
105606	*B. ephippiatus*	Mexico	BBMICH031	20.09873	-100.40507	2739	+		
105626	*B. ephippiatus*	Mexico	BBMICH032	20.07874	-100.39009	2914	+		+
105627	*B. ephippiatus*	Mexico	BBMICH032	20.07874	-100.39009	2914	+		+
105633	*B. ephippiatus*	Mexico	BBMICH032	20.07874	-100.39009	2914	+		
105634	*B. ephippiatus*	Mexico	BBMICH032	20.07874	-100.39009	2914	+		
105640	*B. ephippiatus*	Mexico	BBMICH032	20.07874	-100.39009	2914	+		
105641	*B. ephippiatus*	Mexico	BBMICH032	20.07874	-100.39009	2914	+		
105653	*B. ephippiatus*	Mexico	BBEDM0111	19.75557	-100.75322	2427	+		
105654	*B. ephippiatus*	Mexico	BBEDM0112	19.774	-100.7336	2565	+		
105655	*B. ephippiatus*	Mexico	BBEDM0112	19.774	-100.7336	2565	+		
105656	*B. ephippiatus*	Mexico	BBEDM0112	19.774	-100.7336	2565	+		
105658	*B. ephippiatus*	Mexico	BBEDM0112	19.774	-100.7336	2565	+		
105659	*B. ephippiatus*	Mexico	BBEDM0112	19.774	-100.7336	2565	+		
105660	*B. ephippiatus*	Mexico	BBEDM0112	19.774	-100.7336	2565	+		
105661	*B. ephippiatus*	Mexico	BBEDM0112	19.774	-100.7336	2565	+		+

Table 1.1 (cont.)

Voucher Name	Phenotype	Country	Population	Latitude	Longitude	Altitude	MSAT	COI	WING
105668	*B. ephippiatus*	Mexico	BBEDM0112	19.774	-100.7336	2565	+		
105670	*B. ephippiatus*	Mexico	BBEDM0112	19.774	-100.7336	2565	+		+
105671	*B. ephippiatus*	Mexico	BBEDM0112	19.774	-100.7336	2565	+		
105672	*B. ephippiatus*	Mexico	BBEDM0112	19.774	-100.7336	2565	+		
105686	*B. ephippiatus*	Mexico	BBEDM0113	19.80071	-100.72079	2557	+		
105687	*B. ephippiatus*	Mexico	BBEDM0113	19.80071	-100.72079	2557	+		
105688	*B. ephippiatus*	Mexico	BBEDM0113	19.80071	-100.72079	2557	+		
105690	*B. ephippiatus*	Mexico	BBEDM0113	19.80071	-100.72079	2557	+		+
105691	*B. ephippiatus*	Mexico	BBEDM0113	19.80071	-100.72079	2557	+		+
105693	*B. ephippiatus*	Mexico	BBEDM0113	19.80071	-100.72079	2557	+		
105758	*B. ephippiatus*	Mexico	BBEDM0113	19.80071	-100.72079	2557	+		+
105759	*B. ephippiatus*	Mexico	BBEDM0113	19.80071	-100.72079	2557	+		
105784	*B. ephippiatus*	Mexico	BBMICH173	19.82134	-100.15338	2668	+		
105785	*B. ephippiatus*	Mexico	BBMICH173	19.82134	-100.15338	2668	+		
105790	*B. ephippiatus*	Mexico	BBMICH173	19.82134	-100.15338	2668	+		
105791	*B. ephippiatus*	Mexico	BBMICH173	19.82134	-100.15338	2668	+		
105792	*B. ephippiatus*	Mexico	BBMICH173	19.82134	-100.15338	2668	+		
105793	*B. ephippiatus*	Mexico	BBMICH173	19.82134	-100.15338	2668	+		+
105794	*B. ephippiatus*	Mexico	BBMICH173	19.82134	-100.15338	2668	+		
105795	*B. ephippiatus*	Mexico	BBMICH173	19.82134	-100.15338	2668	+		
105796	*B. ephippiatus*	Mexico	BBMICH173	19.82134	-100.15338	2668	+		
105797	*B. ephippiatus*	Mexico	BBMICH173	19.82134	-100.15338	2668	+		
105798	*B. ephippiatus*	Mexico	BBMICH173	19.82134	-100.15338	2668	+		
105799	*B. ephippiatus*	Mexico	BBMICH173	19.82134	-100.15338	2668	+		
105813	*B. ephippiatus*	Mexico	BBMICH173	19.82134	-100.15338	2668	+		+
105814	*B. ephippiatus*	Mexico	BBMICH173	19.82134	-100.15338	2668	+		
105815	*B. ephippiatus*	Mexico	BBMICH173	19.82134	-100.15338	2668	+		

Table 1.1 (cont.)

Voucher Name	Phenotype	Country	Population	Latitude	Longitude	Altitude	MSAT	COI	WING
105816	*B. ephippiatus*	Mexico	BBMICH173	19.82134	-100.15338	2668	+		+
105817	*B. ephippiatus*	Mexico	BBMICH173	19.82134	-100.15338	2668	+		+
105818	*B. ephippiatus*	Mexico	BBMICH173	19.82134	-100.15338	2668	+		+
105819	*B. ephippiatus*	Mexico	BBMICH173	19.82134	-100.15338	2668	+		
105820	*B. ephippiatus*	Mexico	BBMICH173	19.82134	-100.15338	2668	+		
106091	*B. ephippiatus*	Mexico	BBEDM0911	19.56131	-99.57233	3197	+		
106092	*B. ephippiatus*	Mexico	BBEDM0911	19.56131	-99.57233	3197	+		
106093	*B. ephippiatus*	Mexico	BBEDM0911	19.56131	-99.57233	3197	+		
106094	*B. ephippiatus*	Mexico	BBEDM0911	19.56131	-99.57233	3197	+		+
106095	*B. ephippiatus*	Mexico	BBEDM0911	19.56131	-99.57233	3197	+		
106096	*B. ephippiatus*	Mexico	BBEDM0911	19.56131	-99.57233	3197	+		
106097	*B. ephippiatus*	Mexico	BBEDM0911	19.56131	-99.57233	3197	+		
106098	*B. ephippiatus*	Mexico	BBEDM0911	19.56131	-99.57233	3197	+	+	+
106106	*B. ephippiatus*	Mexico	BBEDM0911	19.56131	-99.57233	3197	+		+
106107	*B. ephippiatus*	Mexico	BBEDM0911	19.56131	-99.57233	3197	+		
106108	*B. ephippiatus*	Mexico	BBEDM0911	19.56131	-99.57233	3197	+		
106121	*B. ephippiatus*	Mexico	BBEDM0912	19.57498	-99.53789	3379	+		
106122	*B. ephippiatus*	Mexico	BBEDM0912	19.57498	-99.53789	3379	+		
106123	*B. ephippiatus*	Mexico	BBEDM0912	19.57498	-99.53789	3379	+		
106131	*B. ephippiatus*	Mexico	BBEDM0912	19.57498	-99.53789	3379	+		
106132	*B. ephippiatus*	Mexico	BBEDM0912	19.57498	-99.53789	3379	+		
106133	*B. ephippiatus*	Mexico	BBEDM0912	19.57498	-99.53789	3379	+		+
106134	*B. ephippiatus*	Mexico	BBEDM0912	19.57498	-99.53789	3379	+		
106135	*B. ephippiatus*	Mexico	BBEDM0912	19.57498	-99.53789	3379	+		+
106136	*B. ephippiatus*	Mexico	BBEDM0912	19.57498	-99.53789	3379	+		
106187	*B. ephippiatus*	Mexico	BBEDM191	19.24678	-99.87074	3555	+		
106188	*B. ephippiatus*	Mexico	BBEDM191	19.24678	-99.87074	3555	+		

Table 1.1 (cont.)

Voucher Name	Phenotype	Country	Population	Latitude	Longitude	Altitude	MSAT	COI	WING
106199	*B. ephippiatus*	Mexico	BBEDM191	19.24678	-99.87074	3555	+		
106200	*B. ephippiatus*	Mexico	BBEDM191	19.24678	-99.87074	3555	+		+
106201	*B. ephippiatus*	Mexico	BBEDM192	19.28359	-99.86399	3145	+		
106202	*B. ephippiatus*	Mexico	BBEDM192	19.28359	-99.86399	3145	+		
106203	*B. ephippiatus*	Mexico	BBEDM192	19.28359	-99.86399	3145	+		
106204	*B. ephippiatus*	Mexico	BBEDM192	19.28359	-99.86399	3145	+		+
106205	*B. ephippiatus*	Mexico	BBEDM192	19.28359	-99.86399	3145	+		
106206	*B. ephippiatus*	Mexico	BBEDM192	19.28359	-99.86399	3145	+		
106207	*B. ephippiatus*	Mexico	BBEDM192	19.28359	-99.86399	3145	+		+
106208	*B. ephippiatus*	Mexico	BBEDM192	19.28359	-99.86399	3145	+		
106209	*B. ephippiatus*	Mexico	BBEDM192	19.28359	-99.86399	3145	+		
106227	*B. ephippiatus*	Mexico	BBEDM192	19.28359	-99.86399	3145	+		+
106229	*B. ephippiatus*	Mexico	BBEDM192	19.28359	-99.86399	3145	+		+
106231	*B. ephippiatus*	Mexico	BBEDM192	19.28359	-99.86399	3145	+		
106232	*B. ephippiatus*	Mexico	BBEDM192	19.28359	-99.86399	3145	+		
106238	*B. ephippiatus*	Mexico	BBEDM192	19.28359	-99.86399	3145	+		
106242	*B. ephippiatus*	Mexico	BBEDM193	19.31145	-99.85837	2946	+		
106243	*B. ephippiatus*	Mexico	BBEDM193	19.31145	-99.85837	2946	+		
106297	*B. ephippiatus*	Mexico	BBEDM151	19.04513	-99.59735	2685	+		
106298	*B. ephippiatus*	Mexico	BBEDM151	19.04513	-99.59735	2685	+		
106299	*B. ephippiatus*	Mexico	BBEDM151	19.04513	-99.59735	2685	+		
106300	*B. ephippiatus*	Mexico	BBEDM151	19.04513	-99.59735	2685	+		+
106301	*B. ephippiatus*	Mexico	BBEDM151	19.04513	-99.59735	2685	+		
106302	*B. ephippiatus*	Mexico	BBEDM151	19.04513	-99.59735	2685	+		
106303	*B. ephippiatus*	Mexico	BBEDM151	19.04513	-99.59735	2685	+		
106304	*B. ephippiatus*	Mexico	BBEDM151	19.04513	-99.59735	2685	+		+
106339	*B. ephippiatus*	Mexico	BBEDM151	19.04513	-99.59735	2685	+		

Table 1.1 (cont.)

Voucher Name	Phenotype	Country	Population	Latitude	Longitude	Altitude	MSAT	COI	WING
106343	*B. ephippiatus*	Mexico	BBEDM152	19.00326	-99.57534	2252	+		
106344	*B. ephippiatus*	Mexico	BBEDM152	19.00326	-99.57534	2252	+		
106345	*B. ephippiatus*	Mexico	BBEDM152	19.00326	-99.57534	2252	+		
106346	*B. ephippiatus*	Mexico	BBEDM152	19.00326	-99.57534	2252	+		
106347	*B. ephippiatus*	Mexico	BBEDM152	19.00326	-99.57534	2252	+		
106354	*B. ephippiatus*	Mexico	BBEDM153	19.03841	-99.56345	2603	+		
106355	*B. ephippiatus*	Mexico	BBEDM153	19.03841	-99.56345	2603	+		
106358	*B. ephippiatus*	Mexico	BBEDM153	19.03841	-99.56345	2603	+		
106359	*B. ephippiatus*	Mexico	BBEDM153	19.03841	-99.56345	2603	+		
106360	*B. ephippiatus*	Mexico	BBEDM153	19.03841	-99.56345	2603	+		+
106361	*B. ephippiatus*	Mexico	BBEDM153	19.03841	-99.56345	2603	+		+
106420	*B. ephippiatus*	Mexico	BBEDM161	19.03181	-99.27492	2614	+		
106421	*B. ephippiatus*	Mexico	BBEDM161	19.03181	-99.27492	2614	+		
106422	*B. ephippiatus*	Mexico	BBEDM161	19.03181	-99.27492	2614	+	+	+
106423	*B. ephippiatus*	Mexico	BBEDM161	19.03181	-99.27492	2614	+		
106424	*B. ephippiatus*	Mexico	BBEDM161	19.03181	-99.27492	2614	+		+
106425	*B. ephippiatus*	Mexico	BBEDM161	19.03181	-99.27492	2614	+		
106456	*B. ephippiatus*	Mexico	BBEDM162	19.0522	-99.31538	2809	+		
106457	*B. ephippiatus*	Mexico	BBEDM162	19.0522	-99.31538	2809	+		
106458	*B. ephippiatus*	Mexico	BBEDM162	19.0522	-99.31538	2809	+		
106459	*B. ephippiatus*	Mexico	BBEDM162	19.0522	-99.31538	2809	+		+
106460	*B. ephippiatus*	Mexico	BBEDM162	19.0522	-99.31538	2809	+		
106461	*B. ephippiatus*	Mexico	BBEDM162	19.0522	-99.31538	2809	+		
106463	*B. ephippiatus*	Mexico	BBEDM162	19.0522	-99.31538	2809	+		+
106464	*B. ephippiatus*	Mexico	BBEDM162	19.0522	-99.31538	2809	+		
106465	*B. ephippiatus*	Mexico	BBEDM162	19.0522	-99.31538	2809	+		
106467	*B. ephippiatus*	Mexico	BBEDM163	19.0732	-99.34222	3104	+		

Table 1.1 (cont.)

Voucher Name	Phenotype	Country	Population	Latitude	Longitude	Altitude	MSAT	COI	WING
106468	*B. ephippiatus*	Mexico	BBEDM163	19.0732	-99.34222	3104	+		
106469	*B. ephippiatus*	Mexico	BBEDM163	19.0732	-99.34222	3104	+		
106472	*B. ephippiatus*	Mexico	BBEDM163	19.0732	-99.34222	3104	+		
106473	*B. ephippiatus*	Mexico	BBEDM163	19.0732	-99.34222	3104	+		+
106488	*B. ephippiatus*	Mexico	BBEDM181	18.97556	-99.9165	2668	+		
106489	*B. ephippiatus*	Mexico	BBEDM181	18.97556	-99.9165	2668	+		
106490	*B. ephippiatus*	Mexico	BBEDM181	18.97556	-99.9165	2668	+		+
106491	*B. ephippiatus*	Mexico	BBEDM181	18.97556	-99.9165	2668	+		
106492	*B. ephippiatus*	Mexico	BBEDM181	18.97556	-99.9165	2668	+		+
106493	*B. ephippiatus*	Mexico	BBEDM181	18.97556	-99.9165	2668	+		
106494	*B. ephippiatus*	Mexico	BBEDM181	18.97556	-99.9165	2668	+		
106495	*B. ephippiatus*	Mexico	BBEDM181	18.97556	-99.9165	2668	+		
106523	*B. ephippiatus*	Mexico	BBEDM182	18.95835	-99.93943	2482	+		+
106524	*B. ephippiatus*	Mexico	BBEDM182	18.95835	-99.93943	2482	+		+
106529	*B. ephippiatus*	Mexico	BBEDM182	18.95835	-99.93943	2482	+		
106530	*B. ephippiatus*	Mexico	BBEDM183	19.00288	-99.89851	2837	+		
106531	*B. ephippiatus*	Mexico	BBEDM183	19.00288	-99.89851	2837	+		
106532	*B. ephippiatus*	Mexico	BBEDM183	19.00288	-99.89851	2837	+		
106533	*B. ephippiatus*	Mexico	BBEDM183	19.00288	-99.89851	2837	+		
106544	*B. ephippiatus*	Mexico	BBEDM183	19.00288	-99.89851	2837	+		
106545	*B. ephippiatus*	Mexico	BBEDM183	19.00288	-99.89851	2837	+		+
106551	*B. ephippiatus*	Mexico	BBEDM183	19.00288	-99.89851	2837	+		
106552	*B. ephippiatus*	Mexico	BBEDM183	19.00288	-99.89851	2837	+		
106555	*B. ephippiatus*	Mexico	BBEDM183	19.00288	-99.89851	2837	+		
106591	*B. ephippiatus*	Mexico	BBEDM123	19.07761	-100.16074	2038	+		+
106633	*B. ephippiatus*	Mexico	BBEDM021	19.5658	-100.75623	2198	+		
106635	*B. ephippiatus*	Mexico	BBEDM021	19.5658	-100.75623	2198	+		

Table 1.1 (cont.)

Voucher Name	Phenotype	Country	Population	Latitude	Longitude	Altitude	MSAT	COI	WING
106636	*B. ephippiatus*	Mexico	BBEDM021	19.5658	-100.75623	2198	+		
106637	*B. ephippiatus*	Mexico	BBEDM021	19.5658	-100.75623	2198	+		+
106638	*B. ephippiatus*	Mexico	BBEDM021	19.5658	-100.75623	2198	+		+
106641	*B. ephippiatus*	Mexico	BBEDM022	19.5396	-100.74709	2184	+		
106642	*B. ephippiatus*	Mexico	BBEDM022	19.5396	-100.74709	2184	+		
106643	*B. ephippiatus*	Mexico	BBEDM022	19.5396	-100.74709	2184	+		
106644	*B. ephippiatus*	Mexico	BBEDM022	19.5396	-100.74709	2184	+		
106645	*B. ephippiatus*	Mexico	BBEDM022	19.5396	-100.74709	2184	+		+
106646	*B. ephippiatus*	Mexico	BBEDM022	19.5396	-100.74709	2184	+		
106647	*B. ephippiatus*	Mexico	BBEDM022	19.5396	-100.74709	2184	+		
106648	*B. ephippiatus*	Mexico	BBEDM022	19.5396	-100.74709	2184	+		
106649	*B. ephippiatus*	Mexico	BBEDM022	19.5396	-100.74709	2184	+		
106650	*B. ephippiatus*	Mexico	BBEDM022	19.5396	-100.74709	2184	+		
106690	*B. ephippiatus*	Mexico	BBEDM023	19.54787	-100.71735	2605	+		
106691	*B. ephippiatus*	Mexico	BBEDM023	19.54787	-100.71735	2605	+		
106696	*B. ephippiatus*	Mexico	BBEDM023	19.54787	-100.71735	2605	+		
106697	*B. ephippiatus*	Mexico	BBEDM023	19.54787	-100.71735	2605	+		+
106698	*B. ephippiatus*	Mexico	BBEDM023	19.54787	-100.71735	2605	+		+
107676	*B. ephippiatus*	Mexico	BBDUR351	28.18932	-107.636	2628	+		
107677	*B. ephippiatus*	Mexico	BBDUR351	28.18932	-107.636	2628	+		
107678	*B. ephippiatus*	Mexico	BBDUR351	28.18932	-107.636	2628	+		
107679	*B. ephippiatus*	Mexico	BBDUR351	28.18932	-107.636	2628	+		+
107680	*B. ephippiatus*	Mexico	BBDUR351	28.18932	-107.636	2628	+		
107681	*B. ephippiatus*	Mexico	BBDUR351	28.18932	-107.636	2628	+		
107682	*B. ephippiatus*	Mexico	BBDUR351	28.18932	-107.636	2628	+		
107683	*B. ephippiatus*	Mexico	BBDUR351	28.18932	-107.636	2628	+		
107684	*B. ephippiatus*	Mexico	BBDUR351	28.18932	-107.636	2628	+		

Table 1.1 (cont.)

Voucher Name	Phenotype	Country	Population	Latitude	Longitude	Altitude	MSAT	COI	WING
107720	*B. ephippiatus*	Mexico	BBDUR351	28.18932	-107.636	2628	+		
107721	*B. ephippiatus*	Mexico	BBDUR351	28.18932	-107.636	2628	+		
107722	*B. ephippiatus*	Mexico	BBDUR351	28.18932	-107.636	2628	+		+
107723	*B. ephippiatus*	Mexico	BBDUR351	28.18932	-107.636	2628	+		+
107765	*B. ephippiatus*	Mexico	BBDUR352	28.20052	-107.60052	2415	+		
107766	*B. ephippiatus*	Mexico	BBDUR352	28.20052	-107.60052	2415	+		
107767	*B. ephippiatus*	Mexico	BBDUR352	28.20052	-107.60052	2415	+		
107768	*B. ephippiatus*	Mexico	BBDUR352	28.20052	-107.60052	2415	+		+
107769	*B. ephippiatus*	Mexico	BBDUR352	28.20052	-107.60052	2415	+		+
107770	*B. ephippiatus*	Mexico	BBDUR352	28.20052	-107.60052	2415	+		
107774	*B. ephippiatus*	Mexico	BBDUR352	28.20052	-107.60052	2415	+		
107905	*B. ephippiatus*	Mexico	BBDUR341	28.20577	-108.15741	2938	+		
107906	*B. ephippiatus*	Mexico	BBDUR341	28.20577	-108.15741	2938	+		
107907	*B. ephippiatus*	Mexico	BBDUR341	28.20577	-108.15741	2938	+		
107908	*B. ephippiatus*	Mexico	BBDUR341	28.20577	-108.15741	2938	+		+
107909	*B. ephippiatus*	Mexico	BBDUR341	28.20577	-108.15741	2938	+		
107910	*B. ephippiatus*	Mexico	BBDUR341	28.20577	-108.15741	2938	+		+
107911	*B. ephippiatus*	Mexico	BBDUR341	28.20577	-108.15741	2938	+		
107912	*B. ephippiatus*	Mexico	BBDUR341	28.20577	-108.15741	2938	+		
107913	*B. ephippiatus*	Mexico	BBDUR341	28.20577	-108.15741	2938	+		
107948	*B. ephippiatus*	Mexico	BBDUR342	28.23322	-108.08427	2194	+		
107949	*B. ephippiatus*	Mexico	BBDUR342	28.23322	-108.08427	2194	+		
107950	*B. ephippiatus*	Mexico	BBDUR342	28.23322	-108.08427	2194	+		
107952	*B. ephippiatus*	Mexico	BBDUR342	28.23322	-108.08427	2194	+		+
107953	*B. ephippiatus*	Mexico	BBDUR342	28.23322	-108.08427	2194	+		+
107954	*B. ephippiatus*	Mexico	BBDUR342	28.23322	-108.08427	2194	+		
107955	*B. ephippiatus*	Mexico	BBDUR343	28.17215	-108.16965	2054	+		

Table 1.1 (cont.)

Voucher Name	Phenotype	Country	Population	Latitude	Longitude	Altitude	MSAT	COI	WING
107956	*B. ephippiatus*	Mexico	BBDUR343	28.17215	-108.16965	2054	+		
107957	*B. ephippiatus*	Mexico	BBDUR343	28.17215	-108.16965	2054	+		
108057	*B. ephippiatus*	Mexico	BBDUR343	28.17215	-108.16965	2054	+		+
108058	*B. ephippiatus*	Mexico	BBDUR343	28.17215	-108.16965	2054	+		
108090	*B. ephippiatus*	Mexico	BBDUR391	27.9616	-108.16497	2334	+		
108091	*B. ephippiatus*	Mexico	BBDUR391	27.9616	-108.16497	2334	+		
108092	*B. ephippiatus*	Mexico	BBDUR391	27.9616	-108.16497	2334	+		
108093	*B. ephippiatus*	Mexico	BBDUR391	27.9616	-108.16497	2334	+		
108094	*B. ephippiatus*	Mexico	BBDUR391	27.9616	-108.16497	2334	+	+	+
108095	*B. ephippiatus*	Mexico	BBDUR391	27.9616	-108.16497	2334	+		
108096	*B. ephippiatus*	Mexico	BBDUR391	27.9616	-108.16497	2334	+		+
108097	*B. ephippiatus*	Mexico	BBDUR391	27.9616	-108.16497	2334	+		
108106	*B. ephippiatus*	Mexico	BBDUR391	27.9616	-108.16497	2334	+		
108107	*B. ephippiatus*	Mexico	BBDUR391	27.9616	-108.16497	2334	+		
108108	*B. ephippiatus*	Mexico	BBDUR391	27.9616	-108.16497	2334	+		
108109	*B. ephippiatus*	Mexico	BBDUR391	27.9616	-108.16497	2334	+		
108110	*B. ephippiatus*	Mexico	BBDUR391	27.9616	-108.16497	2334	+		
108111	*B. ephippiatus*	Mexico	BBDUR391	27.9616	-108.16497	2334	+		+
108112	*B. ephippiatus*	Mexico	BBDUR391	27.9616	-108.16497	2334	+		
108127	*B. ephippiatus*	Mexico	BBDUR392	27.9456	-108.21127	2107	+		
108128	*B. ephippiatus*	Mexico	BBDUR392	27.9456	-108.21127	2107	+		
108129	*B. ephippiatus*	Mexico	BBDUR392	27.9456	-108.21127	2107	+		
108130	*B. ephippiatus*	Mexico	BBDUR392	27.9456	-108.21127	2107	+		+
108131	*B. ephippiatus*	Mexico	BBDUR392	27.9456	-108.21127	2107	+		+
108132	*B. ephippiatus*	Mexico	BBDUR393	27.91308	-108.22372	2097	+		
108133	*B. ephippiatus*	Mexico	BBDUR393	27.91308	-108.22372	2097	+		
108134	*B. ephippiatus*	Mexico	BBDUR393	27.91308	-108.22372	2097	+		

Table 1.1 (cont.)

Voucher Name	Phenotype	Country	Population	Latitude	Longitude	Altitude	MSAT	COI	WING
108273	*B. ephippiatus*	Mexico	BBDUR403	27.95583	-107.60294	2431	+		
108274	*B. ephippiatus*	Mexico	BBDUR403	27.95583	-107.60294	2431	+	+	+
108275	*B. ephippiatus*	Mexico	BBDUR403	27.95583	-107.60294	2431	+		
108276	*B. ephippiatus*	Mexico	BBDUR403	27.95583	-107.60294	2431	+		
108277	*B. ephippiatus*	Mexico	BBDUR403	27.95583	-107.60294	2431	+		
108278	*B. ephippiatus*	Mexico	BBDUR403	27.95583	-107.60294	2431	+		
108279	*B. ephippiatus*	Mexico	BBDUR403	27.95583	-107.60294	2431	+		
108280	*B. ephippiatus*	Mexico	BBDUR403	27.95583	-107.60294	2431	+		+
108281	*B. ephippiatus*	Mexico	BBDUR403	27.95583	-107.60294	2431	+		
108282	*B. ephippiatus*	Mexico	BBDUR403	27.95583	-107.60294	2431	+		+
108283	*B. ephippiatus*	Mexico	BBDUR403	27.95583	-107.60294	2431	+		
108295	*B. ephippiatus*	Mexico	BBDUR404	27.98171	-107.61938	2446	+		+
108296	*B. ephippiatus*	Mexico	BBDUR404	27.98171	-107.61938	2446	+		+
108373	*B. ephippiatus*	Mexico	BBDUR451	27.71887	-107.6776	2461	+		
108374	*B. ephippiatus*	Mexico	BBDUR451	27.71887	-107.6776	2461	+		
108375	*B. ephippiatus*	Mexico	BBDUR451	27.71887	-107.6776	2461	+		
108376	*B. ephippiatus*	Mexico	BBDUR451	27.71887	-107.6776	2461	+		
108377	*B. ephippiatus*	Mexico	BBDUR451	27.71887	-107.6776	2461	+		
108378	*B. ephippiatus*	Mexico	BBDUR451	27.71887	-107.6776	2461	+	+	+
108379	*B. ephippiatus*	Mexico	BBDUR451	27.71887	-107.6776	2461	+		
108417	*B. ephippiatus*	Mexico	BBDUR452	27.68698	-107.72294	2458	+		
108418	*B. ephippiatus*	Mexico	BBDUR452	27.68698	-107.72294	2458	+		
108419	*B. ephippiatus*	Mexico	BBDUR452	27.68698	-107.72294	2458	+		
108421	*B. ephippiatus*	Mexico	BBDUR452	27.68698	-107.72294	2458	+		
108422	*B. ephippiatus*	Mexico	BBDUR452	27.68698	-107.72294	2458	+		+
108423	*B. ephippiatus*	Mexico	BBDUR452	27.68698	-107.72294	2458	+		
108424	*B. ephippiatus*	Mexico	BBDUR453	27.68725	-107.66349	2437	+		

Table 1.1 (cont.)

Voucher Name	Phenotype	Country	Population	Latitude	Longitude	Altitude	MSAT	COI	WING
108425	*B. ephippiatus*	Mexico	BBDUR453	27.68725	-107.66349	2437	+		
108426	*B. ephippiatus*	Mexico	BBDUR453	27.68725	-107.66349	2437	+		
108427	*B. ephippiatus*	Mexico	BBDUR453	27.68725	-107.66349	2437	+		+
108428	*B. ephippiatus*	Mexico	BBDUR453	27.68725	-107.66349	2437	+		+
108431	*B. ephippiatus*	Mexico	BBDUR452	27.68698	-107.72294	2458	+		
108437	*B. ephippiatus*	Mexico	BBDUR453	27.68725	-107.66349	2437	+		+
108572	*B. ephippiatus*	Mexico	BBDUR561	26.81817	-107.26517	2519	+		
108574	*B. ephippiatus*	Mexico	BBDUR561	26.81817	-107.26517	2519	+		
108575	*B. ephippiatus*	Mexico	BBDUR561	26.81817	-107.26517	2519	+		+
108576	*B. ephippiatus*	Mexico	BBDUR561	26.81817	-107.26517	2519	+		+
108577	*B. ephippiatus*	Mexico	BBDUR561	26.81817	-107.26517	2519	+		
108578	*B. ephippiatus*	Mexico	BBDUR561	26.81817	-107.26517	2519	+		
108579	*B. ephippiatus*	Mexico	BBDUR561	26.81817	-107.26517	2519	+		
108580	*B. ephippiatus*	Mexico	BBDUR561	26.81817	-107.26517	2519	+		
108581	*B. ephippiatus*	Mexico	BBDUR561	26.81817	-107.26517	2519	+		
108609	*B. ephippiatus*	Mexico	BBDUR562	26.79728	-107.23918	2554	+		
108610	*B. ephippiatus*	Mexico	BBDUR562	26.79728	-107.23918	2554	+		
108611	*B. ephippiatus*	Mexico	BBDUR562	26.79728	-107.23918	2554	+		
108612	*B. ephippiatus*	Mexico	BBDUR562	26.79728	-107.23918	2554	+		+
108613	*B. ephippiatus*	Mexico	BBDUR562	26.79728	-107.23918	2554	+		
108614	*B. ephippiatus*	Mexico	BBDUR562	26.79728	-107.23918	2554	+		+
108615	*B. ephippiatus*	Mexico	BBDUR562	26.79728	-107.23918	2554	+		
108616	*B. ephippiatus*	Mexico	BBDUR562	26.79728	-107.23918	2554	+		+
108628	*B. ephippiatus*	Mexico	BBDUR562	26.79728	-107.23918	2554	+		
108629	*B. ephippiatus*	Mexico	BBDUR562	26.79728	-107.23918	2554	+		
108664	*B. ephippiatus*	Mexico	BBDUR563	26.79143	-107.21179	2525	+		
108835	*B. ephippiatus*	Mexico	BBDUR581	26.86889	-106.88275	2403	+	+	+

Table 1.1 (cont.)

Voucher Name	Phenotype	Country	Population	Latitude	Longitude	Altitude	MSAT	COI	WING
108836	*B. ephippiatus*	Mexico	BBDUR581	26.86889	-106.88275	2403	+		
108837	*B. ephippiatus*	Mexico	BBDUR581	26.86889	-106.88275	2403	+		+
108838	*B. ephippiatus*	Mexico	BBDUR581	26.86889	-106.88275	2403	+		
108839	*B. ephippiatus*	Mexico	BBDUR581	26.86889	-106.88275	2403	+		+
108840	*B. ephippiatus*	Mexico	BBDUR581	26.86889	-106.88275	2403	+		+
108885	*B. ephippiatus*	Mexico	BBDUR681	26.00865	-106.94693	2392	+		
108886	*B. ephippiatus*	Mexico	BBDUR681	26.00865	-106.94693	2392	+		
108887	*B. ephippiatus*	Mexico	BBDUR681	26.00865	-106.94693	2392	+		
108891	*B. ephippiatus*	Mexico	BBDUR681	26.00865	-106.94693	2392	+	+	+
108892	*B. ephippiatus*	Mexico	BBDUR681	26.00865	-106.94693	2392	+		
108893	*B. ephippiatus*	Mexico	BBDUR681	26.00865	-106.94693	2392	+		
108894	*B. ephippiatus*	Mexico	BBDUR681	26.00865	-106.94693	2392	+		+
108895	*B. ephippiatus*	Mexico	BBDUR681	26.00865	-106.94693	2392	+		
108927	*B. ephippiatus*	Mexico	BBDUR682	26.03756	-106.93732	2588	+		
108928	*B. ephippiatus*	Mexico	BBDUR682	26.03756	-106.93732	2588	+		
108929	*B. ephippiatus*	Mexico	BBDUR682	26.03756	-106.93732	2588	+		
108930	*B. ephippiatus*	Mexico	BBDUR682	26.03756	-106.93732	2588	+		
108931	*B. ephippiatus*	Mexico	BBDUR682	26.03756	-106.93732	2588	+		+
108932	*B. ephippiatus*	Mexico	BBDUR682	26.03756	-106.93732	2588	+		+
108935	*B. ephippiatus*	Mexico	BBDUR682	26.03756	-106.93732	2588	+		
108938	*B. ephippiatus*	Mexico	BBDUR683	26.05774	-106.95726	2588	+		
108939	*B. ephippiatus*	Mexico	BBDUR683	26.05774	-106.95726	2588	+		
108940	*B. ephippiatus*	Mexico	BBDUR683	26.05774	-106.95726	2588	+		
108941	*B. ephippiatus*	Mexico	BBDUR683	26.05774	-106.95726	2588	+		+
108949	*B. ephippiatus*	Mexico	BBDUR681	26.00865	-106.94693	2392	+		
109062	*B. ephippiatus*	Mexico	BBDUR741	25.72864	-106.83629	2491	+		
109063	*B. ephippiatus*	Mexico	BBDUR741	25.72864	-106.83629	2491	+		

Table 1.1 (cont.)

Voucher Name	Phenotype	Country	Population	Latitude	Longitude	Altitude	MSAT	COI	WING
109064	*B. ephippiatus*	Mexico	BBDUR741	25.72864	-106.83629	2491	+		
109069	*B. ephippiatus*	Mexico	BBDUR741	25.72864	-106.83629	2491	+	+	+
109070	*B. ephippiatus*	Mexico	BBDUR741	25.72864	-106.83629	2491	+		
109071	*B. ephippiatus*	Mexico	BBDUR741	25.72864	-106.83629	2491	+		
109072	*B. ephippiatus*	Mexico	BBDUR741	25.72864	-106.83629	2491	+		
109073	*B. ephippiatus*	Mexico	BBDUR741	25.72864	-106.83629	2491	+		
109074	*B. ephippiatus*	Mexico	BBDUR741	25.72864	-106.83629	2491	+		+
109075	*B. ephippiatus*	Mexico	BBDUR741	25.72864	-106.83629	2491	+		
109076	*B. ephippiatus*	Mexico	BBDUR741	25.72864	-106.83629	2491	+		
109077	*B. ephippiatus*	Mexico	BBDUR741	25.72864	-106.83629	2491	+		
109078	*B. ephippiatus*	Mexico	BBDUR741	25.72864	-106.83629	2491	+		+
109079	*B. ephippiatus*	Mexico	BBDUR741	25.72864	-106.83629	2491	+		
109090	*B. ephippiatus*	Mexico	BBDUR741	25.72864	-106.83629	2491	+		+
109102	*B. ephippiatus*	Mexico	BBDUR743	25.77628	-106.80327	2364	+		
109103	*B. ephippiatus*	Mexico	BBDUR743	25.77628	-106.80327	2364	+		
109104	*B. ephippiatus*	Mexico	BBDUR743	25.77628	-106.80327	2364	+		
109105	*B. ephippiatus*	Mexico	BBDUR743	25.77628	-106.80327	2364	+		
109110	*B. ephippiatus*	Mexico	BBDUR743	25.77628	-106.80327	2364	+		+
109188	*B. ephippiatus*	Mexico	BBDUR691	26.13	-106.70805	2108	+		
109189	*B. ephippiatus*	Mexico	BBDUR691	26.13	-106.70805	2108	+		
109190	*B. ephippiatus*	Mexico	BBDUR691	26.13	-106.70805	2108	+		
109191	*B. ephippiatus*	Mexico	BBDUR691	26.13	-106.70805	2108	+		+
109192	*B. ephippiatus*	Mexico	BBDUR691	26.13	-106.70805	2108	+		+
109200	*B. ephippiatus*	Mexico	BBDUR691	26.13	-106.70805	2108	+		
109201	*B. ephippiatus*	Mexico	BBDUR691	26.13	-106.70805	2108	+		
109202	*B. ephippiatus*	Mexico	BBDUR691	26.13	-106.70805	2108	+		
109231	*B. ephippiatus*	Mexico	BBDUR692	26.16352	-106.61576	2723	+		+

Table 1.1 (cont.)

Voucher Name	Phenotype	Country	Population	Latitude	Longitude	Altitude	MSAT	COI	WING
109232	*B. ephippiatus*	Mexico	BBDUR692	26.16352	-106.61576	2723	+		
109233	*B. ephippiatus*	Mexico	BBDUR692	26.16352	-106.61576	2723	+		
109236	*B. ephippiatus*	Mexico	BBDUR692	26.16352	-106.61576	2723	+		
109241	*B. ephippiatus*	Mexico	BBDUR693	26.17471	-106.60452	2670	+		
109242	*B. ephippiatus*	Mexico	BBDUR693	26.17471	-106.60452	2670	+		
109243	*B. ephippiatus*	Mexico	BBDUR693	26.17471	-106.60452	2670	+		
109244	*B. ephippiatus*	Mexico	BBDUR693	26.17471	-106.60452	2670	+		+
109245	*B. ephippiatus*	Mexico	BBDUR693	26.17471	-106.60452	2670	+		
109246	*B. ephippiatus*	Mexico	BBDUR693	26.17471	-106.60452	2670	+		
109247	*B. ephippiatus*	Mexico	BBDUR693	26.17471	-106.60452	2670	+		
109248	*B. ephippiatus*	Mexico	BBDUR693	26.17471	-106.60452	2670	+		+
109477	*B. ephippiatus*	Mexico	BBSIN024	23.04714	-105.44598	1680	+		
109478	*B. ephippiatus*	Mexico	BBSIN024	23.04714	-105.44598	1680	+		
109479	*B. ephippiatus*	Mexico	BBSIN024	23.04714	-105.44598	1680	+		
109484	*B. ephippiatus*	Mexico	BBSIN024	23.04714	-105.44598	1680	+	+	+
109485	*B. ephippiatus*	Mexico	BBSIN024	23.04714	-105.44598	1680	+		+
109515	*B. ephippiatus*	Mexico	BBSIN024	23.04714	-105.44598	1680	+		
109919	*B. ephippiatus*	Mexico	BBNAY141	20.79534	-103.84583	2841	+	+	+
109922	*B. ephippiatus*	Mexico	BBNAY141	20.79534	-103.84583	2841	+		+
109923	*B. ephippiatus*	Mexico	BBNAY141	20.79534	-103.84583	2841	+		+
109924	*B. ephippiatus*	Mexico	BBNAY141	20.79534	-103.84583	2841	+		+
110486	*B. ephippiatus*	Mexico	BBSLP341	21.11976	-99.66409	2640	+		
110487	*B. ephippiatus*	Mexico	BBSLP341	21.11976	-99.66409	2640	+		
110488	*B. ephippiatus*	Mexico	BBSLP341	21.11976	-99.66409	2640	+		
110521	*B. ephippiatus*	Mexico	BBSLP342	21.12629	-99.63838	2594	+		
110527	*B. ephippiatus*	Mexico	BBSLP342	21.12629	-99.63838	2594	+		
110540	*B. ephippiatus*	Mexico	BBSLP343	21.14558	-99.61848	2240	+		

Table 1.1 (cont.)

Voucher Name	Phenotype	Country	Population	Latitude	Longitude	Altitude	MSAT	COI	WING
110542	*B. ephippiatus*	Mexico	BBSLP343	21.14558	-99.61848	2240	+		
110619	*B. ephippiatus*	Mexico	BBOAX175	17.48007	-100.03572	2538	+		+
110629	*B. ephippiatus*	Mexico	BBOAX175	17.48007	-100.03572	2538	+		
110695	*B. ephippiatus*	Mexico	BBOAX141	17.66377	-99.1208	1959	+		+
110730	*B. ephippiatus*	Mexico	BBOAX142	17.69348	-99.013445	2250	+		
110731	*B. ephippiatus*	Mexico	BBOAX142	17.69348	-99.013445	2250	+		
110732	*B. ephippiatus*	Mexico	BBOAX142	17.69348	-99.013445	2250	+		
110733	*B. ephippiatus*	Mexico	BBOAX142	17.69348	-99.013445	2250	+		
110781	*B. ephippiatus*	Mexico	BBOAX142	17.69348	-99.013445	2250	+		
110787	*B. ephippiatus*	Mexico	BBOAX143	17.7011	-99.12556	1999	+		+
111103	*B. ephippiatus*	Mexico	BBOAX261	17.16061	-96.01698	2442	+		+
111108	*B. ephippiatus*	Mexico	BBOAX262	17.14264	-96.03147	2537	+		+
111111	*B. ephippiatus*	Mexico	BBOAX262	17.14264	-96.03147	2537	+		+
111119	*B. ephippiatus*	Mexico	BBOAX263	17.11801	-96.04269	2492	+		+
111196	*B. ephippiatus*	Mexico	BBOAX222	16.19076	-96.39581	2674	+		
111197	*B. ephippiatus*	Mexico	BBOAX222	16.19076	-96.39581	2674	+		
111201	*B. ephippiatus*	Mexico	BBOAX223	16.14865	-96.36588	2804	+		
111202	*B. ephippiatus*	Mexico	BBOAX223	16.14865	-96.36588	2804	+		+
111203	*B. ephippiatus*	Mexico	BBOAX223	16.14865	-96.36588	2804	+		
111204	*B. ephippiatus*	Mexico	BBOAX223	16.14865	-96.36588	2804	+		
111207	*B. ephippiatus*	Mexico	BBOAX223	16.14865	-96.36588	2804	+		
111208	*B. ephippiatus*	Mexico	BBOAX223	16.14865	-96.36588	2804	+		
111209	*B. ephippiatus*	Mexico	BBOAX223	16.14865	-96.36588	2804	+		
111210	*B. ephippiatus*	Mexico	BBOAX223	16.14865	-96.36588	2804	+		
115054	*B. ephippiatus*	Guatemala	BBGUA092	14.8239	-91.3465	2722	+		+
115065	*B. ephippiatus*	Guatemala	BBGUA092	14.8239	-91.3465	2722	+		+
115066	*B. ephippiatus*	Guatemala	BBGUA092	14.824	-91.347	2722	+		

Table 1.1 (cont.)

Voucher Name	Phenotype	Country	Population	Latitude	Longitude	Altitude	MSAT	COI	WING
115067	*B. ephippiatus*	Guatemala	BBGUA092	14.8239	-91.3465	2722	+		+
115069	*B. ephippiatus*	Guatemala	BBGUA092	14.8239	-91.3465	2722	+		+
115165	*B. ephippiatus*	Guatemala	BBGUA092	14.84226	-91.40433	2922	+		+
115202	*B. ephippiatus*	Guatemala	BBGUA111	14.78708	-91.65195	2826	+	+	
115208	*B. ephippiatus*	Guatemala	BBGUA112	14.788	-91.654	2700	+		
115209	*B. ephippiatus*	Guatemala	BBGUA112	14.788	-91.654	2700	+		
115211	*B. ephippiatus*	Guatemala	BBGUA112	14.788	-91.654	2700	+		
115212	*B. ephippiatus*	Guatemala	BBGUA112	14.788	-91.654	2700	+		
115213	*B. ephippiatus*	Guatemala	BBGUA112	14.788	-91.654	2700	+		
115214	*B. ephippiatus*	Guatemala	BBGUA112	14.788	-91.654	2700	+		
115218	*B. ephippiatus*	Guatemala	BBGUA112	14.78815	-91.65405	2700	+		+
115219	*B. ephippiatus*	Guatemala	BBGUA112	14.78815	-91.65405	2700	+		+
115220	*B. ephippiatus*	Guatemala	BBGUA112	14.78815	-91.65405	2700	+		+
115221	*B. ephippiatus*	Guatemala	BBGUA112	14.78815	-91.65405	2700	+		+
115222	*B. ephippiatus*	Guatemala	BBGUA112	14.788	-91.654	2700	+		
115223	*B. ephippiatus*	Guatemala	BBGUA112	14.78815	-91.65405	2700	+		+
115225	*B. ephippiatus*	Guatemala	BBGUA113	14.79372	-91.64734	2674	+		+
115229	*B. ephippiatus*	Guatemala	BBGUA113	14.79372	-91.64734	2674	+		+
115230	*B. ephippiatus*	Guatemala	BBGUA113	14.79372	-91.64734	2674	+		+
115231	*B. ephippiatus*	Guatemala	BBGUA113	14.794	-91.647	2674	+		
115232	*B. ephippiatus*	Guatemala	BBGUA113	14.79372	-91.64734	2674	+		+
115233	*B. ephippiatus*	Guatemala	BBGUA113	14.79372	-91.64734	2674	+		+
115287	*B. ephippiatus*	Guatemala	BBGUA141	15.052	-91.491	2743	+		
115292	*B. ephippiatus*	Guatemala	BBGUA141	15.05189	-91.49088	2743	+		+
115314	*B. ephippiatus*	Guatemala	BBGUA142	15.14374	-92.06654	2865	+		+
115330	*B. ephippiatus*	Guatemala	BBGUA143	15.089	-91.526	2574	+		
115358	*B. ephippiatus*	Guatemala	BBGUA151	15.45755	-91.40934	3157	+		

Table 1.1 (cont.)

Voucher Name	Phenotype	Country	Population	Latitude	Longitude	Altitude	MSAT	COI	WING
115359	*B. ephippiatus*	Guatemala	BBGUA151	15.45755	-91.40934	3157	+		
115361	*B. ephippiatus*	Guatemala	BBGUA151	15.45755	-91.40934	3157	+		
115362	*B. ephippiatus*	Guatemala	BBGUA151	15.45755	-91.40934	3157	+		
115367	*B. ephippiatus*	Guatemala	BBGUA151	15.45755	-91.40934	3157	+		
115368	*B. ephippiatus*	Guatemala	BBGUA151	15.45755	-91.40934	3157	+		
115370	*B. ephippiatus*	Guatemala	BBGUA151	15.45755	-91.40934	3157	+		
115371	*B. ephippiatus*	Guatemala	BBGUA151	15.45755	-91.40934	3157	+		
115372	*B. ephippiatus*	Guatemala	BBGUA151	15.45755	-91.40934	3157	+		+
115373	*B. ephippiatus*	Guatemala	BBGUA151	15.45755	-91.40934	3157	+		
115374	*B. ephippiatus*	Guatemala	BBGUA151	15.45755	-91.40934	3157	+		
115375	*B. ephippiatus*	Guatemala	BBGUA151	15.45755	-91.40934	3157	+		
115376	*B. ephippiatus*	Guatemala	BBGUA151	15.45755	-91.40934	3157	+		
115377	*B. ephippiatus*	Guatemala	BBGUA151	15.45755	-91.40934	3157	+		
115378	*B. ephippiatus*	Guatemala	BBGUA151	15.45755	-91.40934	3157	+		
115399	*B. ephippiatus*	Guatemala	BBGUA151	15.45755	-91.40934	3157	+		
115400	*B. ephippiatus*	Guatemala	BBGUA151	15.45755	-91.40934	3157	+		
115401	*B. ephippiatus*	Guatemala	BBGUA151	15.45755	-91.40934	3157	+		
115402	*B. ephippiatus*	Guatemala	BBGUA151	15.45755	-91.40934	3157	+		+
115403	*B. ephippiatus*	Guatemala	BBGUA151	15.45755	-91.40934	3157	+		
115420	*B. ephippiatus*	Guatemala	BBGUA152	15.42314	-91.94025	3140	+		+
115421	*B. ephippiatus*	Guatemala	BBGUA152	15.42314	-91.94025	3140	+		
115422	*B. ephippiatus*	Guatemala	BBGUA152	15.42314	-91.94025	3140	+		
115423	*B. ephippiatus*	Guatemala	BBGUA152	15.42314	-91.94025	3140	+		+
115424	*B. ephippiatus*	Guatemala	BBGUA152	15.42314	-91.94025	3140	+		
115425	*B. ephippiatus*	Guatemala	BBGUA152	15.42314	-91.94025	3140	+		+
115426	*B. ephippiatus*	Guatemala	BBGUA152	15.42314	-91.94025	3140	+		
115428	*B. ephippiatus*	Guatemala	BBGUA152	15.42314	-91.94025	3140	+		+

Table 1.1 (cont.)

Voucher Name	Phenotype	Country	Population	Latitude	Longitude	Altitude	MSAT	COI	WING
115429	*B. ephippiatus*	Guatemala	BBGUA152	15.42314	-91.94025	3140	+		+
115430	*B. ephippiatus*	Guatemala	BBGUA131	14.75011	-91.46581	2596	+		
115436	*B. ephippiatus*	Guatemala	BBGUA131	14.75011	-91.46581	2596	+		
115529	*B. ephippiatus*	Guatemala	BBGUA171	15.142	-92.063	2712	+		
115598	*B. ephippiatus*	Guatemala	BBGUA172	15.144	-92.067	2865	+		
115599	*B. ephippiatus*	Guatemala	BBGUA172	15.144	-92.067	2865	+		
115602	*B. ephippiatus*	Guatemala	BBGUA172	15.14374	-92.06654	2865	+		+
115603	*B. ephippiatus*	Guatemala	BBGUA172	15.14374	-92.06654	2865	+		+
115619	*B. ephippiatus*	Guatemala	BBGUA172	15.144	-92.067	2865	+	+	
115627	*B. ephippiatus*	Guatemala	BBGUA173	15.151	-92.066	3020	+		
115628	*B. ephippiatus*	Guatemala	BBGUA173	15.15135	-92.06579	3020	+		+
115630	*B. ephippiatus*	Guatemala	BBGUA173	15.151	-92.066	3020	+		
115638	*B. ephippiatus*	Guatemala	BBGUA173	15.151	-92.066	3020	+		
115639	*B. ephippiatus*	Guatemala	BBGUA173	15.151	-92.066	3020	+		
115640	*B. ephippiatus*	Guatemala	BBGUA173	15.151	-92.066	3020	+		
115642	*B. ephippiatus*	Guatemala	BBGUA173	15.15135	-92.06579	3020	+		+
115644	*B. ephippiatus*	Guatemala	BBGUA173	15.15135	-92.06579	3020	+		+
115646	*B. ephippiatus*	Guatemala	BBGUA173	15.15135	-92.06579	3020	+		+
115647	*B. ephippiatus*	Guatemala	BBGUA173	15.151	-92.066	3020	+		
CARTA	*B. ephippiatus*	Costa Rica	Cartago	9.676111111	-83.87722222		+		+
CARTB	*B. ephippiatus*	Costa Rica	Cartago	9.676111111	-83.87722222		+		+
CARTC	*B. ephippiatus*	Costa Rica	Cartago	9.676111111	-83.87722222		+		+
CARTD	*B. ephippiatus*	Costa Rica	Cartago	9.676111111	-83.87722222		+		+
CdeJ-A	*B. ephippiatus*	Mexico	Chiapas	16.803097	-92.277431	1683	+	+	+
CdeJ-B	*B. ephippiatus*	Mexico	Chiapas	16.803097	-92.277431	1683	+	+	+
CdeJ-C	*B. ephippiatus*	Mexico	Chiapas	16.803097	-92.277431	1683	+	+	+
CdeJ-D	*B. ephippiatus*	Mexico	Chiapas	16.803097	-92.277431	1683	+	+	+

Table 1.1 (cont.)

Voucher Name	Phenotype	Country	Population	Latitude	Longitude	Altitude	MSAT	COI	WING
CdeJ-E	*B. ephippiatus*	Mexico	Chiapas	16.803097	-92.277431	1683	+	+	
CPA	*B. ephippiatus*	Honduras	Cusuco	15.49222222	-88.22666667	1092	+	+	+
CPB	*B. ephippiatus*	Honduras	Cusuco	15.49222222	-88.22666667	1092	+	+	+
CPC	*B. ephippiatus*	Honduras	Cusuco	15.49222222	-88.22666667	1092	+	+	+
CPD	*B. ephippiatus*	Honduras	Cusuco	15.49222222	-88.22666667	1092	+	+	+
CPE	*B. ephippiatus*	Honduras	Cusuco	15.49222222	-88.22666667	1092	+	+	+
CPF	*B. ephippiatus*	Honduras	Cusuco	15.49222222	-88.22666667	1092	+	+	+
CPG	*B. ephippiatus*	Honduras	Cusuco	15.49222222	-88.22666667	1092	+	+	+
eph73424	*B. ephippiatus*	Mexico	Chiapas				+	+	
eph74841	*B. ephippiatus*	Mexico	Chiapas	16.8824	-92.2801		+	+	
eph76297	*B. ephippiatus*	Mexico	Chiapas	16.7994	-92.7119	1683	+	+	
eph76358	*B. ephippiatus*	Mexico	Chiapas	16.754	-92.6777		+	+	
eph76640	*B. ephippiatus*	Mexico	Chiapas	15.4494	-92.2656		+	+	
eph76643	*B. ephippiatus*	Mexico	Chiapas	15.4505	-92.3198		+	+	
eph76675	*B. ephippiatus*	Mexico	Chiapas				+	+	
eph76682	*B. ephippiatus*	Mexico	Chiapas	15.2399	-92.2306		+	+	
eph76688	*B. ephippiatus*	Mexico	Chiapas				+	+	
eph76689	*B. ephippiatus*	Mexico	Chiapas	15.4494	-92.2656		+	+	
eph76690	*B. ephippiatus*	Mexico	Chiapas				+		
eph76707	*B. ephippiatus*	Mexico	Chiapas				+		
eph76708	*B. ephippiatus*	Mexico	Chiapas	15.2399	-92.2306		+	+	
eph76713	*B. ephippiatus*	Mexico	Chiapas	15.4505	-92.3198		+	+	
eph76714	*B. ephippiatus*	Mexico	Chiapas	15.4505	-92.3198		+	+	
eph78272	*B. ephippiatus*	Mexico	Chiapas				+	+	
eph78411	*B. ephippiatus*	Mexico	Chiapas				+	+	
eph78503	*B. ephippiatus*	Mexico	Chiapas				+	+	
eph78504	*B. ephippiatus*	Mexico	Chiapas	15.4505	-92.3198		+	+	

Table 1.1 (cont.)

Voucher Name	Phenotype	Country	Population	Latitude	Longitude	Altitude	MSAT	COI	WING
eph78505	*B. ephippiatus*	Mexico	Chiapas				+		
eph78541	*B. ephippiatus*	Mexico	Chiapas				+	+	
eph78545	*B. ephippiatus*	Mexico	Chiapas	15.2343	-92.2234		+	+	
eph78585	*B. ephippiatus*	Mexico	Chiapas				+	+	
eph78590	*B. ephippiatus*	Mexico	Chiapas				+	+	
eph78591	*B. ephippiatus*	Mexico	Chiapas	15.4505	-92.3198		+	+	
LT1	*B. ephippiatus*	Honduras	La Tigra	14.19444444	-87.12972222	1755	+	+	+
LT2-A	*B. ephippiatus*	Honduras	La Tigra	14.19444444	-87.12972222	1807	+		+
LT2-B	*B. ephippiatus*	Honduras	La Tigra	14.19444444	-87.12972222	1807	+		+
LT2-C	*B. ephippiatus*	Honduras	La Tigra	14.19444444	-87.12972222	1807	+	+	+
LT2-D	*B. ephippiatus*	Honduras	La Tigra	14.19444444	-87.12972222	1807	+	+	+
LT2-E	*B. ephippiatus*	Honduras	La Tigra	14.19444444	-87.12972222	1807	+	+	+
LT2-F	*B. ephippiatus*	Honduras	La Tigra	14.19444444	-87.12972222	1807	+	+	+
LT2-G	*B. ephippiatus*	Honduras	La Tigra	14.19444444	-87.12972222	1807	+	+	+
LT2-H	*B. ephippiatus*	Honduras	La Tigra	14.19444444	-87.12972222	1807	+	+	+
LT2-I	*B. ephippiatus*	Honduras	La Tigra	14.19444444	-87.12972222	1807	+	+	+
LT2-J	*B. ephippiatus*	Honduras	La Tigra	14.19444444	-87.12972222	1807	+	+	+
LT2-K	*B. ephippiatus*	Honduras	La Tigra	14.19444444	-87.12972222	1807	+	+	+
LT2-L	*B. ephippiatus*	Honduras	La Tigra	14.19444444	-87.12972222	1807	+	+	+
LT2-M	*B. ephippiatus*	Honduras	La Tigra	14.19444444	-87.12972222	1807	+		
LT2-N	*B. ephippiatus*	Honduras	La Tigra	14.19444444	-87.12972222	1807	+		
LT2-O	*B. ephippiatus*	Honduras	La Tigra	14.19444444	-87.12972222	1807	+		
LT2-P	*B. ephippiatus*	Honduras	La Tigra	14.19444444	-87.12972222	1807	+		+
LT2-Q	*B. ephippiatus*	Honduras	La Tigra	14.19444444	-87.12972222	1807	+		+
LT2-R	*B. ephippiatus*	Honduras	La Tigra	14.19444444	-87.12972222	1807	+		+
MDA	*B. ephippiatus*	Honduras	Montaña de Comayagua	14.4375	-87.56083333	1664	+	+	+
MDB	*B. ephippiatus*	Honduras	Montaña de Comayagua	14.4375	-87.56083333	1664	+	+	+

Table 1.1 (cont.)

Voucher Name	Phenotype	Country	Population	Latitude	Longitude	Altitude	MSAT	COI	WING
MDC	*B. ephippiatus*	Honduras	Montaña de Comayagua	14.4375	-87.56083333	1664	+	+	
MDD	*B. ephippiatus*	Honduras	Montaña de Comayagua	14.4375	-87.56083333	1664	+	+	+
MDE	*B. ephippiatus*	Honduras	Montaña de Comayagua	14.4375	-87.56083333	1664	+	+	+
MDF	*B. ephippiatus*	Honduras	Montaña de Comayagua	14.4375	-87.56083333	1664	+	+	+
MDG	*B. ephippiatus*	Honduras	Montaña de Comayagua	14.4375	-87.56083333	1664	+	+	+
MZ3-A	*B. ephippiatus*	Mexico	Chiapas	15.62381	-92.23264	2050	+	+	+
MZ4-N	*B. ephippiatus*	Mexico	Chiapas	15.62103	-92.28654	2087	+	+	+
SNJ1C	*B. ephippiatus*	Costa Rica	San José	10.02	-84		+		
SNJ2A	*B. ephippiatus*	Costa Rica	San José	10.02	-84		+		+
SNJ2B	*B. ephippiatus*	Costa Rica	San José	10.02	-84		+		
SNJ2C	*B. ephippiatus*	Costa Rica	San José	10.02	-84		+		+
SNJ2D	*B. ephippiatus*	Costa Rica	San José	10.02	-84		+		+
T-A	*B. ephippiatus*	Honduras	Tatumbla	14.018834	-87.096436	1779	+		+
T-B	*B. ephippiatus*	Honduras	Tatumbla	14.018834	-87.096436	1779	+	+	+
T-C	*B. ephippiatus*	Honduras	Tatumbla	14.018834	-87.096436	1779	+	+	+
T-D	*B. ephippiatus*	Honduras	Tatumbla	14.018834	-87.096436	1779	+	+	+
T-E	*B. ephippiatus*	Honduras	Tatumbla	14.018834	-87.096436	1779	+	+	
T-G	*B. ephippiatus*	Honduras	Tatumbla	14.018834	-87.096436	1779	+	+	+
T-H	*B. ephippiatus*	Honduras	Tatumbla	14.018834	-87.096436	1779	+	+	+
T-I	*B. ephippiatus*	Honduras	Tatumbla	14.018834	-87.096436	1779	+	+	+
T-J	*B. ephippiatus*	Honduras	Tatumbla	14.018834	-87.096436	1779	+		+
T-K	*B. ephippiatus*	Honduras	Tatumbla	14.018834	-87.096436	1779	+	+	+
T-L	*B. ephippiatus*	Honduras	Tatumbla	14.018834	-87.096436	1779	+		+
T-M	*B. ephippiatus*	Honduras	Tatumbla	14.018834	-87.096436	1779	+		+
T-N	*B. ephippiatus*	Honduras	Tatumbla	14.018834	-87.096436	1779	+		+
T-O	*B. ephippiatus*	Honduras	Tatumbla	14.018834	-87.096436	1779	+		+

Table 1.1 (cont.)

Voucher Name	Phenotype	Country	Population	Latitude	Longitude	Altitude	MSAT	COI	WING
T-P	*B. ephippiatus*	Honduras	Tatumbla	14.018834	-87.096436	1779	+		+
T-Q	*B. ephippiatus*	Honduras	Tatumbla	14.018834	-87.096436	1779	+		+
T-R	*B. ephippiatus*	Honduras	Tatumbla	14.018834	-87.096436	1779	+		+
T-S	*B. ephippiatus*	Honduras	Tatumbla	14.018834	-87.096436	1779	+		+
U1-A	*B. ephippiatus*	Honduras	Uyuca	14.03055556	-87.08	1638	+	+	+
U1-B	*B. ephippiatus*	Honduras	Uyuca	14.03055556	-87.08	1638	+	+	+
U1-C	*B. ephippiatus*	Honduras	Uyuca	14.03055556	-87.08	1638	+		+
U1-D	*B. ephippiatus*	Honduras	Uyuca	14.03055556	-87.08	1638	+	+	+
U1-E	*B. ephippiatus*	Honduras	Uyuca	14.03055556	-87.08	1638	+	+	+
U1-F	*B. ephippiatus*	Honduras	Uyuca	14.03055556	-87.08	1638	+	+	+
U1-G	*B. ephippiatus*	Honduras	Uyuca	14.03055556	-87.08	1638	+	+	+
U1-H	*B. ephippiatus*	Honduras	Uyuca	14.03055556	-87.08	1638	+		+
U1-I	*B. ephippiatus*	Honduras	Uyuca	14.03055556	-87.08	1638	+	+	+
U1-K	*B. ephippiatus*	Honduras	Uyuca	14.03055556	-87.08	1638	+		+
U1-L	*B. ephippiatus*	Honduras	Uyuca	14.03055556	-87.08	1638	+		+
U1-M	*B. ephippiatus*	Honduras	Uyuca	14.03055556	-87.08	1638	+		+
U1-N	*B. ephippiatus*	Honduras	Uyuca	14.03055556	-87.08	1638	+		+
U1-O	*B. ephippiatus*	Honduras	Uyuca	14.03055556	-87.08	1638	+		+
U1-P	*B. ephippiatus*	Honduras	Uyuca	14.03055556	-87.08	1638	+		+
U1-Q	*B. ephippiatus*	Honduras	Uyuca	14.03055556	-87.08	1638	+		+
U1-R	*B. ephippiatus*	Honduras	Uyuca	14.03055556	-87.08	1638	+		+
U1-S	*B. ephippiatus*	Honduras	Uyuca	14.03055556	-87.08	1638	+		+
U1-U	*B. ephippiatus*	Honduras	Uyuca	14.03055556	-87.08	1638	+		+
VEP01	*B. ephippiatus*	Mexico	Michoacan	19.118402	-101.893329	1204	+	+	+
VEP02	*B. ephippiatus*	Costa Rica	San José	9.566583333	-83.75018333	3140	+	+	+
VEP03	*B. ephippiatus*	Mexico	Chihuahua	28.221098	-108.251971		+	+	+
VEP05	*B. ephippiatus*	Mexico	Guerrero	17.474758	-100.178778		+	+	+

Table 1.1 (cont.)

Voucher Name	Phenotype	Country	Population	Latitude	Longitude	Altitude	MSAT	COI	WING
VEP06	*B. ephippiatus*	Guatemala	Guatemala	15.239095	-90.235607		+		+
VEP07	*B. ephippiatus*	Mexico	Jalisco	17.31736	-96.495108	2814	+	+	+
VEP08	*B. ephippiatus*	Guatemala	Guatemala	15.511595	-91.60564	2700	+		+
VEP09	*B. ephippiatus*	Costa Rica	Puntarenas	10.28396	-84.75961	1520	+	+	+
VEP10	*B. ephippiatus*	Guatemala	Guatemala	15.083336	-89.916665	400	+		
VEP12	*B. ephippiatus*	Mexico	Jalisco	20.0085	-103.70833		+	+	+
VEP13	*B. ephippiatus*	Mexico	Queretaro	21.17631	-99.57348		+	+	+
VEP14	*B. ephippiatus*	Mexico	Chihuahua	28.168724	-108.2131	1219	+	+	+
VEP17	*B. ephippiatus*	Mexico	Chiapas	15.117761	-92.107067		+	+	+
VEP18	*B. ephippiatus*	Costa Rica	San José	10.02	-84	1600	+	+	+
VEP19	*B. ephippiatus*	Mexico	Chiapas	15.120847	-92.096547		+	+	+
VEP20	*B. ephippiatus*	Costa Rica	Cartago	9.7	-83.9	2300	+	+	+
VEP21	*B. ephippiatus*	Mexico	Queretaro	21.13517	-99.63268		+	+	+
VEP23	*B. ephippiatus*	Costa Rica	San José	9.564651	-83.707901	2600	+	+	+
VEP24	*B. ephippiatus*	Costa Rica	Cartago	9.7	-83.9	2300	+	+	+
VEP25	*B. ephippiatus*	Mexico	Jalisco	17.31736	-96.495108	2418	+	+	+
VEP26	*B. ephippiatus*	Mexico	Chihuahua	28.168724	-108.2131	1219	+	+	
VEP27	*B. ephippiatus*	Costa Rica	Cartago	9.676111111	-83.87722222	2600	+	+	+
VEP28	*B. ephippiatus*	Costa Rica	Puntarenas	10.28396	-84.75961	1620	+	+	+
VEP29	*B. ephippiatus*	Mexico	Guerrero	17.474758	-100.178778		+	+	+
VEP33	*B. ephippiatus*	Mexico	Jalisco	20.0085	-103.70833		+	+	+
VEP34	*B. ephippiatus*	Mexico	Queretaro	21.13517	-99.63268		+	+	+
VEP36	*B. ephippiatus*	Mexico	Jalisco	19.6143	-103.56765		+	+	+
VEP38	*B. ephippiatus*	Mexico	Jalisco	19.6143	-103.56765		+	+	+
VEP43	*B. ephippiatus*	Mexico	Guerrero	17.474758	-100.178778		+	+	+
VEP44	*B. ephippiatus*	Honduras	Uyuca	14.03055556	-87.08	1638	+	+	+
VEP45	*B. ephippiatus*	Honduras	Uyuca	14.03055556	-87.08	1638	+	+	+

Table 1.1 (cont.)

Voucher Name	Phenotype	Country	Population	Latitude	Longitude	Altitude	MSAT	COI	WING
VEP46	*B. ephippiatus*	Honduras	Tatumbla	14.018834	-87.096436	1779	+	+	+
VEP47	*B. ephippiatus*	Honduras	Tatumbla	14.018834	-87.096436	1779	+	+	+
VEP50	*B. ephippiatus*	Honduras	La Tigra	14.19444444	-87.12972222	1755	+	+	+
VEP51	*B. ephippiatus*	Honduras	La Tigra	14.19722222	-87.12583333	1807	+	+	+
VEP52	*B. ephippiatus*	Honduras	Montaña de Comayagua	14.43611111	-87.56083333	1664	+	+	+
VEP53	*B. ephippiatus*	Honduras	Montaña de Comayagua	14.4375	-87.56083333	1664	+	+	+
VEP54	*B. ephippiatus*	Honduras	Cusuco	15.49638889	-88.18083333	1092	+	+	+
VEP55	*B. ephippiatus*	Honduras	Cusuco	15.49222222	-88.22666667	1092	+	+	+
VEP56	*B. ephippiatus*	Mexico	Chiapas	16.744444	-92.685		+	+	+
VEP57	*B. ephippiatus*	Mexico	Chiapas	16.744444	-92.685		+	+	+
VEP59	*B. ephippiatus*	Mexico	Chiapas	16.749722	-92.688611	2440	+	+	+
VEP60	*B. ephippiatus*	Mexico	Chiapas	16.749722	-92.688611	2440	+	+	+
VEP61	*B. ephippiatus*	Mexico	Chiapas	16.749722	-92.688611	2440	+	+	+
VEP62	*B. ephippiatus*	Mexico	Chiapas	16.749722	-92.688611	2440	+	+	+
VEP63	*B. ephippiatus*	Mexico	Chiapas	16.749722	-92.688611	2440	+	+	+
VEP64	*B. ephippiatus*	Mexico	Chiapas	16.749722	-92.688611	2440	+	+	+
VEP65	*B. ephippiatus*	Mexico	Chiapas	16.749722	-92.688611	2440	+	+	+
VEP66	*B. ephippiatus*	Mexico	Chiapas	16.749722	-92.688611	2440	+	+	+
VEP67	*B. ephippiatus*	Mexico	Chiapas	16.749722	-92.688611	2440	+	+	+
VEP68	*B. ephippiatus*	Mexico	Chiapas	16.749722	-92.688611	2440	+	+	+
VEP69	*B. ephippiatus*	Mexico	Chiapas	16.803097	-92.277431	1683	+	+	+
VEP70	*B. ephippiatus*	Mexico	Chiapas	16.803097	-92.277431	1683	+	+	+
VEP71	*B. ephippiatus*	Mexico	Chiapas	16.803097	-92.277431	1683	+	+	+
VEP72	*B. ephippiatus*	Mexico	Chiapas	16.803097	-92.277431	1683	+	+	+
VEP73	*B. ephippiatus*	Mexico	Chiapas	16.803097	-92.277431	1683	+	+	+
VEP74	*B. ephippiatus*	Mexico	Chiapas	16.803097	-92.277431	1683	+	+	+
VEP75	*B. ephippiatus*	Mexico	Chiapas	16.803097	-92.277431	1683	+	+	

Table 1.1 (cont.)

Voucher Name	Phenotype	Country	Population	Latitude	Longitude	Altitude	MSAT	COI	WING
VEP76	*B. ephippiatus*	Mexico	Chiapas	16.803097	-92.277431	1683	+	+	+
VEP77	*B. ephippiatus*	Mexico	Chiapas	16.803097	-92.277431	1683	+	+	+
VEP78	*B. ephippiatus*	Mexico	Chiapas	16.803097	-92.277431	1683	+	+	+
VEP79	*B. ephippiatus*	Mexico	Chiapas	16.803097	-92.277431	1683	+	+	+
VEP80	*B. ephippiatus*	Mexico	Chiapas	16.803097	-92.277431	1683	+	+	+
VEP81	*B. ephippiatus*	Mexico	Chiapas	16.803097	-92.277431	1683	+	+	+
45858	*B. wilmattae*	Mexico	Chiapas	15.657	-92.809	1960	+		+
45860	*B. wilmattae*	Mexico	Chiapas	15.657	-92.809	1960	+		+
45900	*B. wilmattae*	Mexico	Chiapas	15.657	-92.809	1960	+		
45903	*B. wilmattae*	Mexico	Chiapas	15.657	-92.809	1960	+		+
45905	*B. wilmattae*	Mexico	Chiapas	15.657	-92.809	1960	+		+
45906	*B. wilmattae*	Mexico	Chiapas	15.657	-92.809	1960	+		+
77026	*B. wilmattae*	Mexico	Chiapas	15.521	-92.302	1836	+		
77027	*B. wilmattae*	Mexico	Chiapas	15.52	-92.299	1896	+		
77028	*B. wilmattae*	Mexico	Chiapas	15.52	-92.299	1896	+		
77029	*B. wilmattae*	Mexico	Chiapas	15.52	-92.299	1896	+		
77030	*B. wilmattae*	Mexico	Chiapas	15.52	-92.299	1896	+		+
77031	*B. wilmattae*	Mexico	Chiapas	15.52	-92.299	1896	+		+
77032	*B. wilmattae*	Mexico	Chiapas	15.52	-92.299	1896	+		
77033	*B. wilmattae*	Mexico	Chiapas	15.52	-92.299	1896	+		+
77036	*B. wilmattae*	Mexico	Chiapas	15.52	-92.299	1896	+		+
79168	*B. wilmattae*	Mexico	Chiapas	16.153	-93.609	1331	+		+
79232	*B. wilmattae*	Mexico	Chiapas	15.339	-92.385	2029	+		
79233	*B. wilmattae*	Mexico	Chiapas	15.339	-92.385	2029	+		+
79253	*B. wilmattae*	Mexico	Chiapas	15.521	-92.302	1836	+		+
79257	*B. wilmattae*	Mexico	Chiapas	15.52	-92.299	1896	+		+
79258	*B. wilmattae*	Mexico	Chiapas	15.52	-92.299	1896	+		+

Table 1.1 (cont.)

Voucher Name	Phenotype	Country	Population	Latitude	Longitude	Altitude	MSAT	COI	WING
79259	*B. wilmattae*	Mexico	Chiapas	15.52	-92.299	1896	+		+
79261	*B. wilmattae*	Mexico	Chiapas	15.52	-92.299	1896	+		+
79303	*B. wilmattae*	Mexico	Chiapas	15.521	-92.302	1836	+		
79305	*B. wilmattae*	Mexico	Chiapas	15.52	-92.299	1896	+		
79464	*B. wilmattae*	Mexico	Chiapas				+		
79915	*B. wilmattae*	Mexico	BBCHI141	15.6197	-92.2099	1785	+		
79916	*B. wilmattae*	Mexico	BBCHI141	15.6197	-92.2099	1785	+		
79918	*B. wilmattae*	Mexico	BBCHI141	15.62	-92.21	1785	+		+
79919	*B. wilmattae*	Mexico	BBCHI141	15.6197	-92.2099	1785	+		
79920	*B. wilmattae*	Mexico	BBCHI141	15.62	-92.21	1785	+		+
79921	*B. wilmattae*	Mexico	BBCHI141	15.6197	-92.2099	1785	+		
79922	*B. wilmattae*	Mexico	BBCHI141	15.6197	-92.2099	1785	+		
79923	*B. wilmattae*	Mexico	BBCHI141	15.6197	-92.2099	1785	+		
79924	*B. wilmattae*	Mexico	BBCHI141	15.6197	-92.2099	1785	+		
79931	*B. wilmattae*	Mexico	BBCHI142	15.6178	-92.2382	2041	+		
79932	*B. wilmattae*	Mexico	BBCHI142	15.6178	-92.2382	2041	+		
79933	*B. wilmattae*	Mexico	BBCHI142	15.6178	-92.2382	2041	+		
79934	*B. wilmattae*	Mexico	BBCHI142	15.618	-92.238	2041	+		+
79935	*B. wilmattae*	Mexico	BBCHI142	15.6178	-92.2382	2041	+		
79937	*B. wilmattae*	Mexico	BBCHI142	15.6178	-92.2382	2041	+		
79938	*B. wilmattae*	Mexico	BBCHI142	15.6178	-92.2382	2041	+		
79939	*B. wilmattae*	Mexico	BBCHI142	15.618	-92.238	2041	+		+
79940	*B. wilmattae*	Mexico	BBCHI142	15.6178	-92.2382	2041	+		
79941	*B. wilmattae*	Mexico	BBCHI142	15.618	-92.238	2041	+		+
79974	*B. wilmattae*	Mexico	BBCHI111	15.3222	-92.3031	1629	+		
79975	*B. wilmattae*	Mexico	BBCHI111	15.3222	-92.3031	1629	+		
79976	*B. wilmattae*	Mexico	BBCHI111	15.3222	-92.3031	1629	+		

Table 1.1 (cont.)

Voucher Name	Phenotype	Country	Population	Latitude	Longitude	Altitude	MSAT	COI	WING
79977	*B. wilmattae*	Mexico	BBCHI111	15.322	-92.303	1629	+		+
79978	*B. wilmattae*	Mexico	BBCHI111	15.3222	-92.3031	1629	+		
79979	*B. wilmattae*	Mexico	BBCHI111	15.322	-92.303	1629	+		+
83798	*B. wilmattae*	Mexico	Chiapas	14.998	-92.165	515	+		+
83799	*B. wilmattae*	Mexico	Chiapas	15.058	-92.191	707	+		+
83800	*B. wilmattae*	Mexico	Chiapas	15.058	-92.191	707	+		+
83801	*B. wilmattae*	Mexico	Chiapas	15.058	-92.191	707	+		+
85653	*B. wilmattae*	Mexico	Chiapas				+		+
85654	*B. wilmattae*	Mexico	Chiapas				+		+
85655	*B. wilmattae*	Mexico	Chiapas				+		+
87331	*B. wilmattae*	Mexico	Chiapas				+		
87332	*B. wilmattae*	Mexico	Chiapas				+		+
87334	*B. wilmattae*	Mexico	Chiapas	15.058	-92.191	707	+		+
92175	*B. wilmattae*	Mexico	BBCHI112	15.3319	-92.2253	2274	+		
92176	*B. wilmattae*	Mexico	BBCHI112	15.3319	-92.2253	2274	+		
92177	*B. wilmattae*	Mexico	BBCHI112	15.3319	-92.2253	2274	+		
92178	*B. wilmattae*	Mexico	BBCHI112	15.3319	-92.2253	2274	+		
92179	*B. wilmattae*	Mexico	BBCHI112	15.332	-92.225	2274	+		+
92180	*B. wilmattae*	Mexico	BBCHI112	15.3319	-92.2253	2274	+		
92181	*B. wilmattae*	Mexico	BBCHI112	15.3319	-92.2253	2274	+		
92200	*B. wilmattae*	Mexico	BBCHI113	15.2958	-92.2413	2460	+		
92201	*B. wilmattae*	Mexico	BBCHI113	15.2958	-92.2413	2460	+		
92202	*B. wilmattae*	Mexico	BBCHI113	15.2958	-92.2413	2460	+		
92204	*B. wilmattae*	Mexico	BBCHI113	15.296	-92.241	2460	+		+
92206	*B. wilmattae*	Mexico	BBCHI113	15.296	-92.241	2460	+		+
92207	*B. wilmattae*	Mexico	BBCHI113	15.2958	-92.2413	2460	+		
92215	*B. wilmattae*	Mexico	BBCHI113	15.2958	-92.2413	2460	+		

Table 1.1 (cont.)

Voucher Name	Phenotype	Country	Population	Latitude	Longitude	Altitude	MSAT	COI	WING
92241	*B. wilmattae*	Mexico	BBCHI101	15.0945	-92.0842	1840	+		
92242	*B. wilmattae*	Mexico	BBCHI101	15.0945	-92.0842	1840	+		
92243	*B. wilmattae*	Mexico	BBCHI101	15.0945	-92.0842	1840	+		
92244	*B. wilmattae*	Mexico	BBCHI101	15.095	-92.084	1840	+		+
92245	*B. wilmattae*	Mexico	BBCHI101	15.0945	-92.0842	1840	+		
92246	*B. wilmattae*	Mexico	BBCHI101	15.0945	-92.0842	1840	+		
92247	*B. wilmattae*	Mexico	BBCHI101	15.095	-92.084	1840	+		+
92268	*B. wilmattae*	Mexico	BBCHI102	15.093	-92.1143	1866	+		
92269	*B. wilmattae*	Mexico	BBCHI102	15.093	-92.1143	1866	+		
92270	*B. wilmattae*	Mexico	BBCHI102	15.093	-92.1143	1866	+		
92272	*B. wilmattae*	Mexico	BBCHI102	15.093	-92.114	1866	+		+
92273	*B. wilmattae*	Mexico	BBCHI102	15.093	-92.1143	1866	+		
92274	*B. wilmattae*	Mexico	BBCHI102	15.093	-92.114	1866	+		+
92275	*B. wilmattae*	Mexico	BBCHI102	15.093	-92.1143	1866	+		
92293	*B. wilmattae*	Mexico	BBCHI103	15.1996	-92.198	1815	+		
92294	*B. wilmattae*	Mexico	BBCHI103	15.1996	-92.198	1815	+		
92295	*B. wilmattae*	Mexico	BBCHI103	15.1996	-92.198	1815	+		
92296	*B. wilmattae*	Mexico	BBCHI103	15.1996	-92.198	1815	+		
92297	*B. wilmattae*	Mexico	BBCHI103	15.2	-92.198	1815	+		+
92298	*B. wilmattae*	Mexico	BBCHI103	15.1996	-92.198	1815	+		
92418	*B. wilmattae*	Mexico	BBCHI131	16.146	-93.594	1358	+		+
115041	*B. wilmattae*	Guatemala	BBGUA092	14.824	-91.347	2722	+		
115053	*B. wilmattae*	Guatemala	BBGUA092	14.8239	-91.3465	2722	+	+	+
115071	*B. wilmattae*	Guatemala	BBGUA093	14.83958	-91.36332	2966	+		+
115072	*B. wilmattae*	Guatemala	BBGUA093	14.84	-91.363	2966	+		
115094	*B. wilmattae*	Guatemala	BBGUA094	14.855	-91.371	2826	+		
115097	*B. wilmattae*	Guatemala	BBGUA094	14.85456	-91.37123	2826	+		+

Table 1.1 (cont.)

Voucher Name	Phenotype	Country	Population	Latitude	Longitude	Altitude	MSAT	COI	WING
115099	*B. wilmattae*	Guatemala	BBGUA094	14.85456	-91.37123	2826	+		+
115158	*B. wilmattae*	Guatemala	BBGUA096	14.84226	-91.40433	2922	+		+
115162	*B. wilmattae*	Guatemala	BBGUA096	14.84226	-91.40433	2922	+		+
115173	*B. wilmattae*	Guatemala	BBGUA097	14.842	-91.388	2943	+		
115174	*B. wilmattae*	Guatemala	BBGUA097	14.842	-91.388	2943	+		
115175	*B. wilmattae*	Guatemala	BBGUA097	14.84196	-91.38822	2943	+		+
115191	*B. wilmattae*	Guatemala	BBGUA111	14.787	-91.652	2826	+		
115192	*B. wilmattae*	Guatemala	BBGUA111	14.78708	-91.65195	2826	+		+
115193	*B. wilmattae*	Guatemala	BBGUA111	14.78708	-91.65195	2826	+		+
115194	*B. wilmattae*	Guatemala	BBGUA111	14.787	-91.652	2826	+		
115195	*B. wilmattae*	Guatemala	BBGUA111	14.787	-91.652	2826	+		
115196	*B. wilmattae*	Guatemala	BBGUA111	14.787	-91.652	2826	+		
115197	*B. wilmattae*	Guatemala	BBGUA111	14.787	-91.652	2826	+		
115198	*B. wilmattae*	Guatemala	BBGUA111	14.787	-91.652	2826	+		
115199	*B. wilmattae*	Guatemala	BBGUA111	14.78708	-91.65195	2826	+		+
115200	*B. wilmattae*	Guatemala	BBGUA111	14.787	-91.652	2826	+		
115201	*B. wilmattae*	Guatemala	BBGUA111	14.787	-91.652	2826	+		
115203	*B. wilmattae*	Guatemala	BBGUA111	14.78708	-91.65195	2826	+		+
115204	*B. wilmattae*	Guatemala	BBGUA111	14.787	-91.652	2826	+		
115205	*B. wilmattae*	Guatemala	BBGUA111	14.787	-91.652	2826	+		
115206	*B. wilmattae*	Guatemala	BBGUA111	14.78708	-91.65195	2826	+		+
115207	*B. wilmattae*	Guatemala	BBGUA111	14.787	-91.652	2826	+		
115215	*B. wilmattae*	Guatemala	BBGUA112	14.788	-91.654	2700	+		
115216	*B. wilmattae*	Guatemala	BBGUA112	14.78815	-91.65405	2700	+		+
115217	*B. wilmattae*	Guatemala	BBGUA112	14.78815	-91.65405	2700	+		+
115237	*B. wilmattae*	Guatemala	BBGUA112	14.83138	-91.49361	2506	+		+
115262	*B. wilmattae*	Guatemala	BBGUA123	14.82856	-91.49358	2514	+		+

Table 1.1 (cont.)

Voucher Name	Phenotype	Country	Population	Latitude	Longitude	Altitude	MSAT	COI	WING
115267	*B. wilmattae*	Guatemala	BBGUA123	14.82856	-91.49358	2514	+		+
115275	*B. wilmattae*	Guatemala	BBGUA123	14.82856	-91.49358	2514	+		+
115293	*B. wilmattae*	Guatemala	BBGUA141	15.05189	-91.49088	2743	+		+
115301	*B. wilmattae*	Guatemala	BBGUA141	15.05189	-91.49088	2743	+		+
115332	*B. wilmattae*	Guatemala	BBGUA143	15.089	-91.526	2574	+		
115333	*B. wilmattae*	Guatemala	BBGUA143	15.08949	-91.52551	2574	+		+
115334	*B. wilmattae*	Guatemala	BBGUA143	15.089	-91.526	2574	+		
115335	*B. wilmattae*	Guatemala	BBGUA143	15.08949	-91.52551	2574	+		+
115341	*B. wilmattae*	Guatemala	BBGUA143	15.089	-91.526	2574	+		
115342	*B. wilmattae*	Guatemala	BBGUA143	15.08949	-91.52551	2574	+		+
115343	*B. wilmattae*	Guatemala	BBGUA143	15.089	-91.526	2574	+		
115344	*B. wilmattae*	Guatemala	BBGUA143	15.08949	-91.52551	2574	+		+
115347	*B. wilmattae*	Guatemala	BBGUA143	15.089	-91.526	2574	+		
115348	*B. wilmattae*	Guatemala	BBGUA143	15.08949	-91.52551	2574	+		+
115349	*B. wilmattae*	Guatemala	BBGUA143	15.089	-91.526	2574	+		
115352	*B. wilmattae*	Guatemala	BBGUA143	15.089	-91.526	2574	+		
115354	*B. wilmattae*	Guatemala	BBGUA143	15.089	-91.526	2574	+		
115527	*B. wilmattae*	Guatemala	BBGUA171	15.142	-92.063	2712	+		
115530	*B. wilmattae*	Guatemala	BBGUA171	15.142	-92.063	2712	+		
115534	*B. wilmattae*	Guatemala	BBGUA171	15.142	-92.063	2712	+		
115535	*B. wilmattae*	Guatemala	BBGUA171	15.142	-92.063	2712	+		
115536	*B. wilmattae*	Guatemala	BBGUA171	15.14215	-92.06251	2712	+		+
115537	*B. wilmattae*	Guatemala	BBGUA171	15.142	-92.063	2712	+		
115538	*B. wilmattae*	Guatemala	BBGUA171	15.142	-92.063	2712	+		
115539	*B. wilmattae*	Guatemala	BBGUA171	15.142	-92.063	2712	+		
115540	*B. wilmattae*	Guatemala	BBGUA171	15.14215	-92.06251	2712	+		+
115541	*B. wilmattae*	Guatemala	BBGUA171	15.142	-92.063	2712	+		

Table 1.1 (cont.)

Voucher Name	Phenotype	Country	Population	Latitude	Longitude	Altitude	MSAT	COI	WING
115542	*B. wilmattae*	Guatemala	BBGUA171	15.14215	-92.06251	2712	+		+
115550	*B. wilmattae*	Guatemala	BBGUA171	15.142	-92.063	2712	+		
115551	*B. wilmattae*	Guatemala	BBGUA171	15.142	-92.063	2712	+		
115552	*B. wilmattae*	Guatemala	BBGUA171	15.142	-92.063	2712	+		
115553	*B. wilmattae*	Guatemala	BBGUA171	15.142	-92.063	2712	+		
115554	*B. wilmattae*	Guatemala	BBGUA171	15.14215	-92.06251	2712	+		+
115555	*B. wilmattae*	Guatemala	BBGUA171	15.14215	-92.06251	2712	+		+
115570	*B. wilmattae*	Guatemala	BBGUA171	15.142	-92.063	2712	+		
115571	*B. wilmattae*	Guatemala	BBGUA171	15.142	-92.063	2712	+		
115572	*B. wilmattae*	Guatemala	BBGUA171	15.142	-92.063	2712	+		
115593	*B. wilmattae*	Guatemala	BBGUA172	15.144	-92.067	2865	+		
115594	*B. wilmattae*	Guatemala	BBGUA172	15.144	-92.067	2865	+		
115600	*B. wilmattae*	Guatemala	BBGUA172	15.144	-92.067	2865	+		
115601	*B. wilmattae*	Guatemala	BBGUA172	15.144	-92.067	2865	+		
115604	*B. wilmattae*	Guatemala	BBGUA172	15.14374	-92.06654	2865	+		+
115606	*B. wilmattae*	Guatemala	BBGUA172	15.144	-92.067	2865	+		
115607	*B. wilmattae*	Guatemala	BBGUA172	15.144	-92.067	2865	+		
115608	*B. wilmattae*	Guatemala	BBGUA172	15.144	-92.067	2865	+		
115609	*B. wilmattae*	Guatemala	BBGUA172	15.144	-92.067	2865	+		
115610	*B. wilmattae*	Guatemala	BBGUA172	15.144	-92.067	2865	+		
115611	*B. wilmattae*	Guatemala	BBGUA172	15.14374	-92.06654	2865	+		+
115612	*B. wilmattae*	Guatemala	BBGUA172	15.144	-92.067	2865	+		
115613	*B. wilmattae*	Guatemala	BBGUA172	15.144	-92.067	2865	+		
115614	*B. wilmattae*	Guatemala	BBGUA172	15.144	-92.067	2865	+		
115615	*B. wilmattae*	Guatemala	BBGUA172	15.14374	-92.06654	2865	+		+
115616	*B. wilmattae*	Guatemala	BBGUA172	15.144	-92.067	2865	+		
115617	*B. wilmattae*	Guatemala	BBGUA172	15.14374	-92.06654	2865	+		+

Table 1.1 (cont.)

Voucher Name	Phenotype	Country	Population	Latitude	Longitude	Altitude	MSAT	COI	WING
115618	*B. wilmattae*	Guatemala	BBGUA172	15.14374	-92.06654	2865	+		+
115620	*B. wilmattae*	Guatemala	BBGUA173	15.151	-92.066	3020	+		
115626	*B. wilmattae*	Guatemala	BBGUA173	15.15135	-92.06579	3020	+		+
115632	*B. wilmattae*	Guatemala	BBGUA173	15.15135	-92.06579	3020	+		+
115633	*B. wilmattae*	Guatemala	BBGUA173	15.15135	-92.06579	3020	+		+
115641	*B. wilmattae*	Guatemala	BBGUA173	15.15135	-92.06579	3020	+		+
115643	*B. wilmattae*	Guatemala	BBGUA173	15.15135	-92.06579	3020	+		+
115844	*B. wilmattae*	Mexico	Chiapas				+		+
115845	*B. wilmattae*	Mexico	Chiapas				+		+
115846	*B. wilmattae*	Mexico	Chiapas				+		+
DSB1-A	*B. wilmattae*	Mexico	Chiapas	15.064531	-92.0812		+	+	+
DSB1-B	*B. wilmattae*	Mexico	Chiapas	15.064531	-92.0812		+	+	+
DSB1-C	*B. wilmattae*	Mexico	Chiapas	15.064531	-92.0812		+	+	+
DSB1-D	*B. wilmattae*	Mexico	Chiapas	15.064531	-92.0812		+	+	+
DSB1-E	*B. wilmattae*	Mexico	Chiapas	15.064531	-92.0812		+	+	+
DSC3-A	*B. wilmattae*	Mexico	Chiapas	15.064531	-92.0812		+	+	+
DSC3-B	*B. wilmattae*	Mexico	Chiapas	15.064531	-92.0812		+	+	+
DSC3-C	*B. wilmattae*	Mexico	Chiapas	15.064531	-92.0812		+	+	
DSC3-D	*B. wilmattae*	Mexico	Chiapas	15.064531	-92.0812		+	+	+
DSC3-E	*B. wilmattae*	Mexico	Chiapas	15.064531	-92.0812		+	+	+
DSC3-F	*B. wilmattae*	Mexico	Chiapas	15.064531	-92.0812		+	+	+
DSC3-G	*B. wilmattae*	Mexico	Chiapas	15.064531	-92.0812		+	+	+
DSC3-H	*B. wilmattae*	Mexico	Chiapas	15.064531	-92.0812		+	+	+
DSC3-I	*B. wilmattae*	Mexico	Chiapas	15.064531	-92.0812		+	+	+
DSCW-A	*B. wilmattae*	Mexico	Chiapas	15.064531	-92.0812		+	+	+
DSCW-B	*B. wilmattae*	Mexico	Chiapas	15.064531	-92.0812		+	+	+
MUTUAL 5161	*B. wilmattae*	Mexico	Chiapas				+	+	

Table 1.1 (cont.)

Voucher Name	Phenotype	Country	Population	Latitude	Longitude	Altitude	MSAT	COI	WING
MUTUAL 5527	*B. wilmattae*	Mexico	Chiapas				+	+	
MUTUAL 9076	*B. wilmattae*	Guatemala	Guatemala				+		
MUTUAL 9416	*B. wilmattae*	Guatemala	Guatemala				+	+	
MZ1-A	*B. wilmattae*	Mexico	Chiapas	15.62469	-92.22035	1840	+	+	+
MZ1-B	*B. wilmattae*	Mexico	Chiapas	15.62469	-92.22035	1840	+	+	+
MZ1-C	*B. wilmattae*	Mexico	Chiapas	15.62469	-92.22035	1840	+	+	+
MZ1-D	*B. wilmattae*	Mexico	Chiapas	15.62469	-92.22035	1840	+	+	+
MZ1-E	*B. wilmattae*	Mexico	Chiapas	15.62469	-92.22035	1840	+	+	+
MZ2-A	*B. wilmattae*	Mexico	Chiapas	15.62628	-92.22637	1989	+	+	+
MZ2-B	*B. wilmattae*	Mexico	Chiapas	15.62628	-92.22637	1989	+	+	+
MZ2-C	*B. wilmattae*	Mexico	Chiapas	15.62628	-92.22637	1989	+	+	+
MZ2-D	*B. wilmattae*	Mexico	Chiapas	15.62628	-92.22637	1989	+	+	+
MZ3-B	*B. wilmattae*	Mexico	Chiapas	15.62381	-92.23264	2050	+	+	+
MZ3-C	*B. wilmattae*	Mexico	Chiapas	15.62381	-92.23264	2050	+	+	+
MZ4-A	*B. wilmattae*	Mexico	Chiapas	15.62103	-92.28654	2087	+	+	+
MZ4-B	*B. wilmattae*	Mexico	Chiapas	15.62103	-92.28654	2087	+	+	+
MZ4-C	*B. wilmattae*	Mexico	Chiapas	15.62103	-92.28654	2087	+	+	+
MZ4-D	*B. wilmattae*	Mexico	Chiapas	15.62103	-92.28654	2087	+	+	+
MZ4-E	*B. wilmattae*	Mexico	Chiapas	15.62103	-92.28654	2087	+	+	+
MZ4-F	*B. wilmattae*	Mexico	Chiapas	15.62103	-92.28654	2087	+	+	+
MZ4-G	*B. wilmattae*	Mexico	Chiapas	15.62103	-92.28654	2087	+	+	+
MZ4-H	*B. wilmattae*	Mexico	Chiapas	15.62103	-92.28654	2087	+	+	+
MZ4-I	*B. wilmattae*	Mexico	Chiapas	15.62103	-92.28654	2087	+	+	+
MZ4-J	*B. wilmattae*	Mexico	Chiapas	15.62103	-92.28654	2087	+	+	+
MZ4-K	*B. wilmattae*	Mexico	Chiapas	15.62103	-92.28654	2087	+	+	+
MZ4-L	*B. wilmattae*	Mexico	Chiapas	15.62103	-92.28654	2087	+	+	+
MZ4-M	*B. wilmattae*	Mexico	Chiapas	15.62103	-92.28654	2087	+	+	+

Table 1.1 (cont.)

Voucher Name	Phenotype	Country	Population	Latitude	Longitude	Altitude	MSAT	COI	WING
MZ4-O	*B. wilmattae*	Mexico	Chiapas	15.62103	-92.28654	2087	+	+	+
MZ5-A	*B. wilmattae*	Mexico	Chiapas	15.60989	-92.2259	2084	+	+	+
MZ5-B	*B. wilmattae*	Mexico	Chiapas	15.60989	-92.2259	2084	+	+	+
MZ6-A	*B. wilmattae*	Mexico	Chiapas	15.60716	-92.21432	1826	+	+	+
MZ7-A	*B. wilmattae*	Mexico	Chiapas	15.58993	-92.28812	2024	+	+	+
MZ7-B	*B. wilmattae*	Mexico	Chiapas	15.58993	-92.28812	2024	+	+	+
MZ7-C	*B. wilmattae*	Mexico	Chiapas	15.58993	-92.28812	2024	+	+	+
MZ7-D	*B. wilmattae*	Mexico	Chiapas	15.58993	-92.28812	2024	+	+	+
MZ7-E	*B. wilmattae*	Mexico	Chiapas	15.58993	-92.28812	2024	+	+	+
MZ7-F	*B. wilmattae*	Mexico	Chiapas	15.58993	-92.28812	2024	+	+	+
VWILM04	*B. wilmattae*	Mexico	Chiapas	15.120847	-92.096547		+	+	+
VWILM06	*B. wilmattae*	Mexico	Chiapas	15.05	-92.283333	1491	+	+	+
VWILM07	*B. wilmattae*	Mexico	Chiapas	15.05	-92.283333	1491	+	+	+
VWILM10	*B. wilmattae*	Mexico	Chiapas	15.09036667	-92.28638333		+		+
wilm76673	*B. wilmattae*	Mexico	Chiapas				+	+	
wilm76687	*B. wilmattae*	Mexico	Chiapas				+	+	
wilm76696	*B. wilmattae*	Mexico	Chiapas	15.3429	-92.219		+	+	
wilm76697	*B. wilmattae*	Mexico	Chiapas				+	+	
wilm76698	*B. wilmattae*	Mexico	Chiapas	15.3429	-92.219		+		
wilm76699	*B. wilmattae*	Mexico	Chiapas	15.3429	-92.219		+	+	
wilm76700	*B. wilmattae*	Mexico	Chiapas	15.3429	-92.219		+	+	
wilm76706	*B. wilmattae*	Mexico	Chiapas	15.3429	-92.219		+	+	
wilm78527	*B. wilmattae*	Mexico	Chiapas				+	+	
wilm78573	*B. wilmattae*	Mexico	Chiapas	15.3429	-92.219		+		
wilm78574	*B. wilmattae*	Mexico	Chiapas				+	+	
wilm78575	*B. wilmattae*	Mexico	Chiapas				+	+	
wilm78576	*B. wilmattae*	Mexico	Chiapas				+	+	

Table 1.1 (cont.)

Voucher Name	Phenotype	Country	Population	Latitude	Longitude	Altitude	MSAT	COI	WING
wilm78577	*B. wilmattae*	Mexico	Chiapas				+	+	
wilm78578	*B. wilmattae*	Mexico	Chiapas	15.3429	-92.219		+	+	
wilm78587	*B. wilmattae*	Mexico	Chiapas				+	+	
wilm78588	*B. wilmattae*	Mexico	Chiapas				+	+	

Table 1.2. Summary of the six analyses run in GENELAND. If a + is indicated under "GPS," a spatial dataset was included in the analysis that consisted of the GPS coordinates for each specimen in UTM format. If a + is indicated under "MORPH," a phenotype dataset was included in the analysis that consisted of the regression residuals of the 20 Procrustes superimposed landmark coordinates for each sample. "N" indicates the total sample size for each analysis and "burnin" indicates the number of iterations discarded before the MCMC chain reached stationarity (I assessed this individually for each analysis). Under "K (logLk)" are the K values for the replicates with the highest log likelihood values with their corresponding log likelihood values (after burnin) in parentheses.

	DNA	GPS	MORPH	N MEX	NUC CA	N	burnin	K (logLk)
1	+	+	+	+	+	606	300	8 (81607.2106)
2	+	+		+	+	606	200	8 (-24524.6806)
3	+	+	+	+		281	200	3 (40686.0608)
4	+	+		+		1229	450	5 (-42727.4268)
5	+	+	+		+	310	200	5 (40414.5477)
6	+	+			+	624	300	6 (-26724.7870)

Table 1.3. Pairwise F_{ST} estimates for major clades and groups in the Bayesian COI phylogeny (Fig. 1.4). EPH = *B. ephippiatus;* WILM = *B. wilmattae.*

		EPH	EPH	EPH	WILM	EPH	EPH	EPH	WILM
		Mexico North of IT	Mexico South of IT Guatemala (c)	Honduras	Mexico South of IT (f)	Costa Rica (h)	Mexico South of IT (i)	Honduras (g)	Mexico South of IT Guatemala (e)
EPH	Mexico South of IT Guatemala (c)	0.64146							
EPH	Honduras	0.71013	0.97734						
WILM	Mexico South of IT (f)	0.77475	0.93866	0.86435					
EPH	Costa Rica (h)	0.90445	0.99081	1.00000	0.96449				
EPH	Mexico South of IT (i)	0.71013	0.97734	0.00000	0.86435	1.00000			
EPH	Honduras (g)	0.90445	0.99081	1.00000	0.96449	1.00000	1.00000		
WILM	Mexico South of IT Guatemala (e)	0.90445	0.99081	1.00000	0.96449	1.00000	1.00000	1.00000	
	B. impatiens	0.87577	0.92398	0.90909	0.90342	0.93548	0.90909	0.93548	0.93548

Table 1.4. Average nucleotide differences within and between major clades and groups in the Bayesian COI phylogeny (Fig. 1.4). EPH = *B. ephippiatus;* WILM = *B. wilmattae.*

		EPH Mexico North of IT	EPH Mexico South of IT Guatemala (c)	EPH Honduras	WILM Mexico South of IT (f)	EPH Costa Rica (h)	EPH Mexico South of IT (i)	EPH Honduras (g)	WILM Mexico South of IT Guatemala (e)	*B. impatiens*
EPH	**Mexico North of IT**	0.11159								
EPH	**Mexico South of IT Guatemala (c)**	0.16609	0.02269							
EPH	**Honduras**	0.25746	0.45401	0.12158						
WILM	**Mexico South of IT (f)**	0.69396	1.12898	1.00580	0.05068					
EPH	**Costa Rica (h)**	0.92478	1.13440	1.00382	1.01591	0.02737				
EPH	**Mexico South of IT (i)**	0.43157	0.87472	0.74340	0.38570	0.63021	0.00000			
EPH	**Honduras (g)**	0.73687	1.06264	0.93132	0.82602	1.18804	0.62244	0.01171		
WILM	**Mexico South of IT Guatemala (e)**	0.55487053	0.751418002	0.765228113	0.755610358	0.75351418	0.616522811	0.869050555	0.00000	
	B. impatiens	1.209371147	1.655610358	1.720221948	1.906411837	1.90431566	1.644019729	1.896547472	1.767324291	0.164364982

Table 1.5. Pairwise net nucleotide distances calculated by STRUCTURE for each K cluster (N=1917; K=6). Comparisons are ordered from largest to smallest net nucleotide distance. Nuc CA = Nuclear Central America; eph = *B. ephippiatus;* wilm = *B. wilmattae*.

Net Nucleotide Distance	A	B
0.1805	Sierra Madre Occidental	Nuc CA (eph/wilm)
0.1623	Sierra Madre Oriental	Nuc CA (eph/wilm)
0.1516	Trans-Mexican Volcanic Belt	Nuc CA (eph/wilm)
0.1465	Sierra Madre del Sur	Nuc CA (eph/wilm)
0.1316	Trans-Mexican Volcanic Belt	Nuc CA (eph)
0.1306	Sierra Madre Occidental	Nuc CA (eph)
0.1252	Sierra Madre Oriental	Nuc CA (eph)
0.1161	Sierra Madre del Sur	Nuc CA (eph)
0.0839	Sierra Madre Occidental	Sierra Madre del Sur
0.0754	Nuc CA (eph/wilm)	Nuc CA (eph)
0.0592	Sierra Madre Occidental	Trans-Mexican Volcanic Belt
0.0565	Sierra Madre Occidental	Sierra Madre Oriental
0.0523	Sierra Madre del Sur	Trans-Mexican Volcanic Belt
0.0337	Sierra Madre Oriental	Sierra Madre del Sur
0.0279	Sierra Madre Oriental	Trans-Mexican Volcanic Belt

Table 1.6. Pairwise comparison matrix of the assignment of individuals to distinct genetic clusters by Geneland (scenario 1) and STRUCTURE (N=1917). Empty cells indicate that a given STRUCTURE cluster has no samples in common with a given GENELAND group. SMOcc= Sierra Madre Occidental; SMOri=Sierra Madre Oriental; TMVB= Trans-Mexican Volcanic Belt; SMdS= Sierra Madre del Sur; Nuc CA (eph)= Nuclear Central America *B. ephippiatus*; Nuc CA (eph/wilm)= Nuclear Central America *B. ephippiatus* and *B. wilmattae;* CR= Costa Rica.

		K (DNA + GPS + MORPH)							
		1	**2**	**3**	**4**	**5**	**6**	**7**	**8**
STRUCTURE	**Nuc CA (eph)**	62	22			27	11		
	Nuc CA (eph/wilm)	6	69	15		40	58		
	TMVB				108				
	SMOri				70				
	SMdS				45				
	CR							15	
	SMOcc				5				53

Table 1.7. Pairwise comparison matrix of the assignment of individuals to distinct genetic clusters by Geneland (scenario 1) and Geneland (scenario 2). Empty cells indicate that a given Geneland (scenario 1) group has no samples in common with a given Geneland (scenario 2) group.

K (DNA + GPS) \ K (DNA + GPS + MORPH)	1	2	3	4	5	6	7	8
1	68				26			
2		91				8		
3			15					
4				228				
5					41			
6						61		
7							15	
8								53

Table 1.8. Pairwise comparison matrix of the assignment of individuals to distinct genetic clusters by Geneland (scenario 2) and STRUCTURE (N=1917). Empty cells indicate that a given STRUCTURE cluster has no samples in common with a given GENELAND group. SMOcc= Sierra Madre Occidental; SMOri=Sierra Madre Oriental; TMVB= Trans-Mexican Volcanic Belt; SMdS= Sierra Madre del Sur; Nuc CA (eph)= Nuclear Central America *B. ephippiatus*; Nuc CA (eph/wilm)= Nuclear Central America *B. ephippiatus* and *B. wilmattae;* CR= Costa Rica.

STRUCTURE \ K (DNA + GPS)	1	2	3	4	5	6	7	8
Nuc CA (eph)	82	28			7	5		
Nuc CA (eph/wilm)	12	71	15		34	56		
TMVB				108				
SMOri				70				
SMdS				45				
CR							15	
SMOcc				5				53

Table 1.9. Pairwise comparison matrix of the assignment of individuals to distinct genetic clusters by Geneland (scenario 3) and STRUCTURE (N=1917). Empty cells indicate that a given STRUCTURE cluster has no samples in common with a given GENELAND group. SMOcc= Sierra Madre Occidental; SMOri=Sierra Madre Oriental; TMVB= Trans-Mexican Volcanic Belt; SMdS= Sierra Madre del Sur.

		DNA + GPS + MORPH		
		1	**2**	**3**
STRUCTURE	**TMVB**	108		8
	SMOri	62		
	SMOcc	5	53	
	SMdS	13		32

Table 1.10. Pairwise comparison matrix of the assignment of individuals to distinct genetic clusters by Geneland (scenario 4) and STRUCTURE (N=1917). Empty cells indicate that a given STRUCTURE cluster has no samples in common with a given GENELAND group. SMOcc= Sierra Madre Occidental; SMOri=Sierra Madre Oriental; TMVB= Trans-Mexican Volcanic Belt; SMdS= Sierra Madre del Sur.

		DNA + GPS				
		1	**2**	**3**	**4**	**5**
STRUCTURE	**SMdS**	98	55			3
	SMOri		278	5	3	14
	SMOcc		1	317	27	1
	TMVB	1	19	8	144	255

Table 1.11. Pairwise comparison matrix of the assignment of individuals to distinct genetic clusters by Geneland (scenario 5) and STRUCTURE (N=664). Empty cells indicate that a given STRUCTURE cluster has no samples in common with a given GENELAND group. eph CHI+GUA+HON = *B. ephippiatus* from Chiapas, Mexico, Guatemala and Honduras; eph HON = *B. ephippiatus* from Honduras; eph CHI = *B. ephippiatus* from Chiapas, Mexico; wilm CHI = *B. wilmattae* from Chiapas, Mexico; wilm CHI + GUA = *B. wilmattae* from Chiapas, Mexico and Guatemala.

		DNA + GPS + MORPH				
		1	**2**	**3**	**4**	**5**
STRUCTURE	**eph CHI + GUA + HON**	86	7	1	10	17
	eph HON	6	34		1	
	eph CHI	2		18		2
	wilm CHI				58	1
	wilm CHI + GUA	1				66

Table 1.12. Pairwise comparison matrix of the assignment of individuals to distinct genetic clusters by Geneland (scenario 6) and STRUCTURE (N=664). Empty cells indicate that a given STRUCTURE cluster has no samples in common with a given GENELAND group. eph CHI+GUA+HON = *B. ephippiatus* from Chiapas, Mexico, Guatemala and Honduras; eph HON = *B. ephippiatus* from Honduras; eph CHI = *B. ephippiatus* from Chiapas, Mexico; wilm CHI = *B. wilmattae* from Chiapas, Mexico; wilm CHI + GUA = *B. wilmattae* from Chiapas, Mexico and Guatemala.

		DNA + GPS					
		1	**2**	**3**	**4**	**5**	**6**
STRUCTURE	**eph CHI + GUA + HON**	133	29	6	6	28	30
	eph HON		42		1	1	
	eph CHI	5		104		2	
	wilm CHI	2			96	8	
	wilm CHI + GUA				1	111	19

Table 1.13. Pairwise Mahalanobis distances between haplotypes groups calculated by MorphoJ for all samples with morphometric and genotypic data (N=606). Comparisons are ordered from most to least different. ** indicates that the permutation test P-value was <0.0001; * indicates that the permutation test P-value was <0.05. Nuc CA = Nuclear Central America; eph = *B. ephippiatus;* wilm = *B. wilmattae*.

Mahalanobis Distance	A	B
5.4231**	Sierra Madre del Sur	Costa Rica
4.9842**	Sierra Madre Oriental	Costa Rica
4.9671**	Trans-Mexican Volcanic Belt	Costa Rica
4.8104**	Sierra Madre Occidental	Costa Rica
4.604**	Nuc CA (eph/wilm)	Costa Rica
4.3081**	Nuc CA (eph)	Costa Rica
3.6631**	Sierra Madre del Sur	Nuc CA (eph/wilm)
3.3902**	Sierra Madre Oriental	Nuc CA (eph/wilm)
3.1576**	Nuc CA (eph)	Nuc CA (eph/wilm)
3.0932**	Sierra Madre Occidental	Nuc CA (eph/wilm)
2.9982**	Sierra Madre del Sur	Sierra Madre Occidental
2.9899**	Sierra Madre Occidental	Nuc CA (eph)
2.9302**	Trans-Mexican Volcanic Belt	Nuc CA (eph/wilm)
2.8991**	Sierra Madre del Sur	Nuc CA (eph)
2.72**	Sierra Madre Oriental	Sierra Madre Occidental
2.5739**	Trans-Mexican Volcanic Belt	Nuc CA (eph)
2.4605**	Trans-Mexican Volcanic Belt	Sierra Madre del Sur
2.3864**	Sierra Madre Oriental	Nuc CA (eph)
2.2854**	Trans-Mexican Volcanic Belt	Sierra Madre Occidental
2.2303**	Trans-Mexican Volcanic Belt	Sierra Madre Oriental
1.3352*	Sierra Madre del Sur	Sierra Madre Oriental

Table 1.14. Pairwise Mahalanobis distances between haplotypes groups calculated by MorphoJ for equal sample size haplotype groups (N=17 for each haplotype group, N=119 total). Comparisons are ordered from most to least different. ** indicates that the permutation test P-value was <0.0001; * indicates that the permutation test P-value was <0.05. Nuc CA = Nuclear Central America; eph = *B. ephippiatus;* wilm = *B. wilmattae*.

Mahalanobis Distance	A	B
8.4982**	Sierra Madre del Sur	Costa Rica
8.3784**	Sierra Madre Oriental	Costa Rica
8.1556**	Trans-Mexican Volcanic Belt	Costa Rica
7.2092**	Sierra Madre Occidental	Costa Rica
6.3474**	Nuc CA (eph/wilm)	Costa Rica
6.1282**	Sierra Madre del Sur	Nuc CA (eph/wilm)
6.0663**	Nuc CA (eph)	Costa Rica
5.9101**	Trans-Mexican Volcanic Belt	Nuc CA (eph/wilm)
5.7076**	Sierra Madre Oriental	Nuc CA (eph/wilm)
5.3348**	Sierra Madre Occidental	Nuc CA (eph/wilm)
5.165**	Nuc CA (eph)	Nuc CA (eph/wilm)
4.9026**	Sierra Madre Occidental	Nuc CA (eph)
4.7405**	Sierra Madre del Sur	Nuc CA (eph)
4.6114**	Trans-Mexican Volcanic Belt	Nuc CA (eph)
4.3754**	Sierra Madre Oriental	Nuc CA (eph)
4.3493**	Sierra Madre del Sur	Sierra Madre Occidental
3.9552**	Trans-Mexican Volcanic Belt	Sierra Madre del Sur
3.8866**	Sierra Madre Oriental	Sierra Madre Occidental
3.3786**	Trans-Mexican Volcanic Belt	Sierra Madre Occidental
3.2525**	Trans-Mexican Volcanic Belt	Sierra Madre Oriental
2.3874*	Sierra Madre del Sur	Sierra Madre Oriental

Figure 1.1. Map illustrating the distinct mountain regions that *B. ephippiatus* and *B. wilmattae* inhabit. There are four major mountains chains in Mexico north of the Isthmus of Tehuantepec (IT), two mountain ranges south of the IT and north of the Nicaraguan Depression (ND), which are further split in Mexico by the Central Depression (CD), and the Talamancan montane forests south of the ND in Costa Rica and Panama.

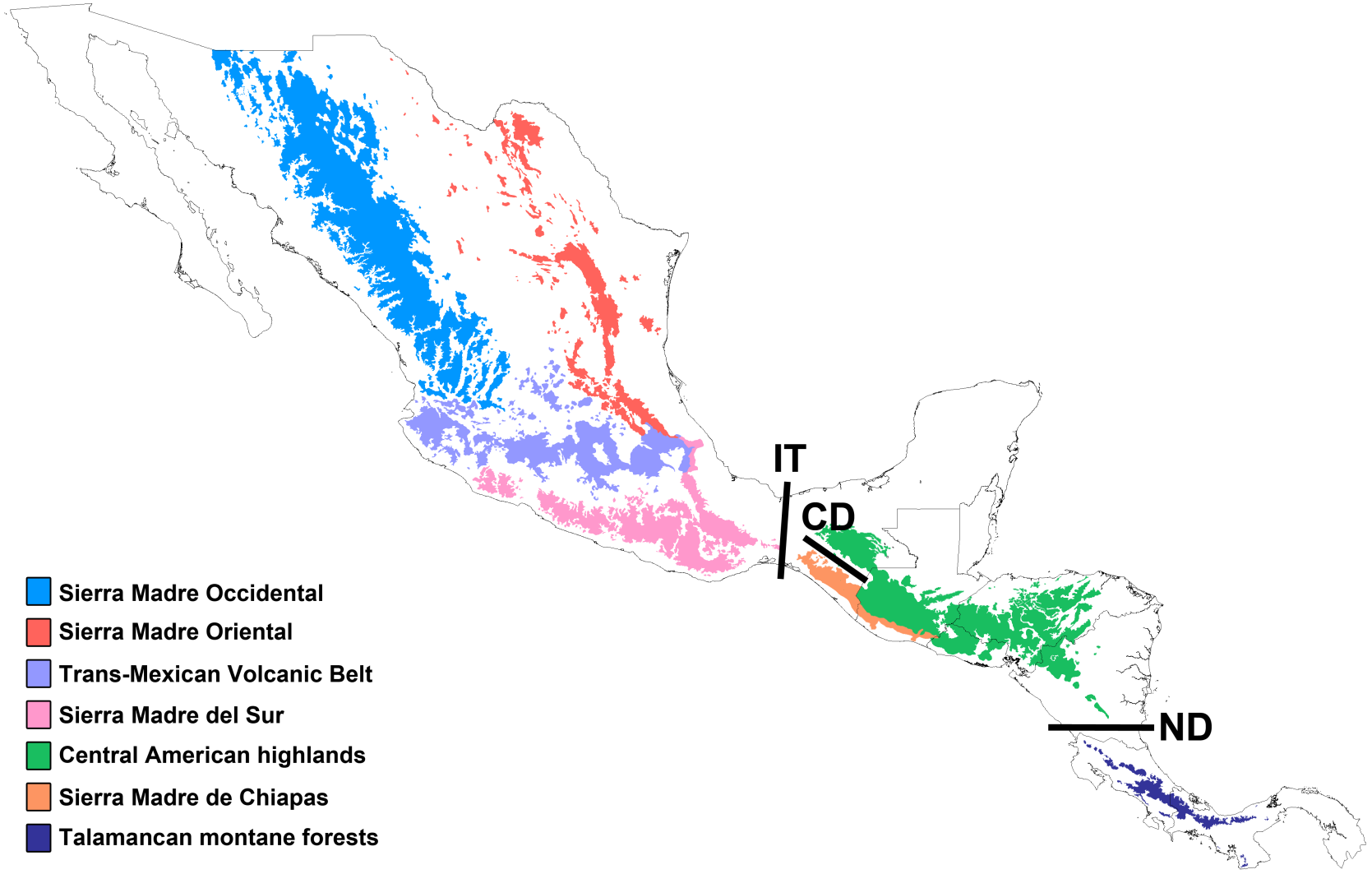

Figure 1.2. A summary of the major results from Duennes *et al.* (2012). Geographic regions and nodes on the COI phylogeny are colored according to the genotypic assignment in the STRUCTURE bar graph in the top right corner. M=Mexico, G=Guatemala, H=Honduras, N=Nicaragua, C=Costa Rica. IT=Isthmus of Tehuantepec, ND=Nicaraguan Depression. Grey-shaded areas of the map represent World Wildlife Federation (WWF) ecoregions in which the species can be found.

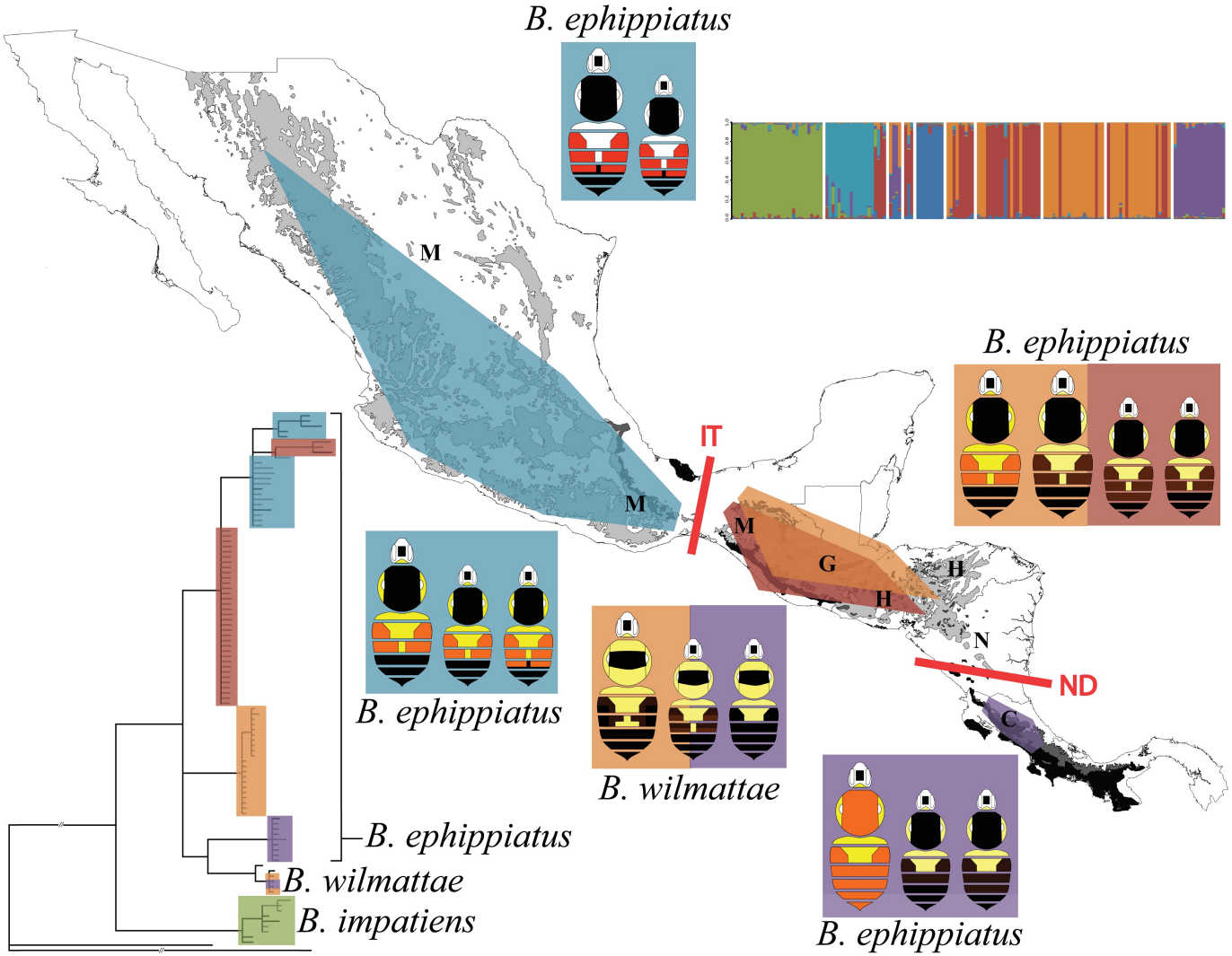

Figure 1.3. Twenty landmark positions on the left forewing that were used for geometric morphometric analyses. Landmark positions were taken from Aytekin *et al.* (2007).

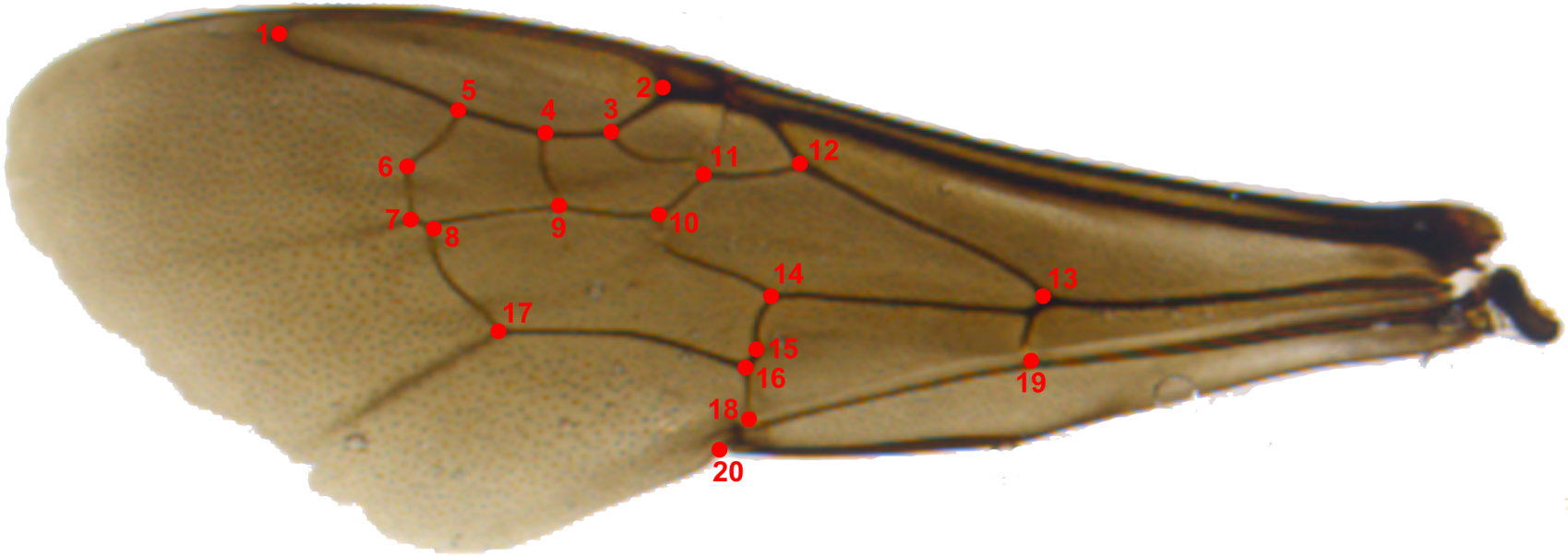

Figure 1.4. Bayesian phylogeny of 811 bp of the COI locus for 254 samples of *B. ephippiatus*, *B. wilmattae* and their sister species. All nodes in the phylogeny are colored according to their assignment in the STRUCTURE analysis of 12 microsatellite loci from the same samples presented in Figure 1.6.

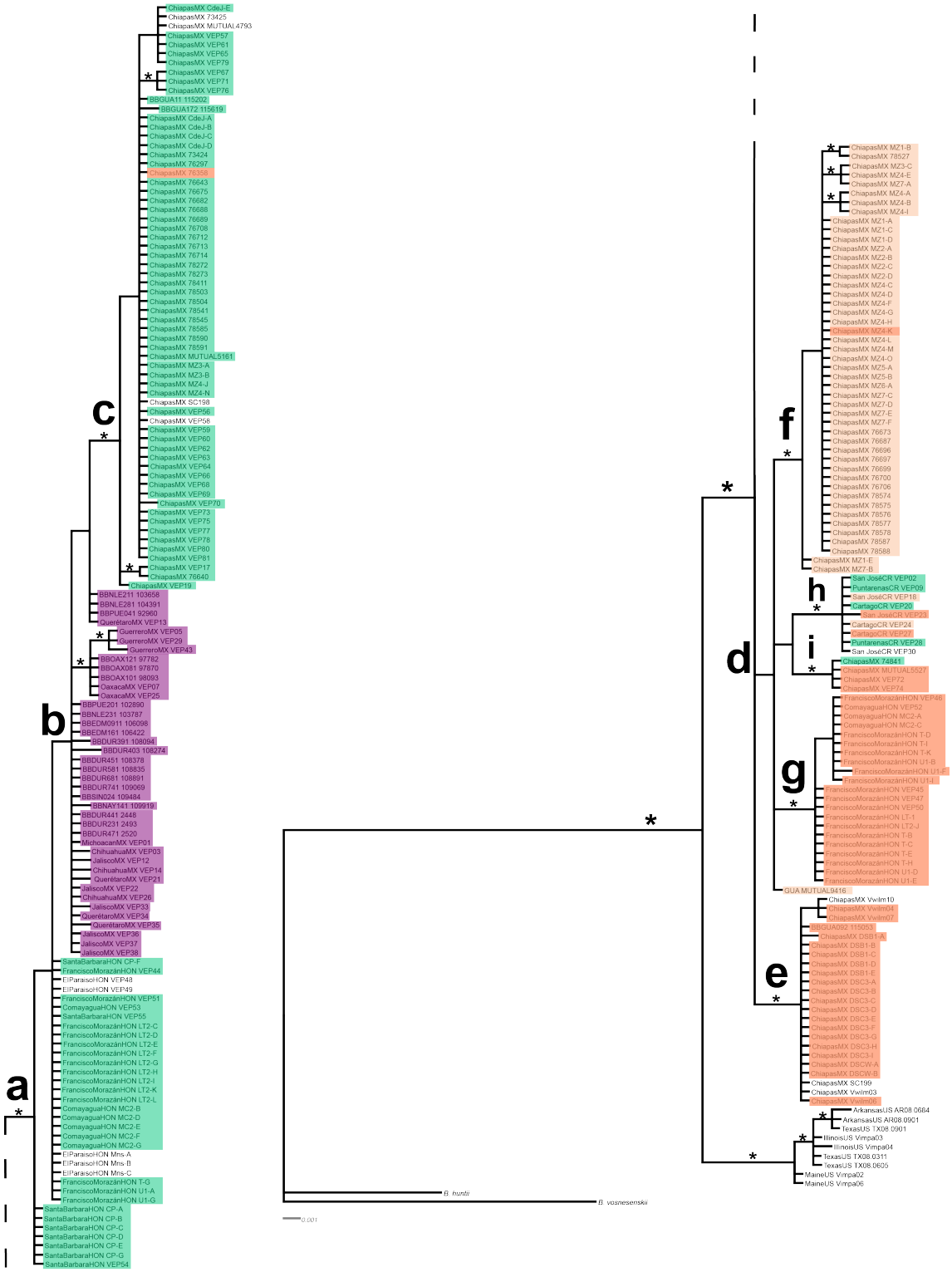

Figure 1.5. Parsimony haplotype network of 811 bp of the COI locus for samples of *B. ephippiatus* and *B. wilmattae.* The size of the circles is relative to the number of samples possessing each haplotype and black dots along connection lines represent steps. Each haplotype is colored to the assignment of each sample in the STRUCTURE analysis of 12 microsatellite loci from the same samples presented in Figure 1.6. Grey-shaded areas represent samples with COI sequence data that were not genotyped for microsatellite data.

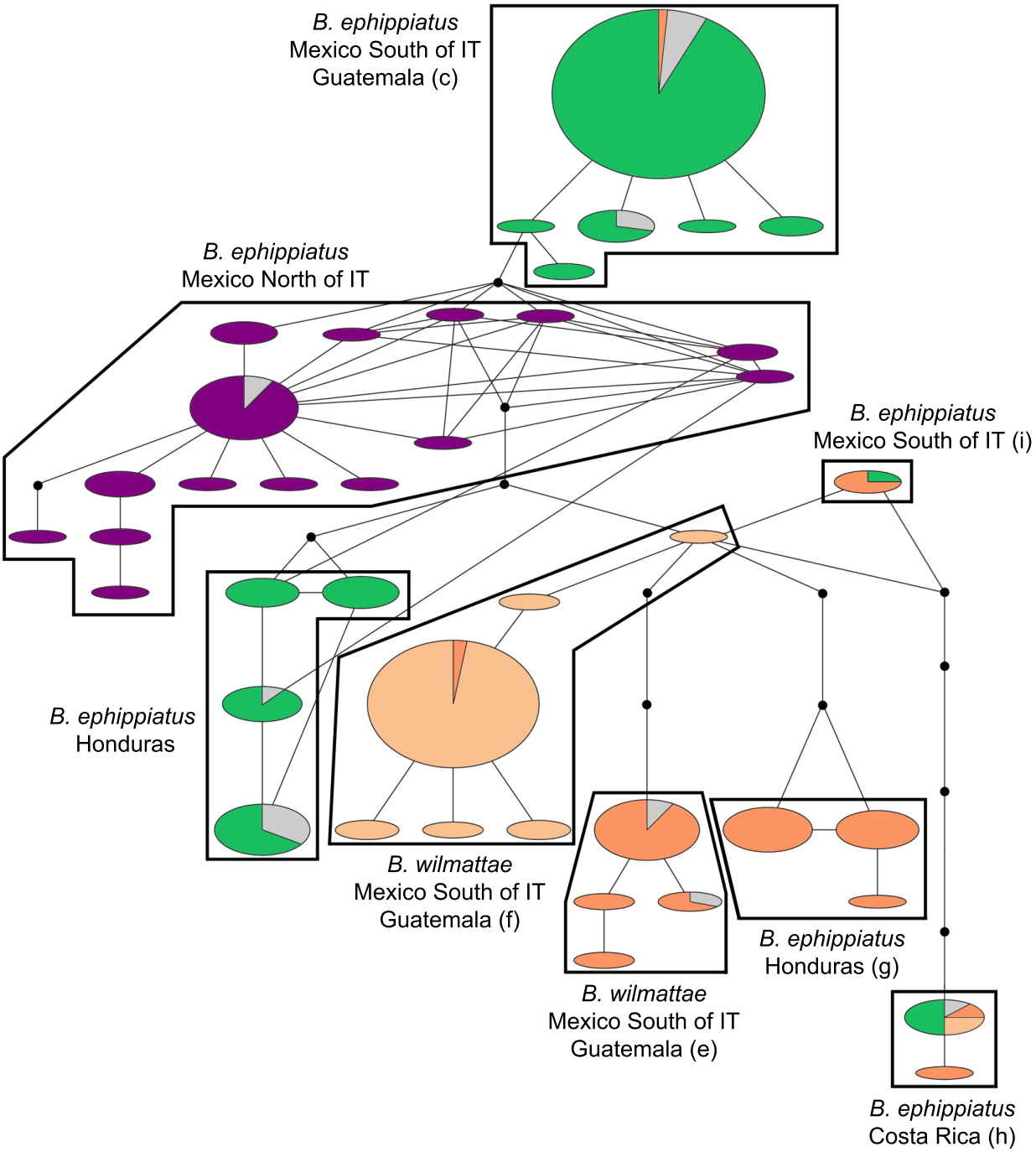

Figure 1.6. A) Bayesian phylogeny of 811 bp of the COI locus for 254 samples of *B. ephippiatus*, *B. wilmattae* and their sister species. All nodes in the phylogeny are colored according to their assignment in the **B)** STRUCTURE analysis of 12 microsatellite loci from the same samples. Individuals in the STRUCTURE graph are ordered and labeled by species designation and geographic location.

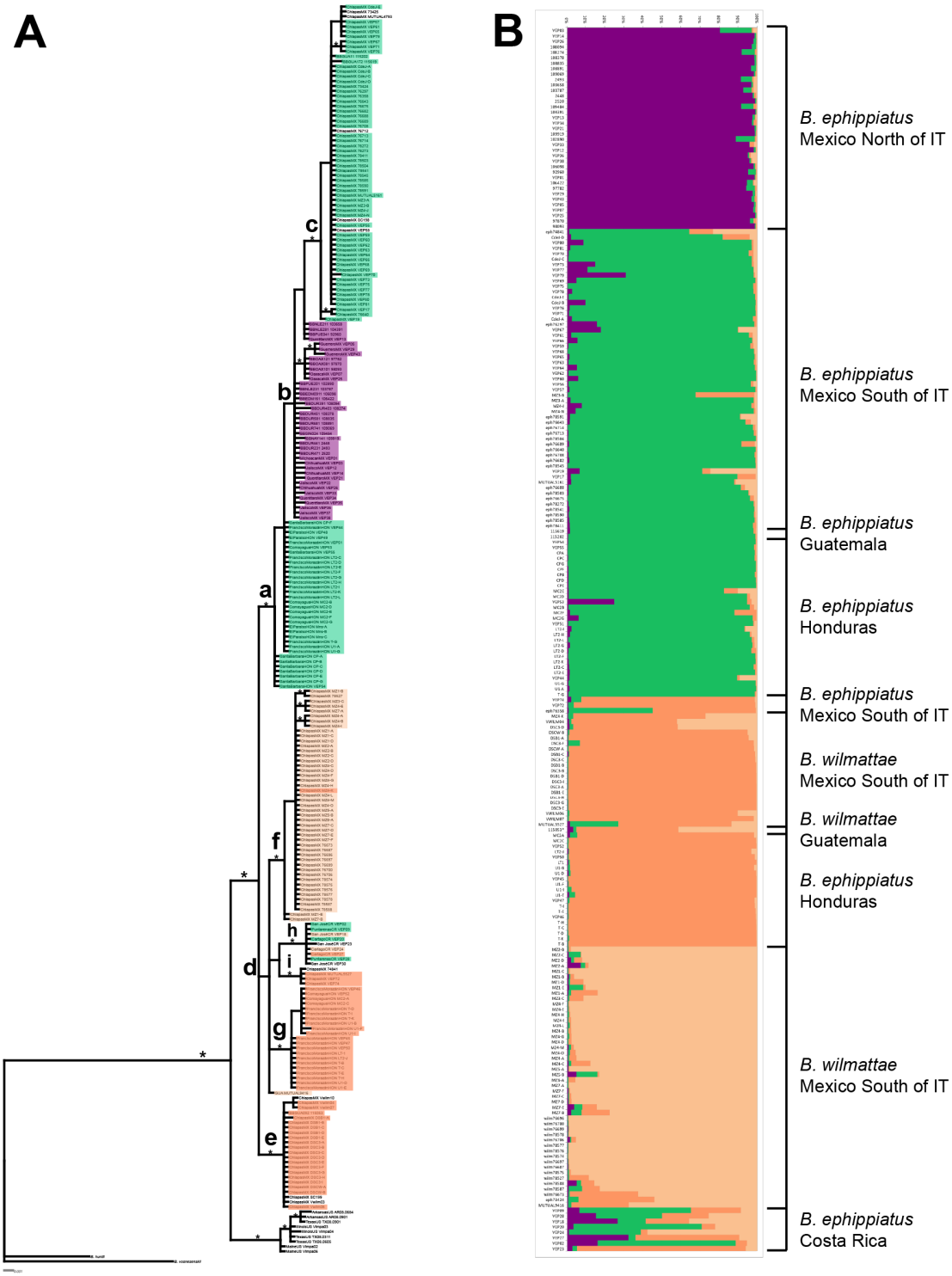

Figure 1.7. Graph of the ΔK values calculated by STRUCTURE HARVESTER for K values from two to nine for the STRUCTURE analysis of samples that were also sequenced at the COI locus.

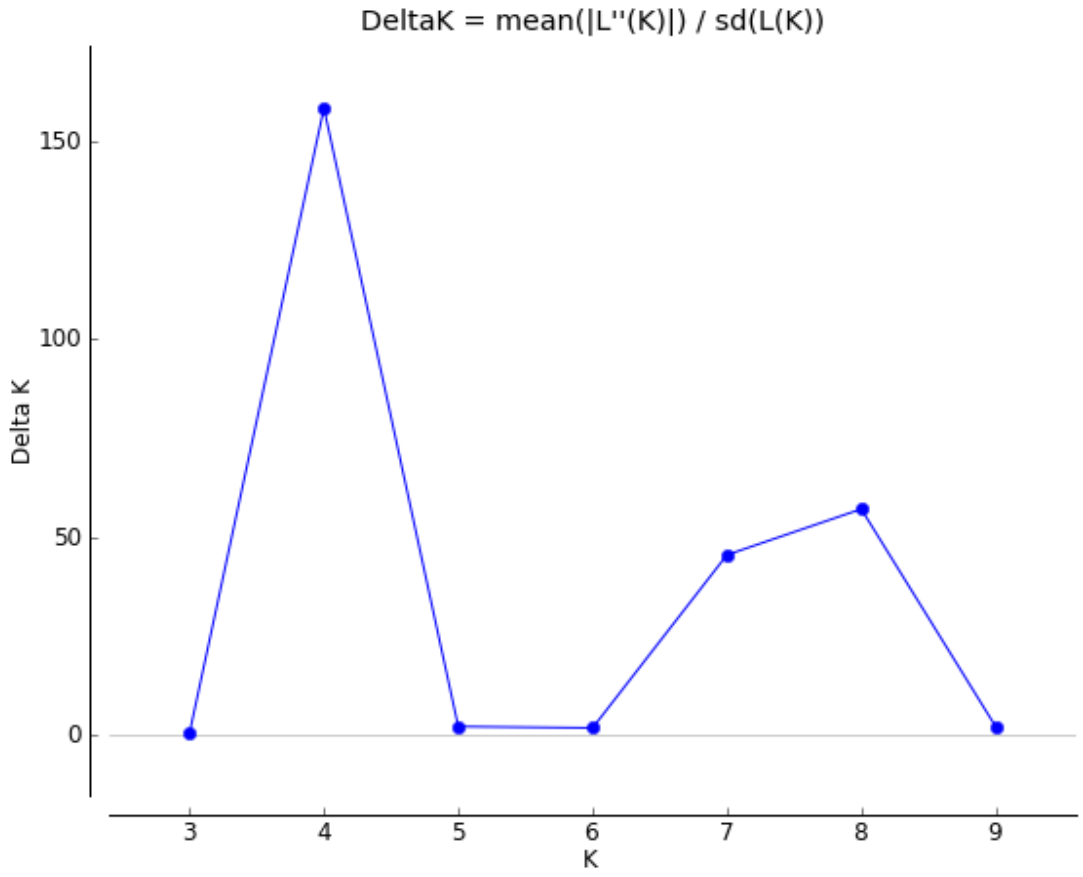

Figure 1.8. Graph of the ΔK values calculated by STRUCTURE HARVESTER for K values from two to nine for the STRUCTURE analysis of all samples with microsatellite genotype data.

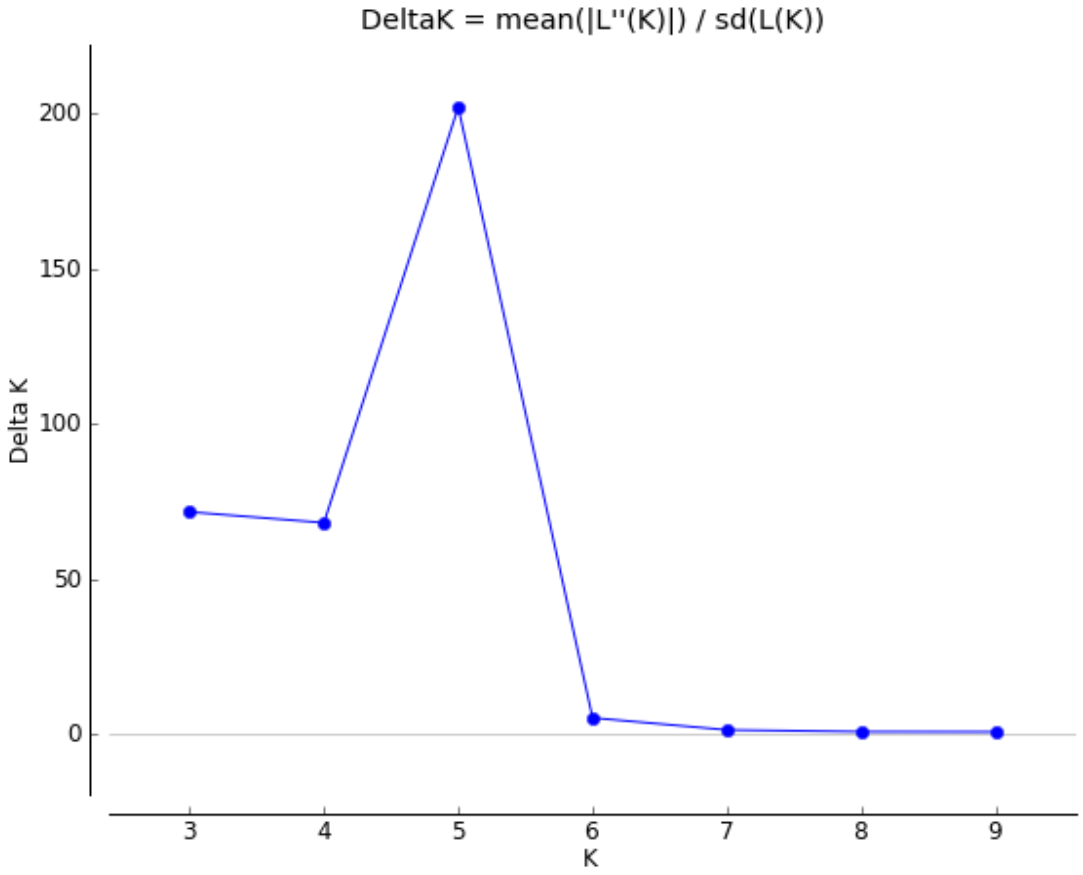

Figure 1.9. Results from the K=5 STRUCTURE analysis of the microsatellite genotype data for all samples. Samples are separated by mountain range and ordered either North to South or East to West depending on the orientation of the mountain range.

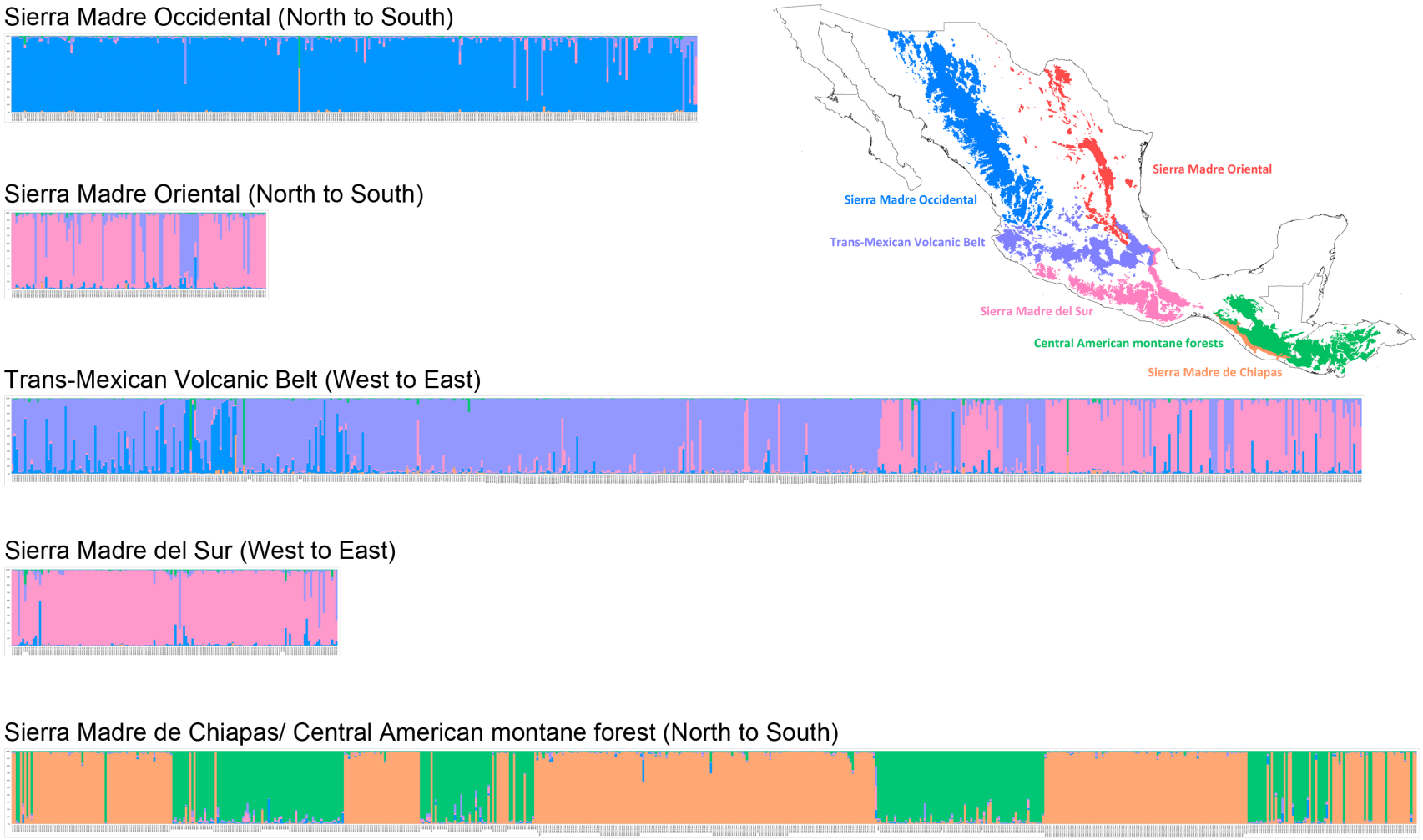

Figure 1.10. Results from the K=6 STRUCTURE analysis of the microsatellite genotype data for all samples. Samples are separated by mountain range and ordered either North to South or East to West depending on the orientation of the mountain range.

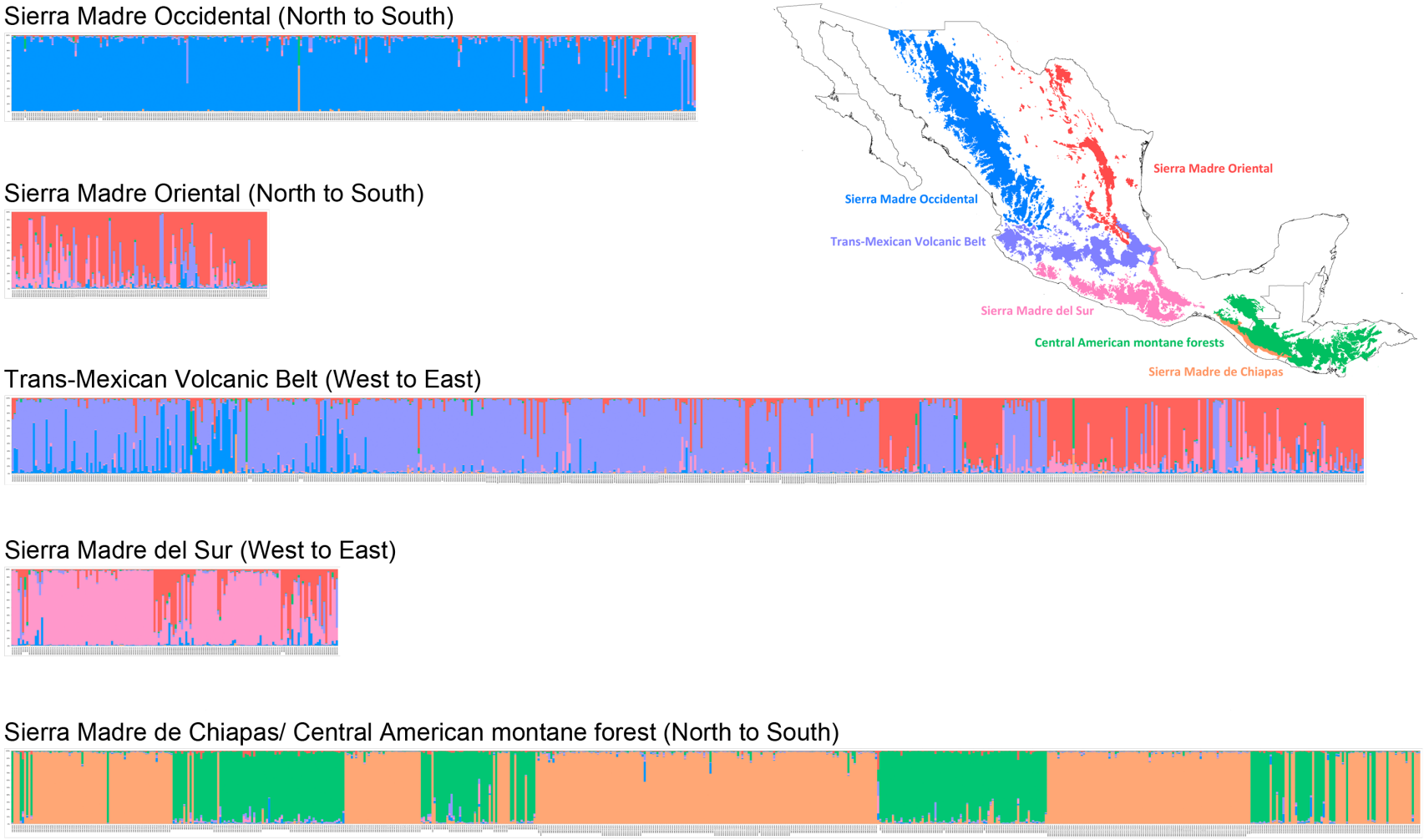

Figure 1.11. Equal sample size STRUCTURE results for K=2-7. Each geographic region and species designation is surrounded by a black box and labeled underneath for each bar graph. SMOcc= Sierra Madre Occidental; SMOri=Sierra Madre Oriental; TMVB= Trans-Mexican Volcanic Belt; SMdS= Sierra Madre del Sur; Nuc CA (eph)= Nuclear Central America *B. ephippiatus*; Nuc CA (eph/wilm)= Nuclear Central America *B. ephippiatus* and *B. wilmattae;* CR= Costa Rica.

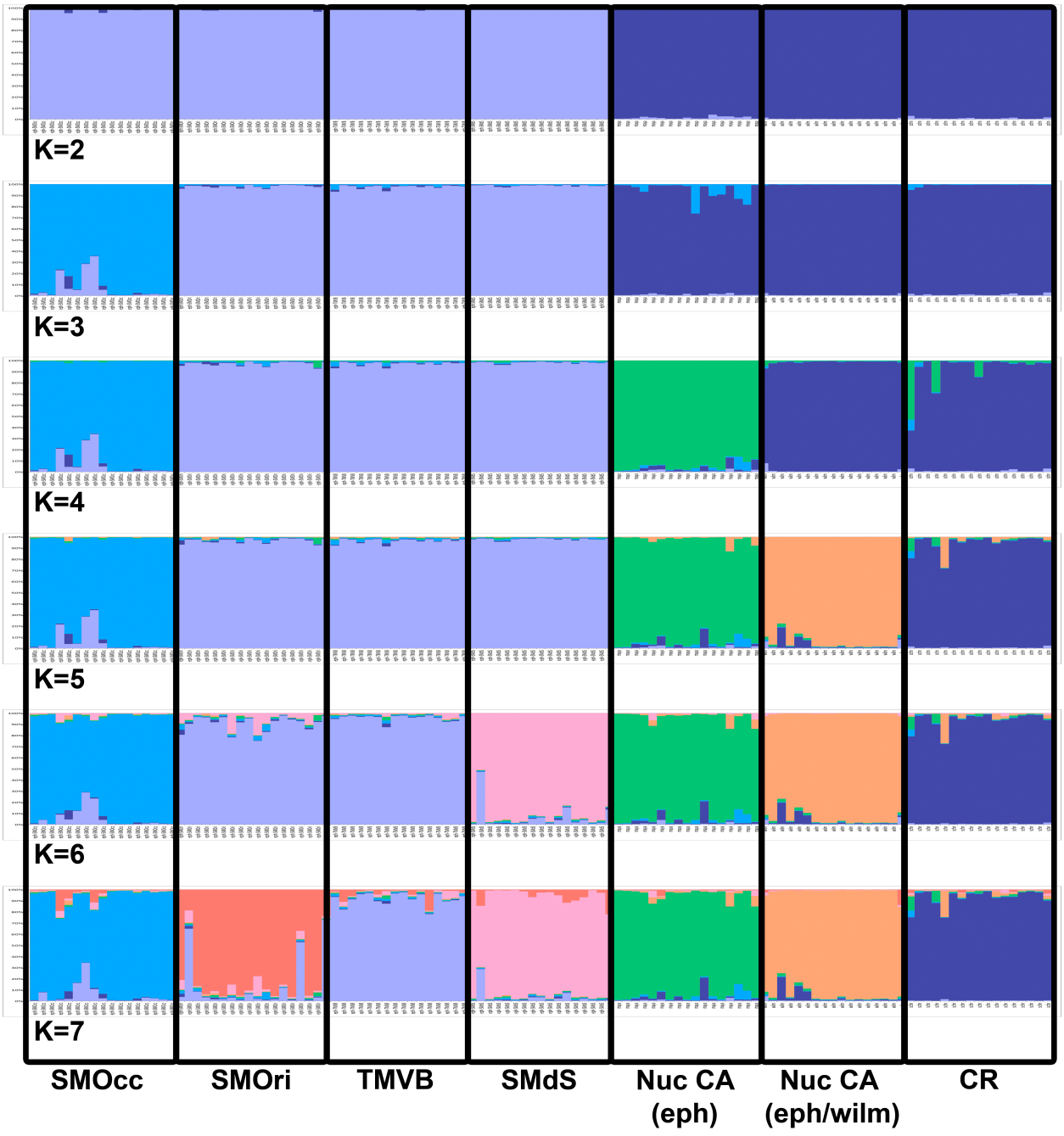

Figure 1.12. STRUCTURE results for K=2-5 for just the samples from Nuclear Central America. Each geographic region and species designation is surrounded by a black box and labeled underneath for each bar graph.

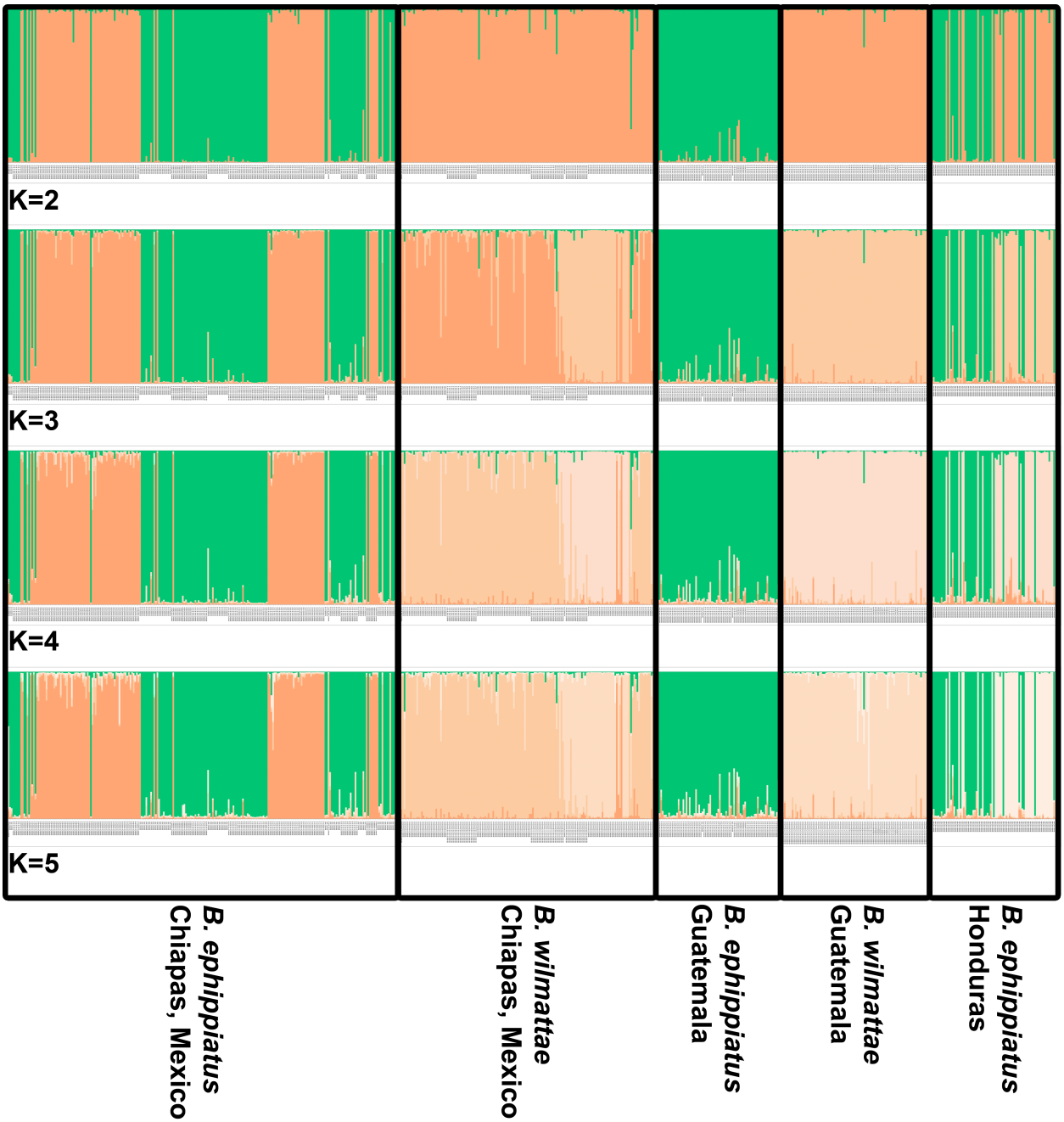

Figure 1.13. Map displaying the geographic distribution of each unique genetic lineage identified by a STRUCTURE analysis of only samples from Nuclear Central America (K=5). Grey-shaded areas of the map represent World Wildlife Federation (WWF) ecoregions in which the species can be found. eph CHI+GUA+HON = *B. ephippiatus* from Chiapas, Mexico, Guatemala and Honduras; eph HON = *B. ephippiatus* from Honduras; eph CHI = *B. ephippiatus* from Chiapas, Mexico; wilm CHI = *B. wilmattae* from Chiapas, Mexico; wilm CHI + GUA = *B. wilmattae* from Chiapas, Mexico and Guatemala.

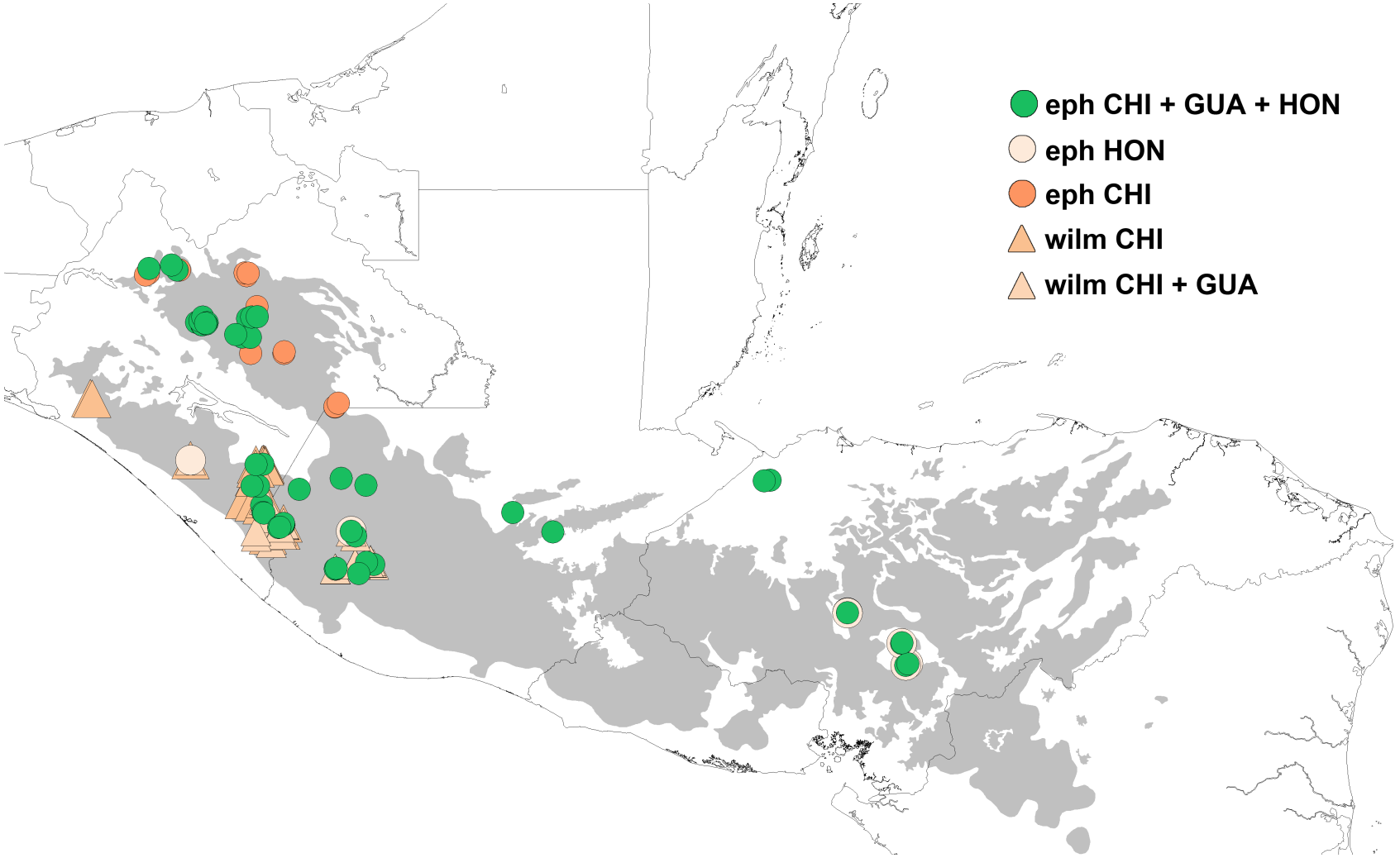

Figure 1.14. Map displaying the geographic distribution of each genetic lineage identified by GENELAND for scenario 1 (Table 1.2). Grey-shaded areas of the map represent World Wildlife Federation (WWF) ecoregions in which the species can be found.

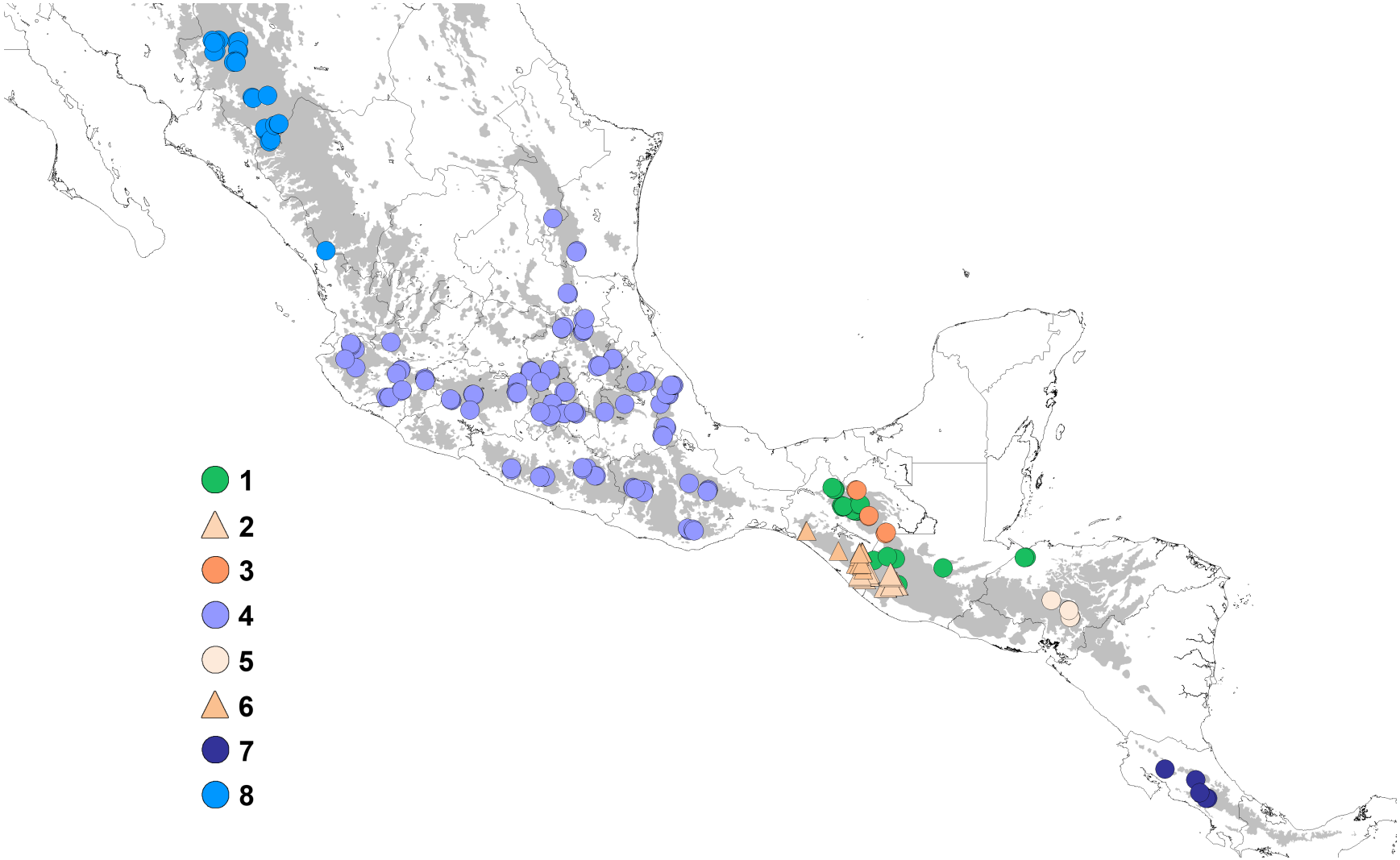

Figure 1.15. Map displaying the geographic distribution of each genetic lineage identified by GENELAND for scenario 2 (Table 1.2). Grey-shaded areas of the map represent World Wildlife Federation (WWF) ecoregions in which the species can be found.

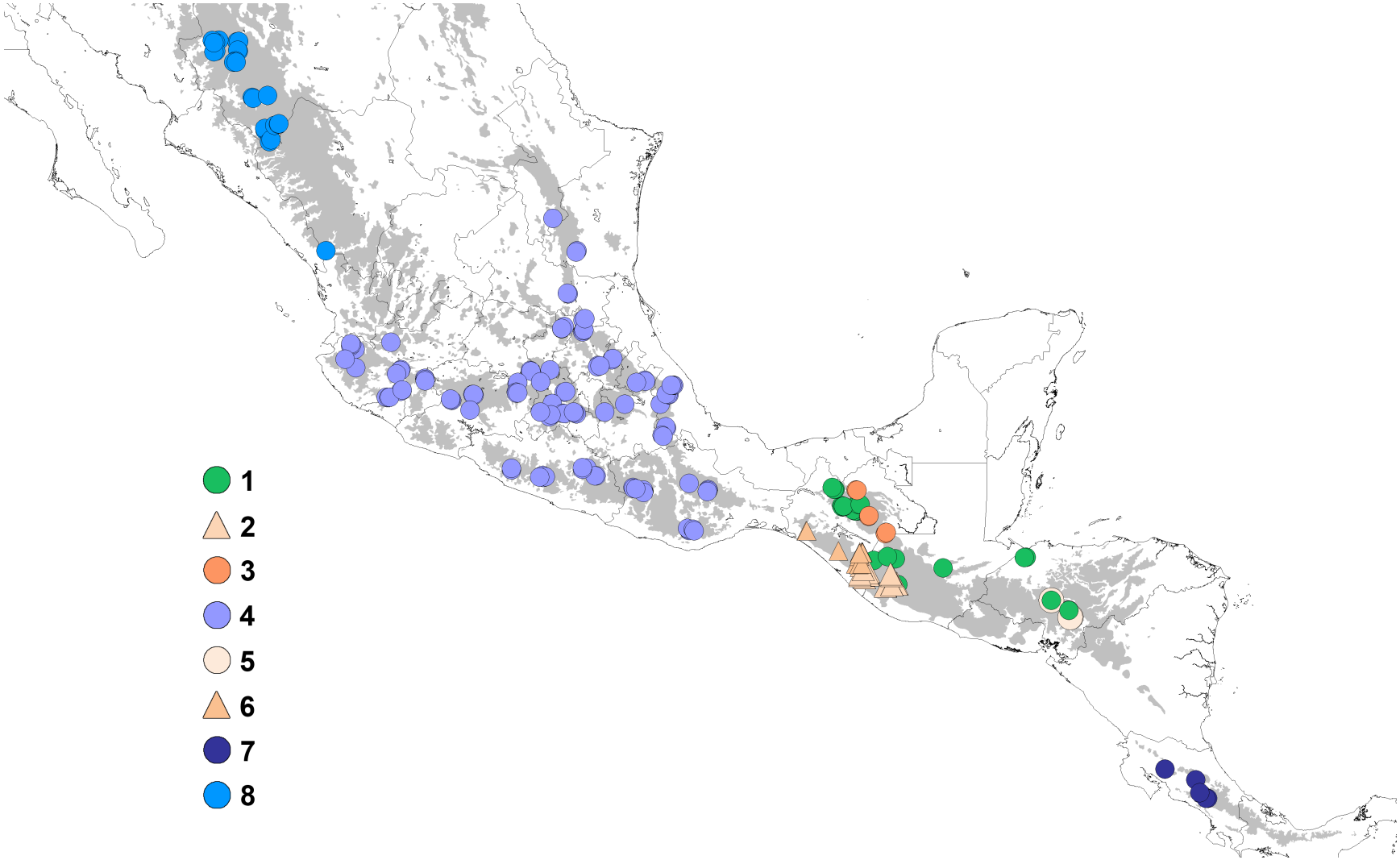

Figure 1.16. Map displaying the geographic distribution of each genetic lineage identified by GENELAND for scenario 3 (Table 1.2). Grey-shaded areas of the map represent World Wildlife Federation (WWF) ecoregions in which the species can be found.

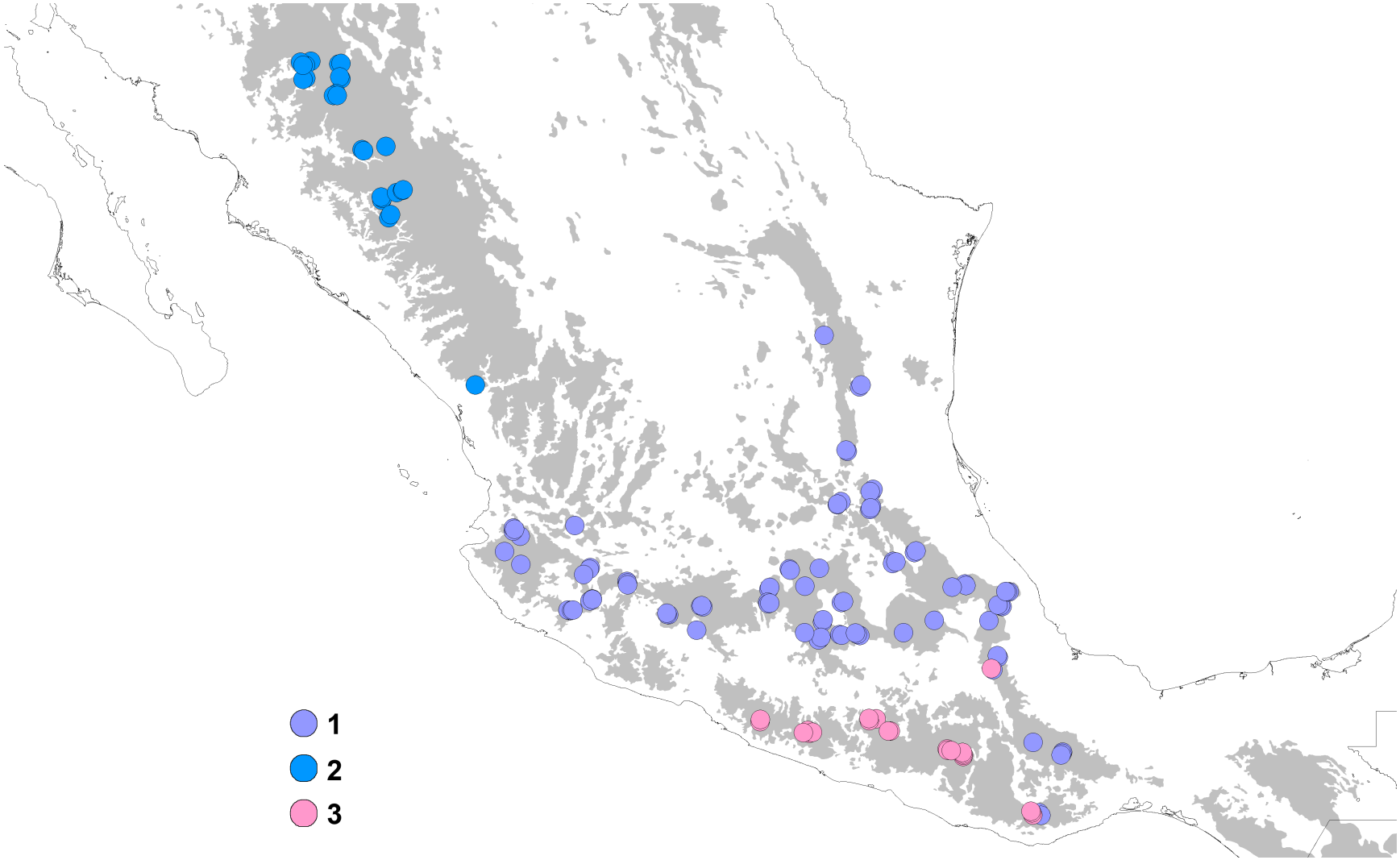

Figure 1.17. Map displaying the geographic distribution of each genetic lineage identified by GENELAND for scenario 4 (Table 1.2). Grey-shaded areas of the map represent World Wildlife Federation (WWF) ecoregions in which the species can be found.

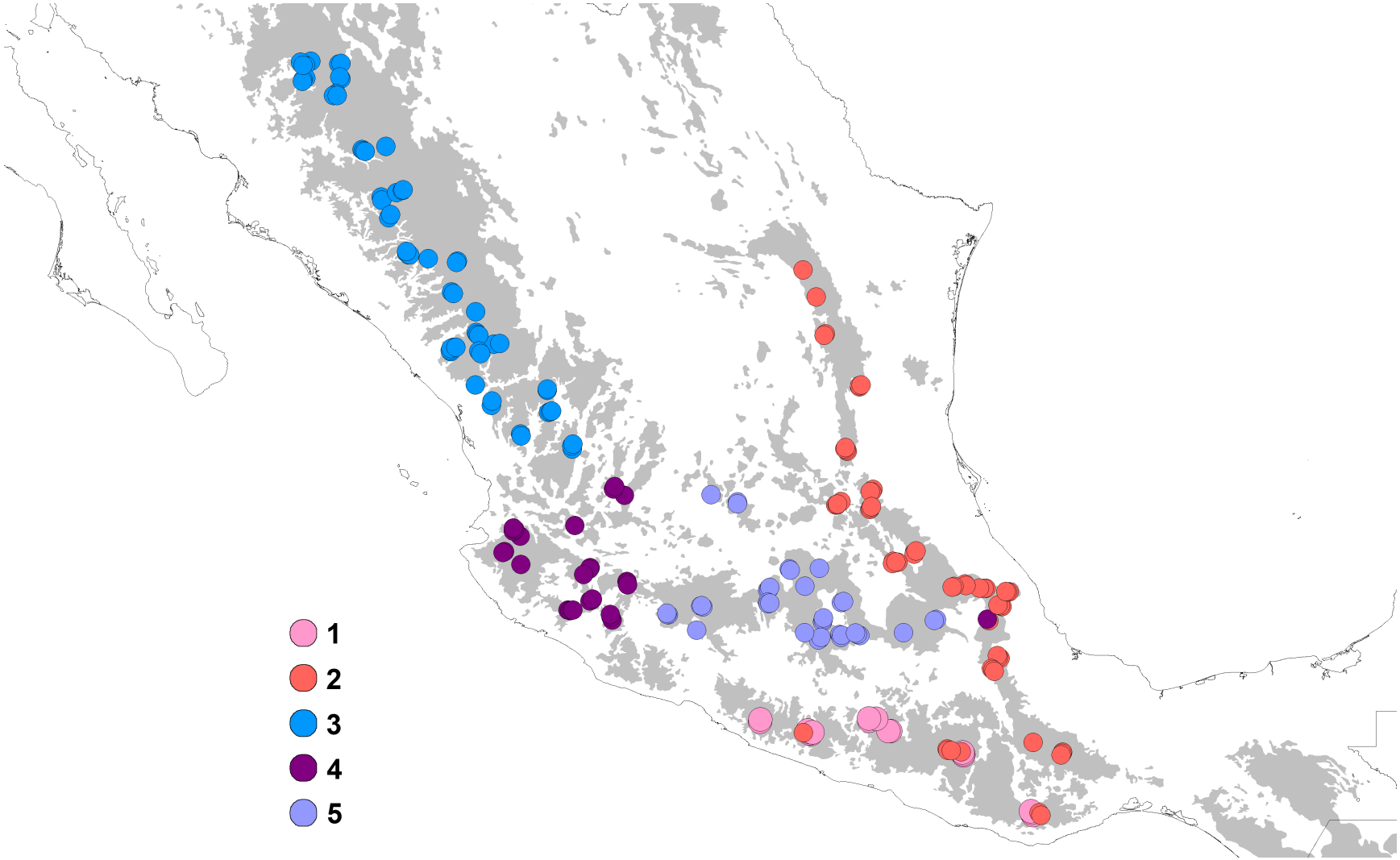

Figure 1.18. Map displaying the geographic distribution of each genetic lineage identified by GENELAND for scenario 5 (Table 1.2). Grey-shaded areas of the map represent World Wildlife Federation (WWF) ecoregions in which the species can be found.

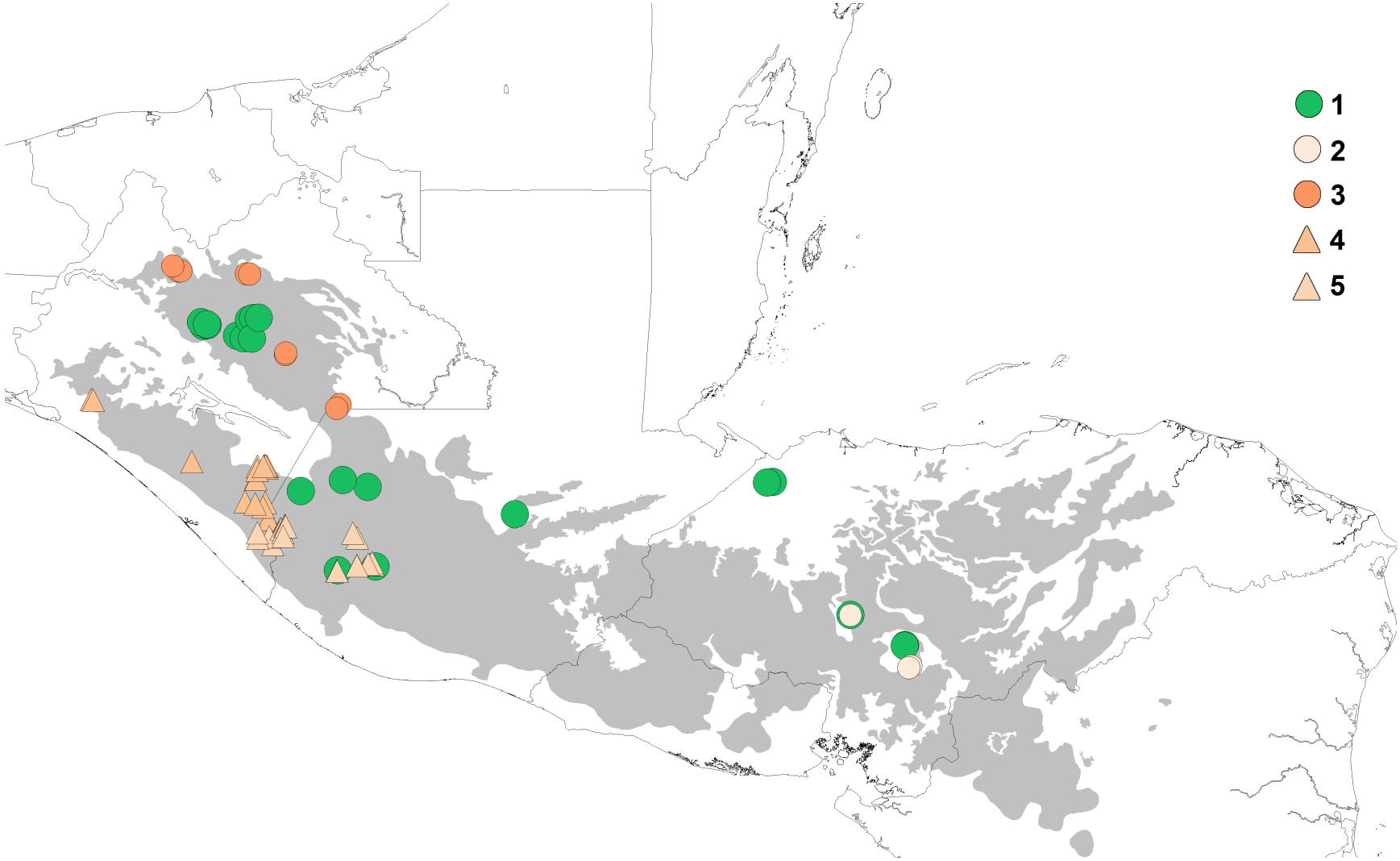

Figure 1.19. Map displaying the geographic distribution of each genetic lineage identified by GENELAND for scenario 6 (Table 1.2). Grey-shaded areas of the map represent World Wildlife Federation (WWF) ecoregions in which the species can be found.

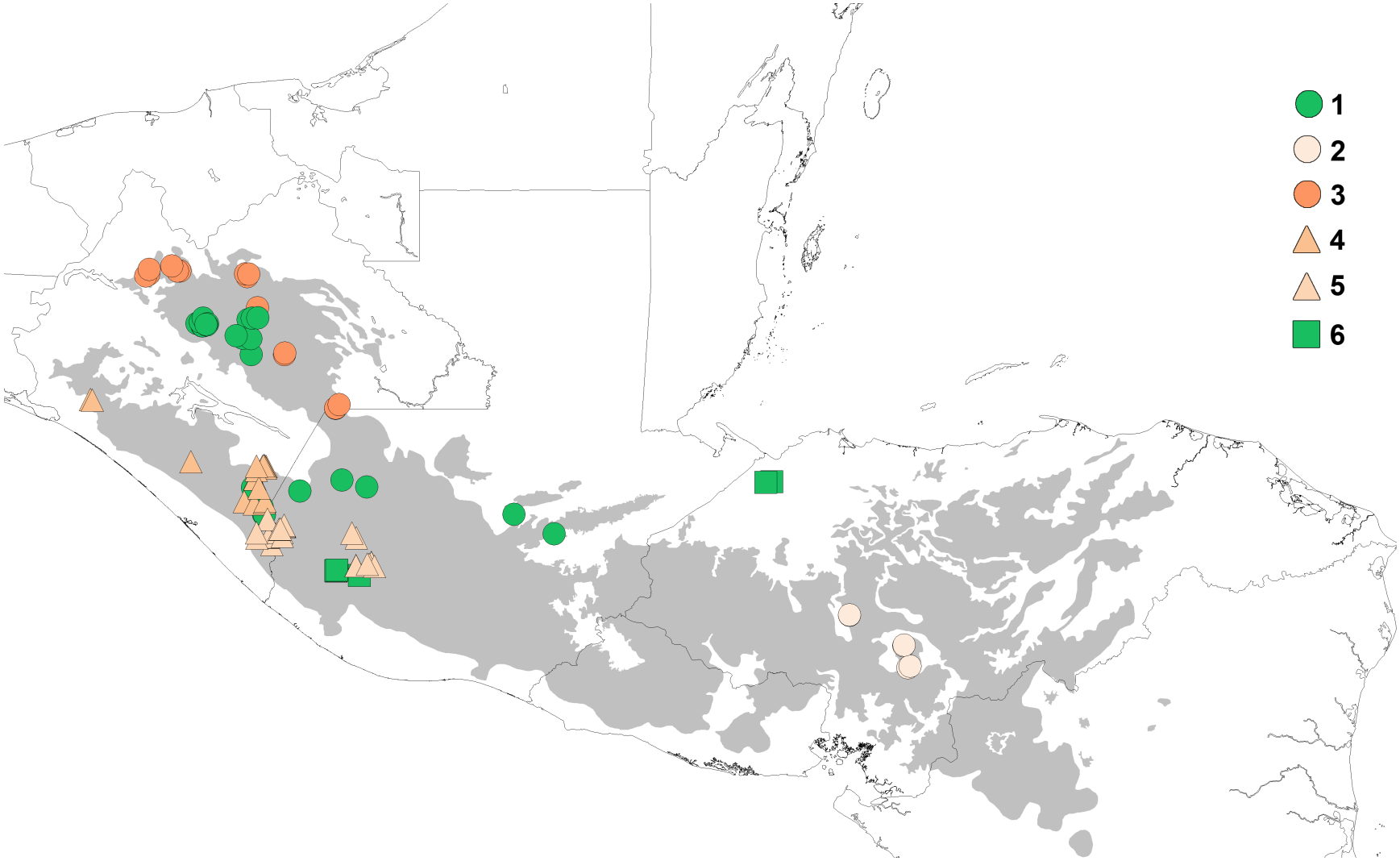

Figure 1.20. Graph of the canonical analysis of variance conducted on all morphometric samples that also had genotype data (N=606). All samples are color-coded according to their genotypic assignment by the K=6 analysis of all samples (N=1917). Nuc CA (eph)= Nuclear Central America *B. ephippiatus*; Nuc CA (eph/wilm)= Nuclear Central America *B. ephippiatus* and *B. wilmattae.*

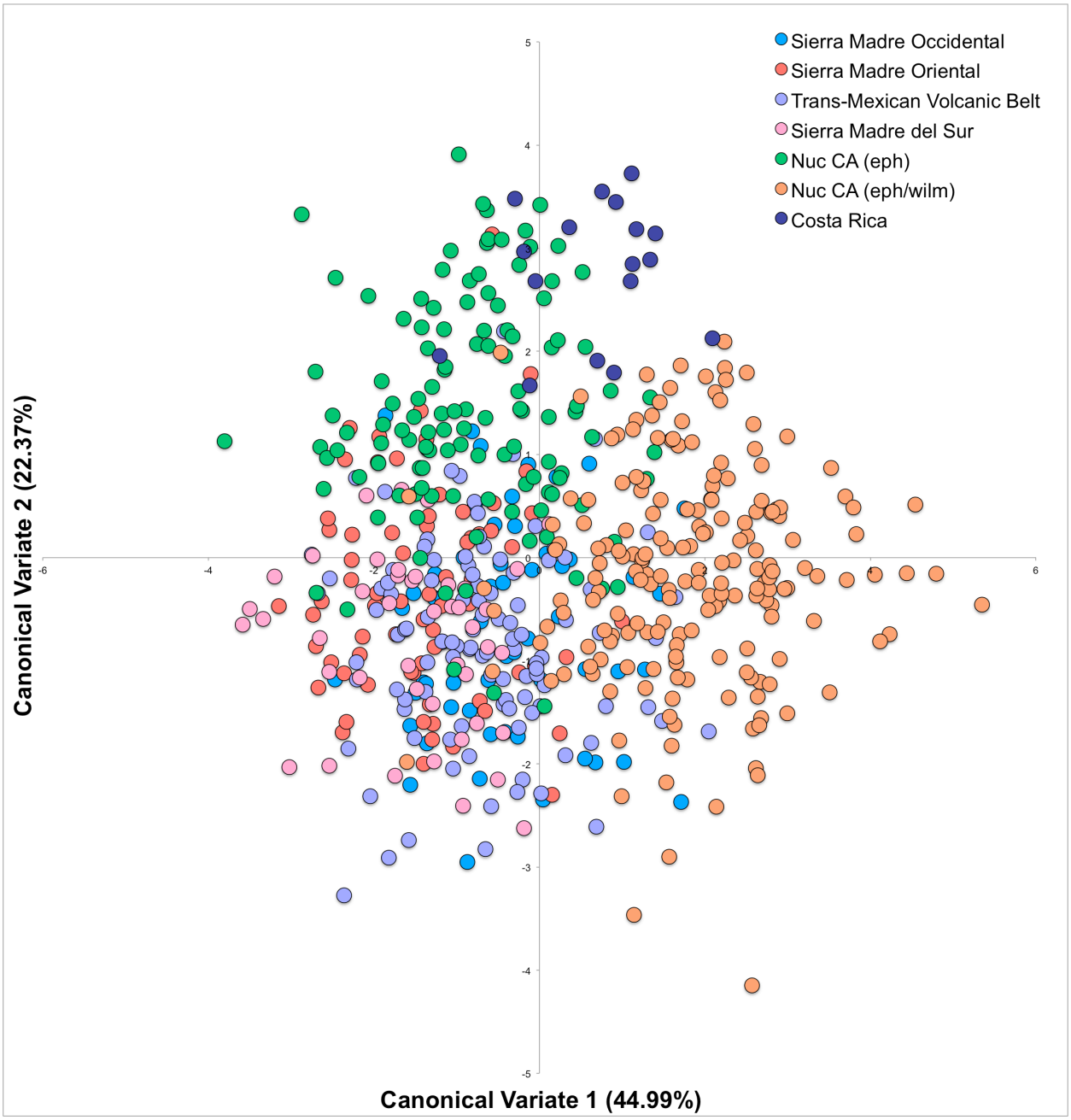

Figure 1.21. Graph of the canonical analysis of variance conducted on equal samples sizes from each region (N=119). All samples are color-coded according to their genotypic assignment by the K=6 analysis of all samples (N=1917). Nuc CA (eph)= Nuclear Central America *B. ephippiatus*; Nuc CA (eph/wilm)= Nuclear Central America *B. ephippiatus* and *B. wilmattae.*

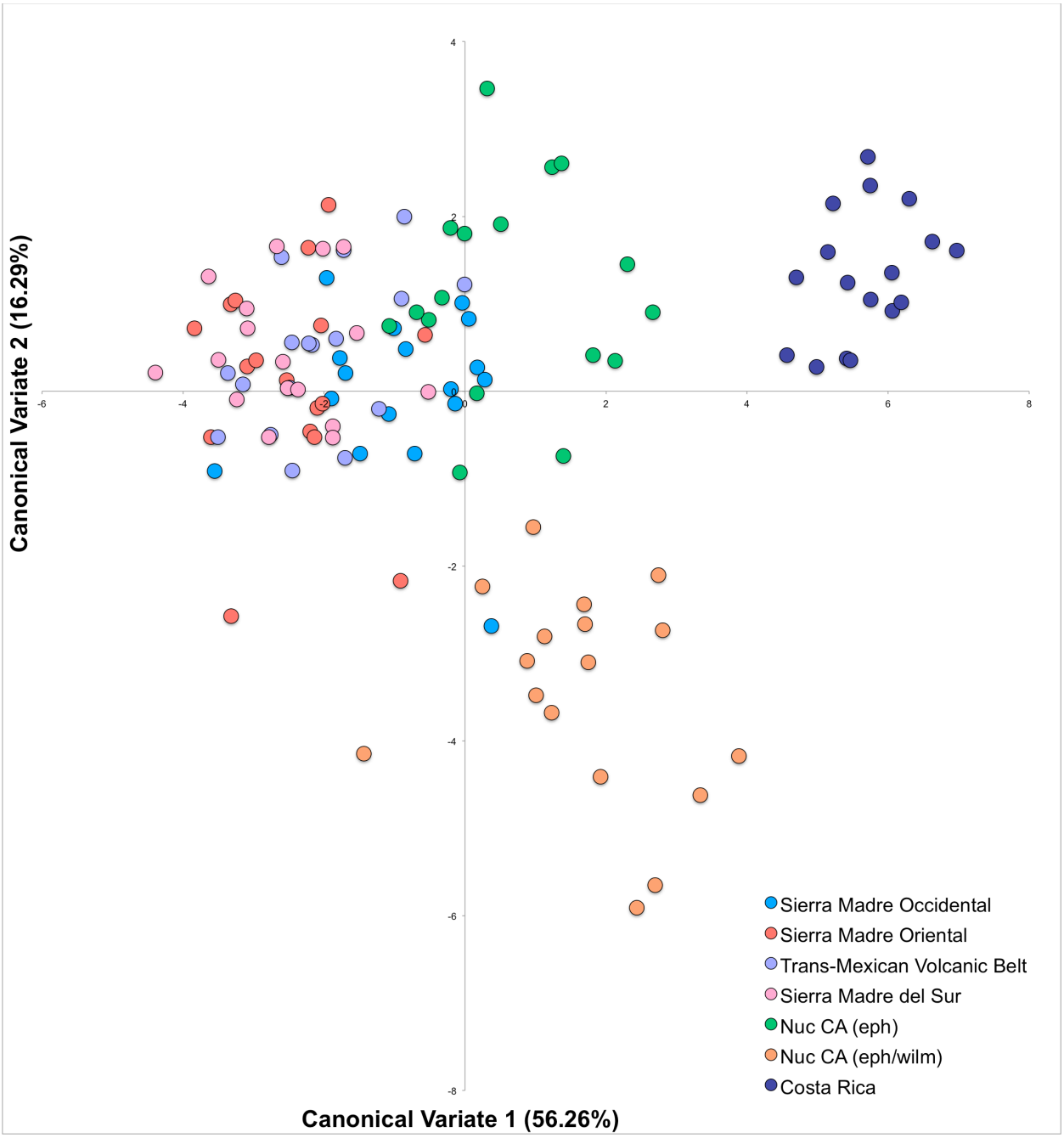

Figure 1.22. Map showing the geographic distribution of the new species that will be described and revised based on the phylogenetic, genotypic, and morphometric data presented here. Grey-shaded areas of the map represent World Wildlife Federation (WWF) ecoregions in which the species can be found. See Chapter Two for a taxonomic revision of the group.

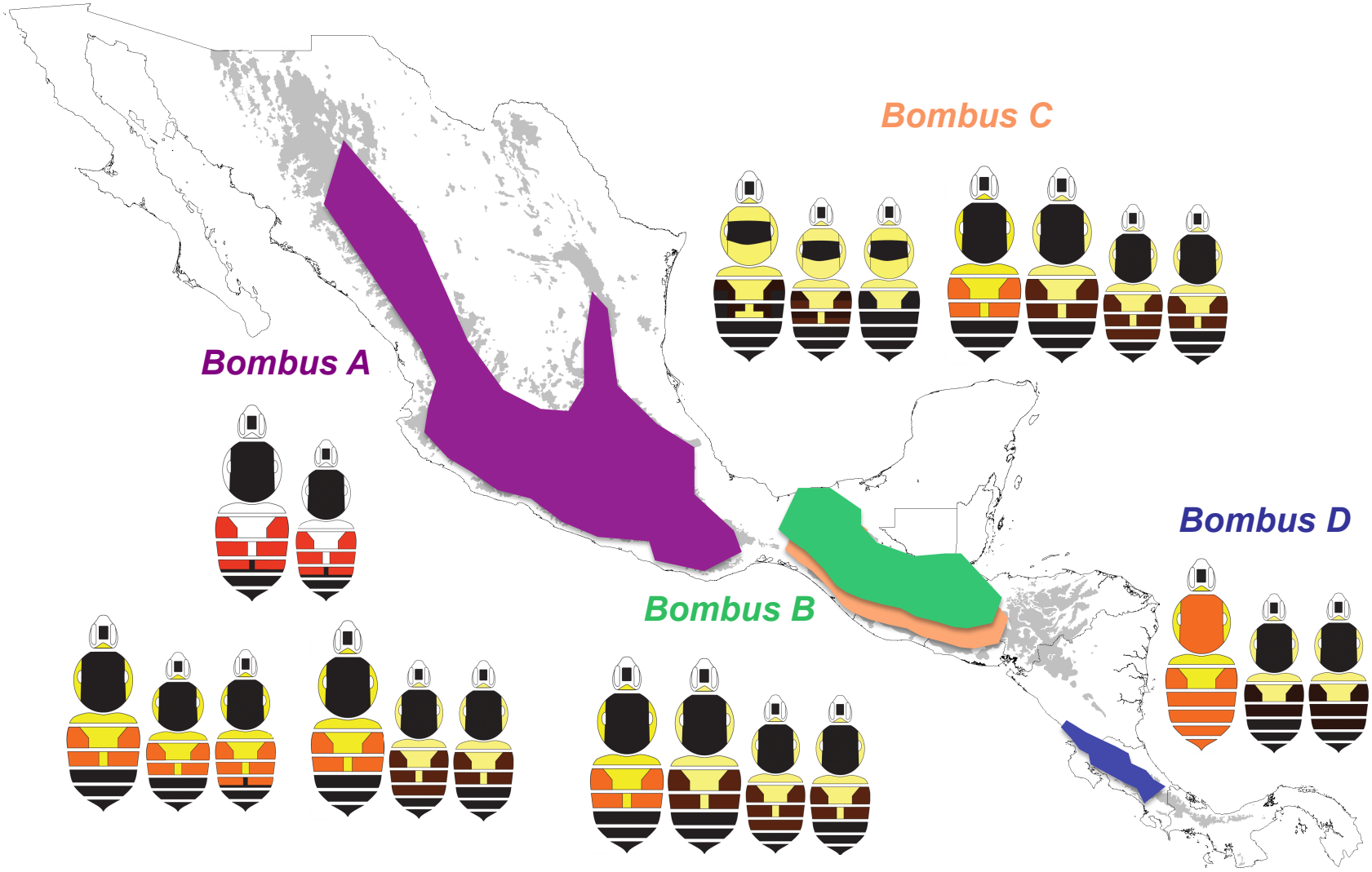

CHAPTER 2: A TAXONOMIC REVISION OF THE *BOMBUS EPHIPPIATUS-BOMBUS WILMATTAE* SPECIES GROUP IN MEXICO AND CENTRAL AMERICA

Abstract

The taxonomic status of the closely related species *Bombus ephippiatus* and *B. wilmattae* has been a source of confusion for taxonomists for nearly 200 years. Since the original descriptions of *B. ephippiatus* and *B. wilmattae*, eight synonyms and four subspecies have been applied to these taxa. Here I present a taxonomic revision of this group, informed by extensive research on phylogenetics, population genetics and wing morphometrics. *Bombus ephippiatus* Say is revised to comprise a more restricted range and *B. wilmattae* Cockerell is revised to include a previously undescribed female color polymorphism. The species *B. schneideri* Friese from Costa Rica and Panama is resurrected and *B. maya* sp. nov. is described. For each species, I provide a detailed description of color pattern polymorphism across geographic distribution.

Introduction

For more than two and a half centuries, bumble bees have been a subject of curiosity for naturalists and biologists worldwide (Linneaus, 1758; Darwin, 1859; Franklin, 1913; Plath, 1934; Heinrich, 2004; Dillon *et al.,* 2006; Cameron *et al.*, 2007; Hines & Williams, 2012). Their social behavior (Free & Butler, 1959), importance as native and commercial pollinators (Goulson, 2010), diversity in nest ecology (Sakagami, 1976) and color patterns (Williams, 2007; Rapti *et al.,* 2014) and, more recently, their decline across a worldwide distribution (Williams, 1986; Goulson *et al.,* 2008; Williams & Osborne, 2009; Cameron *et al.,* 2011; Morales *et al.,* 2013; Bartomeus *et al.,* 2013) make them a rich system for research in multiple disciplines. Taxonomic research has also been extensive. Over 2800 formal names have been applied to the ~250 currently recognized species; on average more than eleven names have been applied to each species (Williams, 1998).

For nearly as long as bumble bees have been studied, taxonomists have been interested in the *B. ephippiatus-B. wilmattae* species group (Duennes *et al.,* 2012). *Bombus ephippiatus* was first described by Thomas Say (Say, 1837), while *B. wilmattae* was originally described by Theodore Cockerell as a subspecies of *B. lateralis* Smith (a synonym of *B. ephippiatus*;

Cockerell, 1912). Since these two original descriptions, six synonyms and four subspecies have been applied to *B. ephippiatus* and two synonyms to *B. wilmattae*. The last thorough revision of the group (Labougle *et al.,* 1985; Labougle, 1990) defined *B. ephippiatus* and *B. wilmattae* as separate species based on subtle morphological differences, but primarily on the presence of a white band of hairs on the pronotum and anterior scutum. These two species were later classified as the single polymorphic species *B. ephippiatus* by Williams (1998). This group's diversity of color pattern polymorphism, extensive range and the mosaic of habitats in which it is found across Mexico and Central America bring into question the status of these taxa as a single polymorphic species, despite the most recent revision of this group.

Throughout Mexico north of the Isthmus of Tehuantepec, *B. ephippiatus* is widely distributed in pine-oak and montane forests from 500m-3600m in the Sierra Madre Occidental, Sierra Madre Oriental, Trans-Mexican Volcanic Belt and the Sierra Madre del Sur with a yellow, black and red color morph throughout the western region and a yellow, black and brown morph throughout the eastern region (Fig. 2.1). In Mexico south of the Isthmus of Tehuantepec to Nicaragua, north of the Nicaragua Depression, the "*B. ephippiatus* phenotype" is co-distributed with the "*B. wilmattae* phenotype" from 1000m-3600m in pine-oak and montane forests in the Sierra Madre de Chiapas and the Central American highlands (Fig. 2.1). Within this region, the *B. ephippiatus* phenotype consists of black and yellow workers with the queens possessing red, brown or black hairs on the abdomen, while the *B. wilmattae* phenotype is distinguished from these by a yellow band of hairs on the pronotum. South of the Nicaraguan Depression, *B. ephippiatus* queens are yellow and orange while males and workers are black and yellow; they live from 1000m-3600m in the Talamancan montane forests of Costa Rica and northern Panama (Fig. 2.1).

A preliminary phylogenetic analysis of *B. ephippiatus* across the range of the putative species revealed significant phylogenetic structure corresponding to geographic barriers throughout Mexico and Central America, corresponding in part to color pattern polymorphisms, with one distinct lineage north of the Isthmus of Tehuantepec, two sympatric lineages south of the Isthmus of Tehuantepec and a single lineage in Costa Rica that is sister to the putative *B. wilmattae* (Duennes *et al.,* 2012). The in-depth population genetic, phylogenetic, and morphometric study presented in Chapter One provides strong evidence to support the conclusion that this group is a complex of species, with barriers to gene flow across the Isthmus

of Tehuantepec and the Nicaraguan Depression (Fig. 2.1). There is also evidence from extensive genetic and morphometric data to support that there are two sympatric species with little to no gene flow between populations south of the Isthmus of Tehuantepec and north of the Nicaraguan Depression. Based on the patterns of genotypic and phenotypic data presented in Chapter One, here I revise this species complex, assigning names to four distinct species.

Materials and Methods

Bumble bee specimens examined for morphological characters of potential use in species diagnostics were predominantly collected by the author or were available in the ethanol collections of Sydney Cameron at the University of Illinois. Two queens and a male specimen (Figs. 2.2-2.4) examined and imaged from Costa Rica belong to the Museum of Comparative Zoology at Harvard University. A single queen (Fig. 2.5) was measured and imaged from the Purdue Entomological Research Collection at Purdue University. Observations of color pattern polymorphism for hundreds of samples within each species were also made during six visits by the author from 2011-2015 to the museum at El Colegio de la Frontera Sur in San Cristobal de las Casas, Mexico. Samples used in this study are listed in Table 1.1, Ch. One.

The morphological features measured and examined in each species were originally defined by Michener (2007); Labougle (1990) used the same traits to describe species from this region. For a list of abbreviations used herein, see Table 2.1. In this work, I build upon previous taxonomic descriptions of this group (Labougle *et al.*, 1985; Labougle, 1990) and therefore include measurements and descriptions of anatomical features examined by previous authors. Images of the male genitalia for each species are included (Fig. 2.6), but I do not describe them in-depth because they have been examined thoroughly by Labougle *et al.* (1985; 1990), and too few male specimens were available to describe robustly the intraspecific genitalic variation within each species.

Ultimately, the decisions to separate these species are based on wing morphometric data as well as genetic data, but the shape differences in the wings between species are nearly imperceptible to the human eye and are not useful as simple diagnostic characters for identification. Thus the wing morphometric data are not discussed further in this chapter.

***Bombus ephippiatus* Say**

Bombus formosus Smith, 1854, type not seen. Synonymized with *B. ephippiatus* and suspected to be from northern Mexico by Cockerell, 1899.

Bombus pulcher Cresson, 1863, type not seen. Synonymized with *B. ephippiatus* by Dalla Torre, 1896. Jalapa, Mexico.

Taxonomic status: *Bombus ephippiatus* is currently recognized as a single polymorphic species from northwest Mexico through Panama (Labougle, 1990) and *B. wilmattae* is considered by some as a color morph of this polymorphic species (Williams, 1998). Based on the detailed evidence presented in Chapter One demonstrating a lack of gene flow across the Isthmus of Tehuantepec, I revise this species to include only populations from Mexico north of the Isthmus of Tehuantepec (Fig. 2.7). While there is considerable population structure and genetic diversity north of the Isthmus of Tehuantepec as demonstrated with the microsatellite genotype data, the low levels of diversity at the COI locus and in the wing morphometric data (see Chapter One) have led me to conclude that these populations are part of a single polymorphic species.

Description: *Dorsal Pile*. There are distinct color pattern polymorphisms throughout the eastern and western ranges of this species in Mexico. A yellow, black and red form predominates throughout the Sierra Madre Occidental, western Trans-Mexican Volcanic Belt and Sierra Madre del Sur and a yellow and black form predominates throughout the Sierra Madre Oriental, eastern Trans-Mexican Volcanic Belt and Sierra Madre del Sur (Fig. 2.7).

Queens and workers, Sierra Madre Occidental, western Trans-Mexican Volcanic Belt and Sierra Madre del Sur (Figs. 2.5 and 2.8): Queens and workers from the western region possess a black patch of pile in the paraocular area and on the vertex of the head (Figs. 2.5B and 2.8B). The pronotum is predominately black, with some yellow hairs interspersed along the midline and laterally at the base of the pronotal lobe. The scutum is entirely black with the exception of some yellow hairs interspersed just posteriorly to corresponding patches on the dorsal pronotum. The sides of the thorax (the mesepisternum, the scrobe and the metepisternum) are covered entirely with yellow hair (Figs. 2.5A and 2.8A). The scutellum is predominately black and sometimes possesses yellow hairs interspersed along the margin with the metanotum and the axilla (Figs. 2.5C and 2.8C). The metanotum possesses lateral patches posterior to the base of the hindwing

comprising predominantly yellow hair, but with short, black hairs located close to the hindwing base. T1 of the metasoma is entirely yellow with the exception of short sparse black hair along the midline (Figs. 2.5D and 2.8D). T2 is yellow medially with orange ferruginous patches laterally that are small anteriorly and gradually widen posteriorly to form "triangles" of orange at each lateral end of the segment. These orange "triangles" that lie laterally on the segment can vary in size, but generally cover a third of the segment in total. T3 is predominately covered with orange ferruginous hair, but possesses a medium to small patch of yellow hair running anteriorly-posteriorly along the midline of the segment. This yellow patch on T3 can vary in size, but is always present. T4 ranges from entirely black hairs to an even mix of orange and black. T5 and T6 are entirely black.

Males, Sierra Madre Occidental,western Trans-Mexican Volcanic Belt and Sierra Madre del Sur (Fig. 2.9): Males from the western region possess a black and yellow mixed patch of pile in the paraocular area, on the clypeus and on the vertex of the head (Fig. 2.9B). The pronotum is covered with a mix of black and yellow hair. The scutum is covered entirely with black hair. The sides of the thorax (the mesepisternum, the scrobe and the metepisternum) are covered entirely with yellow hair (Fig. 2.9A). The scutellum is predominately black and sometimes possesses yellow hairs interspersed along the margin with the metanotum and the axilla (Fig. 2.9C). The metanotum possesses lateral patches posterior to the base of the hindwing comprising predominantly yellow hair, but with short, black hairs located close to the hindwing base. T1 of the metasoma is entirely yellow with the exception of short sparse black hair along the midline (Fig. 2.9D). T2 is yellow medially with orange ferruginous patches laterally that are small anteriorly and gradually widen posteriorly to form "triangles" of orange at each lateral end of the segment. These orange "triangles" that lie laterally on the segment can vary in size, but generally cover a third of the segment in total. T3 is predominately covered with orange ferruginous hair, but possesses a medium to small patch of yellow hair running anteriorly-posteriorly along the midline of the segment. This yellow patch on T3 can vary in size, but is always present. T4 is predominantly covered in orange hairs, with the exception of a midline patch of yellow hairs at the anterior top of the segment and a midline patch of black hairs at the posterior end of the segment. T5-T7 are entirely black.

Queens, workers and males, Sierra Madre Oriental, eastern Trans-Mexican Volcanic Belt and Sierra Madre del Sur (Figs. 2.10-2.12): The dorsal color patterns of queens, workers and

males from the western and eastern regions are the same on all segments as the western patterns with the exception of the colors on T2-T4 of the metasoma in both males and females (Figs. 2.10D, 2.11D and 2.12D). In the eastern region, T2 is yellow medially with brown to black patches laterally that are small anteriorly and gradually widen posteriorly to form "triangles" at each lateral end of the segment. The color in these "triangles" ranges from a brown (the individuals hairs are orange at the root and black at the tip) to a mix of brown and black. In workers but not in queens, sometimes these "triangles" are completely black. These brown/black "triangles" that lie laterally on the segment can vary in size, but generally cover a third of the segment in total. T3 is predominately covered with the same brown/black hair, but also possesses a medium to small patch of yellow hair running anteriorly-posteriorly along the midline of the segment. This yellow patch on T3 can vary in size, but is always present. T4 is covered entirely in black hairs.

Queen. Length of 18-20mm. UID of 2.90-3.11mm. LID of 3.03-3.17mm. Ocelli just below the supraorbital line. IOD of 0.25mm. OOD of 0.63-0.75mm. Clypeus coarse and moderately punctate along the margin with hair; in the center punctation is fine and sparse with no hair. Malar length of 0.63-0.76mm. Malar width of 0.81-0.88mm. Inter-tegular distance of 5.06-5.72mm. Mesobasitarsus length of 3.80-4.05mm. Mesobasitarsus width of 1.27mm. T2 width of 10.10mm.

Worker. Length of 14mm. UID of 2.22-2.27mm. LID of 2.17-2.22mm. Ocelli in the middle of the supraorbital line. IOD of 0.20mm. OOD of 0.55-0.63mm. Clypeus punctuation similar to queen, but with less hair along the margin. Malar length of 0.50-0.58mm. Malar width of 0.88mm. Inter-tegular distance of 3.54-4.05mm. Mesobasitarsus length of 2.78-2.89mm. Mesobasitarsus width of 0.76-0.86mm. T2 width of 6.26-6.36mm.

Male. Length of 15mm. UID of 2.27-2.42mm. LID of 2.19-2.32mm. Ocelli in the middle of the supraorbital line. IOD of 0.18-0.20mm. OOD of 0.55-0.66mm. Clypeus coarse and moderately punctate with hair throughout. Malar length of 0.63-0.66mm. Malar width of 0.81mm. Inter-tegular distance of 3.54-4.30mm. Mesobasitarsus length of 2.78-3.04mm. Mesobasitarsus width of 0.81-0.86mm. T2 width of 6.36-6.87mm. Images of male genitalia are in Fig. 2.6A-B.

Diagnosis: *B. ephippiatus* is similar genetically and in color pattern to *B. maya* (described below), however, this species is distributed throughout the Sierra Madre Occidental, Sierra Madre Oriental, the Trans-Mexican Volcanic Belt and the Sierra Madre del Sur north of the Isthmus of Tehuantepec (Fig. 2.7) where *B. maya* is not found. *Diagnosis note.* There are many sites within the *cytochrome oxidase I* (COI) sequence (Chapter One) that are unique to *B. ephippiatus*, however, population structure within the region as well as saturation (hidden substitutions) make these sites unsuitable as diagnostic characters for the species. Color pattern is useful for differentiation of this species from other sympatric bumble bee species, but it is polymorphic throughout its range and cannot be used as a diagnostic character alone because many of the color patterns present in *B. ephippiatus* are also present in the other species described here. Geographic location is thus the only robust diagnostic character for differentiating this species from the other three species in this complex.

Distribution: *B. ephippiatus* is found in the following states within Mexico: Chihuahua, Colima, Durango, Guanajuato, Guerrero, Hidalgo, Jalisco, Mexico, Michoacán, Morelos, Nayarit, Nuevo Leon, Oaxaca, Puebla, Queretaro, San Luis Potosi, Sinaloa, Tamaulipas, Tlaxcala, Veracruz and Zacatecas (Fig. 2.7).

Types: As is the case with most of Thomas Say's types, the original type of *B. ephippiatus* was damaged and lost. A queen neotype as well as a series of neoparatypes representing different castes and the range of color pattern polymorphism in this species have been designated and housed within the collections of El Colegio de la Frontera Sur in San Cristobal de las Casas, Chiapas, Mexico.

***Bombus maya* sp. nov.**

Taxonomic status: It is likely that the previously described species *B. lateralis* Smith (1879) and *B. vauflavus* Cockerell (1949), as well as the subspecies *Pyrobombus ephippiatus pretiosus* Milliron (1962) belong to either *B. maya* sp. nov. or *B. wilmattae* (described below), but because the only reliable way to identify these cryptic species is with the use of DNA data, none of the type specimens of these species and subspecies can be confirmed with the new species described

here. This species is most similar in phenotype and genotype to *B. ephippiatus*, but robust estimates of gene flow from Chapter One demonstrate that there is no contemporary gene flow across the Isthmus of Tehuantepec, warranting designation as a separate species.

Bombus maya sp. nov. is named in honor of the Maya peoples indigenous throughout the geographic range of this species.

Description: *Dorsal Pile*. Queens and workers (Figs. 2.13-2.16): Queens and workers possess a black patch of pile in the paraocular area and on the vertex of the head (Figs. 2.13B, 2.14B, 2.15B and 2.16B). The pronotum is covered with a mix of black and yellow hairs; this can range from an even mix of yellow and black (Fig. 2.15) to predominantly black (Fig. 2.13 and 2.14), but is always mixed and with more black hairs at the base of the pronotal lobe. The scutum is entirely black with the exception of yellow hairs interspersed along the boundary with the pronotum; these yellow and black mixed patches can lie laterally with a small patch of black between them or are continuous along the edge of the scutum along the pronotum (Figs. 2.13C, 2.14C, 2.15C and 2.16C). The sides of the thorax (the mesepisternum, the scrobe and the metepisternum) are covered entirely with yellow hair (Figs. 2.13A, 2.14A, 2.15A and 2.16A). The scutellum is predominately black with yellow hairs interspersed along the margin with the metanotum and the axilla. The metanotum possesses lateral patches posterior to the base of the hindwing comprising predominantly yellow hair with, but with short, black hairs located close to the hindwing base. T1 of the metasoma is entirely yellow with the exception of short sparse black hair along the midline (Figs. 2.13D, 2.14D, 2.15D and 2.16D). T2 is yellow medially with black and orange ferruginous patches laterally that are small anteriorly and gradually widen posteriorly to form “triangles” at each lateral end of the segment. The color in these “triangles” ranges from an orange with a few black hairs interspersed (Figs. 2.14-2.15) to brown (the individuals hairs are orange at the root and black at the tip; Fig. 2.13) to a mix of brown and black (Fig. 2.16). In workers but not in queens, sometimes these “triangles” are completely black. These orange/brown/black “triangles” that lie laterally on the segment can vary in size, but generally cover a third of the segment in total. T3 is predominately covered with the same orange/brown/black hair, but possesses a medium to small patch of yellow hair running anteriorly-posteriorly along the midline of the segment. This yellow patch on T3 can vary in size,

but is always present. T4 ranges from entirely black hairs to an even mix of orange/brown and black hairs. T5 and T6 are entirely black.

Males (Fig. 2.17): Males possess a black and yellow mixed patch of pile in the paraocular area, on the clypeus and on the vertex of the head (Fig. 2.17B). The pronotum is covered entirely with a mix of black and yellow hair. The scutum is entirely black with the exception of yellow hairs interspersed with black along the boundary with the pronotum; these yellow and black mixed patches can lie laterally with a small patch of black between them or are continuous along the edge of the scutum along the pronotum (Fig. 2.17C). The sides of the thorax (the mesepisternum, the scrobe and the metepisternum) are covered entirely with yellow hair (Fig. 2.17A). The scutellum is predominately black with yellow hairs interspersed along the margin with the metanotum and the axilla. The metanotum possesses lateral patches posterior to the base of the hindwing comprising predominantly yellow hair, but with short, black hairs located close to the hindwing base. T1 of the metasoma is entirely yellow with the exception of short sparse black hair along the midline (Fig. 2.17D). T2 is yellow medially with black and orange ferruginous patches laterally that are small anteriorly and gradually widen posteriorly to form "triangles" at each lateral end of the segment. The color in these "triangles" ranges from an orange with a few black hairs interspersed to brown (the individuals hairs are orange at the root and black at the tip) to a mix of brown and black. These orange/brown/black "triangles" that lie laterally on the segment can vary in size, but generally cover a third of the segment in total. T3 is predominately covered with the same orange/brown/black hair, but possesses a medium to small patch of yellow hair running anteriorly-posteriorly along the midline of the segment. This yellow patch on T3 can have a few black hairs interspersed along the anterior and posterior margins. T4 is covered entirely with black hairs, but can possess some yellow hairs interspersed with the black along the midline and the anterior margin of the segment. T5 is covered entirely with black hairs, but can possess some yellow hairs interspersed with the black along the midline. T6 and T7 are entirely black.

Queen. Length of 21-23mm. UID of 2.97-3.03mm. LID of 3.08mm. Ocelli just below the supraorbital line. IOD of 0.25-0.30mm. OOD of 0.76-0.81mm. Clypeus coarse and moderately punctate along the margin with hair; in the center punctation is fine and sparse with no hair. Malar length of 0.71-0.76mm. Malar width of 1.13-1.18mm. Inter-tegular distance of 6.08mm.

Mesobasitarsus length of 3.65-3.80mm. Mesobasitarsus width of 1.16-1.42mm. T2 width of 9.90-10.10mm.

Worker. Length of 15-16mm. UID of 2.27-2.34mm. LID of 2.29-2.32mm. Ocelli in the middle of the supraorbital line. IOD of 0.20mm. OOD of 0.63mm. Clypeus punctuation similar to queen, but with less hair along the margin. Malar length of 0.45-0.55mm. Malar width of 0.81-0.86mm. Inter-tegular distance of 4.30-4.56mm. Mesobasitarsus length of 2.84-2.94mm. Mesobasitarsus width of 0.91-1.01mm. T2 width of 7.07mm.

Male. Length of 11-14mm. UID of 2.07-2.39mm. LID of 1.79-2.22mm. Ocelli in the middle of the supraorbital line. IOD of 0.15-0.23mm. OOD of 0.53-0.63mm. Clypeus coarse and moderately punctate with hair throughout. Malar length of 0.50-0.63mm. Malar width of 0.63-0.80mm. Inter-tegular distance of 3.34-3.90mm. Mesobasitarsus length of 2.33-2.78mm. Mesobasitarsus width of 0.56-0.76mm. T2 width of 4.95-6.36mm. Images of male genitalia are in Fig. 2.6C-D.

Diagnosis: *B. maya* is similar in color pattern to *B. ephippiatus,* but this species is distributed south of the Isthmus of Tehuantepec throughout the highlands in the state of Chiapas in Mexico, Guatemala and Honduras (Fig. 2.18). Locus 537 in the *cytochrome oxidase I* gene fragment (primers listed in Duennes *et al.,* 2012) is cytosine (C) in *B. maya* and a thymine (T) in *B. wilmattae*.

Diagnosis note: B. wilmattae is sympatric with *B. maya* throughout its range and some populations of *B. ephippiatus* also have the cytosine (C) nucleotide at locus 537, but these two characters (geographic location and nucleotide substitution) together can definitively distinguish *B. maya* from the other species in this complex.

Distribution: *B. maya* is found in the following states in the following countries: Mexico: Chiapas; Guatemala: Baja Verapaz, Huehuetenango, Quetzaltenango, San Marcos, Sololá, Totonicapán, Zacapa; Honduras: Comayagua, El Paraiso, Francisco Morazán, Santa Barbara (Fig. 2.18).

Distribution note: Based on Labougle (1990) and museum records, this species most likely also occurs in El Salvador and Nicaragua, but DNA information is needed to positively ID specimens and the study presented in Chapter One did not have samples from these countries.

Types: A queen holotype as well as a series of paratypes representing different castes and the range of color pattern polymorphism in this species have been designated and housed within the collections of El Colegio de la Frontera Sur in San Cristobal de las Casas, Chiapas, Mexico.

Bombus wilmattae **Cockerell**

Bombus ephippiatus var. d. Handlirsch, 1888. Synonymized with *B. wilmattae* by Franklin, 1913.

Bombus lateralis wilmattae Cockerell, 1912, type examined. Elevated to species by Franklin, 1913.

Bombus guatemalensis nom. nud. Franklin, 1913. Synonymized with *B. wilmattae* by Franklin, 1913.

Bombus alboniger Franklin, 1915, type not seen. Synonymized with *B. wilmattae* by Labougle, 1985.

Taxonomic status: *Bombus wilmattae* is currently recognized by some authors as a separate species (Huth-Schwarz *et al*., 2011a; Huth-Schwarz *et al.,* 2011b) and by others as a variant of *B. ephippiatus* Williams, 1998; Abrahamovich *et al*., 2004). Here I provide robust genetic and morphometric evidence that *B. wilmattae* is a separate species (presented in Chapter One) and revise the species to include worker and queen polymorphisms that do not possess pure white or yellow patches on the pronotum and anterior scutum, thus identical in color pattern to polymorphisms of *B. maya* (previously *B. ephippiatus*). I have examined photos of Cockerell's type of *B. lateralis wilmattae* and have confirmed that this specimen exhibits a color pattern unique to *B. wilmattae* as revised here.

As noted above, it is likely that the previously described species *B. lateralis* Smith (1879) and *B. vauflavus* Cockerell (1949), as well as the subspecies *Pyrobombus ephippiatus pretiosus* Milliron (1962) belong to either *B. maya* sp. nov. or *B. wilmattae*, but because the only reliable way to identify these cryptic species is with the use of DNA data, none of the type specimens of these species and subspecies can be confirmed with the species described here.

The data presented in Chapter One demonstrate strong genetic structure and little to no gene flow at both mitochondrial and nuclear loci within populations of *B. wilmattae*, possibly warranting their designation as separate subspecies or even species. Until further genetic data from males and information on the fine-scale distribution of color patterns across geography can be obtained, I will recognize these genetic groups as part of the single, polymorphic *B. wilmattae* species.

Description: *Dorsal Pile*. Two predominant color pattern phenotypes exist in the queens and workers of this species. The "light pronotum" phenotype matches previous descriptions of *B. wilmattae*; the presence of pure white or yellow patches on the pronotum and anterior scutum was the only reliable diagnostic character used to differentiate *B. wilmattae* from *B. ephippiatus* (Labougle, 1990). The "dark pronotum" phenotype, newly described in this species here, is identical to color pattern variation that can also be found in *B. maya* and *B. ephippiatus* workers, but of the three "dark pronotum" queens identified to this species using DNA data, all possessed only black and yellow hair on T3 and T4. It is possible that males also exhibit the "dark pronotum" phenotype, but only "light pronotum" males were available for description.

"Light pronotum" queens and workers (Figs. 2.19-2.21): Queens and workers possess a black patch of pile in the paraocular area of the face and yellow or white (yellow/white) and black mixed hairs on the vertex of the head (Figs. 2.19B, 2.20B and 2.21B). The pronotum medially is entirely yellow/white and sometimes has very few black hairs interspersed. At the narrowing of the pronotum laterally before the distal lobes there are patches of black and yellow/white hair mixed. The pronotal distal lobes are covered entirely with yellow/white hair with very few black hairs interspersed. The scutum is predominantly black with the exception of entirely yellow/white patches of hair continuous along the boundary with the pronotum; these yellow/white hairs are sometimes mixed with black hairs and sometimes extend posteriorly and medially on the scutum to form a heart-shaped patch of black in the center of the scutum. The sides of the thorax (the mesepisternum, the scrobe and the metepisternum) are covered entirely with yellow/white hair (Figs. 2.19A, 2.20A and 2.21A). The scutellum ranges from being covered almost entirely in yellow/white hair with very few black hairs interspersed to mostly black with a margin of yellow/white hair along the margin with the metanotum and the axilla (Figs. 2.19C, 2.20C and 2.21C). The metanotum possesses lateral patches posterior to the base of

the hindwing comprising predominantly yellow/white hair, but with short, black hairs located close to the hindwing base. T1 of the metasoma is entirely yellow/white with the exception of short sparse black hair along the midline (Figs. 2.19D, 2.20D and 2.21D). T2 is yellow/white medially with black and orange ferruginous patches laterally that are small anteriorly and gradually widen posteriorly to form "triangles" at each lateral end of the segment. The color in these "triangles" ranges from being entirely covered in brown two-tone setae (the individuals hairs are orange at the root and black at the tip) to a mix of brown and black to entirely black. These brown/black "triangles" that lie laterally on the segment can vary in size, but generally cover a third of the segment in total. T3 is predominately covered with the same brown/black hair, but possesses a medium to small patch of yellow/white hair running anteriorly-posteriorly along the midline of the segment. This yellow/white patch on T3 can vary in width and ranges from extending fully anteriorly to posteriorly across the segment to widening anteriorly to only being present anteriorly on the segment. T4-T6 are entirely black.

"Dark pronotum" queens and workers (Fig. 2.22; No queen specimens available for imaging): Queens and workers possess a black patch of pile in the paraocular area and on the vertex of the head (Fig. 2.22B). The pronotum is covered with a mix of black and yellow hairs; this can be an even mix of black and yellow to predominantly black, but is always mixed and with more black hairs at the base of the pronotal lobe. The scutum is entirely black with the exception of yellow hairs interspersed with black along the boundary with the pronotum; these yellow and black mixed patches can lie laterally with a small patch of black between them or are continuous along the anterior boundary of the scutum (Fig. 2.22C). The sides of the thorax (the mesepisternum, the scrobe and the metepisternum) are covered entirely with yellow hair (Fig. 2.22A). The scutellum is predominately black with interspersed yellow hairs along the edge against the metanotum and the axilla. The metanotum possesses lateral patches posterior to the base of the hindwing comprising predominantly yellow hair, but with short, black hairs located close to the hindwing base. T1 of the metasoma is entirely yellow with the exception of short sparse black hair along the midline (Fig. 2.22D). T2 is yellow medially with black and orange ferruginous patches laterally that are small anteriorly and gradually widen posteriorly to form "triangles" at each lateral end of the segment. The color in these "triangles" ranges from an orange and black mix to brown (the individuals hairs are orange at the root and black at the tip; to a mix of brown and black. In queens these "triangles" are always completely black. These

orange/brown/black “triangles” that lie laterally on the segment can vary in size, but generally cover a third of the segment in total. T3 is predominately covered with the same orange/brown/black hair, but possesses a medium to small patch of yellow hair running anteriorly-posteriorly along the midline of the segment. In queens, T3 is always completely black medially. T4 ranges from entirely black hairs to a mix of orange or brown and black hairs. In queens, T4 is always entire black. T5 and T6 are entirely black.

Males (Figs. 2.23-2.24): Males possess a black and yellow mixed patch of pile in the paraocular area, on the clypeus and on the vertex of the head (Figs. 2.23B and 2.24B). The pronotum medially is entirely yellow/white and sometimes has very few black hairs interspersed. At the narrowing of the pronotum laterally before the distal lobes there are patches of black and yellow/white hair mixed. The scutum is predominantly black with the exception of pure yellow/white hairs patches continuous along the boundary with the pronotum; these yellow/white hairs are sometimes mixed with black hairs and sometimes extend posteriorly and medially on the scutum to form a heart-shaped patch of black on the scutum (Figs. 2.23C and 2.24C). The sides of the thorax (the mesepisternum, the scrobe and the metepisternum) are covered entirely with yellow/white hair (Figs. 2.23A and 2.24A). The scutellum can range from being covered almost entirely in yellow/white hair with very few black hairs interspersed to mostly black with a margin of yellow/white hair along the edge against the metanotum and the axilla. The metanotum possesses lateral patches posterior to the base of the hindwing comprising predominantly yellow/white hair, but with short, black hairs located close to the hindwing base. T1 of the metasoma is entirely yellow with the exception of short sparse black hair along the midline (Figs. 2.23D and 2.24D). T2 is yellow medially with black and orange ferruginous patches laterally that are small anteriorly and gradually widen posteriorly to form “triangles” at each lateral end of the segment. The color in these “triangles” ranges from an orange with a few black hairs interspersed (Fig. 2.24D) to brown (the individuals hairs are orange at the root and black at the tip; Fig. 2.23D) to entirely black. These orange/brown/black “triangles” that lie laterally on the segment can vary in size, but generally cover a third of the segment in total. T3 is predominately covered with the same orange/brown/black hair, but possesses a medium to small patch of yellow hair running anteriorly-posteriorly along the midline of the segment. T4 ranges from entirely black hairs to brown hairs to an even mix of orange and black hairs. T5-T7 are entirely black.

Queen. Length of 21-23mm. UID of 2.90-2.92mm. LID of 3.10-3.15mm. Ocelli just below the supraorbital line. IOD of 0.20-0.23mm. OOD of 0.68-0.71mm. Clypeus coarse and moderately punctate along the margin with hair; in the center punctation is fine and sparse with no hair. Malar length of 0.76mm. Malar width of 1.21-1.24mm. Inter-tegular distance of 5.32-5.72mm. Mesobasitarsus length of 3.70-3.80mm. Mesobasitarsus width of 1.16-1.42mm. T2 width of 9.80-10.00mm.
Worker. Length of 15-17mm. UID of 2.27-2.32mm. LID of 2.19-2.24mm. Ocelli in the middle of the supraorbital line. IOD of 0.20-0.23mm. OOD of 0.55-0.58mm. Clypeus punctuation similar to queen, but with less hair along the margin. Malar length of 0.50-0.55mm. Malar width of 0.78-0.88mm. Inter-tegular distance of 4.05-4.15mm. Mesobasitarsus length of 2.68-3.04mm. Mesobasitarsus width of 0.76-0.91mm. T2 width of 6.26-7.17mm.
Male. Length of 16mm. UID of 2.17-2.22mm. LID of 2.04-2.17mm. Ocelli in the middle of the supraorbital line. IOD of 0.20mm. OOD of 0.55mm. Clypeus coarse and moderately punctate with hair throughout. Malar length of 0.55mm. Malar width of 0.71-0.81mm. Inter-tegular distance of 3.90-4.15mm. Mesobasitarsus length of 2.84-2.94mm. Mesobasitarsus width of 0.76-0.96mm. T2 width of 6.46-6.57mm. Images of male genitalia are in Fig. 2.6E-F.

Diagnosis: This species is distributed south of the Isthmus of Tehuantepec throughout the highlands in the state of Chiapas in Mexico, Guatemala and Honduras (Fig. 2.25). Locus 537 in the *cytochrome oxidase I* gene fragment (primers listed in Duennes *et al.* 2012) is a thymine (T) in *B. wilmattae* and a cytosine (C) in *B. maya*.
Diagnosis note: Because some workers and queens can possess color patterns that are identical to color polymorphisms found in *B. maya*, the substitution present at locus 537 in the COI gene fragment is the only robust way to differentiate this species from the sympatric *B. maya*, but if a queen, worker or male of the "light pronotum" phenotype is found, color pattern alone can be used to identify the sample to *B. wilmattae.*

Distribution: *B. wilmattae* is found in the following states in the following countries: Mexico: Chiapas; Guatemala: Baja Verapaz, Huehuetenango, Quetzaltenango, San Marcos, Sololá, Totonicapán; Honduras: Comayagua, El Paraiso, Francisco Morazán (Fig. 2.25).

Distribution note: Based on Labougle (1990) and museum records, this species most likely also occurs in El Salvador and Nicaragua, but DNA information is needed to positively ID specimens and the study presented in Chapter One did not have samples from these countries.

Types: The original worker holotype of *B. lateralis wilmattae* is deposited in the collections of the Smithsonian National Museum of Natural History in Washington DC, USA. A series of neoparatypes representing different castes and the range of color pattern polymorphism in this species have been designated and housed within the collections of El Colegio de la Frontera Sur in San Cristobal de las Casas, Chiapas, Mexico.

Bombus schneideri **Friese**

Bombus schneideri fuliginosus Friese, 1903, type not seen. Synonymized with *B. ephippiatus* by Franklin, 1913.
Bombus schneideri badiocollis Friese, 1916, type not seen. Synonymized with *B. ephippiatus* by Frison, 1925.
Bombus folsomi Frison, 1922, type not seen. Synonymized with *B. ephippiatus* by Starr, 1989.
Bombus ephippiatus varigatus Frison, 1925, type not seen.

Taxonomic status: *Bombus schneideri* is currently recognized as a color variant of the polymorphic, widespread *B. ephippiatus* (Labougle, 1990). The genetic and morphometric information presented in Chapter One provide robust evidence that *B. ephippiatus* in Costa Rica (and presumably also Panama) are a separate species; therefore I am resurrecting the original species name given to this group in Costa Rica.

Description: *Dorsal Pile*. The queens of *B. schneideri* are strikingly different in color pattern to the queens and workers, with bright orange or orange and black mixed hair where black is present on the workers and males (Fig. 2.26).

Queens (Figs. 2.2-2.3): Queens possess a black and orange mixed patch of pile in the paraocular area of the face and on the vertex of the head (Figs. 2.2B and 2.3B). The pronotum is predominantly orange with very few black hairs interspersed. The scutum is entirely covered in

orange hairs (Figs. 2.2C and 2.3C). The sides of the thorax (the mesepisternum, the scrobe and the metepisternum) are covered entirely with yellow hair (Figs. 2.2A and 2.3A). The scutellum is entirely orange with a few black hairs interspersed near the midline. The metanotum is covered with short feathered black hairs. T1 of the metasoma is entirely yellow with the exception of short sparse black hair along the midline (Figs. 2.2D and 2.3D). T2 is yellow medially with orange ferruginous patches laterally that are small anteriorly and gradually widen posteriorly to form "triangles" at each lateral end of the segment. These orange "triangles" that lie laterally on the segment can vary in size, but generally cover a third of the segment in total. T3-T5 are entirely orange. T6 is predominantly covered in black hair with orange hairs interspersed.

Queen variation: The pattern described above for queens appears to be the most common morph, but another variant exists where all regions orange in color in the pattern described above are a mix of orange and black hairs (Fig. 2.26). These queens appear to be smaller in size than the queens displaying pure orange hair throughout the body.

Workers (Fig. 2.27): Workers possess a black patch of pile in the paraocular area and on the vertex of the head (Fig. 2.27B). The pronotum is covered with a mix of black and yellow hairs; this can be an even mix of black and yellow to predominantly black, but is always mixed and with more black hairs at the base of the pronotal lobe. The scutum is entirely black with the exception of yellow hairs interspersed with black along the boundary with the pronotum; these yellow and black mixed patches can lie laterally with a small patch of black between them or are continuous along the anterior boundary of the scutum (Fig. 2.27C). The sides of the thorax (the mesepisternum, the scrobe and the metepisternum) are covered entirely with yellow hair (Fig. 2.27A). The scutellum is predominately black with yellow hairs interspersed along the margin with the metanotum and the axilla. The metanotum possesses lateral patches posterior to the base of the hindwing comprising predominantly yellow hair with, but with short, black hairs located close to the hindwing base. T1 of the metasoma is entirely yellow with the exception of short sparse black hair along the midline ((Fig. 2.27D). T2 is yellow medially with brown (the individuals hairs are orange at the root and black at the tip) hairs laterally that are small anteriorly and gradually widen posteriorly to form "triangles" at each lateral end of the segment. The color in these "triangles" always consists of two-toned brown setae. These brown "triangles" that lie laterally on the segment can vary in size, but generally cover a third of the segment in

total. T3 is entirely covered with the same brown two-toned hair. T4 ranges from entirely brown two-toned hairs to covered entirely with black hair. T5 and T6 are entirely black.

Males (Figs. 2.4): The males are identical in color pattern to the workers, except the brown two-toned patches on T2 and T3 also have orange ferruginous hairs interspersed with the brown hairs (Fig. 2.4D). T7 is covered entirely with black hairs.

Queen. Length of 20-23mm. UID of 2.65-2.95mm. LID of 2.77-3.03mm. Ocelli just below the supraorbital line. IOD of 0.20-0.23mm. OOD of 0.66-0.76mm. Clypeus coarse and moderately punctate along the margin with hair; in the center punctation is fine and sparse with no hair. Malar length of 0.63-0.71mm. Malar width of 1.06-1.24mm. Inter-tegular distance of 5.47-5.67mm. Mesobasitarsus length of 3.44-3.95mm. Mesobasitarsus width of 1.06-1.27mm. T2 width of 8.48-9.60mm.

Worker. Length of 13-15mm. UID of 2.19-2.22mm. LID of 2.09-2.17mm. Ocelli in the middle of the supraorbital line. IOD of 0.18-0.20mm. OOD of 0.55-0.58mm. Clypeus punctuation similar to queen, but with less hair along the margin. Malar length of 0.50mm. Malar width of 0.76-0.81mm. Inter-tegular distance of 3.65-4.15mm. Mesobasitarsus length of 2.48-2.73mm. Mesobasitarsus width of 0.66-0.86mm. T2 width of 5.96-6.26mm.

Male. Length of 17-18mm. UID of 2.27-2.29mm. LID of 2.22-2.29mm. Ocelli in the middle of the supraorbital line. IOD of 0.20mm. OOD of 0.55mm. Clypeus coarse and moderately punctate with hair throughout. Malar length of 0.55mm. Malar width of 0.66-0.88mm. Inter-tegular distance of 3.85-4.25mm. Mesobasitarsus length of 2.89-2.94mm. Mesobasitarsus width of 0.71-0.81mm. T2 width of 6.06-7.27mm. Images of male genitalia are in Fig. 2.6G-H.

Diagnosis: This species is distributed throughout montane regions of Costa Rica and northern Panama (Fig. 2.26). Queens possess a distinctive color pattern with orange pile covering the dorsum of the thorax and lower abdomen (Fig. 2.26). *B. schneideri* possesses a thymine (T) at locus 537 in the *cytochrome oxidase I* gene fragment.

Diagnosis note: B. wilmattae also possesses a thymine (T) nucleotide at locus 537 and the color patterns of workers and males are identical to some color variants of *B. maya* and *B. wilmattae*, but geographic location and nucleotide substitution together can definitively distinguish *B. schneideri* from the other species in this complex.

Distribution: *B. schneideri* is found in the following states in the following countries: Costa Rica: Cartago, San José, Puntarenas; Panama: Chiriquí (Fig. 2.26).

Types: The queen holotype of *B. schneideri,* as well as the queen types for *B. schneideri fuliginosus* and *B. schneideri badiocollis* are deposited at the Museum Für Naturkunde in Berlin, Germany. The queen type of *B. folsomi* is deposited at The Academy of Natural Sciences of Drexel University in Philadelphia, Pennsylvania, USA. The male type of *B. ephippiatus variegatus* is deposited at the University of Michigan Museum of Zoology in Ann Arbor, Michigan, USA.

References

Bartomeus I, Ascher JS, Gibbs J, Danforth BN, Wagner DL, Hedtke SM, Winfree R. 2013. Historical changes in northeastern US bee pollinators related to shared ecological traits. Proceedings of the *National Academy of Sciences of the United States of America* 110: 4656-4660.

Cameron SA, Hines HM, Williams PH. 2007. A comprehensive phylogeny of the bumble bees (*Bombus*). *Biological Journal of the Linnean Society* 91: 161-188.

Cameron SA, Lozier JD, Strange JP, Koch JB, Cordes N, Solter LF, Griswold TL. 2011. Patterns of widespread decline in North American bumble bees. *Proceedings of the National Academy of Sciences of the United States of America* 108: 662-667.

Cockerell TDA. 1899. Catálogo de las abejas de México. *México: Secretaría de Fomento* 19.

Cockerell TDA. 1912. Descriptions and records of bees—XLV. *The Annals and Magazine of Natural History* 10: 21.

Cockerell TDA. 1949. Bees from Central America, principally Honduras. *Proceedings of the United States National Museum* 98: 486-487.

Cresson ET. 1863. List of the North American species of *Bombus* and *Apathus*. *Proceedings of the Entomological Society of Philadelphia* 2: 108.

Dalla Torre CG. 1896. *Catalogus Hymenopterorum hucusque descriptorum systematicus et synonymicus*. Lipsiae: *Guilelmi Engelmann* 10: 518.

Darwin C. 1859. *The Origin of Species by Means of Natural Selection, or, the Preservation of Favoured Races in the Struggle for Life.* London, UK: Murray.

Dillion ME, Frazier MR, Dudley R. 2006. Into thin air: physiology and evolution of alpine insects. *Integrative and Comparative Biology* 46: 49-61.

Duennes MA, JD Lozier, HM Hines, SA Cameron. 2012. Geographical patterns of genetic divergence in the widespread Mesoamerican bumble bee *Bombus ephippiatus* (Hymenoptera: Apidae). *Molecular Phylogenetics and Evolution* 64: 219-231.

Franklin HJ. 1913. The Bombidae of the New World. *Transactions of the American Entomological Society* 38: 177-486.

Franklin HJ. 1915. Notes on Bombidae, with descriptions of new forms (Hym.). *Entomological News and Proceedings of the Entomological Sections of the Academy of Natural Sciences of Philadelphia* 26: 409-410.

Free JB, Butler CG. 1959. *Bumblebees*. London, UK: Collins New Naturalist.

Friese H. 1903. Neue Bombus-Arten aus der neotropischen Region. (Hym.). *Zeitschrift Für Systematische Hymenopterologie Und Dipterologie* 3: 253.

Friese H. 1916. Zur Bienenfauna von Costa Rica (Hym.). *Stettiner Entomologische Zeitung* 77: 288.

Frison TH. 1922. Systematic and biological notes on bumblebees (Bremidae; Hymenoptera). *Transactions of the American Entomological Society* 48: 322.

Frison TH. 1925. Contribution to the classification of the Bremidae (Bumble-bees) of Central and South America. *Transactions of the American Entomological Society* 51: 139.

Goulson D, Lye GC, Darvill B. 2008. Decline and conservation of bumble bees. *Annual Review of Entomology* 53: 191-208.

Handlirsch A. 1888. Die hummelsammlung des k.k. naturhistorischen hofmuseums. *Annalen des Naturhistorischen Museums in Wien* 3: 233.

Heinrich B. 2004. *Bumblebee economics (with a new preface)*. Cambridge, MA: Harvard University Press.

Hines HM, Williams P. 2012. Evolution of Müllerian mimicry in the highly color polymorphic bumble bee *Bombus trifaciatus* and its comimics. *Zoological Journal of the Linnean Society* 166: 805-826.

Labougle JM, Ito M, Okazawa T. 1985. The species of the genus *Bombus* (Hymenoptera: Apidae) of Chiapas, Mexico and Guatemalal; with a morphometric and altitudinal analysis. *Folia Entomólgica Mexicana* 64: 55-72.

Labougle JM. 1990. *Bombus* of México and Central America (Hymenoptera, Apidae). *The University of Kansas Science Bulletin* 54: 35-73.

Linnaeus C. 1758. *Systema naturae per regna tria naturae, secundum classes, ordines, genera, species, cum characteribus, differentiis, synonymis, locis. Holmiae* 579.

Michener C. 2007. *The Bees of the World, second edition*. Baltimore, MD: The Johns Hopkins University Press.

Milliron HE. 1962. Taxonomic notes on some American bumblebees (Hymenoptera: Apidae; Bombinae). *Canadian Entomologist* 94: 731.

Morales CL, Arbetman MP, Cameron SA, Aizen MA. 2013. Rapid ecological replacement of a native bumble bee by invasive species. *Frontiers in Ecology and the Environment* 11:529-534.

Plath OE. 1934. Bumblebees and their ways. New York, NY: The Macmillan Company.

Rapti Z, Duennes MA, Cameron SA. 2014. Defining the colour pattern phenotype in bumble bees (*Bombus*): a new model for evo devo. *Biological Journal of the Linnean Society* 113: 384-404.

Sakagami SF. 1976. Specific differences in the bionomic characters of bumblebees: a comparative review. *Journal of the Faculty of Science Hokkaido University* 20: 390-447.

Say T. 1837. Part XVII – Descriptions of new species of North American Hymenoptera, and observations on some already described. *Boston Journal of Natural History* 1: 414.

Smith F. 1854. *Catalogue of Hymenopterous Insects in the Collection of the British Museum. Part II. Apidae*. London, UK: British Museum.

Smith F. 1879. *Descriptions of New Species of Hymenoptera in Collection of the British Museum.* London, UK: British Museum.

Starr CK. 1989. *Bombus folsomi* and the origin of Philippine bumble bees (Hymenoptera: Apidae). *Systematic Entomology* 14: 411.

Williams PH. 1986. Environmental change and the distributions of British bumble bees (*Bombus* Latr.). *Bee World* 67: 50-61.

Williams PH. 1998. An annotated checklist of bumble bees with an analysis of patterns of description (Hymenoptera: Apidae, Bombini). *Bulletin of the Natural History Museum of London (Entomology)* 67: 128.

Williams P. 2007. The distribution of bumblebee colour patterns worldwide: possible significance for thermoregulation, crypsis, and warning mimicry. *Biological Journal of the Linnean Society* 92: 97-118.

Williams PH, Osborne JL. 2009. Bumblebee vulnerability and conservation world-wide. *Apidologie* 40: 367-387.

Table 2.1. A list of abbreviations used in the species descriptions and the anatomical features they reference. These same abbreviations are used by Labougle (1990).

Abbreviation	Anatomical feature
UID	Upper Interocular Distance
LID	Lower Interocular Distance
IOD	Interocellar Distance
OOD	Ocellocular Distance
T-N	Metasomal tergum number N

Figure 2.1. Distribution of *B. ephippiatus* and *B. wilmattae* as they are currently recognized taxonomically. Points represent samples used for the population genetic analyses of Chapter One, as well as localities listed by Labougle (1990). Grey-shaded areas of the map represent World Wildlife Federation (WWF) ecoregions in which both species can be found. The Isthmus of Tehuantepec (IT) and the Nicaraguan Depression (ND) are highlighted.

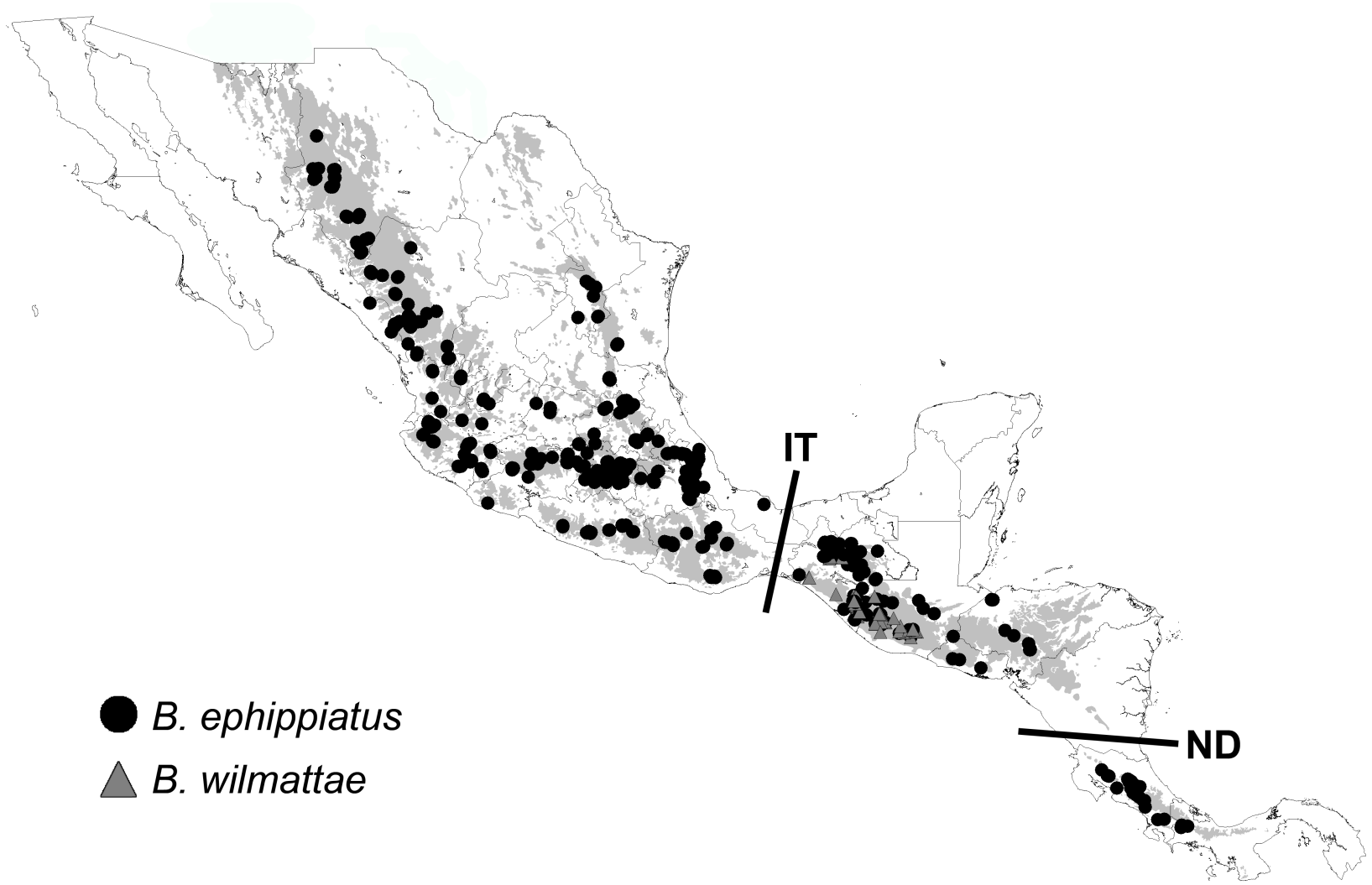

Figure 2.2. Images of a larger queen representative of the newly resurrected species, *Bombus schneideri*. A) view of the ride side B) view of the head C) view of the dorsal thorax D) view of the dorsal abdomen.

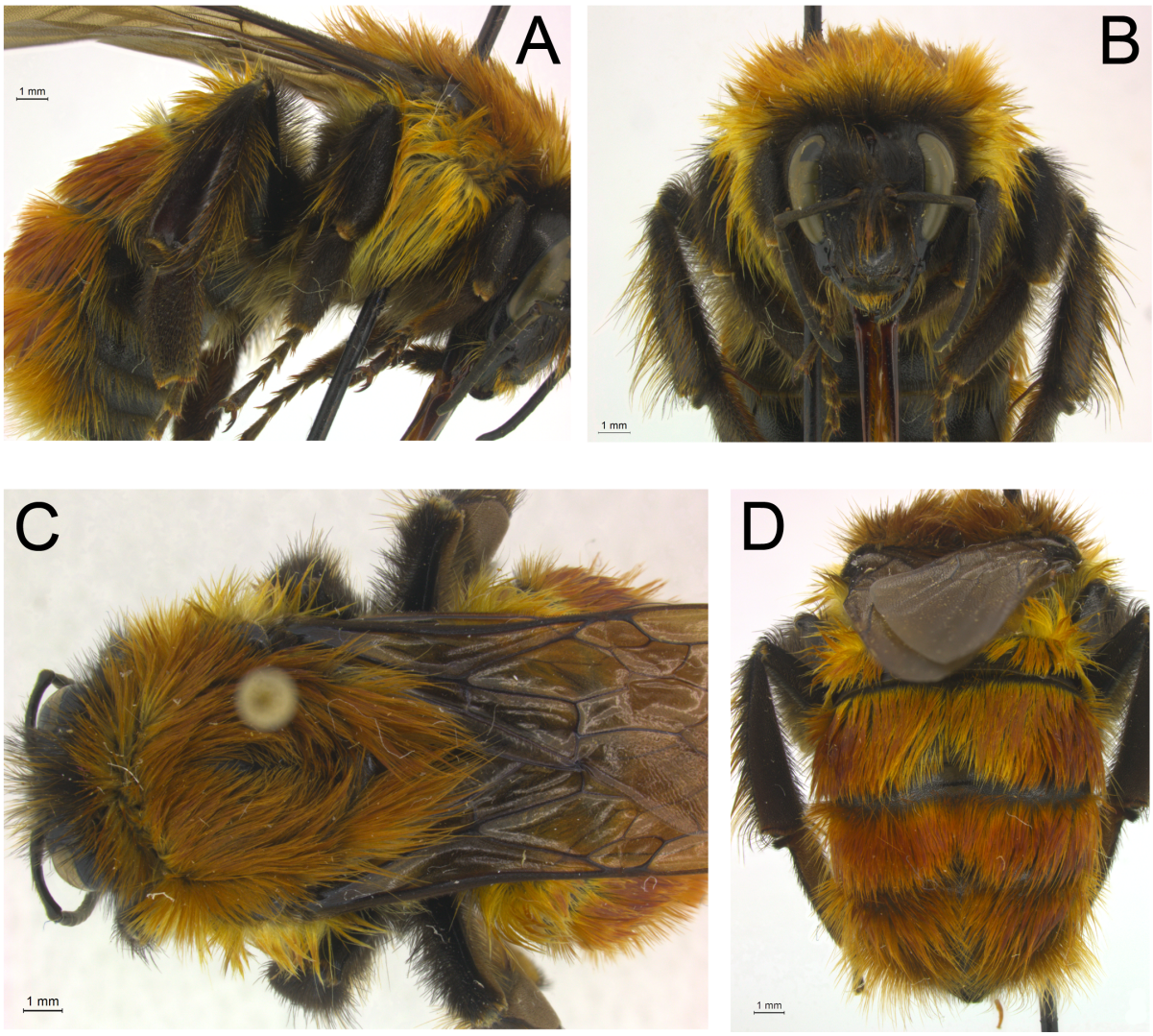

Figure 2.3. Images of a smaller queen representative of the newly resurrected species, *Bombus schneideri*. A) view of the ride side, B) view of the head, C) view of the dorsal thorax and D) view of the dorsal abdomen.

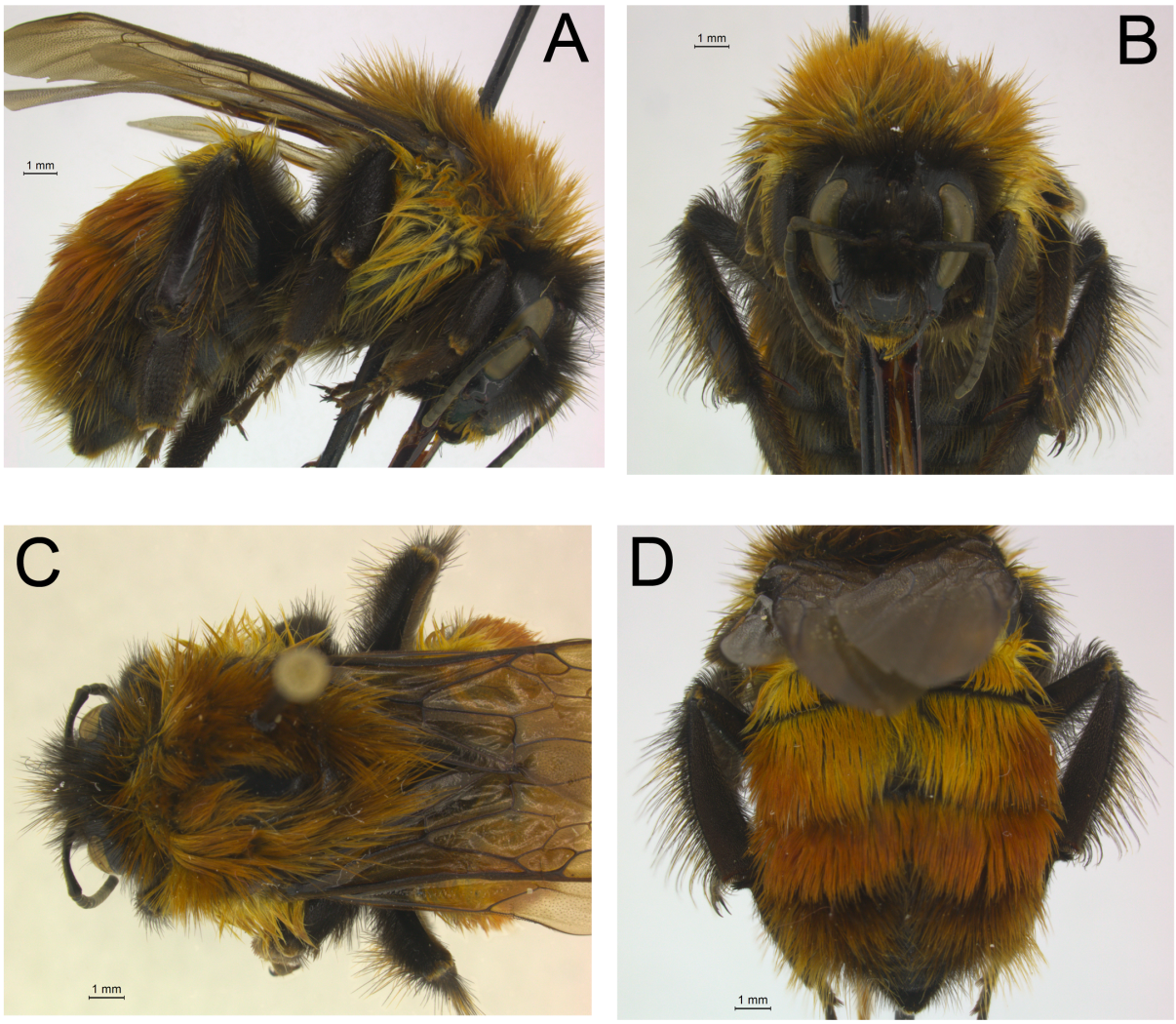

Figure 2.4. Images of a male representative of the newly resurrected species, *Bombus schneideri*. A) view of the ride side, B) view of the head, C) view of the dorsal thorax and D) view of the dorsal abdomen.

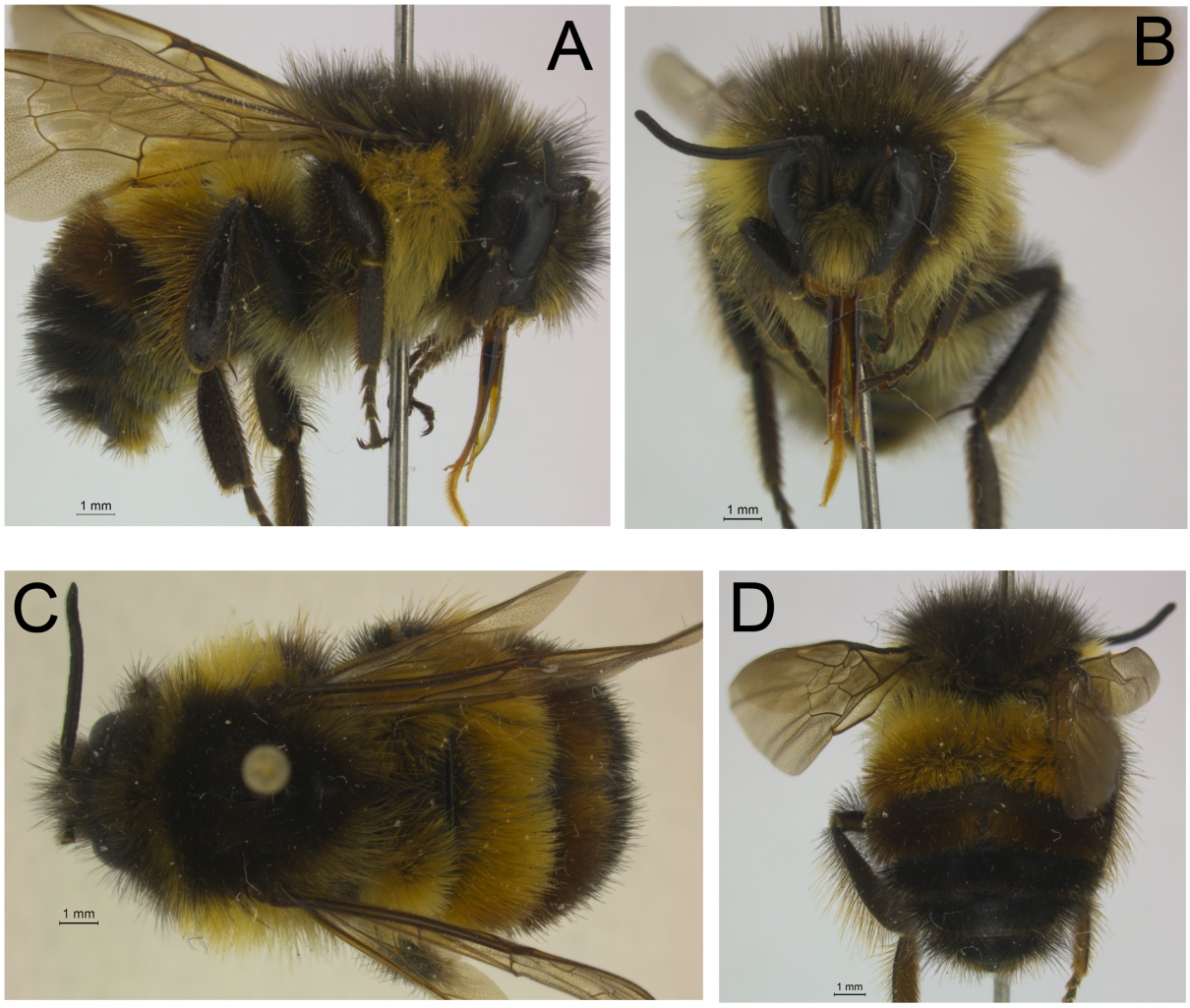

Figure 2.5. Images of a queen representative from the Western region of the distribution of the revised species *Bombus ephippiatus.* A) view of the ride side, B) view of the head, C) view of the dorsal thorax and D) view of the dorsal abdomen.

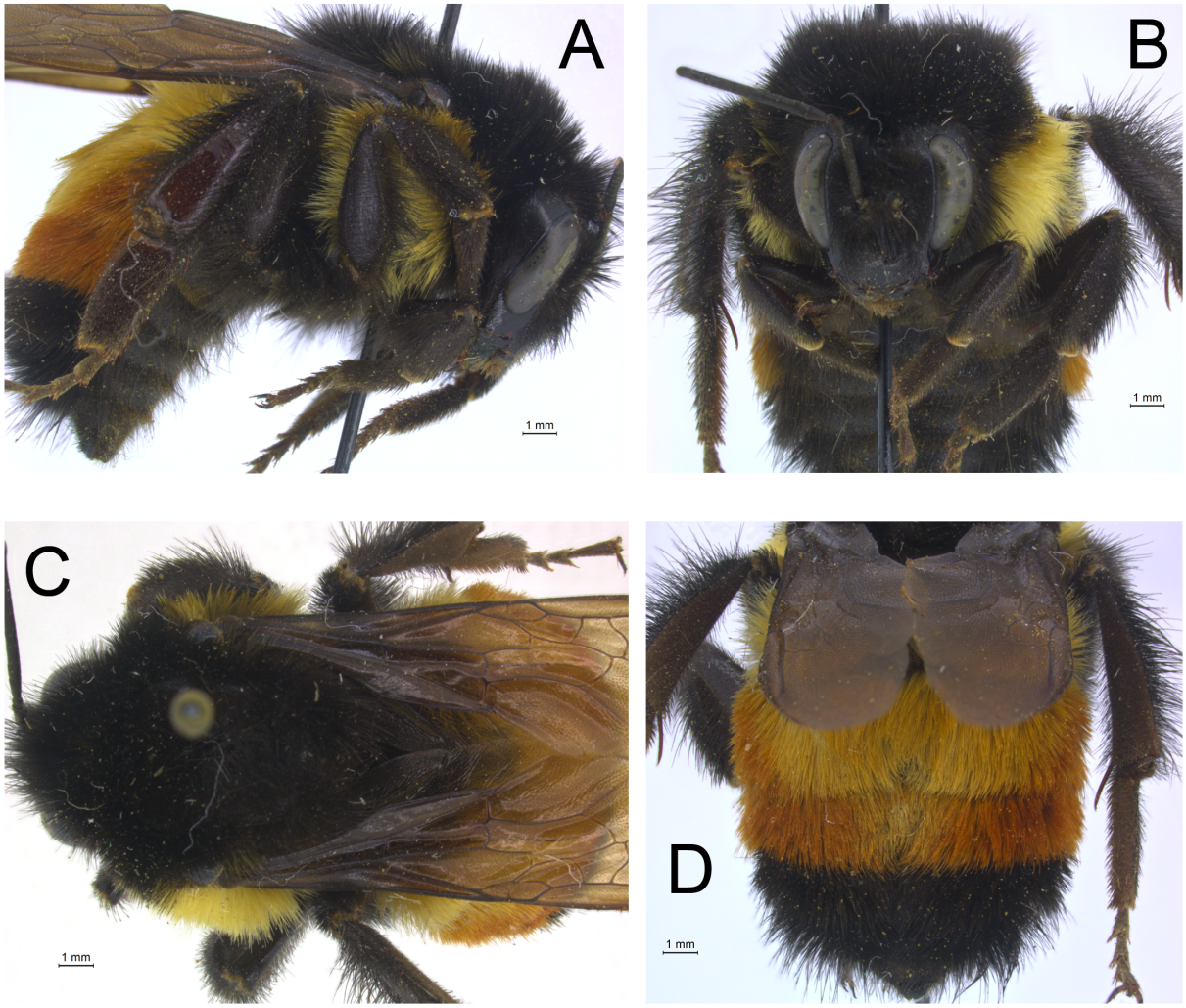

Figure 2.6. Dorsal and vental images of the male genitalia of the species described. A) ventral *B. ephippiatus,* B) dorsal *B. ephippiatus*, C) ventral *B. maya*, D) dorsal *B. maya,* E) ventral *B. wilmattae,* F) dorsal *B. wilmattae*, G) ventral *B. schneideri*, H) dorsal *B. schneideri.*

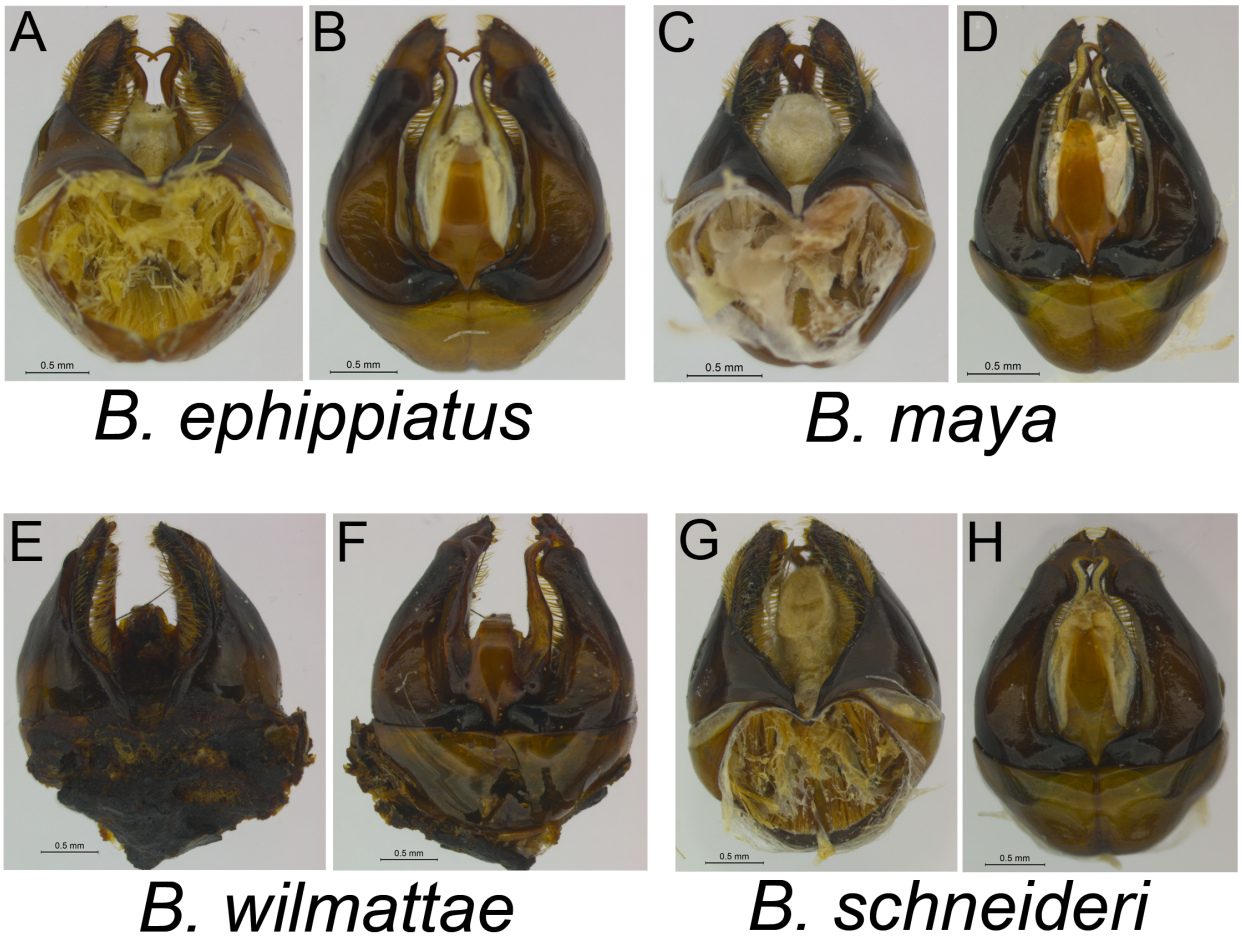

Figure 2.7. Geographic distribution of the revised *B. ephippiatus* as well as the range of color pattern variation it exhibits across its range. Sample points represent specimens that have been confirmed to belong to *B. ephippiatus* (i.e. samples used for genetic analyses in Chapter One). Grey-shaded areas of the map represent World Wildlife Federation (WWF) ecoregions of suitable habitat for the species. Larger bees represent queen color patterns, bees with an additional seventh abdominal segment represent male color patterns and the others are worker color patterns.

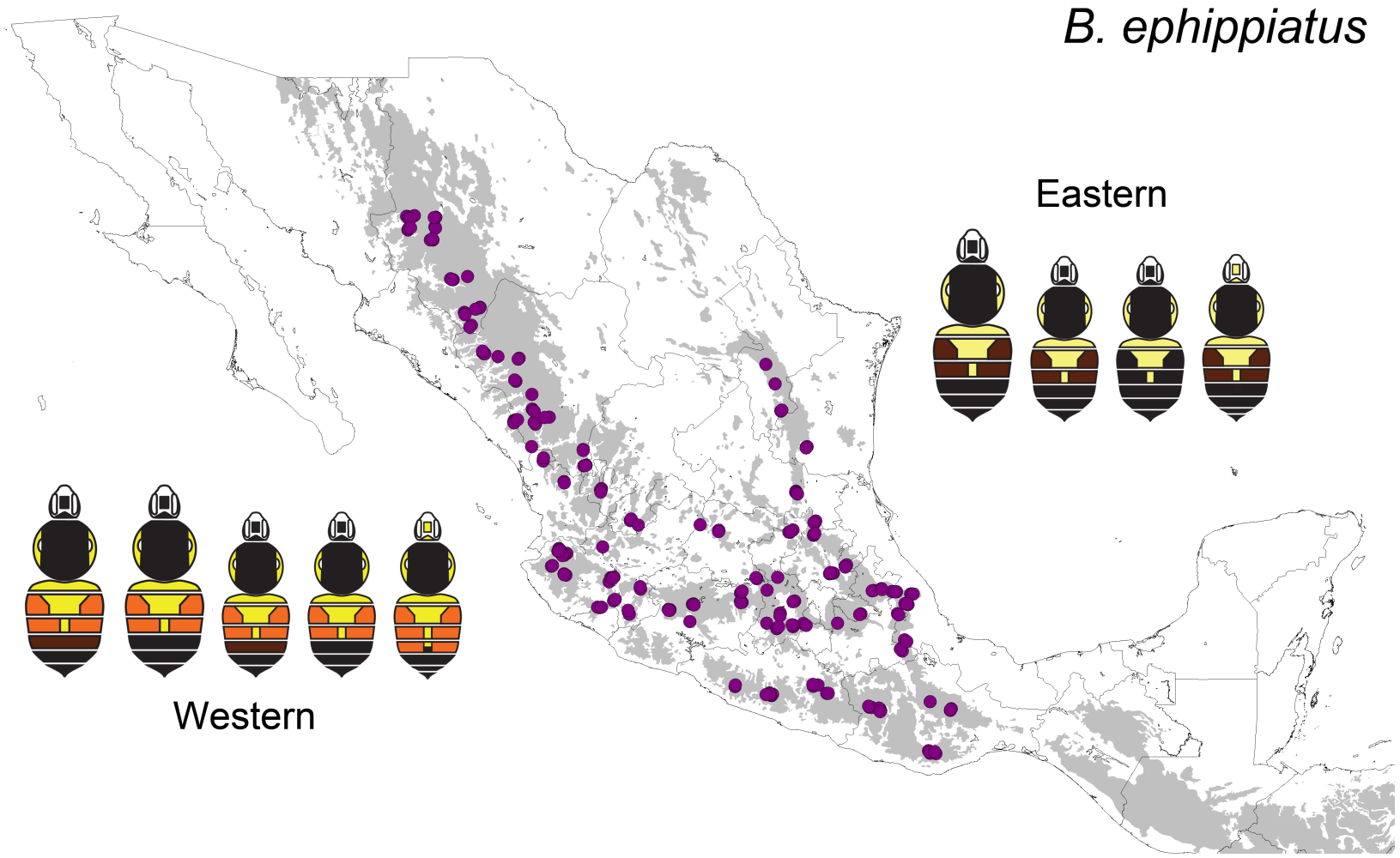

Figure 2.8. Images of a worker representative from the Western region of the distribution of the revised species *Bombus ephippiatus.* A) view of the ride side, B) view of the head, C) view of the dorsal thorax and D) view of the dorsal abdomen.

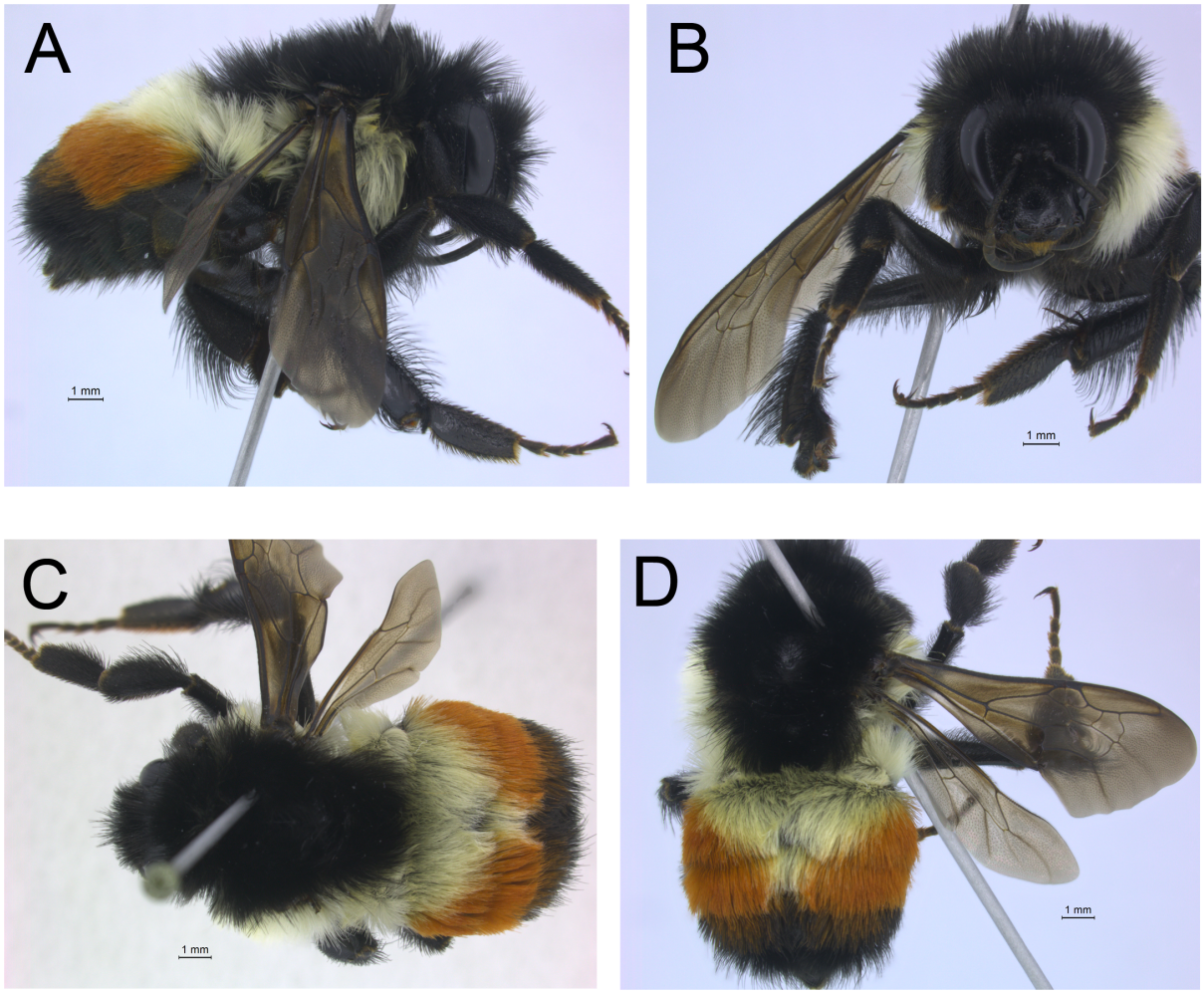

Figure 2.9. Images of a male representative from the Western region of the distribution of the revised species *Bombus ephippiatus.* A) view of the ride side, B) view of the head, C) view of the dorsal thorax and D) view of the dorsal abdomen.

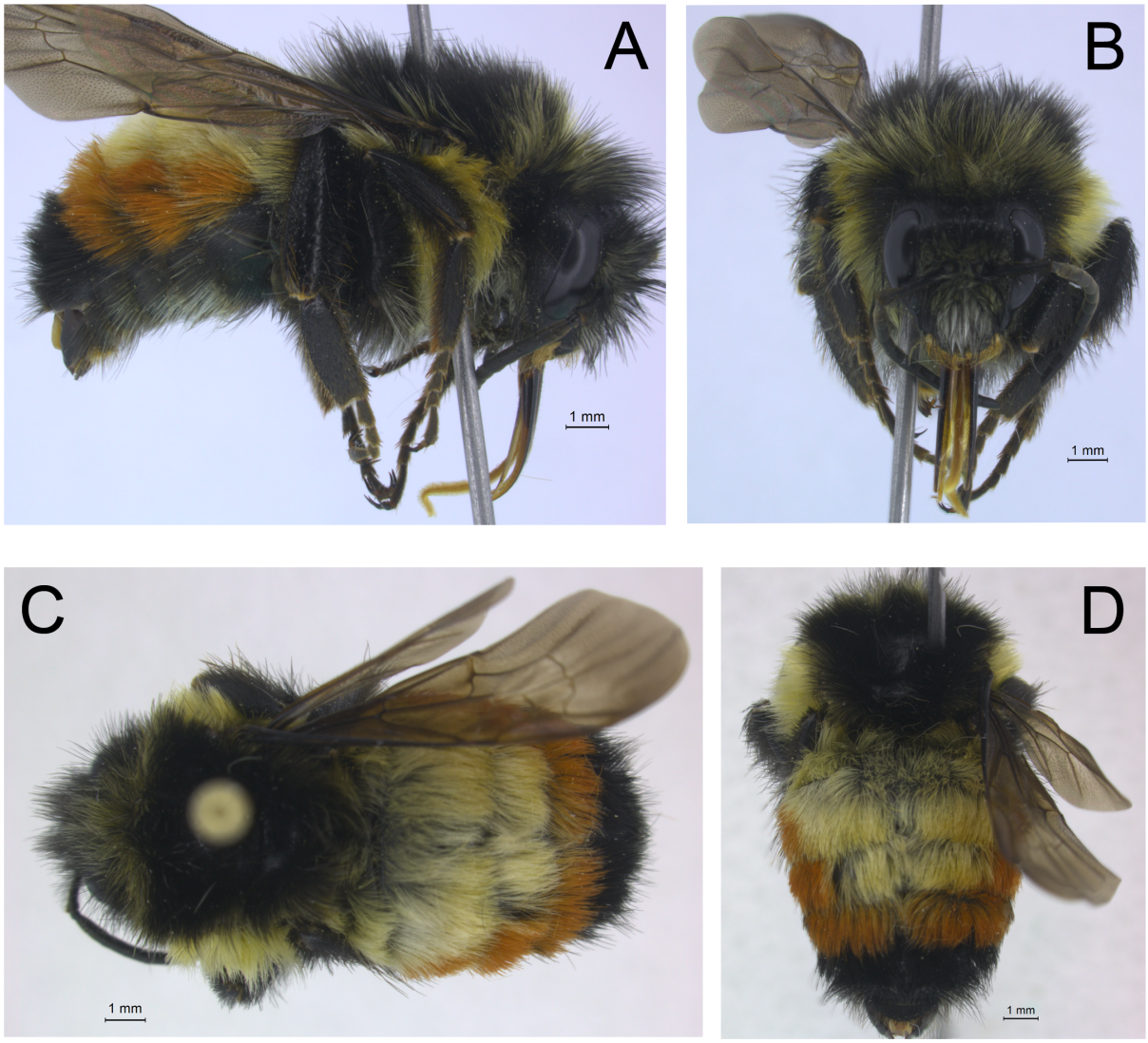

Figure 2.10. Images of a queen representative from the Eastern region of the distribution of the revised species *Bombus ephippiatus.* A) view of the ride side, B) view of the head, C) view of the dorsal thorax and D) view of the dorsal abdomen.

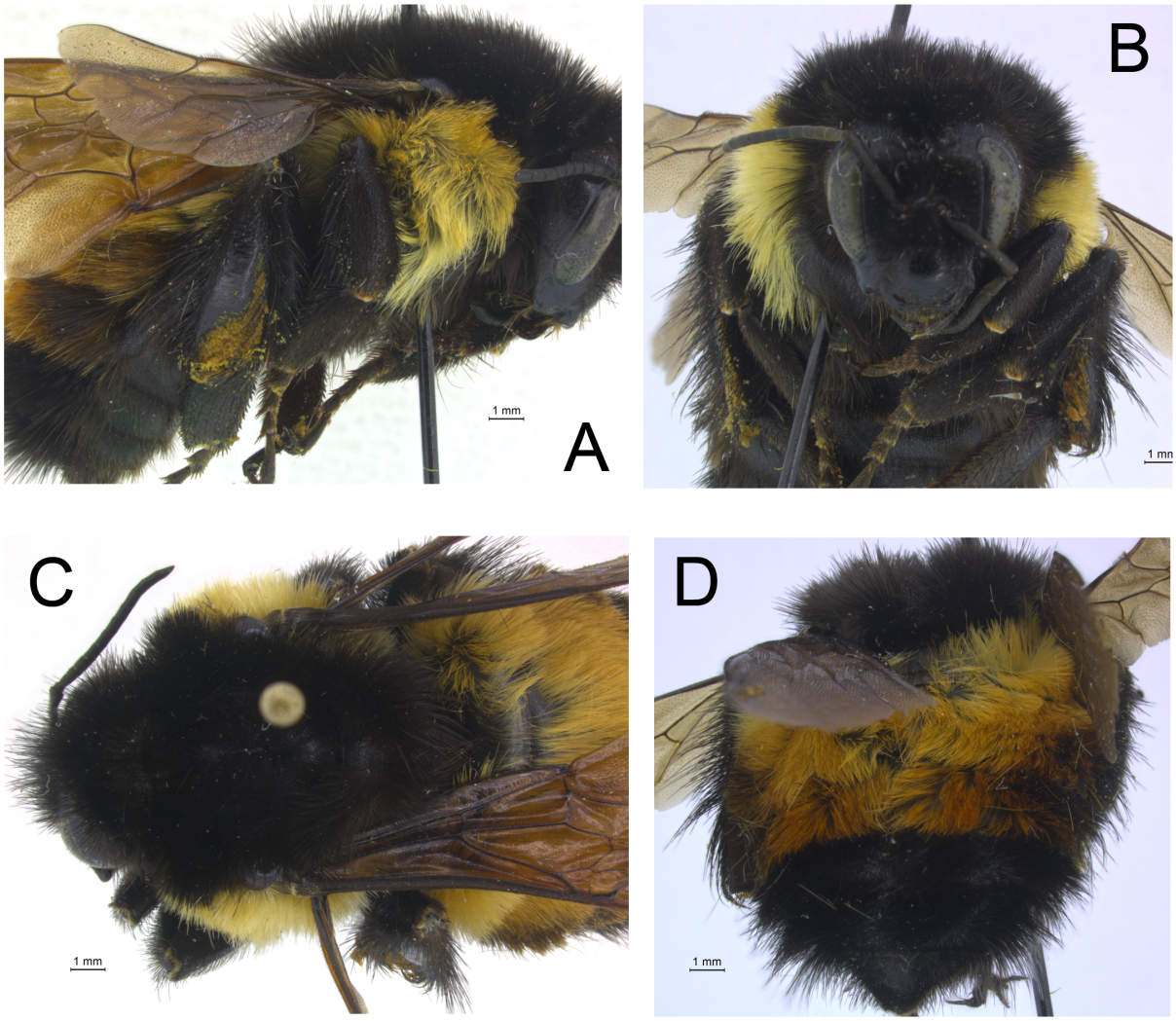

Figure 2.11. Images of a worker representative from the Eastern region of the distribution of the revised species *Bombus ephippiatus.* A) view of the ride side, B) view of the head, C) view of the dorsal thorax and D) view of the dorsal abdomen.

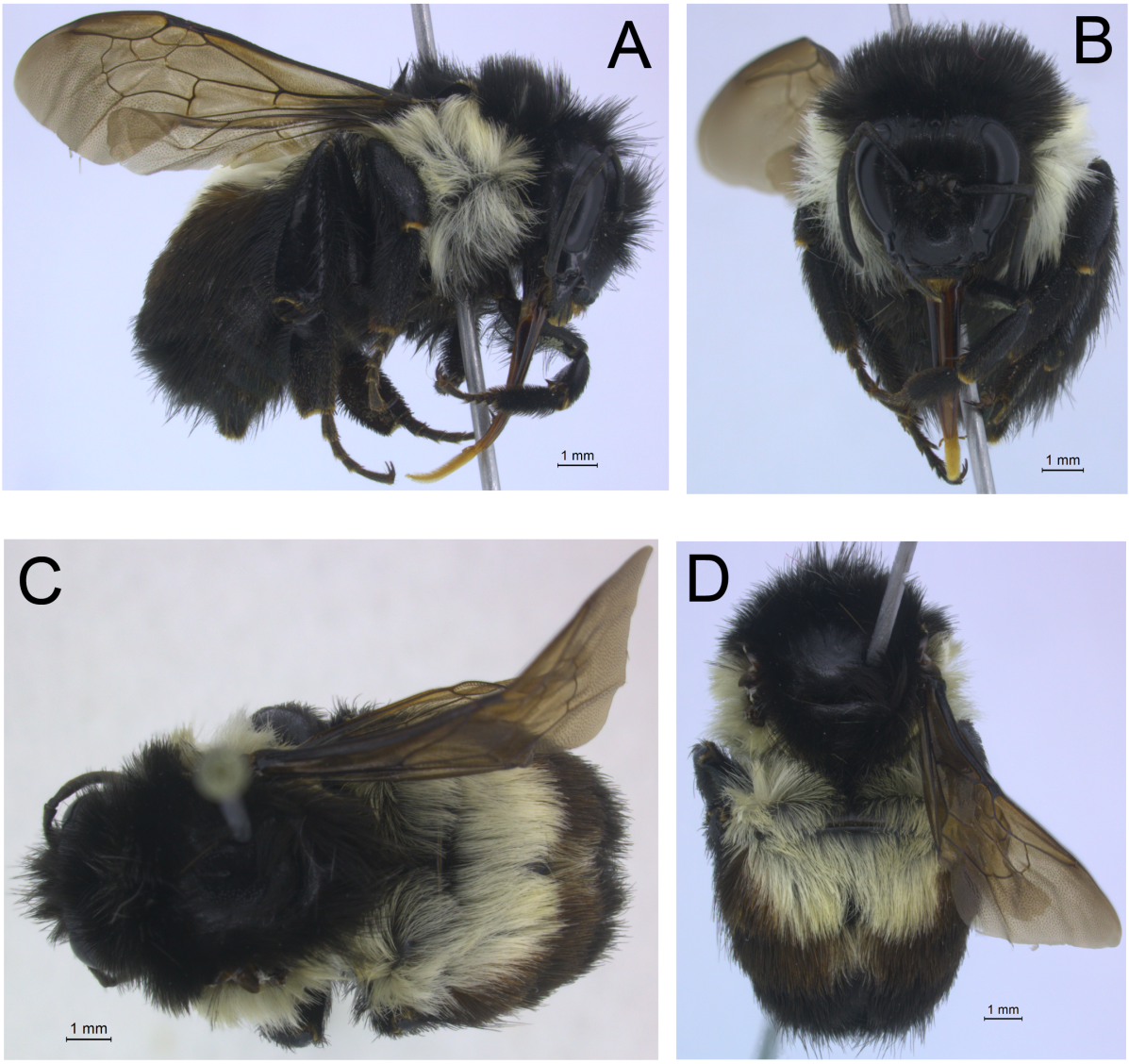

Figure 2.12. Images of a male representative from the Eastern region of the distribution of the revised species *Bombus ephippiatus.* A) view of the ride side, B) view of the head, C) view of the dorsal thorax and D) view of the dorsal abdomen.

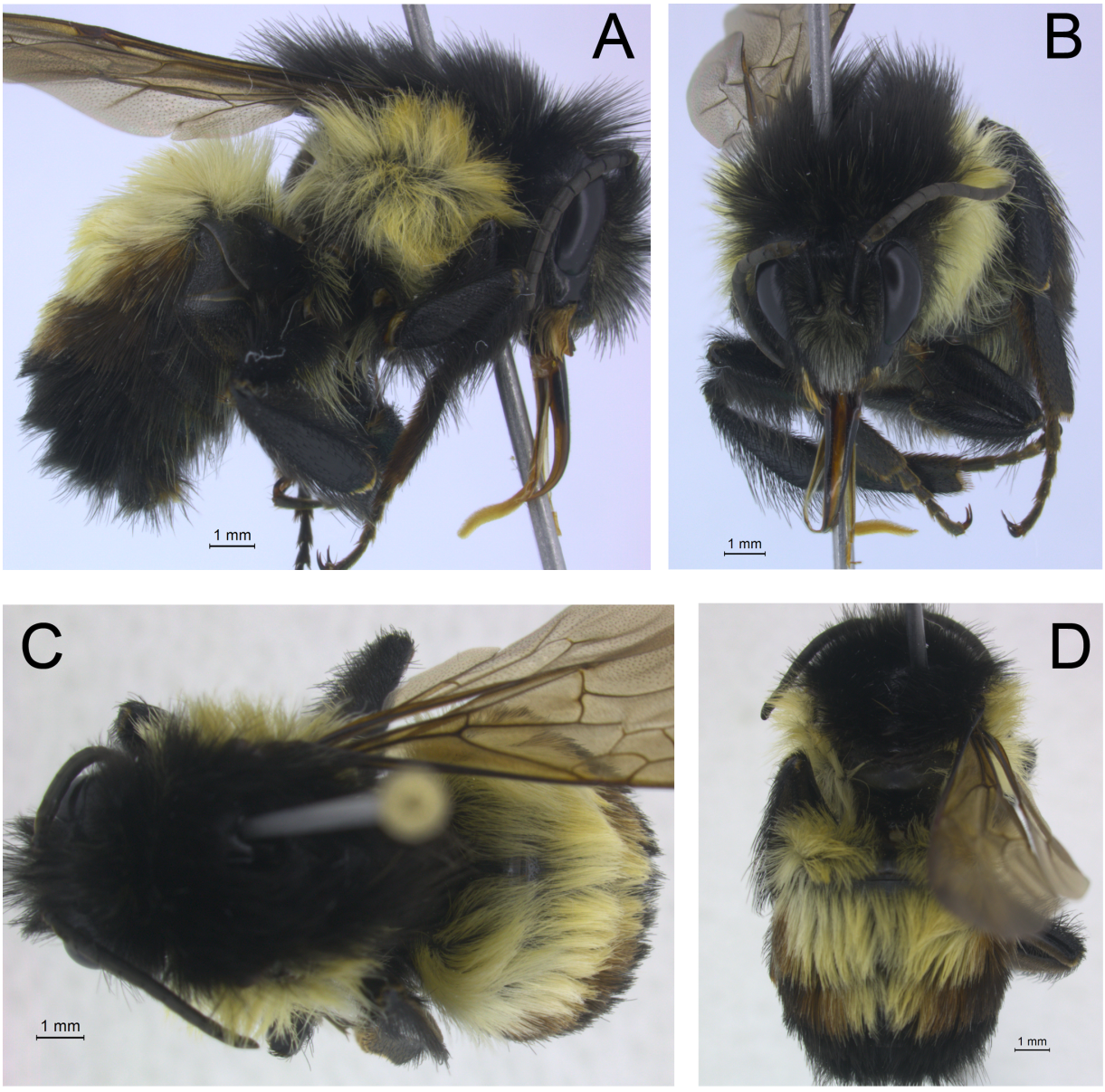

Figure 2.13. Images of a queen representative displaying a brown abdomen color variant of *Bombus maya* sp. nov. A) view of the ride side, B) view of the head, C) view of the dorsal thorax and D) view of the dorsal abdomen.

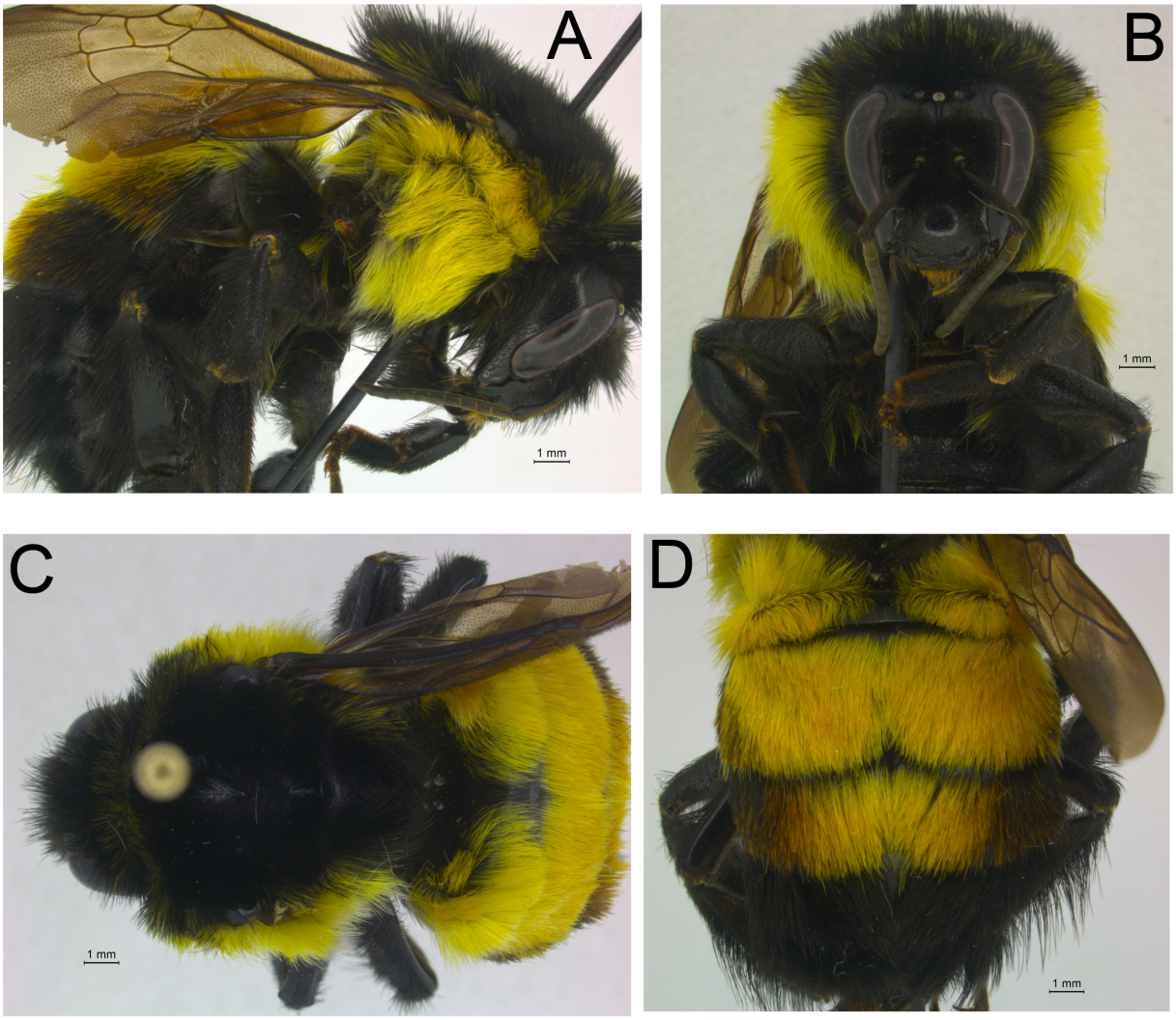

Figure 2.14. Images of a queen representative displaying an orange abdomen color variant of *Bombus maya* sp. nov. A) view of the ride side, B) view of the head, C) view of the dorsal thorax and D) view of the dorsal abdomen.

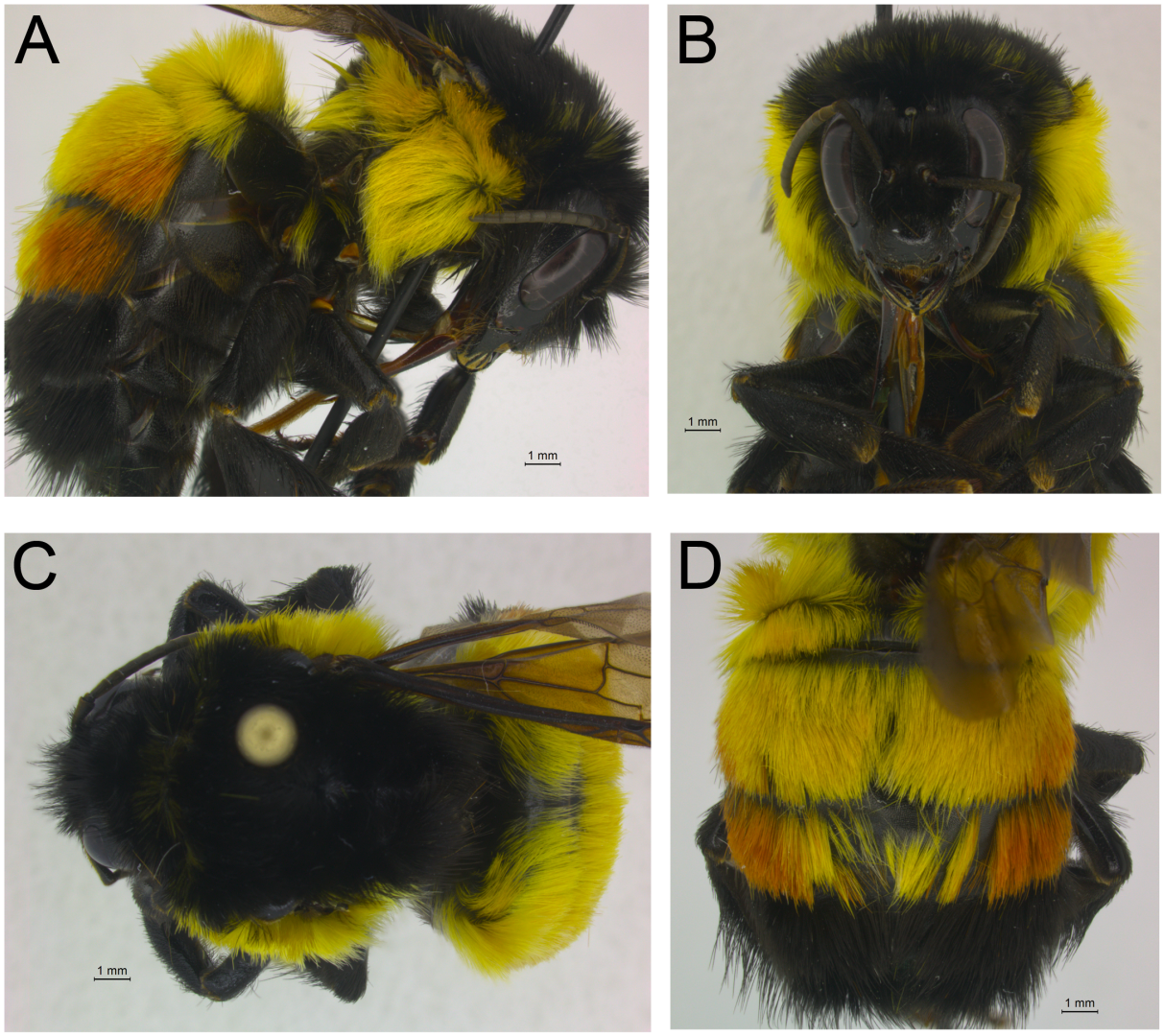

Figure 2.15. Images of a queen representative displaying a yellow pronotum color variant of *Bombus maya* sp. nov. A) view of the ride side, B) view of the head, C) view of the dorsal thorax and D) view of the dorsal abdomen.

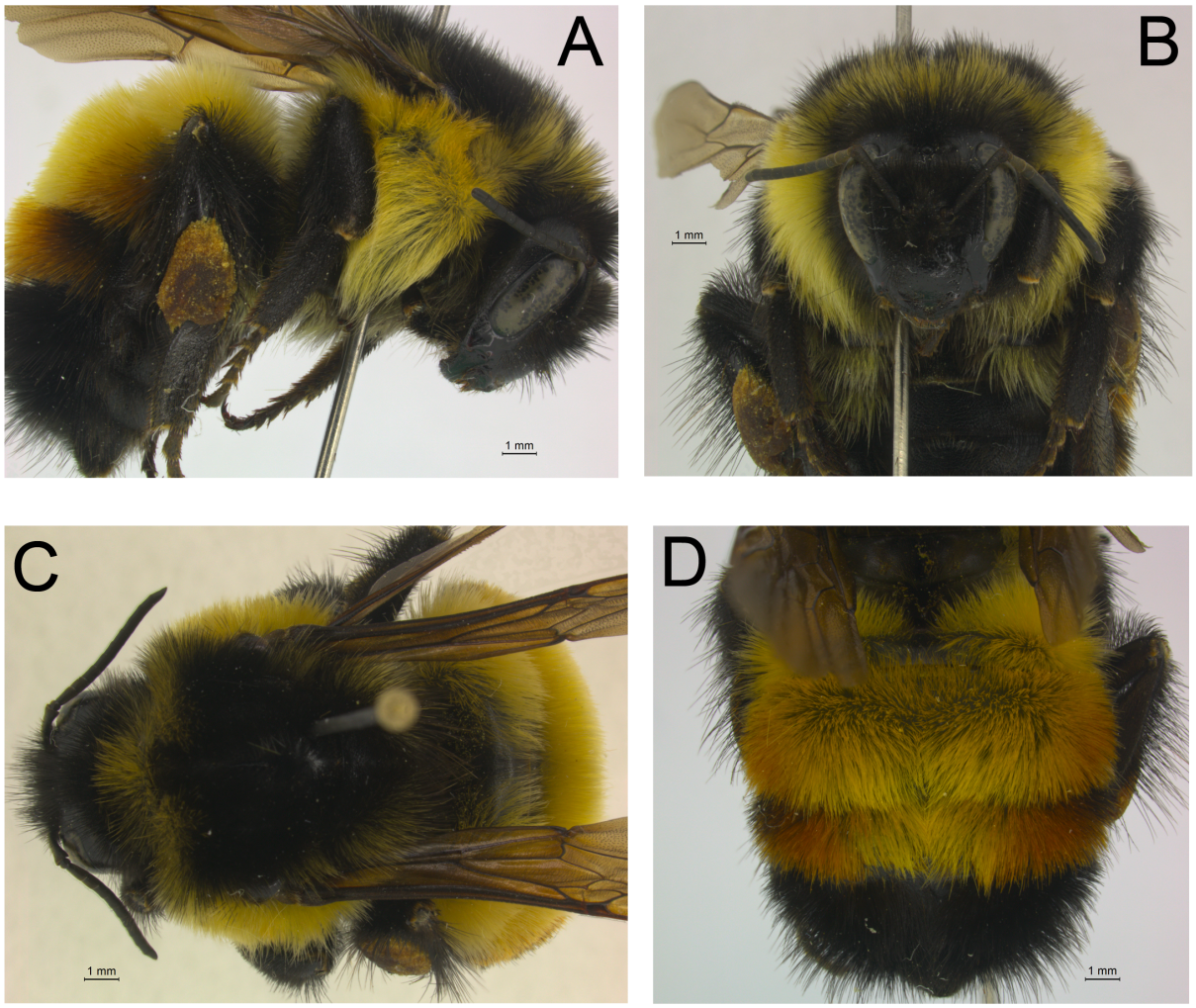

Figure 2.16. Images of a worker representative of *Bombus maya* sp. nov. A) view of the ride side, B) view of the head, C) view of the dorsal thorax and D) view of the dorsal abdomen.

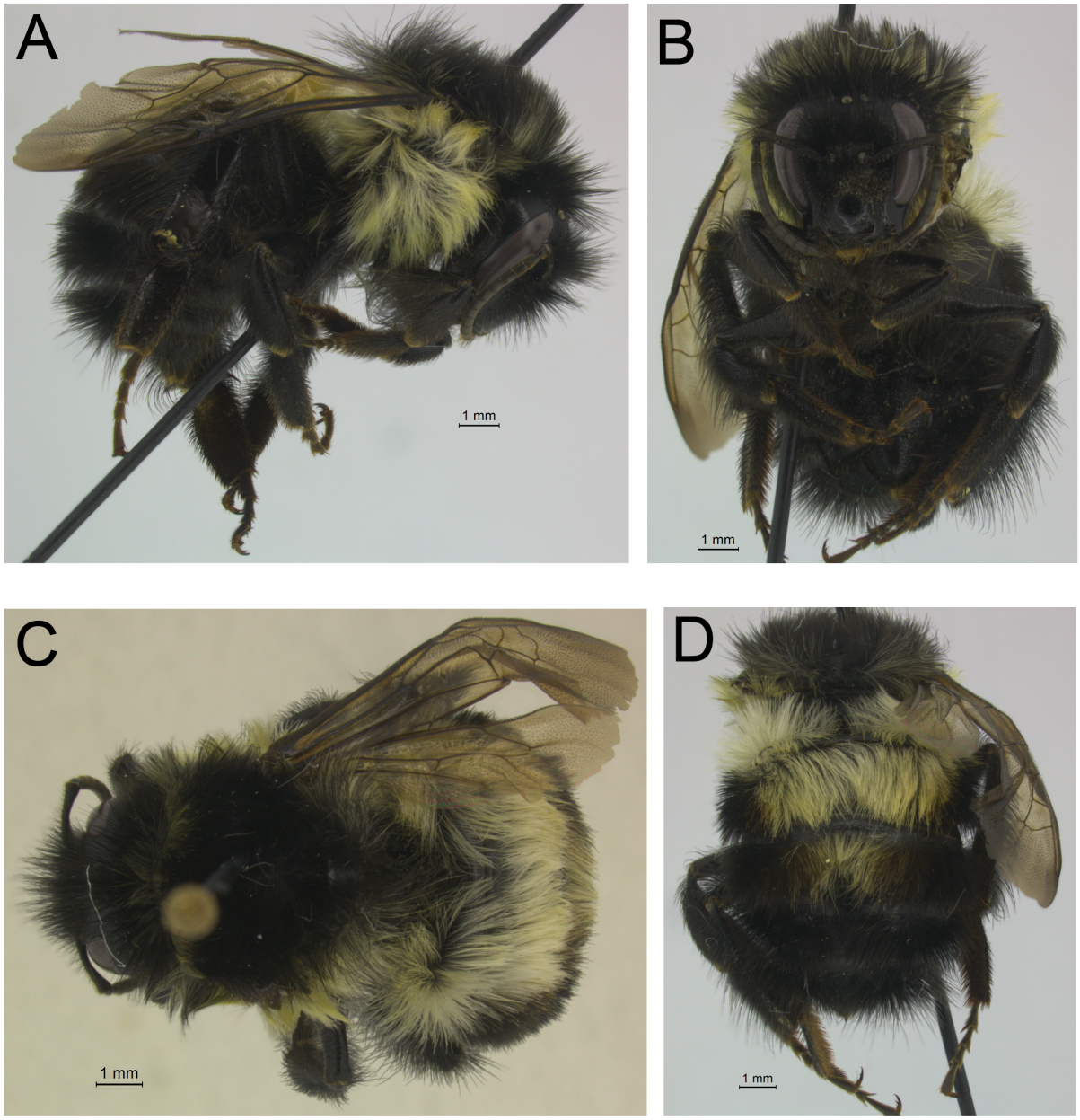

Figure 2.17. Images of a male representative of *Bombus maya* sp. nov. A) view of the ride side, B) view of the head, C) view of the dorsal thorax and D) view of the dorsal abdomen.

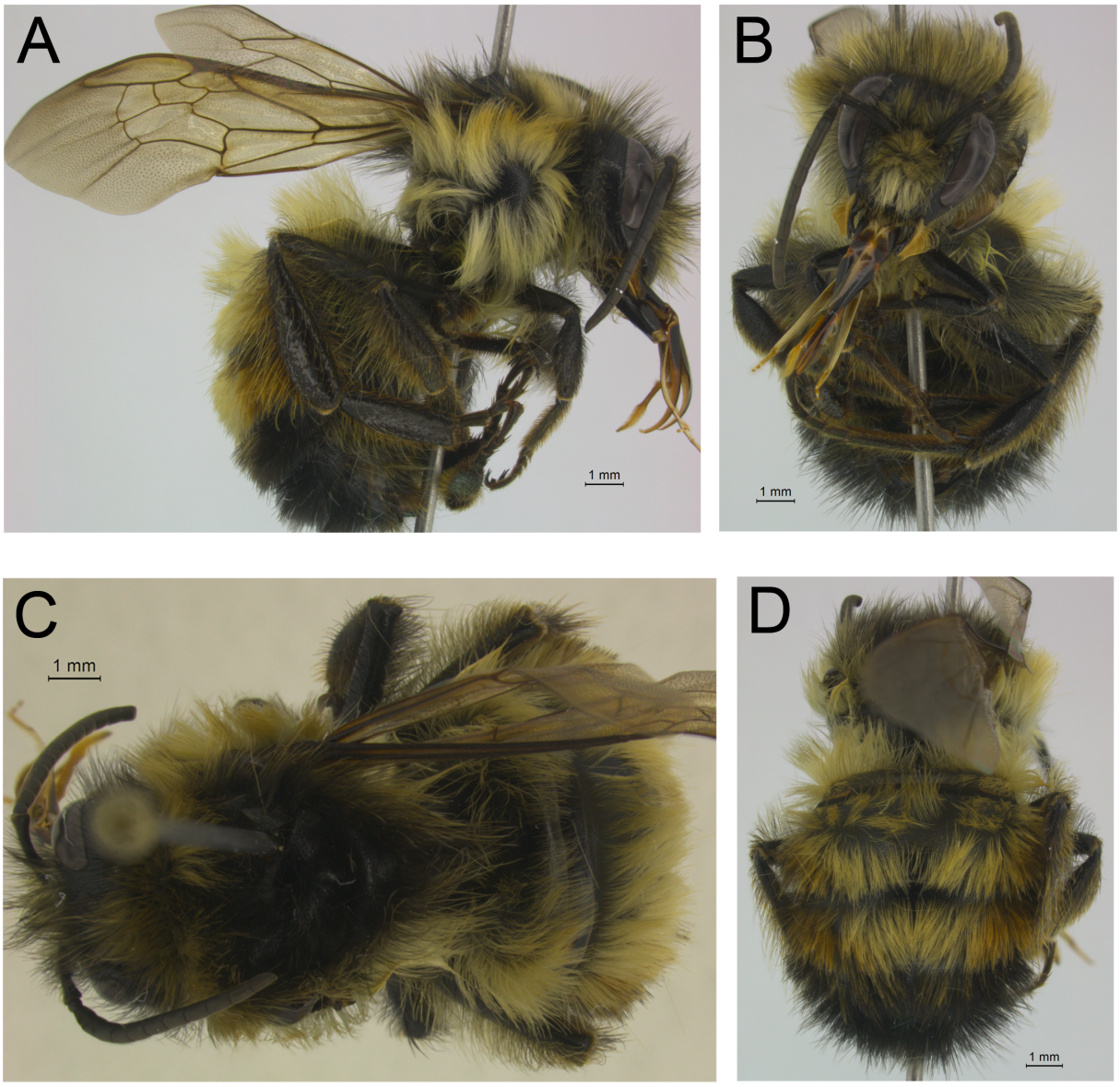

Figure 2.18. Geographic distribution of *B. maya* sp. nov. as well as the range of color pattern variation it exhibits across its range. Sample points represent specimens that have been confirmed to belong to *B. maya* sp. nov. (i.e. samples used for genetic analyses in Chapter One). Grey-shaded areas of the map represent World Wildlife Federation (WWF) ecoregions of suitable habitat for the species. Larger bees represent queen color patterns, bees with an additional seventh abdominal segment represent male color patterns and the others are worker color patterns.

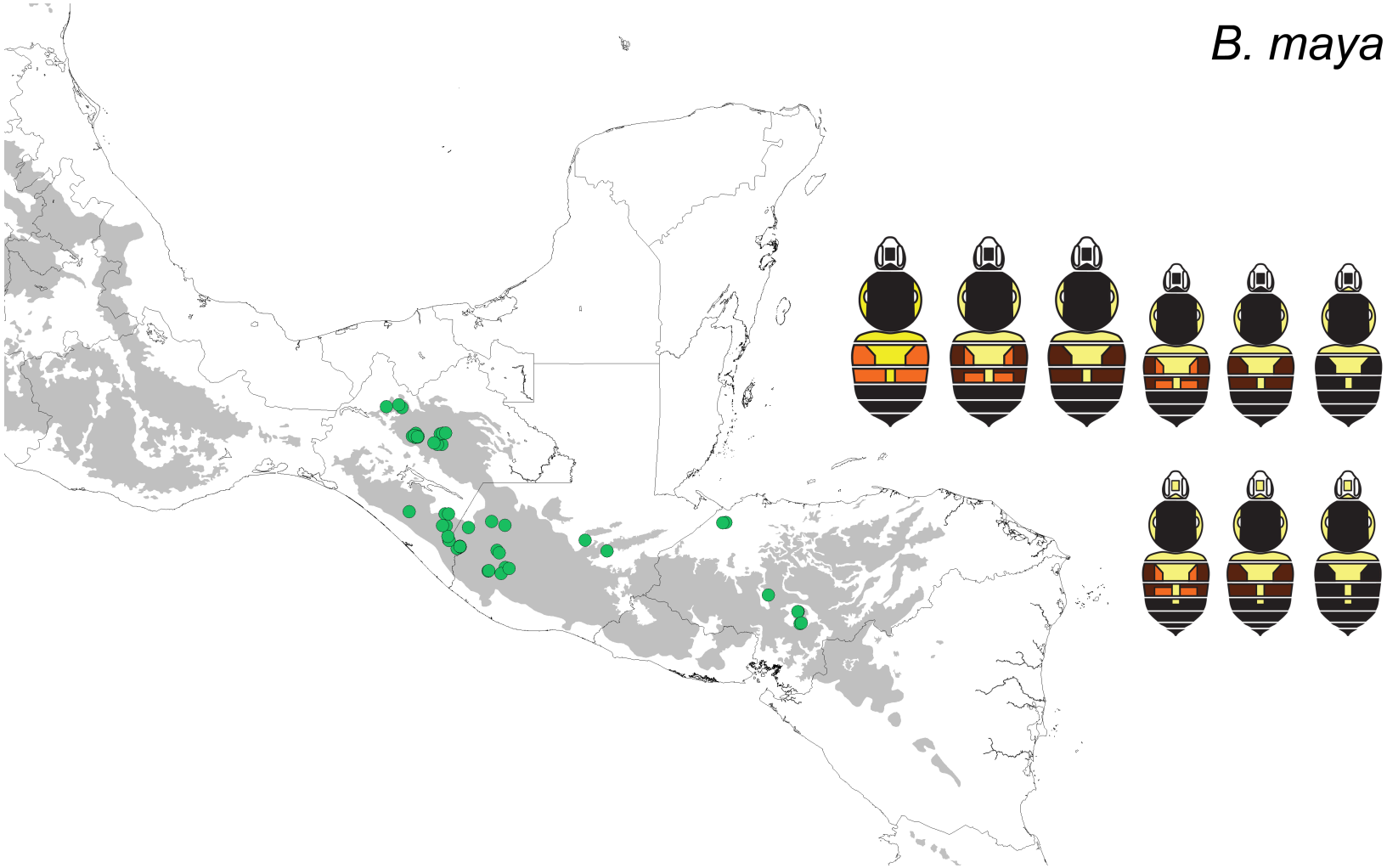

Figure 2.19. Images of a queen representative displaying the bright yellow color variant of the revised *B. wilmattae*. A) view of the ride side, B) view of the head, C) view of the dorsal thorax and D) view of the dorsal abdomen.

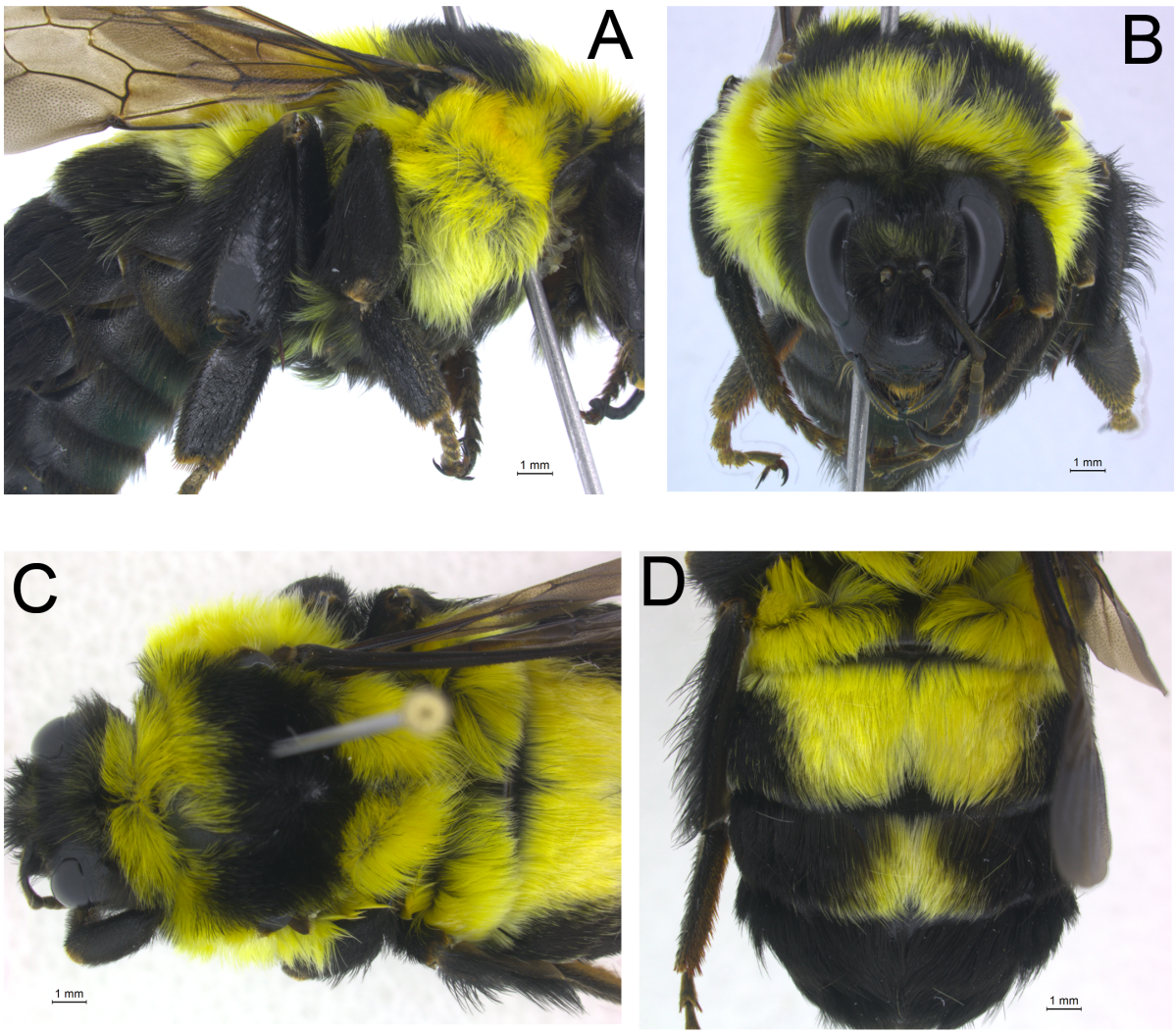

Figure 2.20. Images of a queen representative displaying the pale yellow color variant of the revised *B. wilmattae*. A) view of the ride side, B) view of the head, C) view of the dorsal thorax and D) view of the dorsal abdomen.

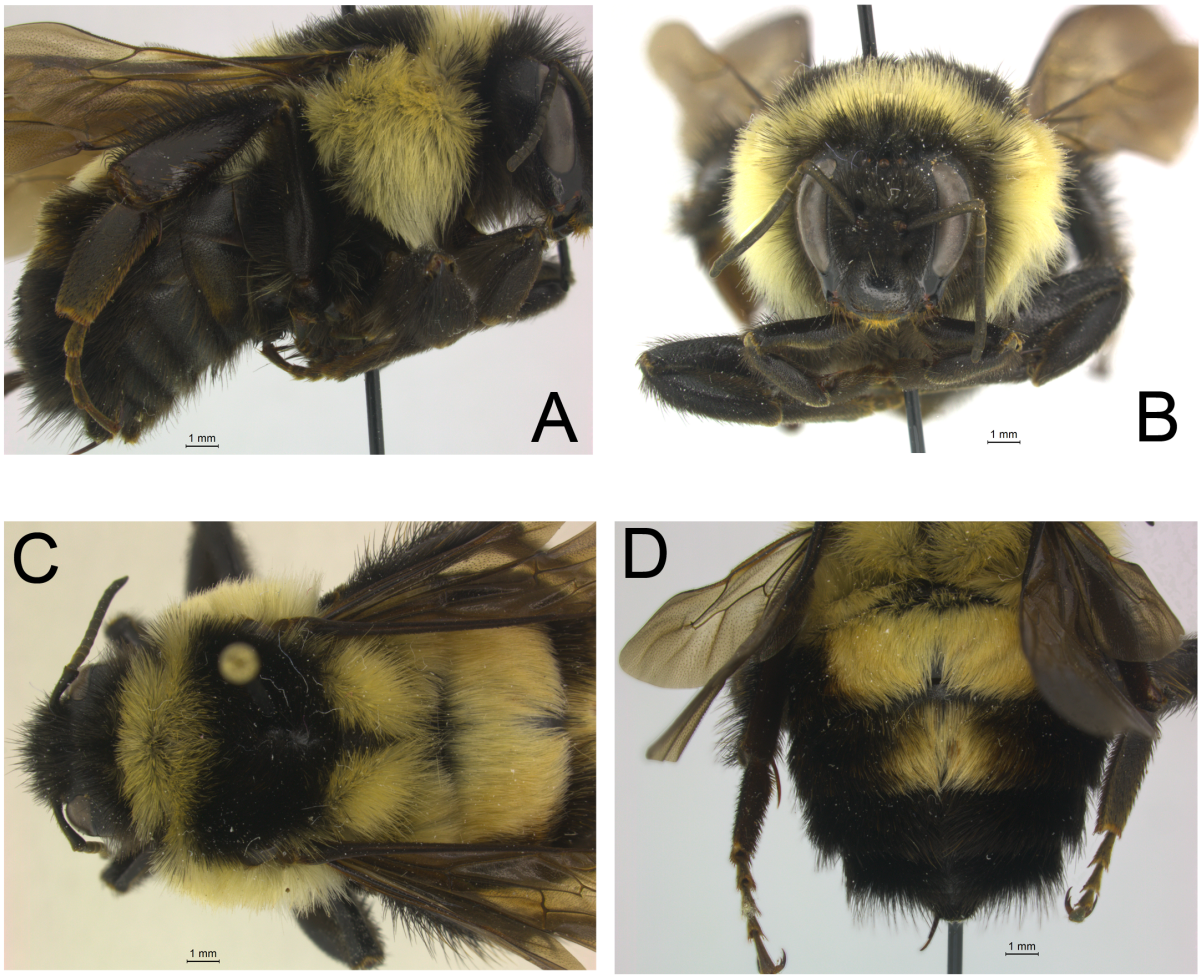

Figure 2.21. Images of a worker representative displaying the yellow pronotum color variant of the revised *B. wilmattae*. A) view of the ride side, B) view of the head, C) view of the dorsal thorax and D) view of the dorsal abdomen.

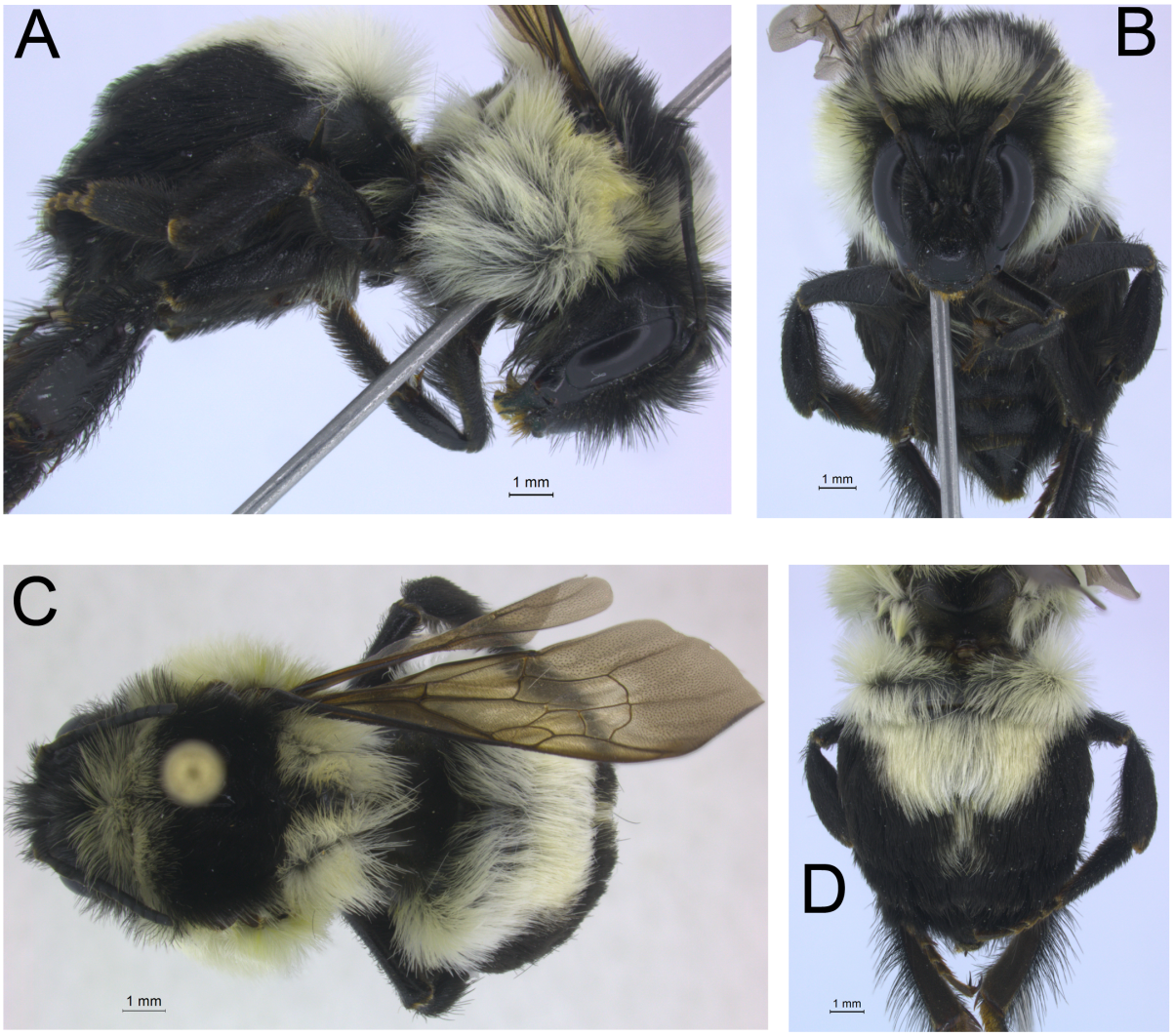

Figure 2.22. Images of a worker representative displaying the dark pronotum color variant of the revised *B. wilmattae*. A) view of the ride side, B) view of the head, C) view of the dorsal thorax and D) view of the dorsal abdomen.

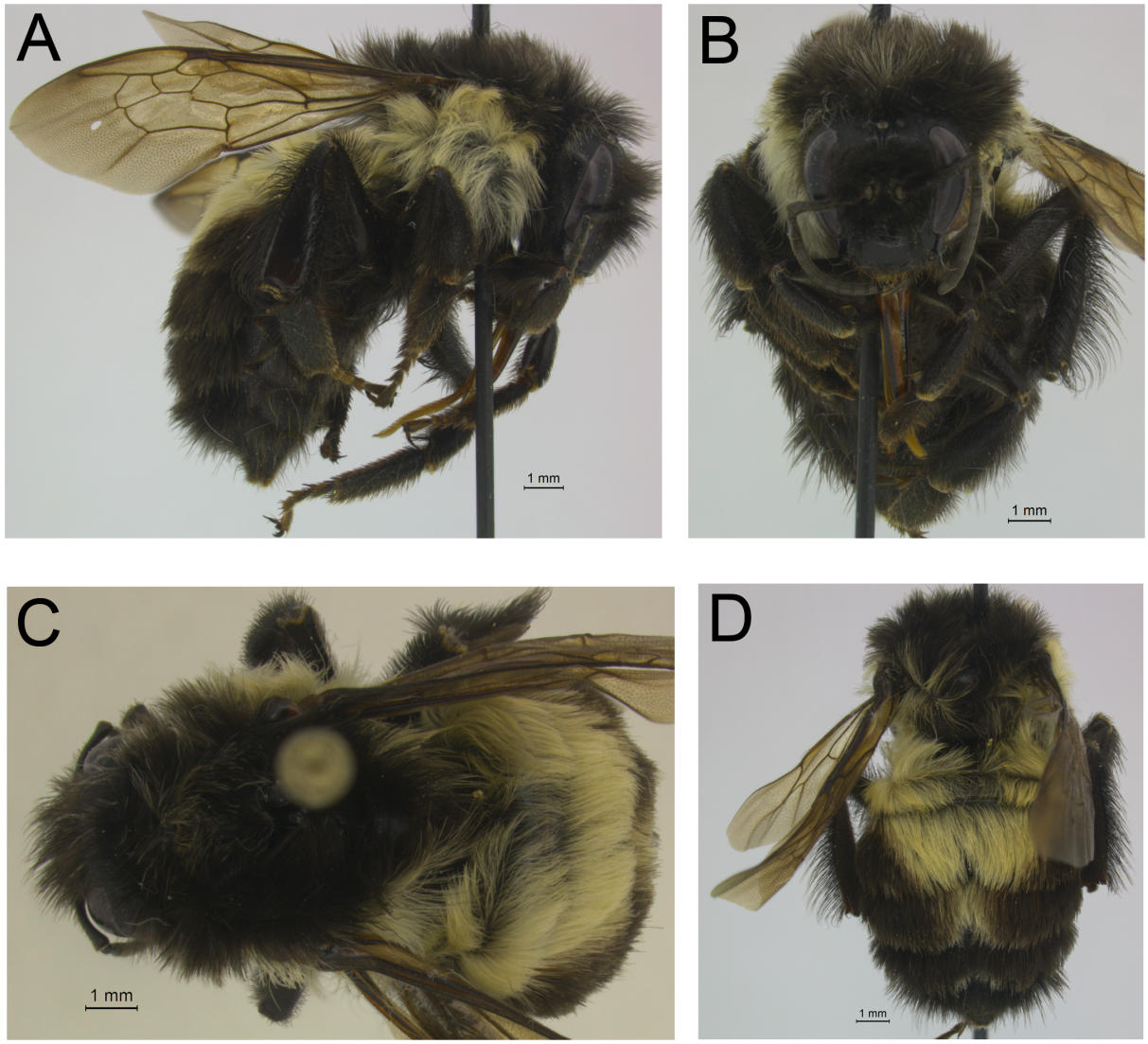

Figure 2.23. Images of a male representative displaying the dark abdomen color variant of the revised *B. wilmattae*. A) view of the ride side, B) view of the head, C) view of the dorsal thorax and D) view of the dorsal abdomen.

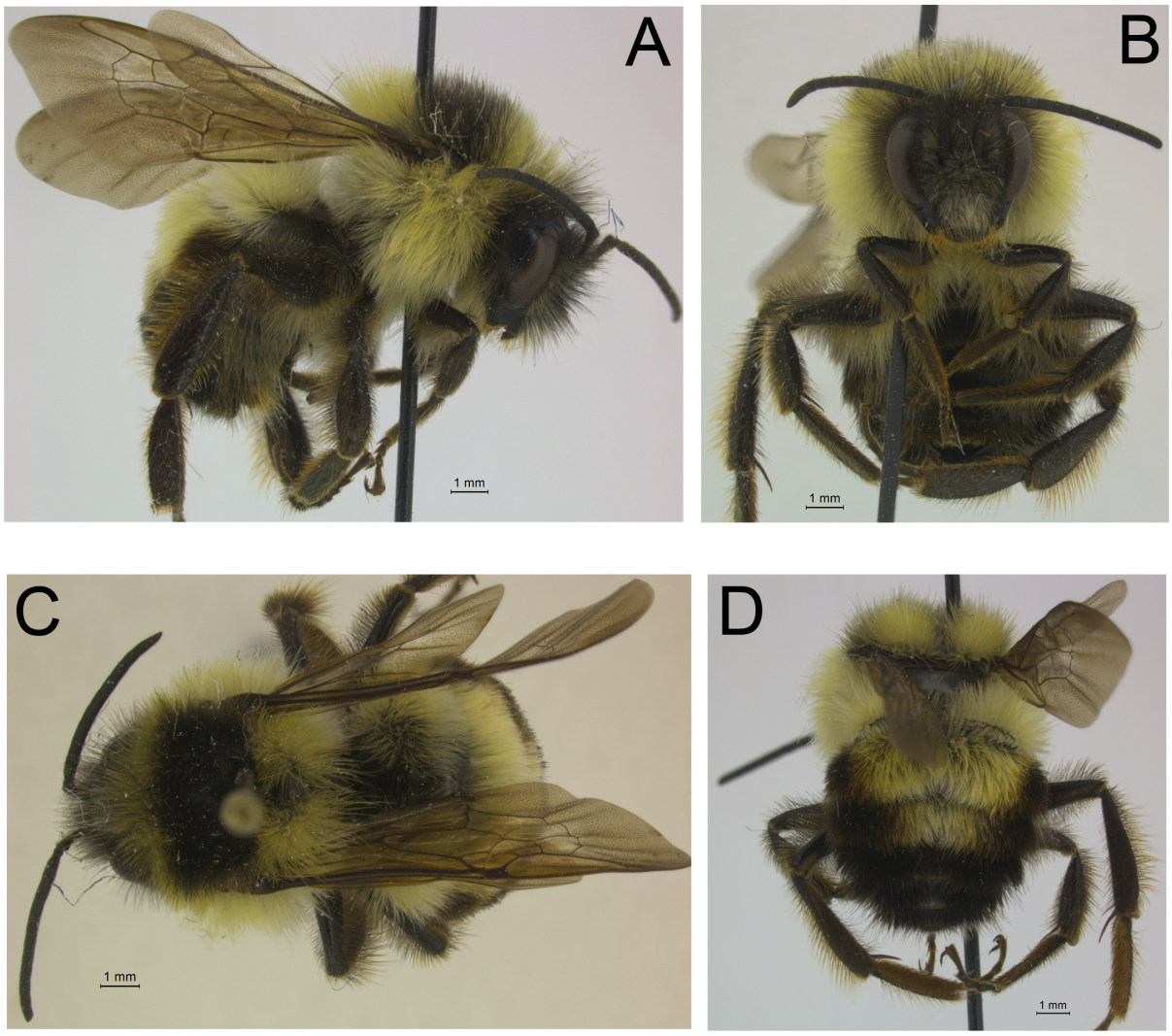

Figure 2.24. Images of a male representative displaying the orange abdomen color variant of the revised *B. wilmattae*. A) view of the ride side, B) view of the head, C) view of the dorsal thorax and D) view of the dorsal abdomen.

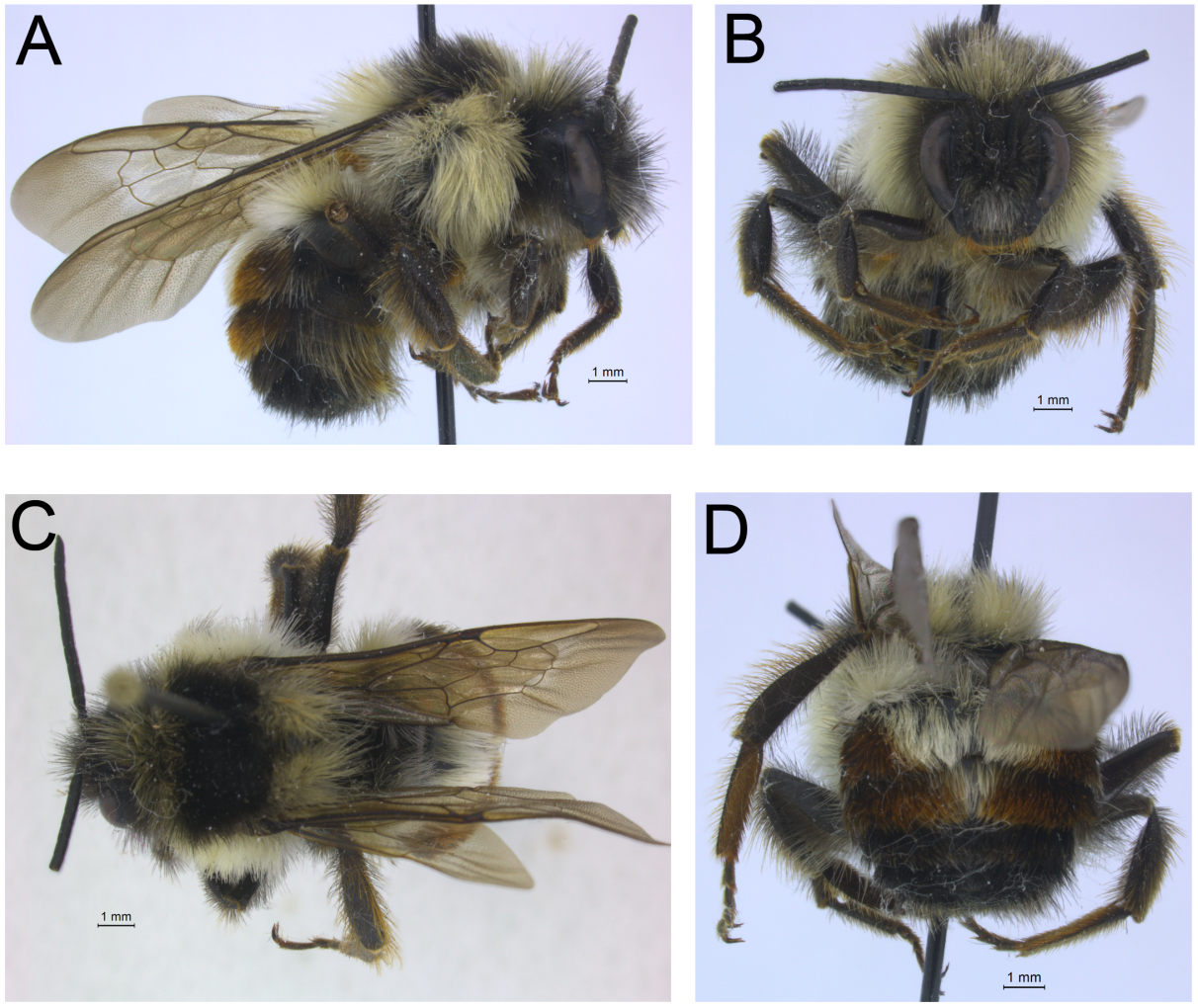

Figure 2.25. Geographic distribution of the revised *B. wilmattae* as well as the range of color pattern variation it exhibits across its range. Sample points represent specimens that have been confirmed to belong to *B. wilmattae* (i.e. samples used for genetic analyses in Chapter One). Grey-shaded areas of the map represent World Wildlife Federation (WWF) ecoregions of suitable habitat for the species. Larger bees represent queen color patterns, bees with an additional seventh abdominal segment represent male color patterns and the others are worker color patterns.

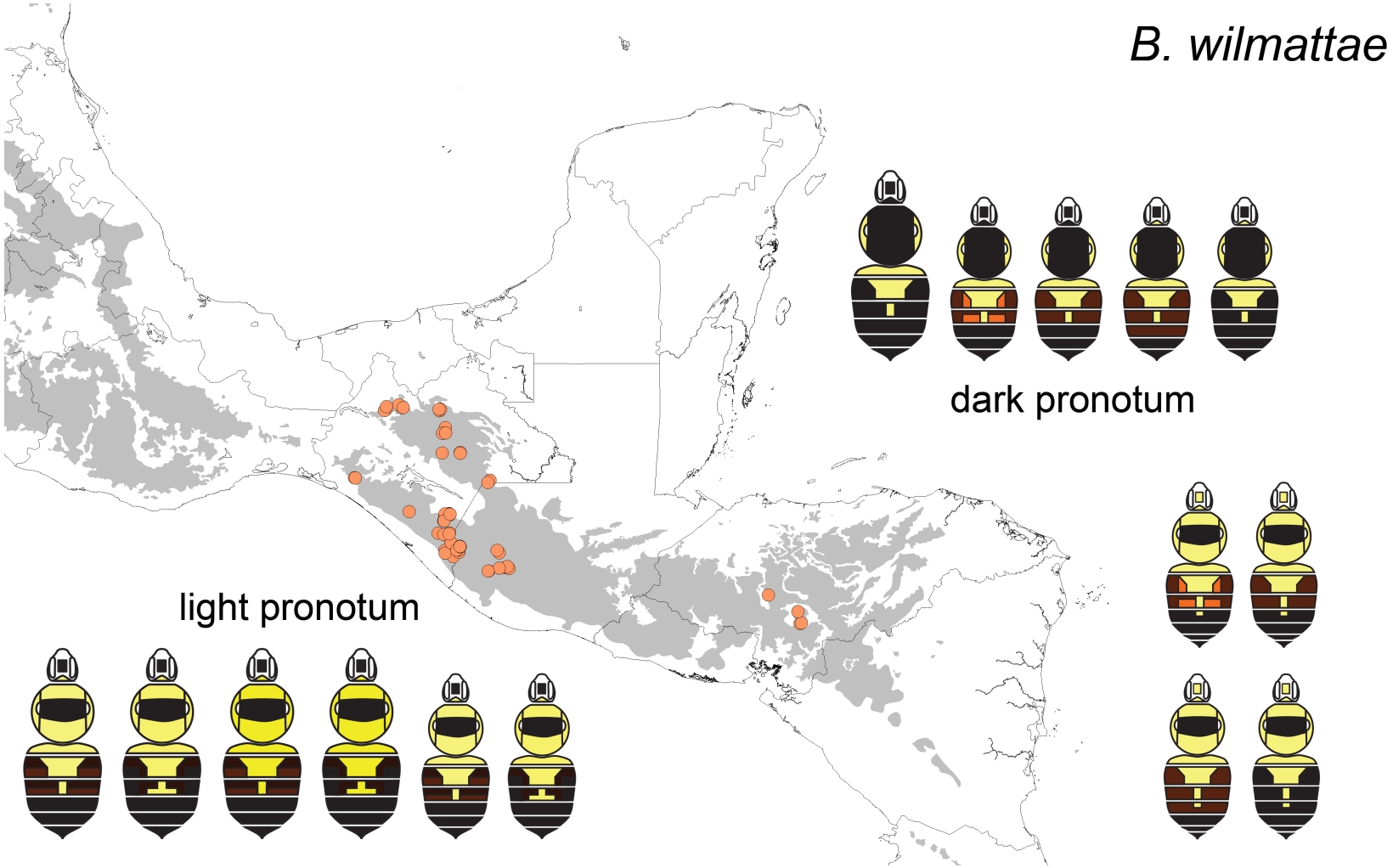

Figure 2.26. Geographic distribution of the resurrected *B. schneideri* as well as the range of color pattern variation it exhibits across its range. Sample points represent specimens that have been confirmed to belong to *B. schneideri* (i.e. samples used for genetic analyses in Chapter One). Grey-shaded areas of the map represent World Wildlife Federation (WWF) ecoregions of suitable habitat for the species. Larger bees represent queen color patterns, bees with an additional seventh abdominal segment represent male color patterns and the others are worker color patterns.

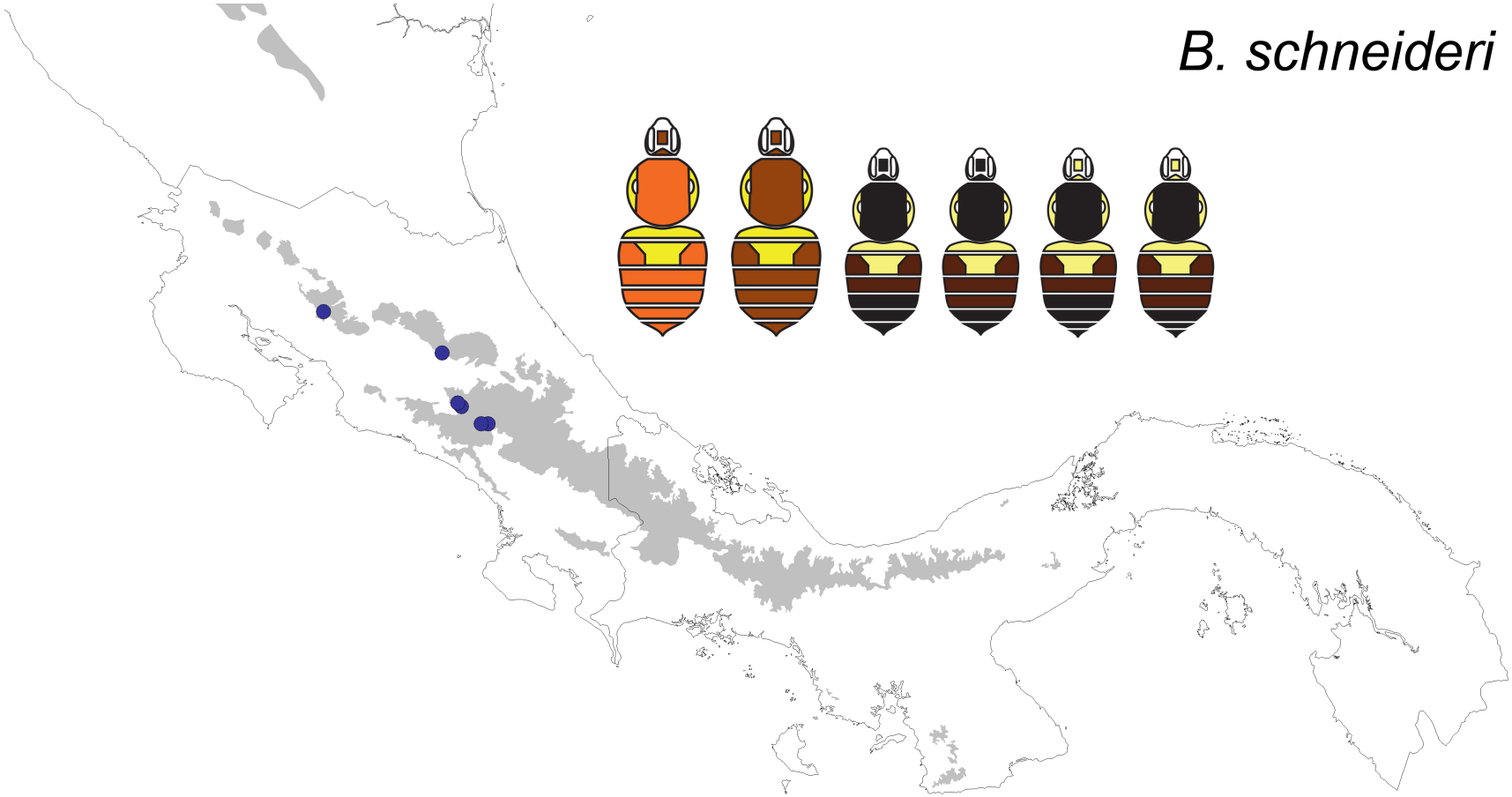

Figure 2.27. Images of a worker representative of the newly resurrected species, *Bombus schneideri*. A) view of the ride side, B) view of the head, C) view of the dorsal thorax and D) view of the dorsal abdomen.

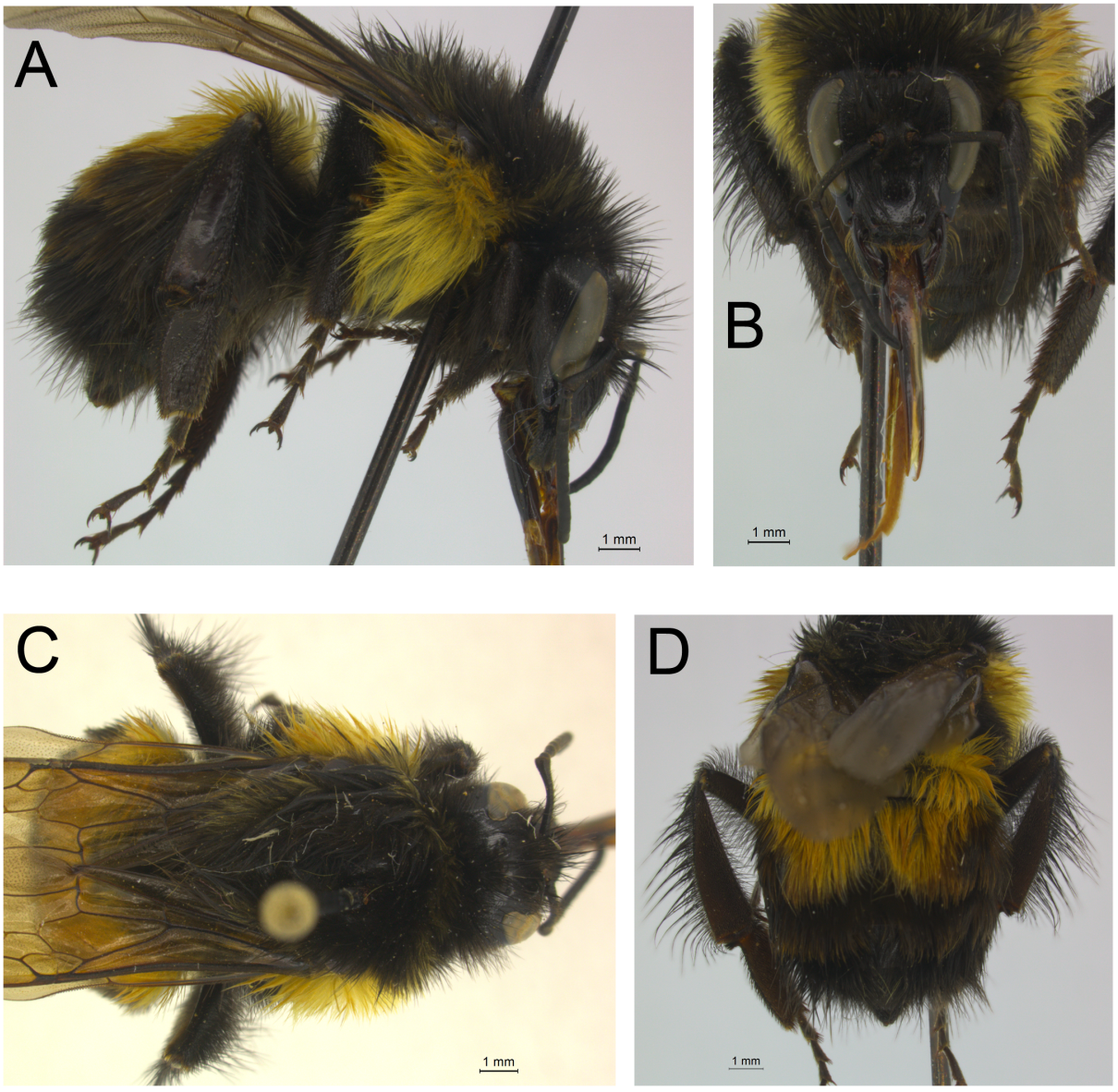

CHAPTER 3: DEFINING THE COLOR PATTERN PHENOTYPE IN BUMBLE BEES (*BOMBUS*): A NEW MODEL FOR EVO DEVO[1]

Abstract

Few insects exhibit the striking color pattern radiation found in bumble bees (*Bombus*), which have diversified globally into a wide range of colors and patterns. Their potent sting is often advertised by conspicuous bands of contrasting color commonly mimicked by scores of harmless (Batesian mimics) and noxious species (Müllerian co-mimics). Despite extensive documentation of color pattern diversification, next to nothing is known about the genetic regulation of pattern formation in bumble bees, hindering progress toward a more general model of the evolution of color pattern mimicry. A critical first step in understanding the color pattern genotype is an unambiguous understanding of the phenotype under selection, which has not been objectively defined in bumble bees. Here, we quantitatively define the principal color pattern elements that comprise the phenotype array across all species. Matrix analysis of meticulously scored color patterns of ~95% of described species indicates there are 12 discrete primary 'ground plan' elements in common among all species, many of which correspond to segmentation patterning. Additional secondary elements characterize individual species and geographic variants. The boundaries of these elements appear to correspond with expression patterns of Hox genes in *Drosophila* and *Apis* but also suggest novel post-*Hox* specialization of abdominal patterning. Our findings provide the first foundation for exploring candidate genes regulating adaptive pattern variation in bumble bees and broaden the framework for understanding common genetic mechanisms of pattern evolution in insects.

Introduction

Color pattern variation and convergence among organisms provide stunning examples of adaptive evolution, the genetic regulation of which is in the early stages of discovery (Wittkopp

[1]This chapter appeared in its entirety in © 2014 The Linnean Society of London, Biological Journal of the Linnean Society, 2014, 113, 384–404. Rapti Z, Duennes MA, Cameron SA. Defining the colour pattern phenotype in bumble bees (*Bombus*): a new model for evo devo. This article is reprinted with permission of the publisher and is available from http://onlinelibrary.wiley.com and using DOI: 10.1111/bij.12356

et al., 2002; Hoekstra & Nachman, 2003; Steiner *et al.,* 2009; Hines *et al.,* 2011; Manceau *et al.*, 2011; Goncalves, Hoekstra & de Freitas, 2011; Reed *et al*., 2011; Martin *et al.*, 2012; Papa *et al*., 2013). To broaden our understanding of pattern evolution and the developmental genetics underlying color pattern adaptation, we present a promising new system for study, the bumble bees (*Bombus*), which exhibit exceptional diversity in adaptive color patterns (Williams, 2007; Hines & Williams, 2012). Within a geographic region, unrelated species often converge on a common pattern (Williams, 2007; Hines & Williams, 2012), while many species also diverge into distinct color pattern sublineages across different parts of their geographic range (Vogt, 1909; Vogt, 1911; Ings *et al.,* 2010; Duennes *et al.,* 2012; Hines & Williams, 2012), forming color pattern complexes with other local congeners (Hines & Williams, 2012). Using a novel quantitative analysis of the world's bumble bee fauna, we show that 12 homologous pattern elements constitute the ground plan for the elaboration of the vast array of color patterns observed among hundreds of species. The boundaries of these elements, many of which correspond to segmental divisions, appear to correspond with known expression patterns of Hox genes in *Drosophila* and *Apis*, but also suggest post-*Hox* specialization of patterning that may be novel.

Renowned for their robust size, venomous sting and brightly colored dorsal banding patterns, bumble bees have undergone some of the most remarkable color pattern radiations among animals (Plowright & Owen, 1980; Williams, 2007; Hines & Williams, 2012). Their potent sting is advertised in many species by conspicuous banding patterns that are commonly mimicked by scores of harmless species (Batesian mimics) such as flies (Waldbauer *et al.,* 1977) and beetles (Heinrich, 2012), and noxious relatives (Müllerian co-mimics) alike. Comparison of *Bombus* color pattern complexes with the *Bombus* phylogeny (Cameron *et al.,* 2007) suggests that extant color patterns have evolved recently with respect to bumble bee evolution (Hines & Williams, 2012). Despite a long history of taxonomic and geographical study of bumble bee color patterns (Vogt, 1909; Vogt, 1911; Williams, 1991; Williams, 2007; Ings *et al.,* 2010; Duennes *et al.,* 2012; Hines & Williams, 2012), nothing is known about the underlying developmental genetic regulation of the pattern. Classical genetic research conducted on two species more than three decades ago showed that either a single locus (unidentified) of two alleles (*B. melanopygus*) or more complex polygenic inheritance (*B. rufocinctus*) can govern pigment switches in coloration (Owen & Plowright, 1980; Owen & Plowright, 1988).

In stark contrast to these two sole pioneering genetic analyses of *Bombus* pattern variation, extensive molecular genetic and developmental research on color pattern regulation of butterfly wings (Nijhout, 1991; Mallet & Joron, 1999; Tong *et al.,* 2012) has recently propelled the genus *Heliconius* to the level of a model system for evo devo studies of pattern evolution (Joron *et al.,* 2006; Counterman *et al.* 2010; Hines *et al*., 2011) and mimicry. Yet the visually striking and simpler banding patterns of bumble bees, which should be at least as attractive for developmental genetic investigations of mimetic evolution, have not been introduced into evo devo research. As a first step in this direction, we argue that a clear understanding of the actual phenotype under selection is needed. Indeed, establishing standardized definitions of the homologous wing pattern elements among diverse butterflies (Schwanwitsch, 1924; Süffert, 1927; Nijhout & Wray, 1986; Nijhout & Wray, 1988) provided the important link between descriptive taxonomy of wing pattern variation and the more recent explorations of common molecular genetic mechanisms underlying the regulation of wing patterns (Nijhout, 1991; Reed *et al.*, 2011).

While we know that bumble bee color patterns vary in the position, shape and color of dorsal hair (branched setae) patches (Williams, 2007), we still lack a standardized definition of homologous pattern elements that account for the diverse array of species phenotypes. A recent study of *Bombus* color patterns by Williams (2007) provided important quantitative evidence that similar patterns are geographically clustered, an important finding consistent with mimicry theory. However, the degree of resolution used in scoring color pattern, while useful to investigate "gross resemblance effects" among species (Williams, 2007), was on a scale far coarser than that required for an analysis with emphasis on evolutionary developmental processes. In particular, Williams (2007) *a priori* divided the dorsum into 24 elements, in an intuitive fashion, and introduced a set of rules to classify color patterns into groups according to three features: tail color; pale band color and pale band position. These were simplifications of the patterns, introduced for the purpose of estimating intuitive resemblance for grouping purposes. In contrast, we make no *a priori* assumptions as to what the elements are and include many more distinguishable pigment classes. The essential nature of our approach is to use high-resolution grid cell mapping of all color transitions across the dorsum, allowing the data in a transition matrix to reveal the pattern elements *a posteriori* via quantitative spatial analysis.

Materials and Methods

Species selection, morphology and scoring color pattern

Bumble bees were taken from both ethanol and pinned collections (Table 3.1). Ethanol-preserved specimens are preferred because they are more likely to preserve the setal pigments in tact, as opposed to dry specimens, in which colorfulness, particularly of red and yellow hues, decreases over time. Before scoring a color pattern, ethanol-preserved specimens were allowed to dry (5-10 min) in open air on a KimWipe®; any remaining ethanol was absorbed by dabbing with a KimWipe® and the setae were fluffed with a fine camel hair brush.

For color pattern scoring, one exemplar was randomly selected to represent each of 204 social species and 18 social parasitic (*Psithyrus*) species (Table 3.1), which is equivalent to ~95% of all described *Bombus* species (Cameron *et al.,* 2007). To mitigate the effects of gender differences on the analysis, we focused on females (foragers and reproductive females). Multiple exemplars were included for three species of the subgenus *Pyrobombus* (*B. ephippiatus*, *B. ternarius* and *B. pyrenaeus*) to separately assess intra-specific variation in the characterization of color pattern elements.

In the first step to distinguish color pattern elements, we scored the color pattern (Fig. 3.1A) for each species exemplar onto a standardized template representing the dorsal thoracic and abdominal surface (dorsum) (Fig. 3.1B). Each scored species was a minutely detailed representation of the pigmentation pattern of the setae across the dorsum (Fig. 3.1C). The standardized template was developed as a composite of several worker bees from which all setae were removed (shaved), exposing the segmentation pattern and other morphological landmarks (sclerites and sutures) on the bare dorsal cuticle. A few individuals were sufficient for constructing the template because bumble bees are morphologically homogeneous relative to other bees (Michener, 2007). All templates were scaled to the same size to allow direct comparison across all exemplars. The thoracic dorsum consists of three true segments: the pronotum, mesonotum and metanotum (Fig. 3.2A). The mesonotum is subdivided into two distinct sclerites (not true segments), a larger anterior scutum and a posterior scutellum, separated from one another by the scutoscutellar suture. The metasomal (abdominal) dorsum has six true visible segments (tergites 1–5) and the pygidial plate (tergite 6) (Fig. 3.2B). Additional cuticular landmarks include an anteroposterior dorsal midline (or groove) and two mesoscutal parapsidal lines (see thorax in Fig. 3.3B), which correspond to the attachment sites of the

dorsoventral indirect flight muscles. A dissecting stereoscopic zoom microscope (Leica model S6E) was used to magnify each bee for accuracy and precision in documenting the morphology and scoring the color patterns, and standard reference illumination was provided by an ACE® light source with EKE halogen lamp (Schott Fostec), with dimmer set at 80, at a distance of approximately 7 cm from the specimen.

Distinct colors of setae were scored by a single observer (MAD) and matched by eye to a specific PANTONE® color chip (Table 3.2) held against the bee's pile under the microscope. Pantone colors were selected from a total of 1,114 hues from the PANTONE® FORMULA GUIDE/solid coated (4^{th} edition, 2^{nd} printing). Color matching of setae to Pantone swatches is known to be relatively well correlated with color variables (hue and saturation) obtained objectively using spectrophotometry (Hill, 1998). For recording the color pattern onto the template (Fig. 3.1C), each of the 16 Pantone colors selected was used to match a colored pencil (Table 3.2), matched by eye against a Pantone chip under the same EKE halogen lighting conditions. Mixed setae of two colors as well as banded setae comprising two or three pigments were also observed (Table 3.2). We also determined reflectance quantitatively using a Cary 5G UV-VIS-NIR spectrophotometer at the Frederick Seitz Materials Research Lab Laser and Spectroscopy Facility (175-3300nm wavelength range for light sources, measurement angle 60 degrees incidence, with broad acceptance angle under diffuse reflection) calibrated with a 0% reflectance standard (black carbon tape) and a 100% diffuse reflectance standard. Each of eight abdominal tergites (T2) covered with setae representing one of the eight pure (unmixed) hues (Table 3.2, colors 1-6, 8, 9), was mounted onto a cylindrical SEM specimen mount (12.5 x 10mm). To control for possible spectral reflection from underlying cuticle, T2 with all setae removed was also measured. Readings were taken every nanometer from 3000 (infrared) to 100 (ultra-violet) nm. Figure 3.4 represents only that portion of the spectrum visible both to humans (400-700 nm) and to UV-sensitive birds (300-800 nm). Each of the eight pure colors identified using human visual perception were clearly distinguished with the spectrophotometer (Fig. 3.4).

Quantifying color pattern and identifying areas of color transition

To statistically resolve the pattern elements, we quantified congruent zones of low and high frequency color transitions in common among ~95% of bumble bee species (Table 3.1) To score the position and estimate the frequencies of color transitions across the dorsum, we quantified

the color pattern of each species exemplar by transposing the pattern onto a transparent square grid matrix (Apollo® transparency film) of 550 equal-size grid cells (Fig. 3.1D) overlaid onto the scored color pattern template (Fig. 3.1C). The size of the matrix (19 columns x 44 rows) was selected to depict the overall shape of the bee anatomy with high resolution, minimal edge effects and maximum accuracy. The 550 grid cells that fell within the outline of the scored template corresponded to the color pattern, which was then converted to binary digits (0 and 1) across the matrix (0=single color in a cell, 1=two or more colors in a cell, representing a transition from one color to another; equally mixed setae, e.g., yellow and black mixed, were scored 0 if the mixture was uniform within a grid cell). The 286 grid cells of the 19 x 44 matrix that fell outside the margins of the bee template were assigned a value of -1 and ignored in analyses.

To quantify areas of color uniformity from areas of high color changeover for all species combined, we created a sum matrix (Fig. 3.1E, Fig. 3.5) by summing the 1 scores in each of the 550 analogous grid cells of all species matrices (implemented in MATLAB R2012a). The sum matrix was manually inspected to ensure accuracy of data entry. To determine that the socially parasitic species, which may mimic their social hosts, would not influence the color transition results, we constructed sum matrices both with and without the social parasites (Fig. 3.5). Results were unaffected by inclusion of the parasitic taxa (Fig. 3.5A, B). Separate sum matrices were constructed for the three species for which we scored more than 10 exemplars each to investigate intraspecific pattern change (Fig. 3.6). For the Perl programming language (v5.10.0) script written to implement the matrix addition procedure in MATLAB, see Appendix A1.

Determining color pattern elements

Color pattern elements were initially recognized as zones of little or no color transition (areas of high color uniformity) bounded by zones exhibiting relatively high frequencies of color transition among all species exemplars. Pattern elements were tested for significance using permutation (randomization) tests, which allow us to determine whether an observed difference between mean transition frequency along an element boundary (group 1) and mean transition frequency within an element (group 2) is large enough to reject the null hypothesis that the two frequencies are not significantly different (Appendix A2). After calculating the difference in means between the two groups we pooled all the transition values of both groups, then randomly

reassigned the pooled values to the two groups and recalculated the difference in mean transition frequency. With 5000 randomizations we generated a distribution of the set of calculated differences to test the null hypothesis. The p-value (one-tailed) represents the proportion of sampled permutations in which the difference in means was ≥ the original observed difference. After evaluating the p-values for all potential elements tested, we established a conservative threshold ($p < 0.0002$) for recognizing primary elements found in common among all species exemplars. Additional elements emerge with p-values above 0.0002 (0.00021 to 0.03), which we consider as secondary elements (Appendix A3). We also performed permutation tests to examine differentiation or fusion of elements in each of the three species representing different degrees of color pattern polymorphism across their ranges: *B ephippiatus* (highly polymorphic), *B. pyranaeus* (intermediate) and *B. ternarius* (monomorphic) (Fig. 3.6).

Analysis of segmental boundaries

To determine if transitions in color pattern commonly occur along true segment boundaries or other margins between sclerites, such as thoracic sutures (Fig. 3.2), we overlaid the sum matrix (Fig. 3.1E) onto a morphology template indicating the position of these dorsal features (Fig. 3.2). We counted the total number of transitions in each matrix cell that corresponded to one of the morphological boundaries. Of the 550 matrix cells, 102 (18.54%) fell along a true segment boundary (Fig. 3.2B) and 11 fell along a sclerite boundary (scutoscutellar suture) on the mesonotum (Fig. 3.2A). The remaining 437 cells (79.45%) were characterized as not belonging to any morphological feature. Using a permutation test, we tested the null hypothesis that the mean frequency of color transitions in cells along the morphological boundaries is not significantly different to the mean frequency of the remaining 437 cells (Appendix A4).

Color location analysis

Numerical values were assigned to each of 19 observed color classes for all 204 exemplars— nine unmixed colors (Fig. 3.1) and 10 mixed setal or banded setal colors (Table 3.2). To determine the position and frequency of each color across the dorsum of each exemplar, a transparent square grid matrix (Fig. 3.1D) was overlaid onto each scored color pattern (Fig. 3.1C) and each cell was assigned a color class (1-19). When two colors were present within one grid cell we used a >50% rule: the cell was assigned the color comprising >50% of the cell area.

Any grid cell falling on an element boundary was assigned a priori to the element above or below it for color assignment by aligning the square grid matrix to a blank bee template (Fig. 3.1B) and using the >50% rule to determine which segment contained the greater fraction of the cell. The 204 color matrices were summed for each color class, generating 19 color sum matrices (Fig. 3.7, Fig. 3.8), each containing the total frequency of that color in each cell summed over all 204 species. Each of the 19 matrices was used to calculate the average frequency of occurrence of each color for each element (averaged over all cells comprising the element). All cells comprising each element were used to create heat maps of the most common colors (Fig. 3.7) and histograms of color distributions for each element (Fig. 3.9) to explore what colors were most common in each element. To control for the effect of element size (the number of grid cells it contained), we divided the frequency of the color by the total number of grid cells per element.

To test for association between colors and pattern elements, we conducted principal components analysis (PCA) of the mean frequency of each color for each element using the FactoMineR package (Lê, Josse & Husson, 2008) in RStudio (v0.98) (Fig. 3.10). Due to the high frequency of black across all of the elements, a correlation matrix was used to normalize for the overall differences in variance. Only the most common colors were used (those occurring on all the elements), thus excluding tawny, white/yellow mixed, white/orange mixed, orange/yellow mixed, two-banded black/orange, two-banded white/orange, two-banded black/white, and three-banded pigmentation.

Color adjacency analysis

To assess how hue changes between adjacent elements, we generated pairwise color change matrices. Ten pairwise matrices (Table 3.3), one for each pair of adjacent elements, including all 19 color classes (19 x 19) were constructed as follows. One cell per element was chosen belonging to or near the dorsal midline where color transitions rarely occur. Figure 3.11 indicates which cells were chosen for each pairwise comparison. Next, the color transitions from element N to element N+1 were recorded for each of the 19 color classes. The transition matrix entry (i, j) corresponds to the number of transitions from color i in element N to color j in element N+1. For instance, the 19 matrix entries along the main diagonal (Table 3.3) correspond to the number of times each of the 19 colors between the two adjacent elements does not change. There are 5 transition matrices for the thorax and 5 for the abdomen. No matrix was generated for element 6

on the posterior thorax and 7 on the anterior abdomen. To be certain that cells along the midline did not have undue influence on the results, we also constructed transition matrices from cells not occurring along the midline and found no difference in results.

Results

Bumble bee color pattern elements

We generated a total of 222 individual color transition matrices, including 204 for the social species and 18 for the parasitic species. We hypothesized that color pattern elements would be characterized by zones of high color uniformity (no/little change in color across a body region), separated by zones of high color changeover (potentially representing a boundary between elements). Zones that exhibited obvious high frequencies of color transitions in the sum matrix (Fig. 3.1E) were thus defined as boundaries separating discrete elements. Permutation tests (Appendix A2) of the frequency values along each boundary zone relative to adjacent zones of low color transition frequency revealed 12 elements (10 boundaries between elements) ($P < 0.0002$) found in common among hundreds of species: six thoracic and six abdominal elements (Fig. 3.3A, Table 3.4). These 12 *Bombus* ground plan elements delineate the basic organization of the color pattern into anterior-posterior compartments across the dorsum. They consist of a sequence of dorsal bands running from the anterior thorax to the posterior abdomen (Fig. 3.3A). Here we present a nomenclature of these primary elements (Table 3.4, Appendix B).

Ground plan pattern elements correlate with segmentation boundaries

Overlaying the sum matrix (Fig. 3.1E) onto a second matrix (Fig. 3.2B) that highlighted all cells representing the dorsal segmentation boundaries (102/550 cells, 18.5%) and a third (Fig. 3.2A) highlighting the suture separating the mesoscutal sclerites (scutum and scutellum) (11/160 mesonotum cells, 6.9%), revealed that color transitions occur on segmental boundaries significantly more frequently than expected based on a null hypothesis of random distribution of cell transition frequencies (permutation test, $P < 0.0002$) (Appendix A4). The scutoscutellar suture was also a zone of significant color transition ($P < 0.0002$).

Separating the 12 ground plan elements are 10 element boundaries (Fig. 3.3A), seven of which correspond to adult segmentation boundaries (Fig. 3.3B). Four pattern elements (elements

2-5) comprising the mesonotum are, however, partly or fully independent of adult segment boundaries, including the posterior margin of element 2, which falls in the upper third of the scutum, elements 3 and 4, which are entirely independent of adult segmentation (although the posterior margin of element 4 is marked by a suture separating it from the scutellum), and element 5 (scutellar band) shares only its posterior margin with the metanotal segment boundary (Fig. 3.3A).

Among all 204 species, the area of highest color transition occurred along the segment boundary separating tergites (T) 3 and 4 (Fig. 3.1E), between elements 9 and 10 (Fig. 3.3A) (mean transition frequency of 17 grid cells comprising boundary = 112.7647 ±3.8166; > 54% of bees displayed transitions along this boundary). Anteriorly, the T2-T3 segmentation boundary separating elements 8 and 9 displayed the next highest color turnover (mean transition frequency of 19 boundary grid cells = 99.8947 ±3.2642; > 48% of bees displayed transitions along boundary). In contrast, the central spot on the thorax (center of element 4) exhibited no color transitions (Fig. 3.1E) and relatively little shift in color occurred between the central (element 3) and posterior (element 4) scutum (mean transition frequency of 15 boundary grid cells = 18.0667 ±2.4339; 7%-10% of bees, depending on which of 15 cells, displayed transitions along boundary).

Spatial distribution of secondary elements

Not all *Bombus* species have all 12 of the primary elements evident; some may deviate from the ground plan, but not in a random fashion. Elements may fuse to form a uniform color in some species (the most extreme example being species of a single color) or become subdivided transversely or longitudinally in others. These "secondary" patterns are stereotypical and appear to be important in species-specific individualization of color pattern. We found five secondary tergal elements (Fig. 3.3A, Appendix A3) that appear frequently among the species (permutation tests $P < 0.03$, Table 3.4): a medial notch of black hair on tergal band 1, and lateral patches of different widths of contrasting color on tergal bands 2, 3 and 4 (Fig. 3.3A), which correspond roughly in position to the dorsolateral convexities of the tergal discs (Michener, 2007).

We also explored 3 species individually to determine whether the 12 pattern elements were conserved in taxa that display different degrees of intraspecific color pattern polymorphism. *B. ephippiatus* (highly polymorphic), *B. pyrenaeus* (moderately polymorphic) and *B. ternarius*

(monomorphic) exhibited many of the ground plan elements, but fusion of two or three adjacent elements was common in each species (Fig. 3.6). Fusion of elements is interpreted from the absence of significant color transition ($P > 0.05$, permutation test) between one primary element and the next, resulting in uniform coloration between 2 or more adjacent elements. For instance, *B. ternarius* displays fusion of central and posterior thoracic elements 3+4+5, and tergal elements 8+9, 11+12 (Fig. 3.6A); in *B. pyrenaeus*, central thoracic elements 3+4, and tergal elements 7+8 and 9-12 merge, respectively (Fig. 3.6B); and in *B. ephippiatus*, anterior and central thoracic elements 2+3+4 merge, as do anterior tergal elements 7+8 and the tail elements 11+12 (Fig. 3.6C).

What colors are located where

We distinguished nine pure setal pigments (Fig. 3.1) among the pattern elements of 204 species. These were not randomly distributed across the dorsum (Fig. 3.7 - Fig. 3.10). Black was the most frequently expressed pigment (Fig. 3.7A) in more than 25% of exemplars. It was found in at least some frequency in all pattern elements (Fig. 3.9), most frequently in the setae covering the central thorax (element 3 mean frequency = 58.45% ± 3.66, element 4 = 71.2% ± 6.08, element 5 = 31.81.% ± 3.69) and tergal band 3 (element 9 =54.03% ± 4.68). Various orange pigments (Fig. 3.7E, F) were found most frequently in the tail region (tergal bands 4-6). Different shades of yellow (Fig. 3.7C, D) were most commonly displayed on the anterior and posterior regions of the thorax (elements 1, 2 and posteriorly 5) and tergal bands 1 and 2 (elements 7, 8), thus flanking the black elements. Pale orange occurs commonly in elements 2, 5 and 8 (Fig. 3.7G). White is mostly congruent with the occurrence of yellow but is also found commonly in the tail (Fig. 3.7H). Mixtures of colored setae also occur, commonly as black+yellow on the pronotum (Fig. 3.7B), and rarely, banded setae are observed: two-banded (black basally with orange or yellow apically) and even 3-banded setae (black-orange-white (Fig. 3.8 A-J).

Principal components analysis indicated that elements and colors grouped congruently into three principal clusters (Fig. 3.10). A map of the color classes used in this analysis (Fig. 3.10A) showed that colors similar in hue mapped to similar dimensions for PC1 and PC2, which explain >70% of the variation in the color frequency data across the elements. White is an exception as it clusters with the orange pigments, reflecting its common expression in the tail region where

orange is also most commonly expressed. Additionally, PCA (Fig. 3.10B) indicated that elements 10, 11, and 12 form a distinct cluster of orange-pigmented tail elements (Fig. 3.7E, F); elements 1, 2, 5, 7, and 8 form a cluster of principally yellow hues (Fig. 3.7C, D); elements 3, 4, and 9 form a looser cluster of the predominantly black elements (Fig. 3.7A); and element 6 (metanotum), which has predominantly mixed black+yellow hair (Fig. 3.7B), falls out separately on the PC map between yellow and black elements.

Conspicuous patterns of association between colors

Pairwise color association matrices were constructed to examine trends in the co-occurrence of colors between each of the 12 elements (Table 3.3). We examined the nine most frequently observed colors, plus 10 less commonly encountered colors among the exemplars. The matrices, representing frequencies of transition between any two colors for adjacent elements, suggest important color trends. The most prominent trend is the conservation of color between any two adjacent elements (Table 3.3). The most common shifts between adjacent elements are from yellow to black or black to yellow, except between element 9 and tail element 10, which most commonly transitions from black to orange. Two notable shifts involving mixed setae occur on the anterior and posterior thorax: black+yellow mixed on element 1 transitions to pure yellow on element 2, and pure yellow posteriorly on element 5 transitions to black+yellow mixed on element 6.

Discussion

We have shown that 12 dorsal pattern elements in bumble bees constitute the ground plan for the elaboration of the vast array of color patterns observed among species. We have presented a nomenclature of these elements that provides a new comparative model for understanding color pattern evolution. We have shown that all but four of the major pattern elements are delimited in position, shape and color by the adult segmentation boundaries, and that transitions from one color to another occur along these boundaries. Non-segmental thoracic elements 2-5 (Fig. 3.3A) subdivide the mesonotum into four compartments, each of which can express different pigmentation and may be under separate regulation. These may correspond to the compartmentalization of clonally distinct populations of cells found in thoracic T2 of *Drosophila*

melanogaster (Lawrence, 1992). A study of larval bumble bee parasegmentation patterns would provide an obvious test of this hypothesis.

Moreover, principal transition zones tend to divide the thoracic and metasomal dorsum broadly into anterior, central and posterior partitions of color. The anterior thorax is circumscribed by the pronotal and anterior scutal bands (elements 1 and 2), a central zone is bounded by the mesoscutal and posterior scutal bands (elements 3 and 4), and a posterior scutellar zone is bounded by elements 5 and 6. Likewise, the abdominal dorsum (tergal bands 1-6) tends toward a subdivision into three broad zones of color along the anterior-posterior axis: an anterior zone comprising tergal bands 1 and 2, a strongly demarcated central tergal band 3, and a posterior zone or "tail," which is differentiated by tergal bands 4-6. These broader zones of color may be under selection for maximizing aposematic coloration.

Secondary or subordinate patterns arise medially and laterally on the abdomen. For example, tergal band 1 often has a notch or central patch of black setae, and patches of contrasting color arise laterally on tergal bands 2-4 and are not entirely circumscribed by segmentation boundaries. They may arise as gradients of pigmentation originating either from the lateral margins of the tergites or from the dorsal midline, and may be important in differentiating species-specific patterns. We also recognize that some species show additional patterns, such as double bands or arches of contrasting pigmentation within some of the tergal elements, again most commonly on tergal bands 2-4 (Fig. 3.3B). The width of the bands may be equal, splitting a segment into two equivalent rows, or unequal, a wide anterior band and a thin posterior stripe of contrasting setae anterior to the segment boundary of the next element (Fig. 3.1E). Arch-shaped patterns (Fig. 3.3B) may vary in shape from shallow and wide to deep and narrow. A notch of contrasting black setae may interrupt the arch posteromedially. The developmental genetic regulation of these patterns is ripe for comparative investigation.

Adaptive coloration in bumble bees

Bumble bee hairs, which are branched and feathery, as in all bees, serve multiple adaptive roles, from enhancing pollen collection to thermoregulation (Michener, 2007). They also evolved to display a stunning array of divergent species-specific color patterns and convergent aposematic patterns comprising Müllerian mimicry complexes that function to warn predators. Our quantitative investigation of coloration trends in *Bombus* has revealed that black is by far the

most common color expressed across species, with the highest frequency (77%) occurring in the central thoracic region. The high frequency of black suggests that it might be serving as a ground plan pigment, adjacent to which other colors occur, thus creating a high contrast, aposematic signal. The high frequency of black in the center of the thorax (Fig. 3.7A) could reflect a thermoregulatory function as it covers the powerful flight muscles that are often used to regulate body temperature (Heinrich, 2004). Interestingly, the highest color transitions occur on elements 9 and 10 (tergal bands 3 and 4). In general, transitions occur more frequently on the abdomen than the thorax, possibly because this region is usually oriented towards an approaching predator.

Various orange pigments occur in high frequency in the tail elements (Fig. 3.7E, F), suggesting that these orange pigment classes may be derived from the same pigment but varies in density within the setae. A similar chemical pathway could also explain the different classes of yellow (pale yellow- pale orange, and white), all of which are highly expressed in the anterior and the posterior thoracic regions, and in the anterior region of the abdomen (Fig. 3.7C, D, G, H).

The color transition matrices reveal that colors are most often preserved between adjacent elements (Table 3.3). Nonetheless, changes from yellow to black or black to yellow are among the most common changes in color (Table 3.3), and likely result in maximum contrast (Williams, 2007). The fact that the ventral surface patterning is pale and lacks the sharp contrasting coloration of the dorsum further suggests an adaptive function of the dorsal pattern elements. An exception to the aposematic pattern are those taxa that are thought to display cryptic coloration in grassland areas, where blending in to background vegetation is advantageous (Williams, 2007). Bumble bee color patterns are also commonly mimicked with high fidelity by a diverse array of flies, particularly those of the families Syrphidae (hover or drone flies) and Asilidae (robber flies). The *Bombus* ground plan may thus define the principal patterns of these diverse Batesian mimics, and experimental research may discover a similar or identical underlying developmental origin of the color patterns. Genetic research by Conn (1972) on the syrphid fly *Merodon equestris*, a high fidelity mimic of multiple bumble bee models, revealed that multiple loci with multiple alleles control the color pattern in the thorax and abdomen of these flies, including a ground color locus. Further genetic and population genetic research on bumble bee models and their mimics is critical for understanding their mimetic the evolution.

We emphasize that the *Bombus* ground plan elements are a minimum set of pattern elements describing a generalized bumble bee pattern, each likely to be under independent developmental regulation. Additional secondary elements occur in many species, and many species exhibit intraspecific variation in color pattern as profound as that found among distantly related species. An available comprehensive *Bombus* phylogeny (Cameron *et al.,* 2007) allows us to examine hypothetical ancestral color patterns across the tree, and it is clear that the diverse, segment-specific patterns were there in the earliest evolution of these bees, in contrast to the invariant pigmentation of the abdominal segments of many *Drosophila*, whose segment-specific differentiation of coloration is a recent innovation (Carroll *et al.,* 2005).

Pattern elements and mimicry

These high-resolution color pattern data allow us to examine differences and similarities between the pattern elements of mimetic species. For example, in the western United States there is a complex of multiple polymorphic species (*B. bifarius*, *B. melanopygus* and *B. sylvicola*) that form two distinct mimicry rings, one along the Pacific coastal region with black pigmentation on tergal bands 2-3 and one immediately to the intermountain east and north with red pigment replacing black on tergal bands 2-3 (Fig. 3.12); the polymorphic species *B. flavifrons* follows a similar pattern on tergal bands 3-4. Additional monomorphic species converge on these complexes, including *B. huntii* and *B. ternarius* with identical abdominal patterning to the *bifarius* complex, and *B. vosnesenskii* and *B. caliginosus* converging on the black complex. All of these species belong to the large subgenus *Pyrobombus*, so it is possible that the retention of elements among them might be due in part to shared phylogeny. One of the most remarkable pairs of co-mimicking species is the nearly indistinguishable *B. auricomis* and *B. pennsylvanicus* in the eastern United States. Despite belonging to distantly related subgenera of *Bombus,* these two species are difficult to differentiate in the field even for a trained expert. Across all species, it appears that the abdominal elements are highly conserved, while the thoracic elements tend to vary more between members of a mimetic complex, suggesting that the abdominal elements might be more important for conveying aposematic signal to predators.

Pattern formation genes and development

The association of different bands of pigmentation with the anterior-posterior segmentation pattern strongly suggests the importance of segmental boundaries in the formation of bumble bee color pattern. The segments appear to serve as barriers or discontinuities between portions of the body, within which the color pattern elements may evolve independently, each able to deviate somewhat from the ground plan, similar to the role of wing veins in butterflies (Nijhout, 1991) as barriers and sources of pattern induction. We have presented a nomenclature of these elements that suggests a new model framework for testing hypotheses of the underlying evolutionary genetic and developmental regulation of the pattern.

An important question in the evolution of pattern formation is whether the many color patterns are under the control of a large number of structural genes, or alternatively whether regulatory genes, such as transcription factors, simply turn a few master genes on and off. Developmental studies of abdominal color pattern in *Drosophila melanogaster* (Kopp & Duncan, 1997; Kopp & Duncan, 2002; Wittkopp *et al*., 2002) have shown that cuticular striping patterns are controlled by segment polarity genes, including *engrailed* (*en*), *hedgehog* (*hh*), *patched* (*ptc*), and *optomotor-blind* (*omb*), and by homeotic genes that control the identity of serially repeated structures. In the honey bee, expression patterns of *Sex combs reduced* (*Scr*) and *Antennapedia* (*Antp*) in portions of the thorax and central abdominal segments, and of *Ultrabithorax* (*Ubx*) and *abdominal-A* (*abd-A*) in the abdomen correlate both with parasegment and segment boundaries (Walldorf *et al.,* 2000). We speculate that some of these developmental genes expressed early in development may also be regulating color pattern in bumble bees, including *Antp* in thoracic and central abdominal patterning and *Ubx*/abd-A in peripheral abdominal patterning (Walldorf *et al*., 2000), while *abd-B* may activate expression of the red pigmentation in the posterior abdominal segments (Jeong *et al.,* 2006). It is especially notable that color transitions among bumble bee abdominal segments occur across an apparently uniform *Ubx/abd-A* expression domain in the honey bee, suggesting that *Ubx/abd-A* alone are unlikely to explain the bumble bee transitions. It is possible that tergite-specific transcription factors are responsible for segment identity and color pattern variation of the bumble bee abdomen. Given that most insects have stereotypical, unchanging abdominal segments (likely related to the ubiquitous *abd-A* (*Hox 8*) identity, bumble bees appear to exhibit a kind of post-*Hox* specialization of abdominal segments that may be novel. Later in development, likely during mid to late pupal stages, specific pigments themselves

may be synthesized under control of one or more transcription factors that switch different branches of the melanin pathway on or off following the instructions laid down by the segmentation and polarity genes earlier in development (Kopp & Duncan, 2002; Wittkopp *et al*., 2002). While this scenario is hypothetical for bumble bees, evidence for the role of a master gene in the regulation of color patterning in insects comes from the recent discovery that expression of a single transcription factor (*optix*) controls all variation in the red color patterning in the wings of diverse *Heliconius* butterflies (Reed *et al*., 2011).

The principal hair colors of bumble bees are black, yellow, orange, and white. We find that black is by far the most common color across the dorsum, and unpublished work in 2008 by H. Imlay and H. Hines indicates that the black pigment in bumble bee hair is melanin, as is the red pigment. The yellow pigment is not yet identified but is not an ommochrome or carotenoid and appears not to be a pteridine. It is unknown whether white is an actual pigment or the absence of pigment in bumble bees. It would be especially compelling if some or all of the bumble bee pigments were products of melanin biosynthesis, because both upstream and downstream genetic control could be compared directly with at least two other systems, *Drosophila* and butterflies. For instance, downstream regulation of bumble bee color pattern could be under the control of genes that regulate melanin synthesis. In *Drosophila melanogaster*, melanin patterns of the dorsal cuticle are delimited by the spatial regulation and combined expression patterns of the *yellow* and *ebony* genes (Wittkopp *et al.,* 2002); the Yellow protein is required for black melanin production and ebony produces a tan pigment, both of which are necessary for producing inter- and intraspecific phenotypic variation in abdominal pigment stripes (Wittkopp *et al.,* 2002). Black melanin patterns within and between species of both *Drosophila* and butterflies are also regulated upstream by morphogen genes of the Wnt-family of signalling proteins (Martin *et al.,* 2012). It is possible that genetic variation in the expression of similar genes in bumble bees could provide a mechanism for the strikingly rapid evolution of the vast array of both novel and convergent pigment patterns.

Individual bumble bee hairs are usually a single color but in some species they may be banded, with different pigment coloration in the basal and apical regions. Some species even have three-toned hairs (*B. waltoni* setae progress from black to orange to white at the tips). This is a heritable phenotypic character and while the adaptive significance, if any, is unclear, it is

possible that this is controlled by an expression-suppression-expression cycle in pigment production during different phases of setal development (Carroll *et al.,* 2005).

The delineation of bumble bee color pattern elements provides a new model system for investigating the genetic and developmental basis of phenotypic polymorphism, especially as it relates to the evolution of color pattern mimicry. The advantages of the *Bombus* system for understanding pattern evolution include: (1) the widespread radiation of diverse mimicry patterns across the entire genus, with repeated examples of both interspecific convergence and intraspecific divergence, (2) a comprehensive phylogeny of the genus (Cameron *et al.,* 2007) and a high density linkage map (covering ~93% of the genome of at least one species [Stolle *et al.,* 2011]) are available as a framework for understanding the evolution of genetic architecture of pattern polymorphism, (3) the geographic distribution of all species is relatively well documented (Williams, 2007; Hines, 2008), and (4) the bees are large and showy, and the banding patterns are simple and thus relatively easily examined for insights into both the developmental genetic and ecological bases of pigmentation patterns.

Conclusions

Our square-grid matrix analysis of color patterns of 222 bumble bee species (~95% of the described taxa) (Cameron *et al.,* 2007) reveals 12 discrete dorsal color pattern elements (ground plan elements) that are shared across the full range of diverse phenotypes. Further analysis reveals additional secondary medial and lateral patterns that uniquely characterize some species; in other species certain elements may fuse. We show that the boundaries of the ground plan elements, hence their shapes, correspond in part to thoracic and abdominal segmentation patterns, but appear independent of adult segmentation in the central and posterior thoracic region. Our findings provide the scaffold from which to embark on evo devo research on pattern formation. We hypothesize a potential role for highly conserved *Hox* and other regulatory genes in upstream regulation and a role for pigment activation genes in the downstream regulation of color patterns, which appear to evolve rapidly in the presence of local communities of bumble bees.

References

Cameron SA, Hines HM, Williams PH. 2007. A comprehensive phylogeny of the bumble bees (*Bombus*) (2007) *Biological Journal of the Linnean Society* 91:161-188.

Carroll SB, Grenier JK, Weatherbee SD. 2005. *From DNA to Diversity.* Malden, MA: Blackwell Publishing.

Conn DLT. 1972. The genetics of mimetic colour polymorphism in the large narcissus bulb fly, *Merodon equestris* Fab. (Diptera: Syrphidae). *Philosophical Transactions of the Royal Society B*. 264: 353-402).

Counterman BA, Araujo-Perez F, Hines HM, Baxter SW, Morrison CM, Lindstrom DP, Papa R, Ferguson L, Joron M, ffrench-Constant RH, Smith CP, Nielsen DM, Chen R, adaptation: the population genetics of Müllerian mimicry in *Heliconius erato*. *PLoS Genetics* 6: e1000796.

Duennes MA, Lozier JD, Hines HM, Cameron SA. 2012. Geographical patterns of genetic divergence in the widespread bumble bee *Bombus ephippiatus* (Hymenoptera: Apidae). *Molecular Phylogenetics and Evolution* 64: 219-231.

Goncalves G, Hoekstra HE, de Freitas TRO. 2011. Striking coat colour variation in tuco-tucos (Rodentia: Ctenomyidae): a role for the melanocortin-1 receptor? *Biological Journal of the Linnean Society* 105: 665-680.

Heinrich B. 2004. *Bumblebee Economics.* Cambridge, MA: Harvard University Press.

Heinrich B. 2012. A heretofore unreported instant color change in a beetle, *Nicrophorus tomentosus* Weber (Coleoptera: Silphidae). *Northeastern Naturalist* 19: 245-252.

Hill GE. 1998. An easy, inexpensive means to quantify plumage coloration. *Journal of Field Ornithology* 69: 353-363.

Hines HM, Williams PH. 2012. Mimetic colour pattern evolution in the highly polymorphic *Bombus trifasciatus* (Hymenoptera: Apidae) species complex and its comimics. *Zoological Journal of the Linnean Society Lond*on 166: 805-826.

Hines HM, Counterman BA, Papa R, de Moura PA, Cardoso MZ, Linares M, Mallet J, Reed RD, Jiggins CD, Kronforst MR, McMillan WO. 2011. A wing patterning gene redefines the mimetic history of *Heliconius* butterflies. *Proceedings of the National Academy of Science USA* 108: 19666-19671.

Hines HM. 2008. Historical biogeography, divergence times, and diversification patterns of bumble bees (Hymenoptera: Apidae: *Bombus*). *Systematic Biol*ogy 57: 58-75.

Hoekstra HE, Nachman MW. 2003. Different genes underlie adaptive melanism in different populations of pocket mice. *Molecular Ecology* 12: 1185-94.

Ings TC, Ings NL, Chittka, L, Rasmont P. 2010. A failed invasion? Commercially introduced pollinators in Southern France. *Apidologie* 41: 1-13.

Jeong S, Rokas A, Carroll B. 2006. Gain and loss in *Drosophila* evolution. *Cell* 125: 1387-1399.

Joron M, Jiggins CD, Papanicolaou A, McMillan WO. 2006. *Heliconius* wing patterns: an evo-devo model for understanding phenotypic diversity. *Heredity* 97: 157–167.

Kopp A, Duncan I. 1997. Control of cell fate and polarity in the adult abdominal segments of *Drosophila* by optomotor-blind. *Development* 124: 3715–3726.

Kopp A, Duncan I. 2002. Anteroposterior patterning in adult abdominal segments of *Drosophila. Developmental Biology* 242: 15–30.

Lawrence PA. 1992. *The Making of a Fly: The Genetics of Animal Design* Oxford, UK: Blackwell Science.

Lê S, Josse J, Husson F. 2008. FactoMineR: An R package for multivariate analysis. *Journal of Statistical Software.* 25: 1-18.

Mallet J, Joron M. 1999. Evolution of diversity in warning color and mimicry: polymorphisms, shifting balance and speciation. *Annual Review of Ecology and Systematics* 30: 201-233.

Manceau M, Domingues VS, Mallarino R, Hoekstra HE. 2011. The developmental role of Agouti in color pattern evolution. *Science* 331: 1062-1065.

Martin A, Papa R, Nadeau NJ, Hill RI, Counterman BA, Halder G, Jiggins CD, Kronforst MR, Long AD, McMillan WO, Reed RD. 2012. Diversification of complex butterfly wing patterns by repeated regulatory evolution of a *Wnt* ligand. *Proceedings of the National Academy of Science USA* 109: 12632-12637.

Michener CD. 2007. *The Bees of the World*, 2nd ed. Baltimore, MD: Johns Hopkins University Press.

Nijhout HF, Wray GA. 1986. Homologies in the colour patterns of the genus *Charaxes* (Lepidoptera: Nymphalidae). *Biological Journal of the Linnean Society* 28: 387-410.

Nijhout HF, Wray GA. 1988. Homologies in the colour patterns of the genus *Heliconius* (Lepidoptera: Nymphalidae). *Biological Journal of the Linnean Society* 33: 345-365.

Nijhout HF. 1991. *The Development and Evolution of Butterfly Wing Patterns*. Washington, DC: Smithsonian Institution Press.

Owen RE, Plowright RC. 1980. Abdominal pile color dimorphism in the bumble bee, *Bombus melanopygus*. *Journal of Heredity* 71: 241-247.

Owen RE, Plowright RC. 1988. Inheritance of metasomal pile colour variation in the bumble bee *Bombus rufocinctus* Cresson (Hymenoptera: Apidae). *Canadian Journal of Zoology* 66: 1172-1178.

Papa R, Kapan DD, Counterman BA, Maldonado K, Lindstrom DP, Reed RD, Nijhout HF, Hrbek T, McMillan WO. 2013. Multi-allelic major effect genes interact with minor effect QTLs to control adaptive color pattern variation in *Heliconius erato*. *PLoS One* 8: e57033.

Plowright RC, Owen RE. 1980. The evolutionary significance of bumble bee color patterns: A mimetic interpretation. *Evolution* 34: 622-37.

Reed RD, *et al*. 2011. *optix* drives the repeated convergent evolution of butterfly wing pattern mimicry. *Science* 333: 1137-1141.

Schwanwitsch BN. 1924. On the groundplan of wing-pattern in nymphalids and certain other families of rhopolacerous Lepidoptera. *Proceedings of the Zoological Society of London ser. B* 34: 509-528.

Steiner CC, Römpler H, Boettger LM, Schöneberg T, Hoekstra HE. 2009. The genetics basis of phenotypic convergence in beach mice: similar pigmentation patterns but different genes. *Molecular Biology and Evolution* 26: 35-45.

Stolle E, Wilfert L, Schmid-Hempel R, Schmid-Hempel P, Kube M, Reinhardt R, Moritz RFA. 2011. A second generation genetic map of the bumblebee *Bombus terrestris* (Linnaeus, 1978) reveals slow genome and chromosome evolution in the Apidae. *BMC Genomics* 12: 48.

Süffert E. 1927. Zur vergleichende Analyse der Schmetterlingszeichnung. *Biologisches Zentralblatt* 47: 385-413.

Tong X, Lindemann A, Monteiro A. 2012. Differential involvement of Hedgehog signaling in butterfly wing and eyespot development. *PLoS ONE* 7: e51087.

Vogt O. 1909. Studien über das Artproblem. 1. Mitteilung. Über das Variieren der Hummeln. 1. Teil. *Sitzungsberichte der Gesellschaft naturforschender Freunde zu Berlin* 1909: 28-84.

Vogt O. 1911. Studien über das Artproblem. 2. Mitteilung. Über das Variieren der Hummeln. 2. Teil. (Schluss). *Sitzungsberichte der Gesellschaft Naturforschender Freunde Zu Berlin* 1911: 31–74.

Waldbauer GP, Sternburg JG, CT Maier. 1977. Phenological relationships of wasps, bumblebees, their mimics, and insectivorous birds in an Illinois sand area. *Ecology* 58: 583-91.

Walldorf U, Binner P, Fleig R. 2000. Hox genes in the honey bee *Apis mellifera*. *Development Genes and Evolution* 210: 483-492.

Williams PH. 1991. The bumble bees of the Kashmir Himalaya (Hymenoptera: Apidae, Bombini). *Bulletin of the British Museum (Natural History) (Entomology)* 60: 1-204.

Williams PH. 2007. The distribution of bumblebee colour patterns worldwide: possible significance for thermoregulation, crypsis, and warning mimicry. *Biological Journal of the Linnean Society* 92: 97-118.

Wittkopp PJ, True JR, Carroll SB. 2002. Reciprocal functions of *Drosophila* Yellow and Ebony proteins development and evolution of pigment patterns. *Development* 129: 1849-1858.

Table 3.1. List of species exemplars for color pattern analysis, including associated specimen vouchers, female caste (worker or queen), and source of specimen identification. All samples are housed either in the Cameron lab or at the Illinois Natural History Survey, University of Illinois. [CP: new specimen for color pattern research, maintained in Cameron lab; SC: voucher specimen used in previous study by Cameron et al. 2007, maintained in Cameron lab; INHS: new specimen for color pattern research, maintained at the Illinois Natural History Survey. *Psithyrus* specimens are indicated by an asterisk (*).

Species	Voucher #	Caste	Determined by
affinis	CP312	worker	SA Cameron
alagesianus	SC085	worker	P Rasmont
alboanalis	CP144	worker	HM Hines
alpinus	SC029	worker	PH Williams
anachoreta	INHS225111	worker	Skorikov
appositus	CP289	worker	PH Williams
ardens	CP400	worker	PH Williams
argillaceus	CP221	worker	P Rasmont
armeniacus	SC080	worker	P Rasmont
asiaticus	CP78A	worker	PH Williams
atratus	SC295	worker	R Brooks
atripes	SC066	worker	PH Williams
auricomus	CP313	worker	SA Cameron
avanus	SC272	worker	PH Williams
avinoviellus	CP36A	worker	PH Williams
baeri	INHS239756	worker	C Rasmussen
balteatus	CP014	queen	P Rasmont
*barbutellus**	INHS313115	female	Lubischew
bellicosus	INHS239893	worker	unknown
bicoloratus	INHS239899	worker	Frison
bifarius	SC208	worker	PH Williams
bimaculatus	CP55	queen	HM Hines
biroi	SC210	worker	PH Williams
*bohemicus**	INHS326118	female	V Popov
borealis	CP314	queen	HM Hines
braccatus	INHS015374	worker	PH Williams
brachycephalus	SC201	queen	SA Cameron
*branickii**	INHS326171	female	V Popov
brasiliensis	CP315	worker	CD Michener
breviceps	SC190	worker	HM Hines
brodmannicus	CP401	worker	P Rasmont
californicus	CP423	worker	HM Hines

Table 3.1 (cont.)

Species	Voucher #	Caste	Determined by
caliginosus	CP450	worker	HM Hines
*campestris**	SC040	female	B Cederberg
centralis	SC146	worker	HM Hines
cingulatus	CP402	worker	B Cederberg
*citrinus**	CP101	female	H Hines
coccineus	SC137	queen	C Rasmussen
confusus	INHS230525	worker	Alfketi
consobrinus	CP223	worker	PH Williams
convexus	CP316	worker	PH Williams
crotchii	SC071	worker	R Thorp
cryptarum	SC127	worker	HM Hines
cullumanus	CP317	worker	P Rasmont
czerskii	INHS240803	worker	unkown
dahlbomii	SC016	queen	PH Williams
defector	INHS240828	worker	Skorikov
deuteronymus	CP318	worker	PH Williams
digressus	CP319	worker	PH Williams
diligens	SC171	worker	PH Williams
distinguendus	INHS230323	worker	unknown
diversus	SC120	worker	S Huang
ecuadorius	INHS230380	worker	Milliron
ephippiatus	VEP01	worker	HM Hines
erzurumensis	SC126	worker	P Rasmont
excellens	CP414	worker	HM Hines
exil	SC232	worker	HM Hines
eximius	SC049	worker	PH Williams
fedtschenkoi	INHS213770	worker	Skorikov
*fernaldae**	CP097	female	H Hines
fervidus	CP282	queen	SA Cameron
festivus	SC104	worker	HM Hines
filchnerae	CP412	worker	PH Williams
flavescens	SC181	worker	HM Hines
*flavidus**	INHS328169	female	V Popov
flavifrons	CP403	worker	SA Cameron
flaviventris	SC275	worker	PH Williams
fragrans	SC061	worker	P Rasmont
franklini	SC204	worker	R Thorp
fraternus	SC031	worker	SA Cameron
frigidus	CP404	worker	HM Hines

Table 3.1 (cont.)

Species	Voucher #	Caste	Determined by
friseanus	CP220	worker	HM Hines
funebris	CP225	queen	HM Hines
funeriarius	SC214	worker	PH Williams
genalis	INHS243282	worker	unkown
gerstaeckeri	SC065	worker	P Rasmont
grahami	SC273	worker	PH Williams
griseocollis	CP224	queen	SA Cameron
haematurus	INHS244473	worker	Pittioni
haemorrhoidalis	SC191	worker	HM Hines
handlirschi	SC132	worker	PH Williams
handlirschianus	SC068	worker	P Rasmont
haueri	SC293	worker	HM Hines
hedini	SC129	worker	PH Williams
himalayanus	INHS333222	worker	unknown
hortorum	CP245	worker	B Cederberg
hortulanus	CP256	worker	PH Williams
humilis	CP77	worker	P Rasmont
huntii	CP152	worker	HM Hines
hyperboreus	CP213	queen	B Cederberg
hypnorum	INHS247415	worker	Moorsel
hypocrita	SC123	worker	S Huang
ignitus	SC096	worker	PH Williams
imitator	CP309	worker	PH Williams
impatiens	CP103	worker	HM Hines
impetuosus	SC165	worker	PH Williams
incertus	INHS245896	worker	Skorikov
infrequens	CP115	worker	PH Williams
*insularis**	CP098	female	H Hines
jonellus	CP148	worker	P Rasmont
kashmirensis	SC121	worker	HM Hines
keriensis	CP031	queen	PH Williams
koreanus	SC277	queen	HM Hines
ladakhensis	CP222	worker	PH Williams
laesus	SC052	worker	P Rasmont
lapidarius	CP34A	worker	P Rasmont
lapponicus	CP405	worker	P Rasmont
lemniscatus	CP116	worker	PH Williams
lepidus	CP149	worker	PH Williams
longipes	SC194	worker	PH Williams

Table 3.1 (cont.)

Species	Voucher #	Caste	Determined by
lucorum	SC048	worker	PH Williams
luteipes	CP154	worker	PH Williams
magregori	SC231	queen	R Ayala
marussinus	INHS248176	worker	Skorikov
*maxillosus**	CP099	female	unknown
medius	CP283	worker	R Ayala
melaleucus	INHS242955	worker	unknown
melanopygus	CP406	worker	HM Hines
melanurus	CP72	queen	PH Williams
mendax	SC019	worker	PH Williams
mesomelas	SC037	worker	PH Williams
mexicanus	CP320	worker	H Imlay
miniatus	CP258	worker	PH Williams
mixtus	CP321	worker	HM Hines
moderatus	CP017	worker	HM Hines
modestus	CP147	worker	P Mardulyn
monticola	CP407	worker	P Rasmont
*morawitzianus**	INHS334202	female	V Popov
morio	CP76	worker	C Rasmussen
morrisoni	CP228	worker	T Griswold
mucidus	SC059	worker	P Rasmont
muscorum	CP322	queen	PH Williams
neoboreus	CP211	worker	A Scholl
nevadensis	SC002	queen	PH Williams
niveatus	CP080	worker	P Rasmont
nobilis	CP231	worker	PH Williams
*norvegicus**	CP100	female	B Cederberg
oberti	SC234	worker	PH Williams
occidentalis	SC026	worker	PH Williams
opifex	SC175	worker	C Rasmussen
opulentus	INHS248983	worker	unknown
parthenius	SC076	worker	PH Williams
pascuorum	SC023	worker	PH Williams
patagiatus	CP214	queen	PH Williams
pensylvanicus	CP111	worker	HM Hines
perplexus	SC166	worker	PH Williams
persicus	SC054	queen	P Rasmont
personatus	SC138	worker	PH Williams
picipes	CP408	worker	PH Williams

Table 3.1 (cont.)

Species	Voucher #	Caste	Determined by
polaris	CP212	worker	A Scholl
pomorum	CP299A	worker	P Rasmont
portchinsky	INHS251974	worker	Skorikov
pratorum	CP001	worker	P Rasmont
pressus	SC239	worker	PH Williams
pseudobaicalensis	SC253	worker	PH Williams
pullatus	CP68A	worker	HM Hines
pyrenaeus	CP045	worker	HM Hines
*quadricolor**	INHS334228	female	V Popov
religiosus	SC141	worker	PH Williams
remotus	SC118	worker	PH Williams
robustus	SC050	queen	PH Williams
rotundiceps	INHS247997	worker	Frison
rubicundus	CP020A	queen	P Reina
ruderarius	SC047	worker	PH Williams
ruderatus	CP324	queen	M Otterstatter
rufipes	SC294	worker	CD Michener
rufocinctus	CP025	queen	A Scholl
rufofasciatus	SC133	worker	PH Williams
*rupestris**	SC009	female	B Cederberg
sandersoni	CP156	worker	HM Hines
schrencki	CP305	queen	PH Williams
securus	SC142	worker	PH Williams
semenovianus	INHS244762	worker	Frison
semenoviellus	INHS244763	worker	Skorikov
senex	INHS244764	worker	Frison
shaposhnikovi	CP420	worker	P Rasmont
sibiricus	SC274	worker	HM Hines
sichelii	SC034	worker	PH Williams
simillimus	CP260	worker	PH Williams
sitkensis	CP145	worker	PH Williams
*skorikovi**	SC159	female	PH Williams
sonani	INHS252896	worker	Frison
sonorus	SC051	worker	T Griswold
soroeensis	CP421	worker	P Rasmont
sporadicus	CP325	queen	PH Williams
steindachneri	SC267	worker	R Ayala
subterraneus	CP079	worker	PH Williams
subtypicus	INHS253093	worker	Skorikov

Table 3.1 (cont.)

Species	Voucher #	Caste	Determined by
*suckleyi**	SC091	female	PH Williams
sulfureus	SC064	queen	HM Hines
supremus	SC101	worker	HM Hines
sushkini	SC143	worker	HM Hines
sylvarum	SC110	worker	PH Williams
*sylvestris**	CP102	female	P Rasmont
sylvicola	CP057A	worker	HM Hines
tanguticus	INHS253110	worker	Richards
ternarius	CP081	worker	SA Cameron
terrestris	CP425	worker	B Cederberg
terricola	CP019A	worker	HM Hines
transversalis	CP065A	worker	HM Hines
tricornis	SC148	worker	PH Williams
trifasciatus	SC015	worker	PH Williams
trinominatus	SC229	worker	HM Hines
tucumanus	SC276	queen	SA Cameron
tunicatus	CP022A	queen	PH Williams
turkestanicus	INHS248263	worker	Skorikov
unicus	INHS333205	worker	Skorikov
ussurensis	CP029A	worker	PH Williams
vagans	SC044	worker	SA Cameron
vandykei	SC149	worker	HM Hines
*variabilis**	CP103	female	R Ayala
velox	SC094	worker	P Rasmont
*vestalis**	CP104	female	A Scholl
veteranus	SC187	worker	A Scholl
vorticosus	SC124	worker	HM Hines
vosnesenskii	CP059A	worker	HM Hines
waltoni	CP038A	worker	SA Cameron
weisi	CP422	worker	R Ayala
wilemani	SC182	worker	HM Hines
wilmattae	Vwilm04	worker	HM Hines
wurflenii	CP011A	worker	SA Cameron
zonatus	SC063	worker	HM Hines

Table 3.2. Color legend of non-technical names matched to Pantone® colors applied to each of the nine distinct setal colors of 204 bumble bee exemplars. Orange-brown (color 7), while a distinctive hue, always occurred as intermixed with black setae. The additional color classes (10-19) refer to mixed setal colors (mixtures of yellows and oranges with black or white) or to multi-hued (multi-toned) banded setae. Colors listed in column 1 refer to the color class we used for scoring. Colored pencil names in column 2 refer to the colors of each Prismacolor® Premier Colored Pencil; in parentheses is the color-matched Pantone number of each color. Colored pencils that begin with I00- or B00- are from the Felissimo Color Museum colored pencil set (200 colored pencils), followed by the matched Pantone number in parentheses.

code #	color	colored pencil
1	white	Cool Grey 10% (7541 C)
2	pale yellow	Cream (7499 C), Jasmine (7401 C), I00402 (7499 C)
3	bright yellow	I00104 (102 C), I00206 (123 C), Spanish Orange (116 C)
4	pale orange	Goldenrod (131 C), I00308 (138 C)
5	orange	Yellowed Orange (1375 C), B00205 (150 C)
6	orange-red	Orange (1585 C), Pale Vermillion (1645 C)
7	orange-brown	Pumpkin Orange (166 C)
8	tawny	B00201 (148 C), B00401 (149 C)
9	black	Black (440 C)
10	black/white mixed	
11	black/yellow mixed	
12	black/orange mixed	
13	white/yellow mixed	
14	white/orange mixed	
15	orange/yellow mixed	
16	black/orange banded	
17	white/orange banded	
18	black/white banded	
19	three-banded	

Table 3.3. Ten pairwise matrices display the association of colors between two adjacent elements (Fig. 3.11). We examined all 19 color classes for the 12 primary elements. Row and column numbers (1-19) represent the 19 pigment classes identified from 204 exemplar species (Table 3.1). Each row x column (19 x 19) grid cell entry indicates the frequency of association for any two colors found on adjacent elements (e.g., elements 1, 2, Fig. 3.11). We do not include comparisons of element 6 (last thoracic element) and 7 (first abdominal element) because of the structural break between them. Highlighted grid cells are those for which the color association between elements occurred at least once.

Elements 1, 2

Element 1 \ Element 2	1	2	3	4	5	6	7	8	9	10	11	12	13	14	15	16	17	18	19
1	7	0	0	0	0	0	0	0	0	2	0	0	0	0	0	0	0	0	0
2	0	41	0	0	0	0	0	0	0	0	2	0	0	0	0	0	0	0	0
3	0	0	23	0	0	0	0	0	0	0	0	0	0	0	0	0	0	0	0
4	0	0	0	8	0	0	0	0	0	0	0	1	0	0	0	0	0	0	0
5	0	0	0	0	5	0	0	0	0	0	0	0	0	0	0	0	0	0	0
6	0	0	0	0	0	1	0	0	0	0	0	1	0	1	0	0	0	0	0
7	0	0	0	0	0	0	0	0	0	0	0	0	0	0	0	0	0	0	0
8	0	0	0	0	0	0	0	0	0	0	0	0	0	0	0	0	0	0	0
9	1	0	0	0	0	0	0	0	22	0	3	0	0	0	0	0	0	0	0
10	7	0	0	0	0	0	0	0	1	7	0	0	0	0	0	0	0	0	0
11	0	23	9	0	0	0	0	0	2	0	27	0	0	0	0	0	0	0	0
12	0	0	0	3	0	2	0	0	2	0	0	1	0	0	0	0	0	0	0
13	0	0	0	0	0	0	0	0	0	0	0	0	1	0	0	0	0	0	0
14	0	0	0	0	0	0	0	0	0	0	0	0	0	0	0	0	0	0	0
15	0	0	0	0	0	0	0	0	0	0	0	0	0	0	0	0	0	0	0
16	0	0	0	0	0	0	0	0	0	0	0	0	0	0	0	0	0	0	0
17	0	0	0	0	0	0	0	0	0	0	0	0	0	0	0	0	0	0	0
18	0	0	0	0	0	0	0	0	0	0	0	0	0	0	0	0	0	1	0
19	0	0	0	0	0	0	0	0	0	0	0	0	0	0	0	0	0	0	0

Table 3.3 (cont.)

Elements 2,3

Element 2 \ Element 3	1	2	3	4	5	6	7	8	9	10	11	12	13	14	15	16	17	18	19
1	5	0	0	0	0	0	0	0	9	0	0	0	0	0	0	0	0	0	0
2	0	16	0	0	0	0	0	0	30	0	7	0	0	0	0	1	0	0	0
3	0	0	12	0	0	0	0	0	14	0	2	0	0	0	0	0	0	0	0
4	0	0	0	8	0	0	0	0	2	0	0	0	0	0	0	0	0	0	0
5	0	0	0	0	4	0	0	0	1	0	0	0	0	0	0	0	0	0	0
6	0	0	0	0	0	3	0	0	1	0	0	0	0	0	0	0	0	0	0
7	0	0	0	0	0	0	0	0	0	0	0	0	0	0	0	0	0	0	0
8	0	0	0	0	0	0	0	0	0	0	0	0	0	0	0	0	0	0	0
9	0	0	0	0	0	0	0	0	53	0	0	0	0	0	0	0	0	0	0
10	0	0	0	0	0	0	0	0	4	2	0	0	0	0	0	0	0	0	0
11	0	0	0	0	0	0	0	0	15	0	11	0	0	0	0	0	0	0	0
12	0	0	0	0	0	0	0	0	0	0	0	2	0	0	0	0	0	0	0
13	0	0	0	0	0	0	0	0	1	0	0	0	0	0	0	0	0	0	0
14	0	0	0	0	0	0	0	0	0	0	0	0	0	0	0	0	0	0	0
15	0	0	0	0	0	0	0	0	0	0	0	0	0	0	0	0	0	0	0
16	0	0	0	0	0	0	0	0	0	0	0	0	0	0	0	0	0	0	0
17	0	0	0	0	0	0	0	0	0	0	0	0	0	0	0	0	0	0	0
18	0	0	0	0	0	0	0	0	0	0	0	0	0	0	0	0	0	1	0
19	0	0	0	0	0	0	0	0	0	0	0	0	0	0	0	0	0	0	0

Element 3, 4

Element 3 \ Element 4	1	2	3	4	5	6	7	8	9	10	11	12	13	14	15	16	17	18	19
1	2	0	0	0	0	0	0	0	3	0	0	0	0	0	0	0	0	0	0
2	0	8	0	0	0	0	0	0	7	0	1	0	0	0	0	0	0	0	0
3	0	0	5	0	0	0	0	0	7	0	0	0	0	0	0	0	0	0	0
4	0	0	0	7	0	0	0	0	0	0	0	1	0	0	0	0	0	0	0
5	0	0	0	0	4	0	0	0	0	0	0	0	0	0	0	0	0	0	0
6	0	0	0	0	0	3	0	0	0	0	0	0	0	0	0	0	0	0	0
7	0	0	0	0	0	0	0	0	0	0	0	0	0	0	0	0	0	0	0
8	0	0	0	0	0	0	0	0	0	0	0	0	0	0	0	0	0	0	0
9	0	0	0	0	0	0	0	0	##	0	0	0	0	0	0	0	0	0	0
10	0	0	0	0	0	0	0	0	0	2	0	0	0	0	0	0	0	0	0
11	0	1	0	0	0	0	0	0	9	0	10	0	0	0	0	0	0	0	0
12	0	0	0	0	0	0	0	0	0	0	0	2	0	0	0	0	0	0	0
13	0	0	0	0	0	0	0	0	0	0	0	0	0	0	0	0	0	0	0
14	0	0	0	0	0	0	0	0	0	0	0	0	0	0	0	0	0	0	0
15	0	0	0	0	0	0	0	0	0	0	0	0	0	0	0	0	0	0	0
16	0	0	0	0	0	0	0	0	0	0	0	0	0	0	0	1	0	0	0
17	0	0	0	0	0	0	0	0	0	0	0	0	0	0	0	0	0	0	0
18	0	0	0	0	0	0	0	0	0	0	0	0	0	0	0	0	0	1	0
19	0	0	0	0	0	0	0	0	0	0	0	0	0	0	0	0	0	0	0

Table 3.3 (cont.)

Elements 4, 5

Element 4 \ Element 5	1	2	3	4	5	6	7	8	9	10	11	12	13	14	15	16	17	18	19
1	2	0	0	0	0	0	0	0	1	0	0	0	0	0	0	0	0	0	0
2	0	9	0	0	0	0	0	0	0	0	1	0	0	0	0	0	0	0	0
3	0	0	5	0	0	0	0	0	0	0	0	0	0	0	0	0	0	0	0
4	0	0	0	8	0	0	0	0	0	0	0	0	0	0	0	0	0	0	0
5	0	0	0	0	5	0	0	0	0	0	0	0	0	0	0	0	0	0	0
6	0	0	1	0	0	3	0	0	0	0	0	0	0	0	0	0	0	0	0
7	0	0	0	0	0	0	0	0	0	0	0	0	0	0	0	0	0	0	0
8	0	0	0	0	0	0	0	0	0	0	0	0	0	0	0	0	0	0	0
9	8	22	12	2	0	0	0	0	70	1	17	5	0	0	0	0	0	0	0
9	2	0	0	0	0	0	0	0	0	2	0	0	0	0	0	0	0	0	0
11	0	9	0	0	0	0	0	0	2	0	13	0	0	0	0	0	0	0	0
12	0	0	0	1	0	0	0	0	0	0	0	1	0	0	0	0	0	0	0
13	0	0	0	0	0	0	0	0	0	0	0	0	0	0	0	0	0	0	0
14	0	0	0	0	0	0	0	0	0	0	0	0	0	0	0	0	0	0	0
15	0	0	0	0	0	0	0	0	0	0	0	0	0	0	0	0	0	0	0
16	0	0	0	0	0	0	0	0	0	0	0	0	0	0	0	1	0	0	0
17	0	0	0	0	0	0	0	0	0	0	0	0	0	0	0	0	0	0	0
18	0	0	0	0	0	0	0	0	0	0	0	0	0	0	0	0	0	1	0
19	0	0	0	0	0	0	0	0	0	0	0	0	0	0	0	0	0	0	0

Elements 5, 6

Element 5 \ Element 6	1	2	3	4	5	6	7	8	9	10	11	12	13	14	15	16	17	18	19
1	5	0	0	0	0	0	0	0	4	5	0	0	0	0	0	0	1	0	0
2	0	25	0	0	0	0	0	0	8	0	18	0	0	0	0	0	0	0	0
3	0	0	11	0	0	0	0	0	5	0	4	0	0	0	0	0	0	0	0
4	0	0	0	8	0	0	0	0	0	0	0	3	0	0	0	0	0	0	0
5	0	0	0	0	4	0	0	0	0	0	0	1	0	0	0	0	0	0	0
6	0	0	0	0	0	2	0	0	1	0	0	0	0	0	0	0	0	0	0
7	0	0	0	0	0	0	0	0	0	0	0	0	0	0	0	0	0	0	0
8	0	0	0	0	0	0	0	0	0	0	0	0	0	0	0	0	0	0	0
9	1	3	1	0	1	0	0	0	44	3	8	0	0	0	0	0	0	0	0
10	1	0	0	0	0	0	0	0	2	1	0	0	0	0	0	0	0	0	0
11	0	3	2	0	0	0	0	0	9	0	12	0	0	0	0	0	0	0	0
12	0	1	0	1	0	2	0	0	2	0	0	0	0	0	0	0	0	0	0
13	0	0	0	0	0	0	0	0	0	0	0	0	0	0	0	0	0	0	0
14	0	0	0	0	0	0	0	0	0	0	0	0	0	0	0	0	0	0	0
15	0	0	0	0	0	0	0	0	0	0	0	0	0	0	0	0	0	0	0
16	0	1	0	0	0	0	0	0	0	0	0	0	0	0	0	0	0	0	0
17	0	0	0	0	0	0	0	0	0	0	0	0	0	0	0	0	0	0	0
18	0	0	0	0	0	0	0	0	0	0	0	0	0	0	0	0	0	1	0
19	0	0	0	0	0	0	0	0	0	0	0	0	0	0	0	0	0	0	0

Table 3.3 (cont.)

Elements 7, 8

Element 7 \ Element 8	1	2	3	4	5	6	7	8	9	10	11	12	13	14	15	16	17	18	19
1	8	3	0	0	0	0	0	0	3	2	1	0	0	0	0	0	0	0	0
2	0	47	0	1	1	1	0	1	3	0	6	0	0	0	0	0	0	0	0
3	0	0	20	1	0	0	0	0	3	0	0	0	0	0	0	0	0	0	0
4	0	0	0	7	0	0	0	0	0	0	0	0	0	0	0	0	0	0	0
5	0	0	0	0	4	0	0	0	0	0	0	1	0	0	0	0	0	0	0
6	0	0	0	0	0	2	0	0	0	0	0	0	0	0	0	0	0	0	0
7	0	0	0	0	0	0	0	0	0	0	0	0	0	0	0	0	0	0	0
8	0	0	0	0	0	0	0	1	0	0	0	0	0	0	0	0	0	0	0
9	3	11	3	1	1	4	0	0	36	0	7	4	0	0	0	0	0	0	0
10	0	0	0	0	0	1	0	0	0	0	0	0	0	0	0	0	0	0	0
11	0	4	1	0	0	0	0	0	0	0	2	0	0	0	0	0	0	0	0
12	0	0	0	2	0	0	0	0	0	0	0	4	0	0	0	0	0	0	0
13	0	0	0	0	0	0	0	0	0	0	0	0	0	0	0	0	0	0	0
14	0	0	0	0	0	0	0	0	0	0	0	0	0	0	0	0	0	0	0
15	0	1	0	1	1	0	0	0	0	0	0	0	0	0	0	0	0	0	0
16	0	0	0	0	0	0	0	0	0	0	0	0	0	0	0	0	0	0	0
17	0	0	0	0	0	0	0	0	0	0	0	0	0	0	0	0	0	0	0
18	0	0	0	0	0	0	0	0	0	0	0	0	0	0	0	0	0	0	0
19	0	0	0	0	0	0	0	0	0	0	0	0	0	0	0	0	0	0	1

Elements 8, 9

Element 8 \ Element 9	1	2	3	4	5	6	7	8	9	10	11	12	13	14	15	16	17	18	19
1	3	0	0	0	0	0	0	0	8	0	0	0	0	0	0	0	0	0	0
2	0	17	0	2	1	1	0	0	30	0	0	2	0	0	0	0	0	0	0
3	0	1	11	0	2	2	0	0	8	0	0	0	0	0	0	0	0	0	0
4	0	0	0	7	0	0	0	0	6	0	0	0	0	0	0	0	0	0	0
5	0	0	0	0	4	0	0	0	3	0	0	0	0	0	0	0	0	0	0
6	0	0	0	0	0	14	0	0	0	0	0	0	0	0	0	0	0	0	0
7	0	0	0	0	0	0	0	0	0	0	0	0	0	0	0	0	0	0	0
8	0	0	0	0	0	0	0	0	1	0	0	0	0	0	0	0	0	0	0
9	1	5	0	1	0	1	0	0	50	0	2	2	0	0	0	0	0	0	0
10	0	0	0	0	0	0	0	0	0	1	0	0	0	0	0	0	0	0	0
11	0	0	0	0	0	1	0	0	8	0	2	1	0	0	0	0	0	0	0
12	0	0	0	0	1	0	0	0	1	0	0	1	0	0	0	0	0	0	0
13	0	0	0	0	0	0	0	0	0	0	0	0	0	0	0	0	0	0	0
14	0	0	0	0	0	0	0	0	0	0	0	0	0	0	0	0	0	0	0
15	0	0	0	0	1	1	0	0	0	0	0	0	0	0	0	0	0	0	0
16	0	0	0	0	0	0	0	0	0	0	0	0	0	0	0	0	0	0	0
17	0	0	0	0	0	0	0	0	0	0	0	0	0	0	0	0	0	0	0
18	0	0	0	0	0	0	0	0	0	0	0	0	0	0	0	0	0	0	0
19	0	0	0	0	0	0	0	0	0	0	0	0	0	0	0	0	1	0	0

Table 3.3 (cont.)

Elements 9, 10

Element 9 \ Element 10	1	2	3	4	5	6	7	8	9	10	11	12	13	14	15	16	17	18	19
1	2	0	0	0	0	0	0	0	1	0	0	0	0	0	0	0	0	0	0
2	0	13	0	0	1	0	0	0	9	0	3	2	0	0	0	1	0	0	0
3	0	0	5	0	0	1	0	0	4	0	1	0	0	0	0	0	0	0	0
4	0	1	0	4	0	0	0	0	1	0	0	0	0	0	1	0	0	0	0
5	0	0	0	0	10	0	0	0	2	0	0	1	0	0	0	0	0	0	0
6	1	2	0	0	0	19	0	0	0	0	0	0	0	1	1	0	0	0	0
7	0	0	0	0	0	0	0	0	0	0	0	0	0	0	0	0	0	0	0
8	0	0	0	0	0	0	0	0	0	0	0	0	0	0	0	0	0	0	0
9	14	9	2	0	18	17	0	0	37	1	2	1	0	0	0	0	0	0	0
10	0	0	0	0	0	0	0	0	0	1	0	0	0	0	0	0	0	0	0
11	0	1	0	1	1	0	0	0	1	0	2	0	0	0	0	0	0	0	0
12	0	0	0	0	4	3	0	0	0	0	1	0	0	0	0	0	0	0	0
13	0	0	0	0	0	0	0	0	0	0	0	0	0	0	0	0	0	0	0
14	0	0	0	0	0	0	0	0	0	0	0	0	0	0	0	0	0	0	0
15	0	0	0	0	0	0	0	0	0	0	0	0	0	0	0	0	0	0	0
16	0	0	0	0	0	0	0	0	0	0	0	0	0	0	0	0	0	0	0
17	0	0	0	0	0	0	0	0	0	0	0	0	0	0	0	0	1	0	0
18	0	0	0	0	0	0	0	0	0	0	0	0	0	0	0	0	0	0	0
19	0	0	0	0	0	0	0	0	0	0	0	0	0	0	0	0	0	0	0

Elements 10, 11

Element 10 \ Element 11	1	2	3	4	5	6	7	8	9	10	11	12	13	14	15	16	17	18	19
1	16	0	0	0	0	0	0	0	5	0	0	0	0	0	0	0	0	0	0
2	0	27	0	0	0	0	0	0	8	0	0	0	0	0	1	0	0	0	0
3	0	0	5	0	0	0	0	0	2	0	1	0	0	0	0	0	0	0	0
4	0	0	0	4	0	0	0	0	0	0	0	0	0	1	0	0	0	0	0
5	0	0	0	0	33	0	0	0	1	0	0	1	0	0	0	0	0	0	0
6	2	0	0	0	0	35	0	0	1	0	0	1	0	0	0	0	0	0	0
7	0	0	0	0	0	0	0	0	0	0	0	0	0	0	0	0	0	0	0
8	0	0	0	0	0	0	0	0	0	0	0	0	0	0	0	0	0	0	0
9	1	2	2	1	1	0	0	0	37	1	0	1	0	0	0	0	0	0	0
10	1	0	0	0	0	0	0	0	0	1	0	0	0	0	0	0	0	0	0
11	0	2	0	0	1	0	0	0	1	0	0	0	0	1	0	0	0	0	0
12	0	0	0	0	1	0	0	0	1	0	0	0	0	0	0	0	0	0	0
13	0	0	0	0	0	0	0	0	0	0	0	0	0	0	0	0	0	0	0
14	0	0	0	0	0	0	0	0	0	0	0	0	0	0	0	0	0	0	0
15	0	0	0	0	0	0	0	0	0	0	0	1	0	0	0	0	0	0	0
16	0	1	0	0	0	0	0	0	0	0	0	0	0	0	0	0	0	0	0
17	1	0	0	0	0	0	0	0	0	0	0	0	0	0	0	0	1	0	0
18	0	0	0	0	0	0	0	0	0	0	0	0	0	0	0	0	0	1	0
19	0	0	0	0	0	0	0	0	0	0	0	0	0	0	0	0	0	0	0

Table 3.3 (cont.)

Elements 11, 12

Element 11 \ Element 12	1	2	3	4	5	6	7	8	9	10	11	12	13	14	15	16	17	18	19
1	17	0	0	0	0	0	0	0	4	1	0	0	0	0	0	0	0	0	0
2	0	15	0	0	0	1	0	0	12	0	4	0	0	0	0	0	0	0	0
3	0	1	2	0	0	0	0	0	1	0	0	0	0	0	0	0	0	0	0
4	0	0	0	3	0	0	0	0	1	0	0	1	0	0	0	0	0	0	0
5	0	0	0	0	32	0	0	0	3	0	0	1	0	0	0	0	0	0	0
6	1	0	0	0	0	26	0	0	3	0	0	3	0	0	1	0	0	0	0
7	0	0	0	0	0	0	0	0	0	0	0	0	0	0	0	0	0	0	0
8	0	0	0	0	0	0	0	0	0	0	0	0	0	0	0	0	0	0	0
9	0	0	1	1	1	0	0	0	52	0	0	1	0	0	0	0	0	0	0
10	0	0	0	0	1	0	0	0	0	0	0	0	0	0	0	0	0	0	0
11	0	0	1	0	0	0	0	0	4	0	0	0	0	1	0	0	0	0	0
12	0	0	0	0	1	0	0	0	1	0	0	2	0	0	0	0	0	0	0
13	0	0	0	0	0	0	0	0	0	0	0	0	0	0	0	0	0	0	0
14	0	0	0	1	0	0	0	0	0	0	0	0	0	0	0	0	0	0	0
15	0	0	0	0	0	0	0	0	0	0	1	0	0	0	0	0	0	0	0
16	0	0	0	0	0	0	0	0	0	0	0	0	0	0	0	0	0	0	0
17	0	0	0	0	0	0	0	0	0	0	0	0	0	0	0	0	1	0	0
18	0	0	0	0	0	0	0	0	0	0	0	0	0	0	0	0	0	1	0
19	0	0	0	0	0	0	0	0	0	0	0	0	0	0	0	0	0	0	0

Table 3.4. Nomenclature of *Bombus* pattern elements, including the numerical coding of the 12 ground plan elements ordered along the anterior-posterior axis of the dorsum, and the letter coding of the secondary elements (a-e).

Element	Name	Position	*P*-value
Ground plan (Primary) elements			
1	Pronotal band	Pronotum	0.0002
2	Anterior scutal band	Anterior scutum	0.0002
3	Central scutal band	Central scutum	0.0002
4	Posterior scutal band	Posterior scutum	0.0002
5	Scutellar band	Scutellum	0.0002
6	Metanotal band	Metanotum	0.0002
7	Tergal band 1	Tergite 1	0.0002
8	Tergal band 2	Tergite 2	0.0002
9	Tergal band 3	Tergite 3	0.0002
10	Tergal band 4	Tergite 4	0.0002
11	Tergal band 5	Tergite 5	0.0002
12	Tergal band 6	Tergite 6	0.0002
Secondary elements			
a	T1 medial notch	Tergite 1 central disc	0.006
b	T2 narrow dorsolateral patch	Tergite 2 lateral disc	0.028
c	T2 wide dorsolateral patch	Tergite 2 lateral disc	0.022
d	T3 dorsolateral patch	Tergite 3 lateral disc	0.0004
e	T4 dorsolateral patch	Tergite 4 lateral disc	0.003

P-value (1-tailed) based on permutation tests. See Methods and Appendix A.

Figure 3.1. Diagrammatic representation of color pattern scoring and numerical coding of bumble bee patterns for analysis of pattern elements. **(A)** Sample bumble bee (*Bombus ephippiatus*) color pattern, **(B)** template of bumble bee thoracic and abdominal dorsum, **(C)** scored *B. ephippiatus* color pattern, **(D)** square-grid matrix placed over scored color pattern for numerical coding of the pattern (0 = no color transition occurs within a grid cell; 1 = a color transition occurs within a grid cell); **(E)** the result is the sum matrix indicating total counts of color transitions occurring within each of 550 grid cells summed for 204 social *Bombus* species used in the analysis (see supplemental Fig. 1*B* online for social plus parasitic species sum matrix). The color legend (upper left) indicates the 9 distinct hues (white to black) we identified for all species; the color transition legend (upper right) identifies the range in color transition frequency (lowest = 6-10 transitions; highest = 116-120) with each grid cell color of the sum matrix represented here as a heat map of color transitions: green to red indicates the highest color transition values, which occur along pattern element boundaries; blue cells fall within pattern elements. T1-T6 refers to the metasomal tergites. Note that in Hymenoptera, the first true abdominal segment is fused to the thorax so the notation "T" refers to the tergites of the metasoma, which differentiates it from the notation "A" indicating abdominal segments in other insects. See Methods (Identifying Areas of Color Transition) for additional details.

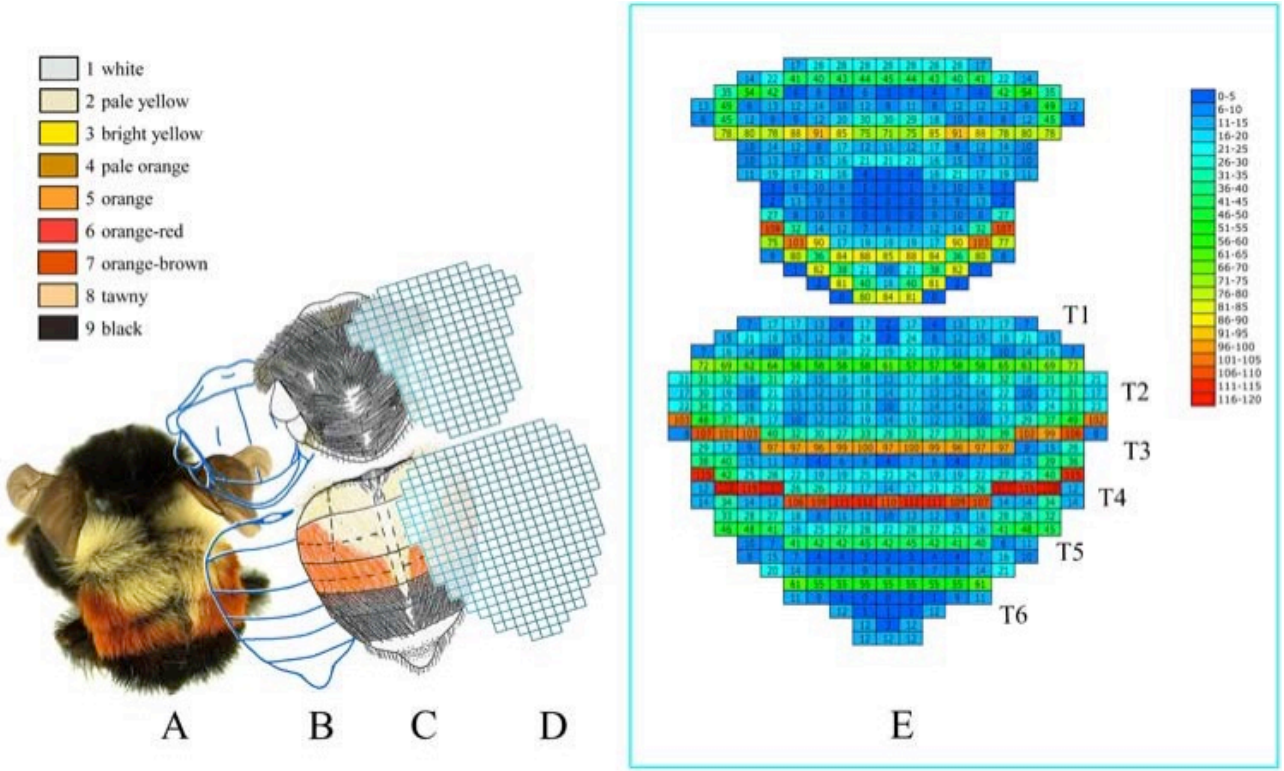

Figure 3.2. (A) scutoscutellar suture (green) separating scutum (purple) and scutellum (blue) comprising the mesonotum)**; (B)** Diagrammatic representation of bumble bee dorsal segmentation boundaries (yellow).

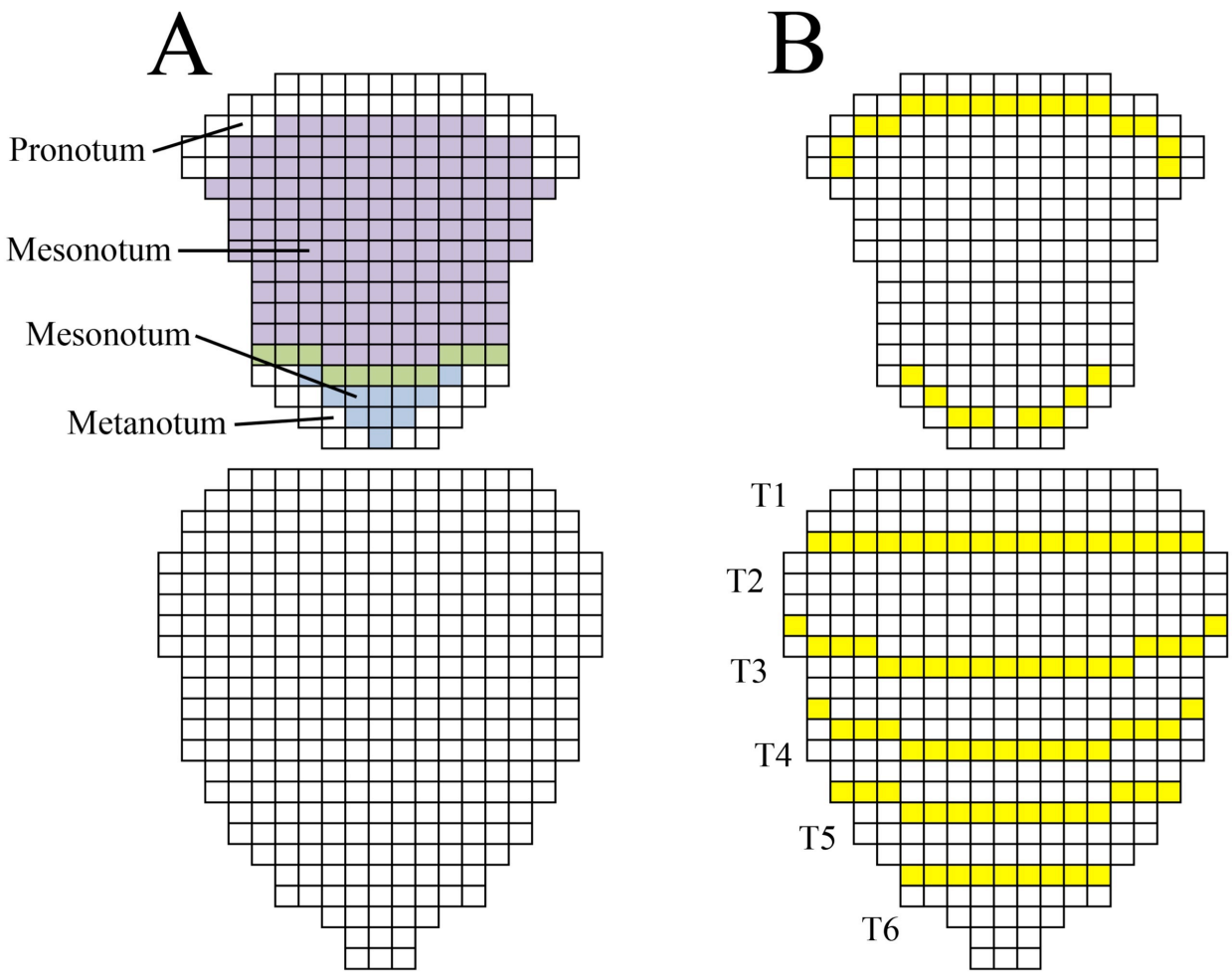

Figure 3.3. (A) Diagrammatic representation of bumble bee dorsal ground plan pattern elements (1-12) and secondary elements (a-e) revealed in color transition analyses. Each element is labeled (also see Table 3.4 and Appendix B), and the associated colored dots identify the correspondingly colored element. **(B)** Template of dorsal morphology showing anterior-posterior sclerite and segmentation boundaries. Additional thoracic morphological features observed on a shaved bee (all setae removed from dorsum) include the dorsal midline and the parapsidal lines on the mesoscutum. Dotted lines on tergite 2 represent some commonly observed species-specific arch patterns formed by contrasting setae relative to the pigmentation of the lateral setae.

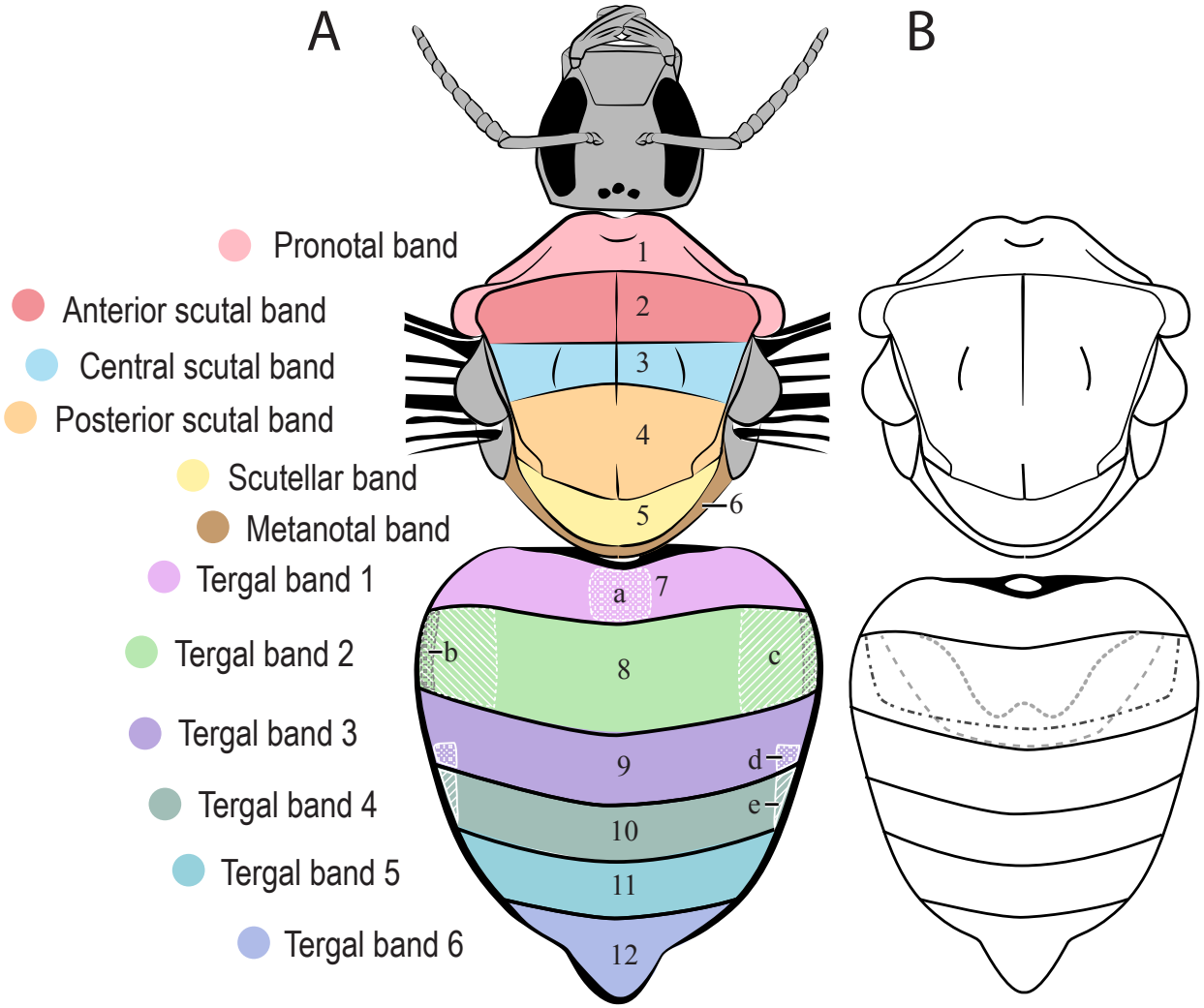

Figure 3.4. Spectrophotometric reflectance curves for each unmixed setal hue (Table 3.2) distinguished among 204 bumble bee species. Orange-brown (Table 3.2, color 7), while a distinctive hue, always occurred as intermixed with black setae, thus was not measured for reflectance. The curves represent diffuse reflectance, indicated by percent reflectance along the Y-axis and wavelength (nm) along the X-axis. White pile is from *Bombus persicus* (SPEC01), pale yellow from *B. impatiens* (SPEC02), bright yellow from *B. fervidus* (SPEC03), pale orange from *B. pomorum* (SPEC04), orange from *B. dahlbomii* (SPEC05), orange-red from *B. rubicundus* (SPEC06), tawny from *B. simillimus* (SPEC07), black from *B. vosnesenskii* (SPEC08), and hairless tergite reflectance from *B. vosnesenskii* (SPEC09). The abrupt vertical translation between 323-324 nm correlates with the position at which the Carey 5G switched detectors, and is an artifact of sample orientation changing relative to the second detector.

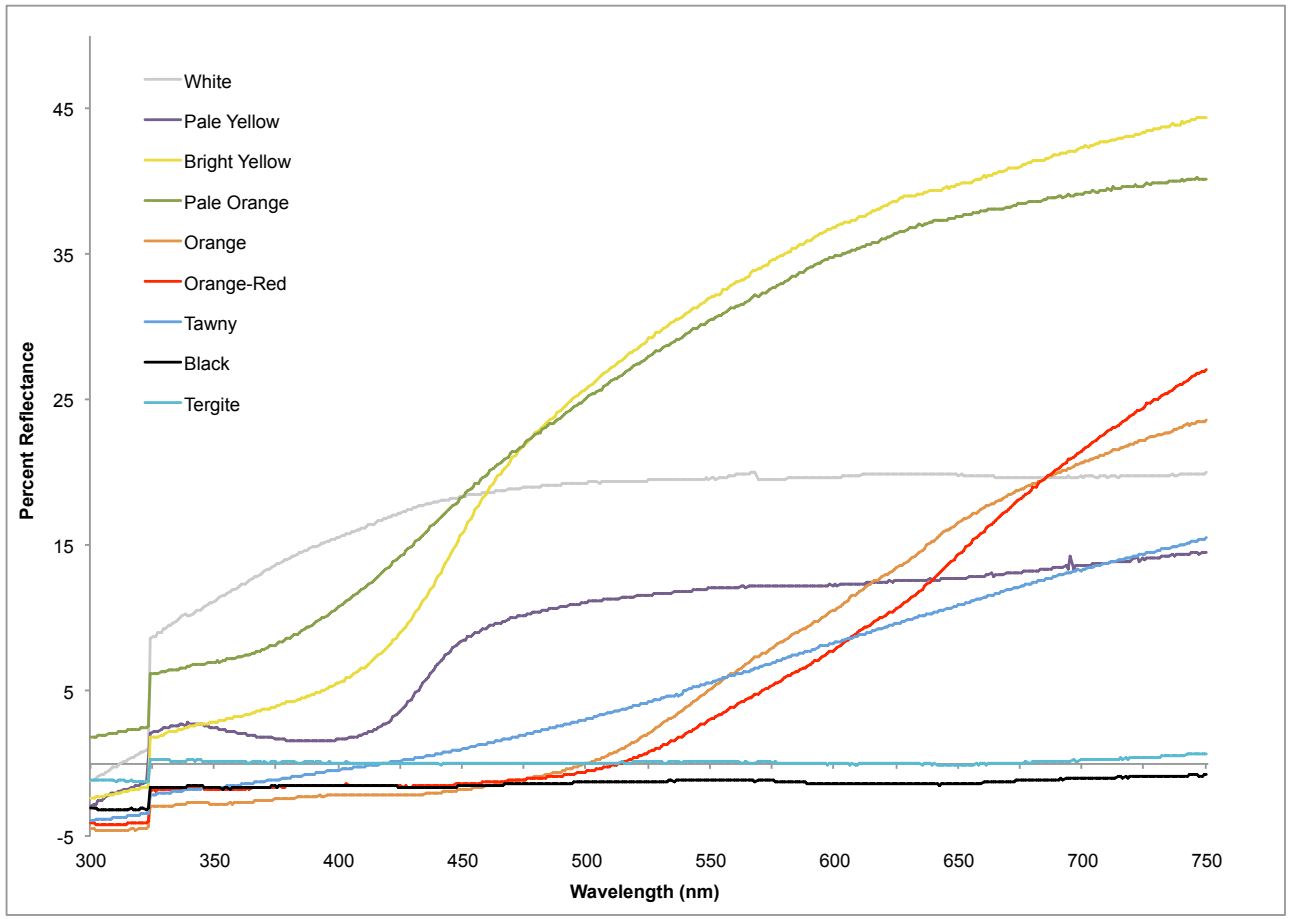

Figure 3.5. (A) Sum matrix of all color transition frequencies for 204 social bumble bee species exemplars. This is identical to that shown in Fig. 3.1E (main text), enlarged for visual clarity. **(B)** Sum matrix of color transition frequencies for 204 social bumble bee species plus 18 species of obligately social parasites of the subgenus *Psithyrus*, indicating identical element boundaries to those of **(A)** when *Psithyrus* are included in the analysis.

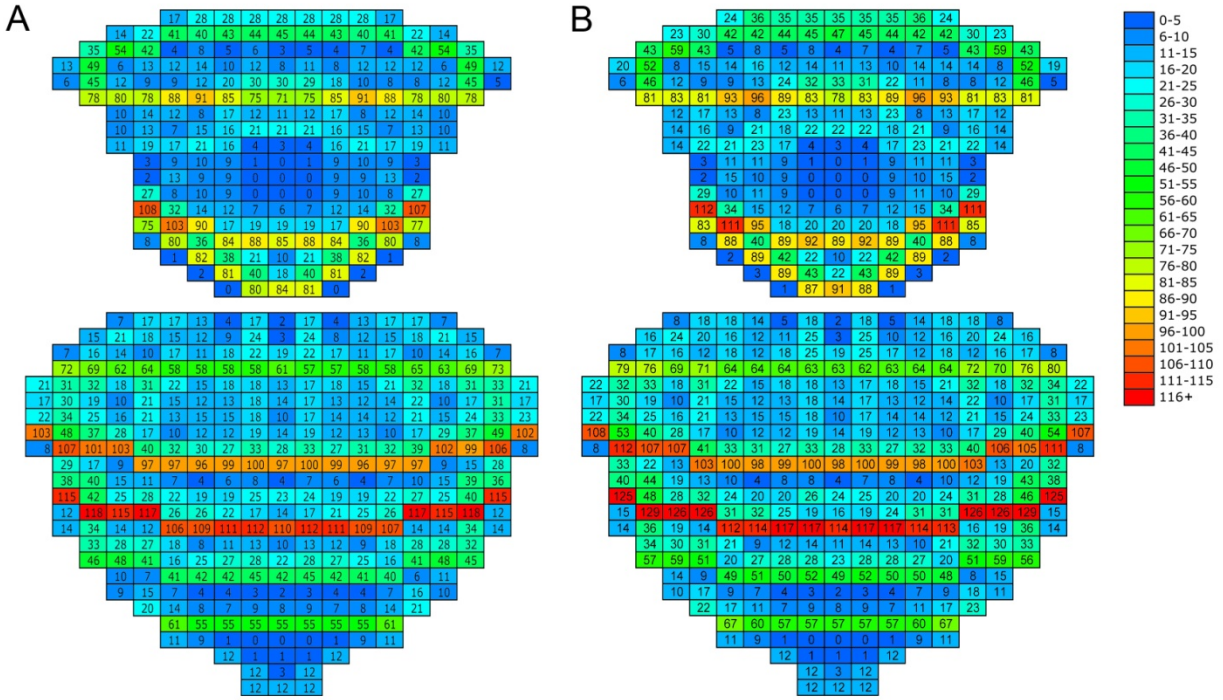

Figure 3.6. To explore whether or not the ground plan elements shared between all species were conserved at the intraspecific-level, we explored the elements within three species with varying levels of polymorphism: *B. ternarius* **(A)**:strongly monomorphic, *B. pyrenaeus* **(B)**: intermediate in pattern variation, and *B. ephippiatus* **(C)**: polymorphic in color pattern. Numbers in each cell represent the total number of changes.

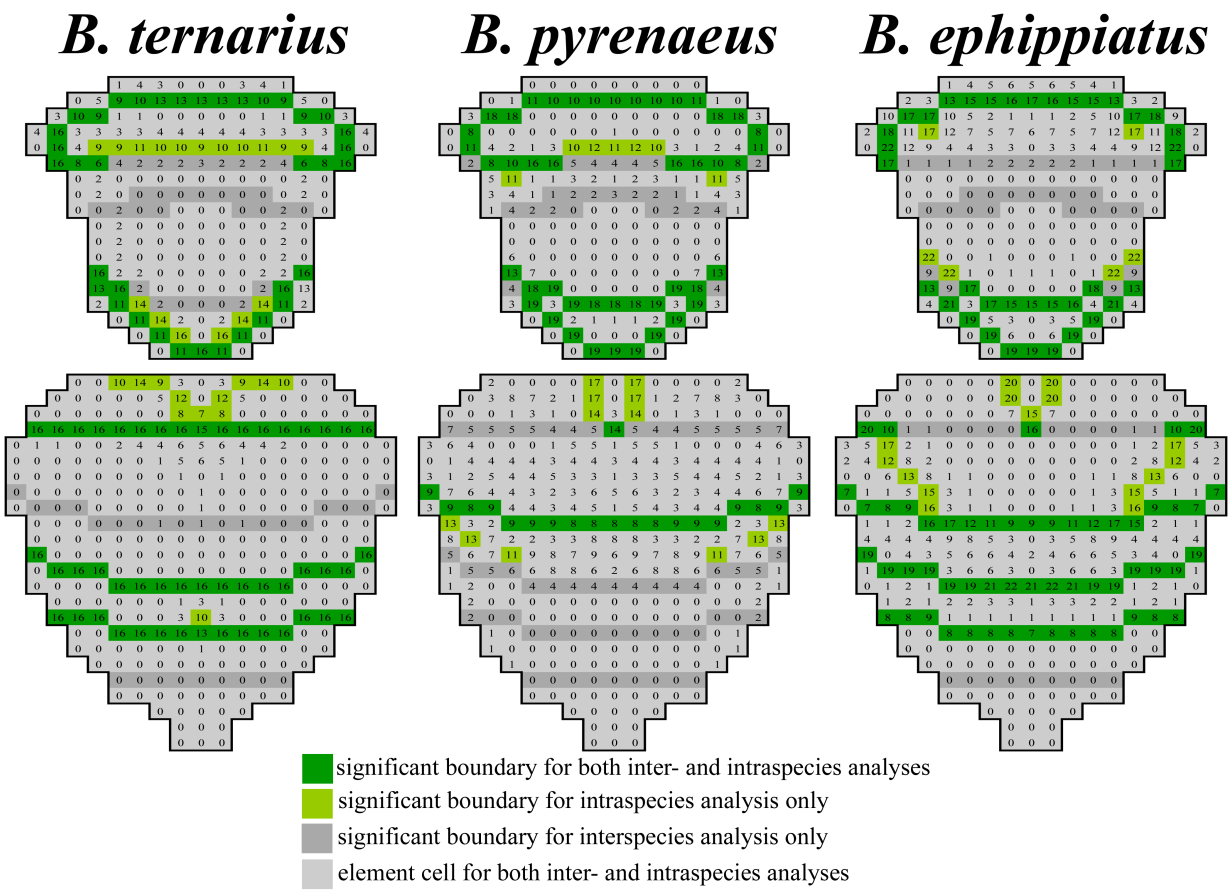

Figure 3.7. Color frequency and heat maps for eight major color classes **(A-H)** (tabulated in Table 3.2) for all 204 species exemplars. The highest frequencies are highlighted for each color (left), and these are also represented as heat maps (right). Range of percentages refer to the highest mean frequencies found for a given pigment. **(A)** black, **(B)** black+yellow mixed, **(C)** pale yellow, **(D)** bright yellow, **(E)** orange-red, **(F)** orange, **(G)** pale orange, **(H)** white.

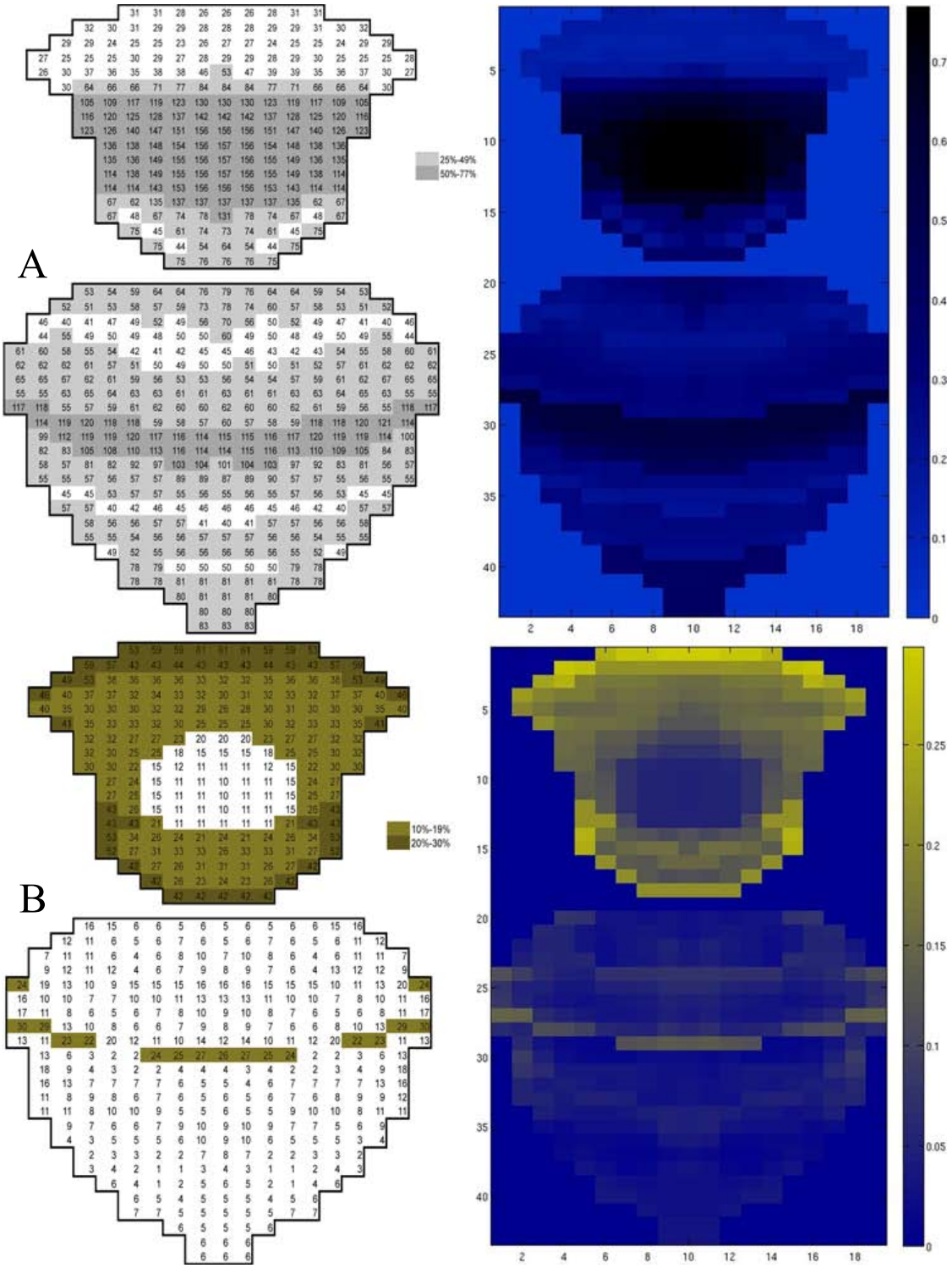

Figure 3.7 (cont.)

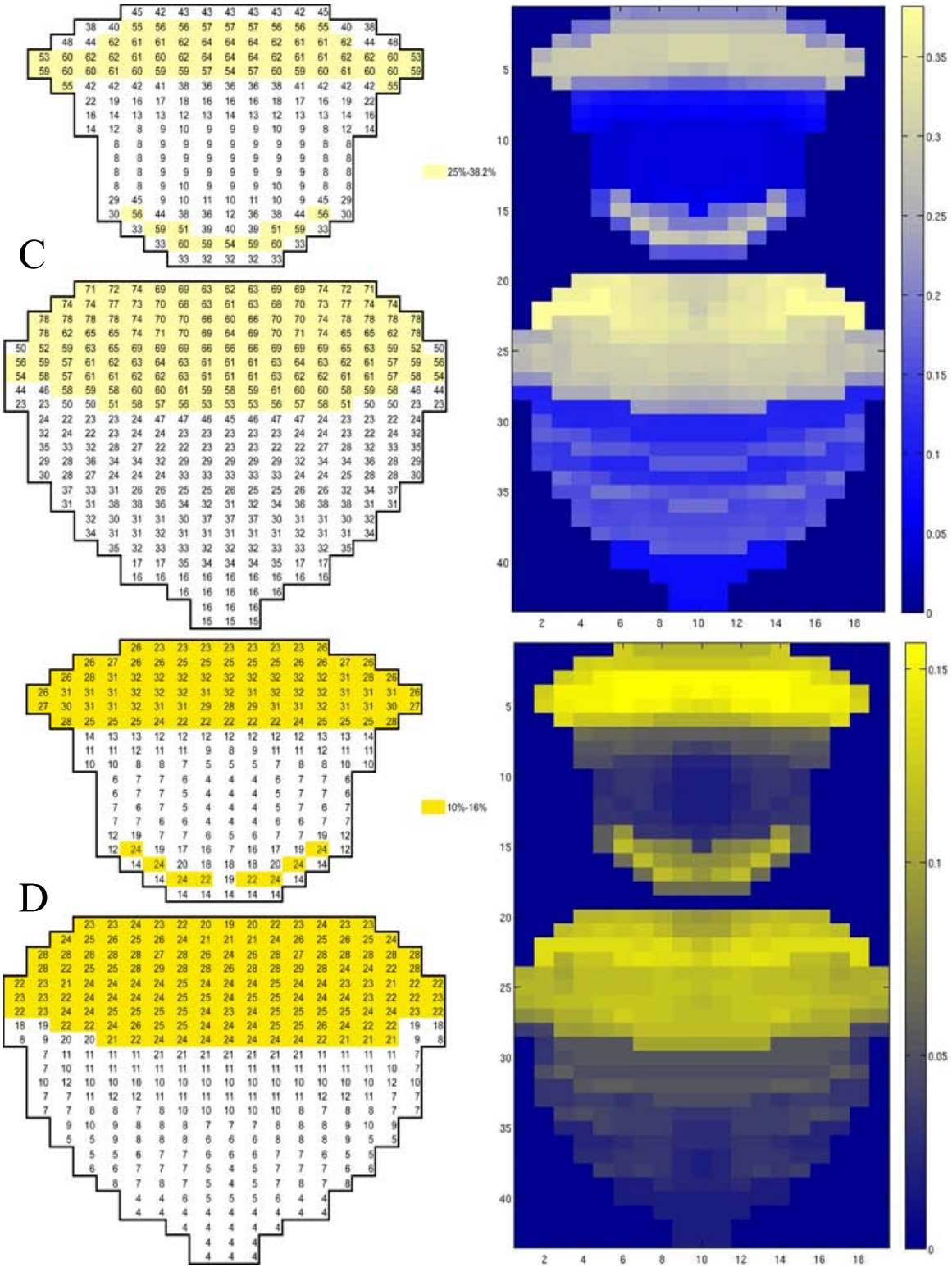

Figure 3.7 (cont.)

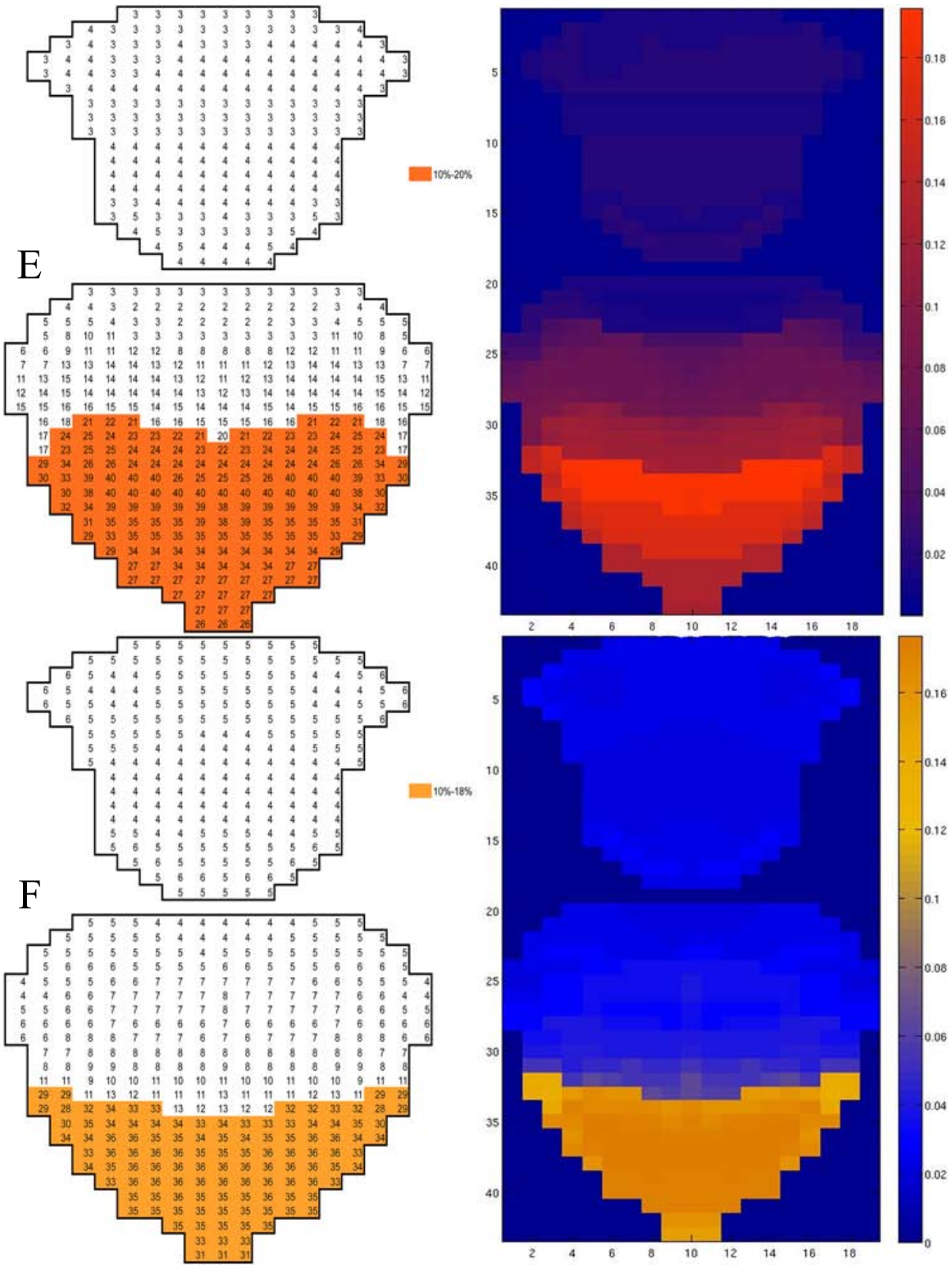

Figure 3.7 (cont.)

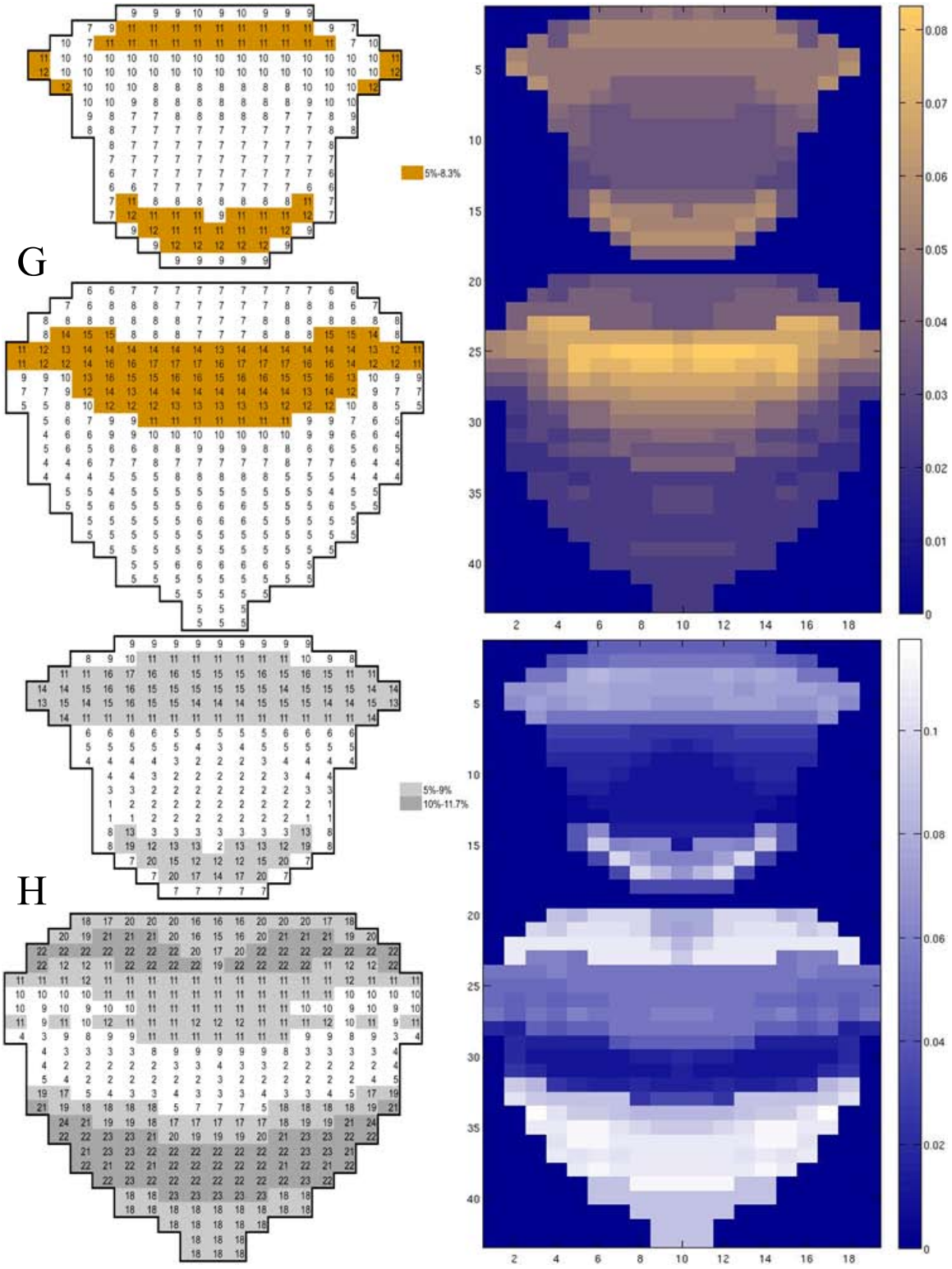

Figure 3.8. (A-J) Color frequency maps for less frequent color classes (Table 3.2) for all 204 species exemplars. A map for the color orange-brown (Table 3.2) is not shown because it appeared only when mixed with another color. Range of percentages shown beside some of the the matrices refer to the highest mean frequencies found for a given pigment.

(A) White and Orange Mixed Setae (left), (B) Orange and Yellow Mixed Setae (right)

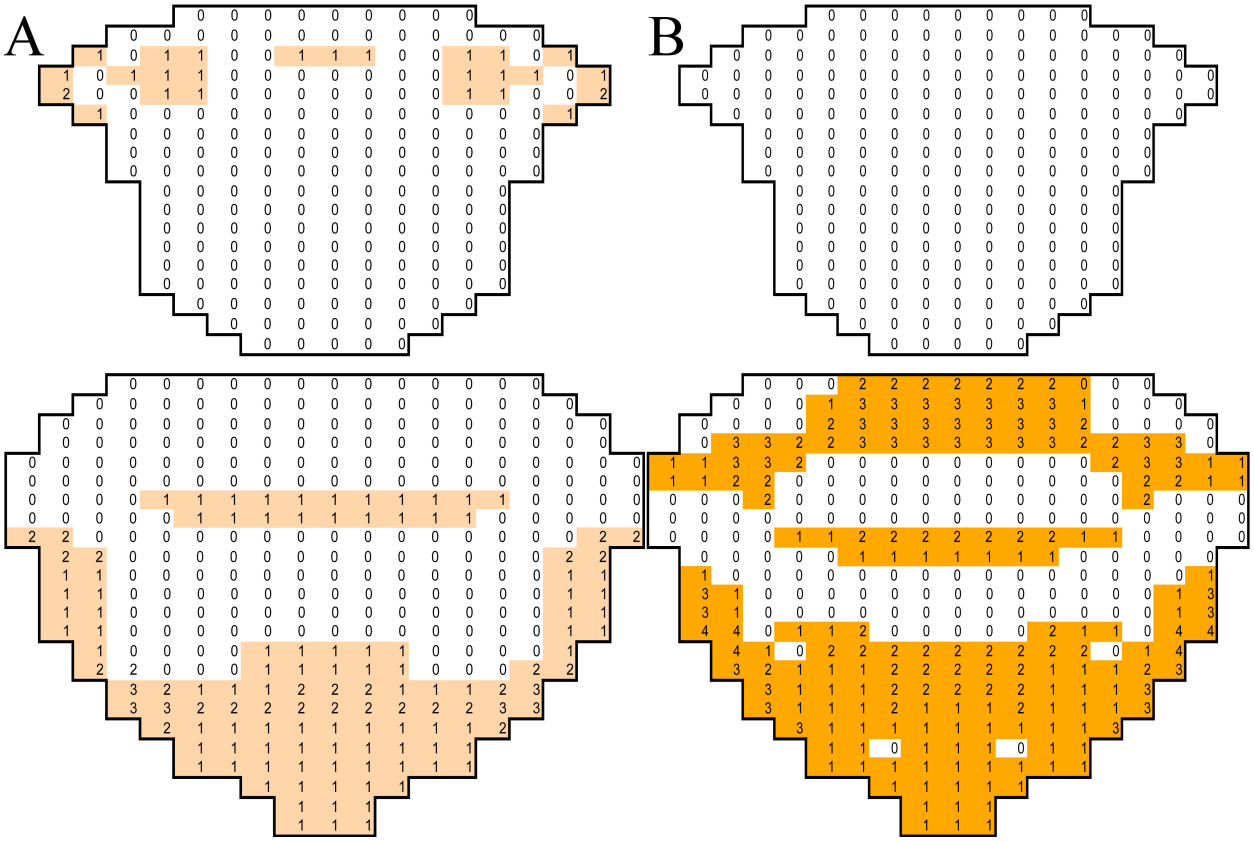

Figure 3.8 (cont.)

(C) Tawny (top left), (D) Black and Yellow Mixed Setae (top right),
(E) Black and Orange Mixed (bottom l.), (F) White and Yelllow mixed (bottom r.)

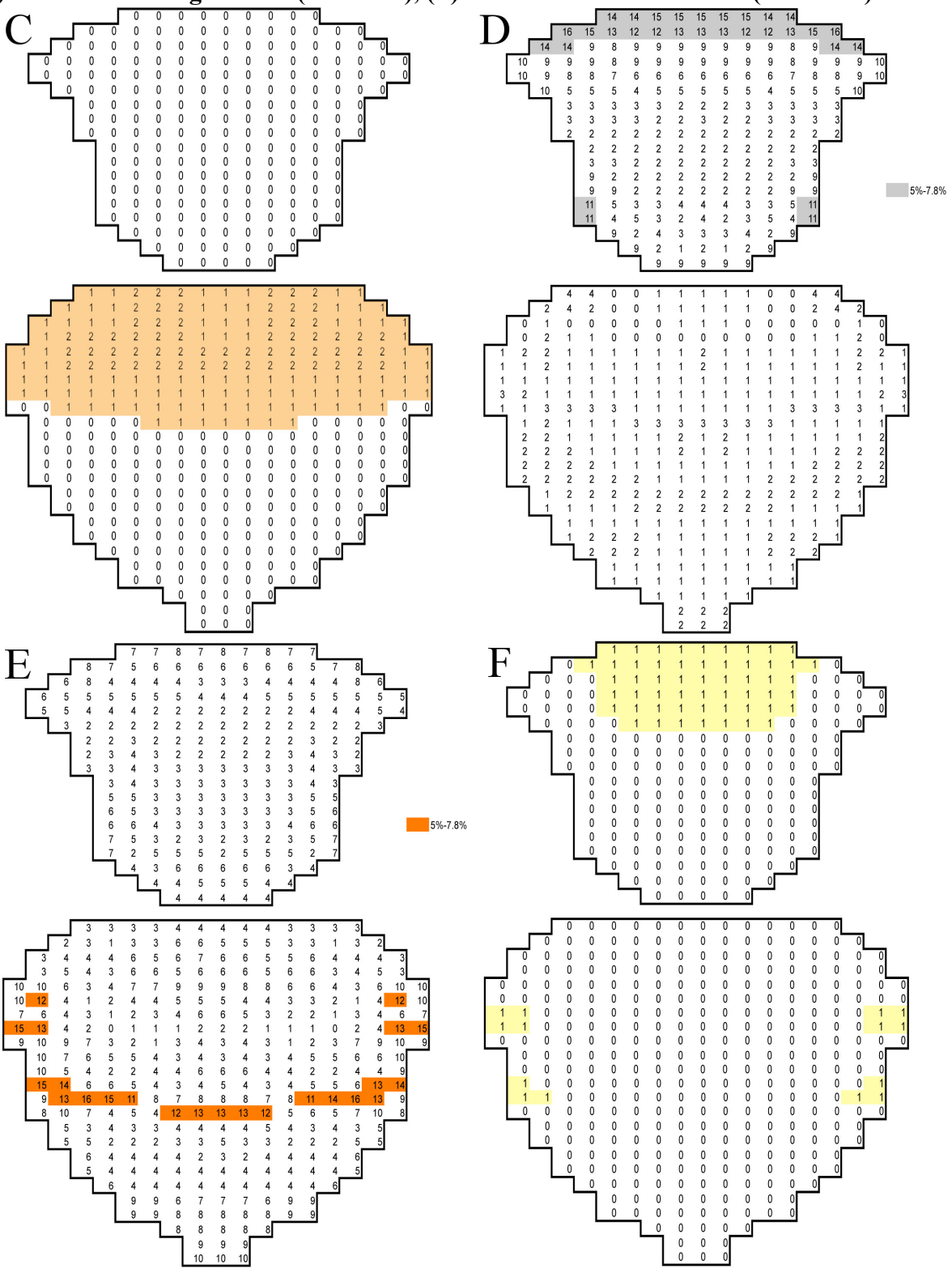

Figure 3.8 (cont.)

(G) Black and Or 2-banded setae (top left), (H) White and Or 2-banded setae (top right)
(I) Black and White 2-banded, (bottom l.), (J) Black/Orang/White 3-banded setae (bott. r.)

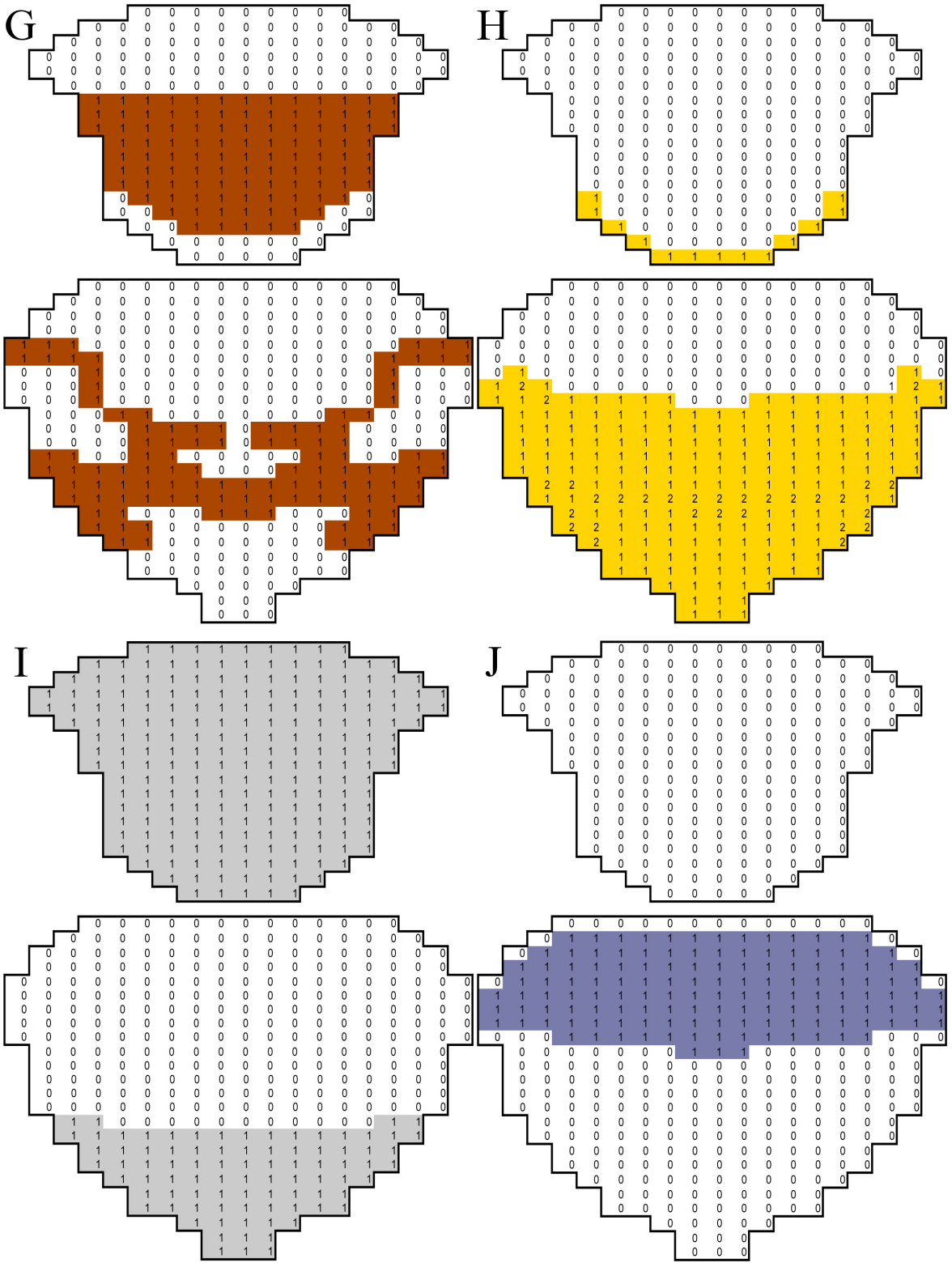

Figure 3.9. (elements 1-l2) Histograms displaying the average frequency of each color category for each of the 12 pattern elements we have delimited. Each figure is colored according to Fig. 3.3 in the main text.

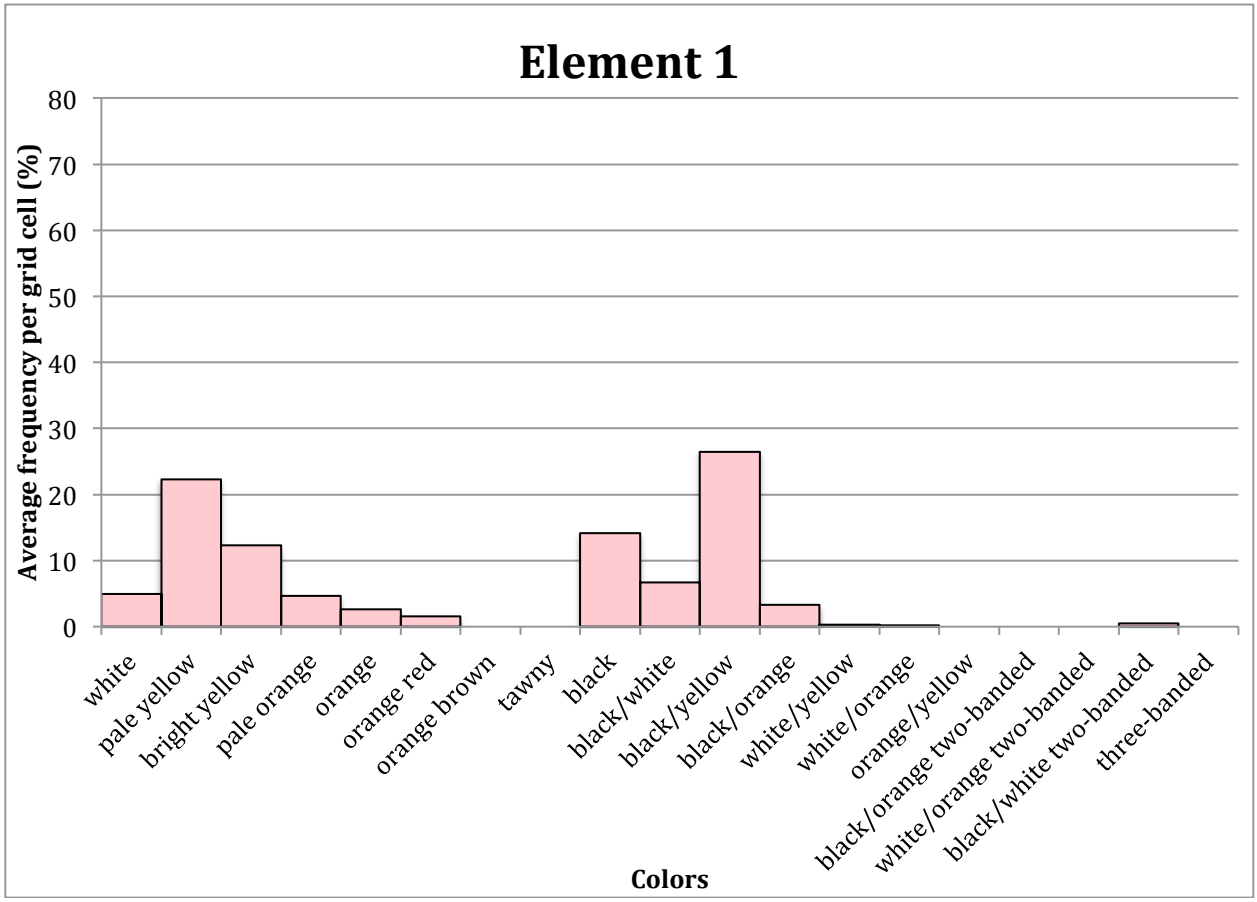

Figure 3.9 (cont.)

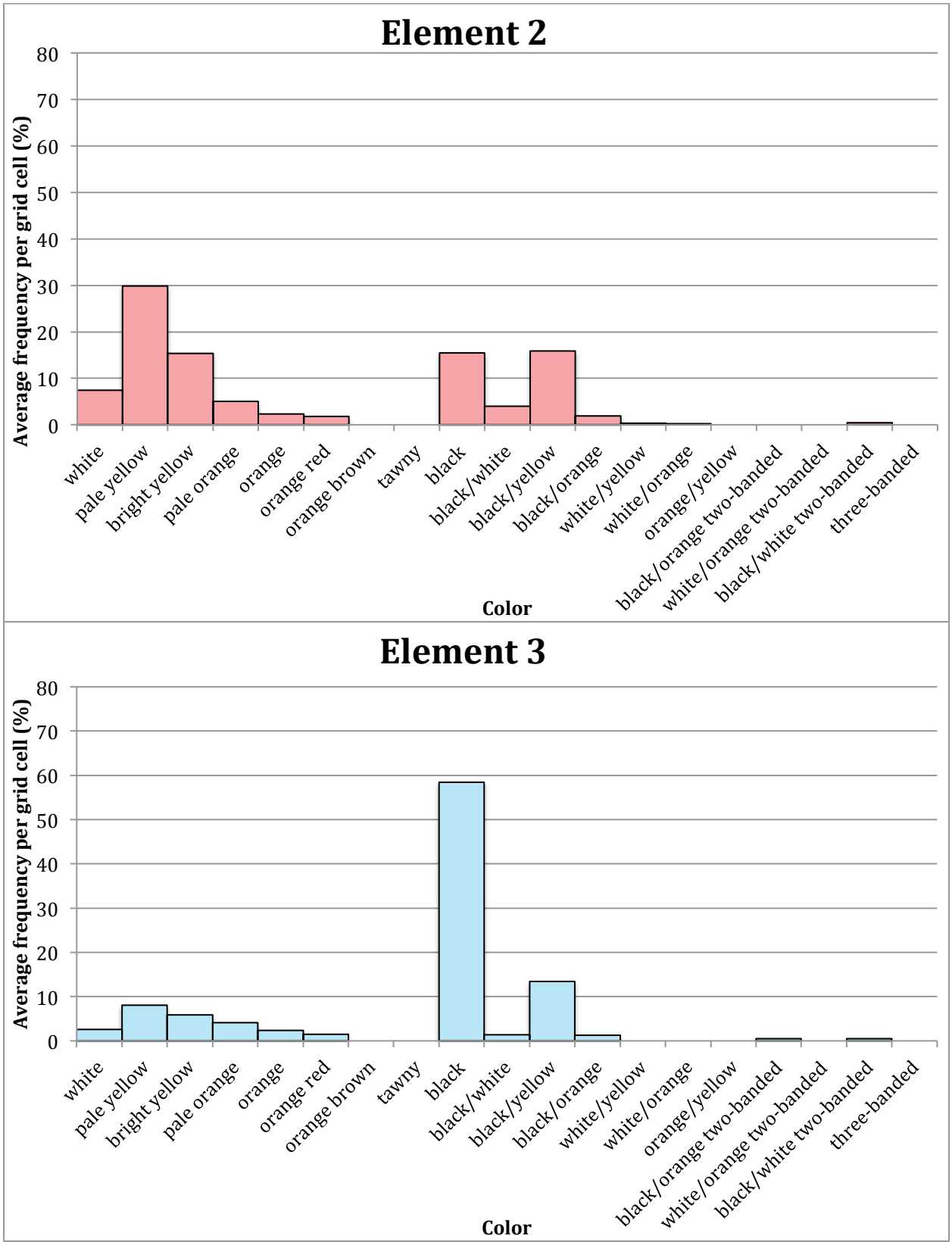

Figure 3.9 (cont.)

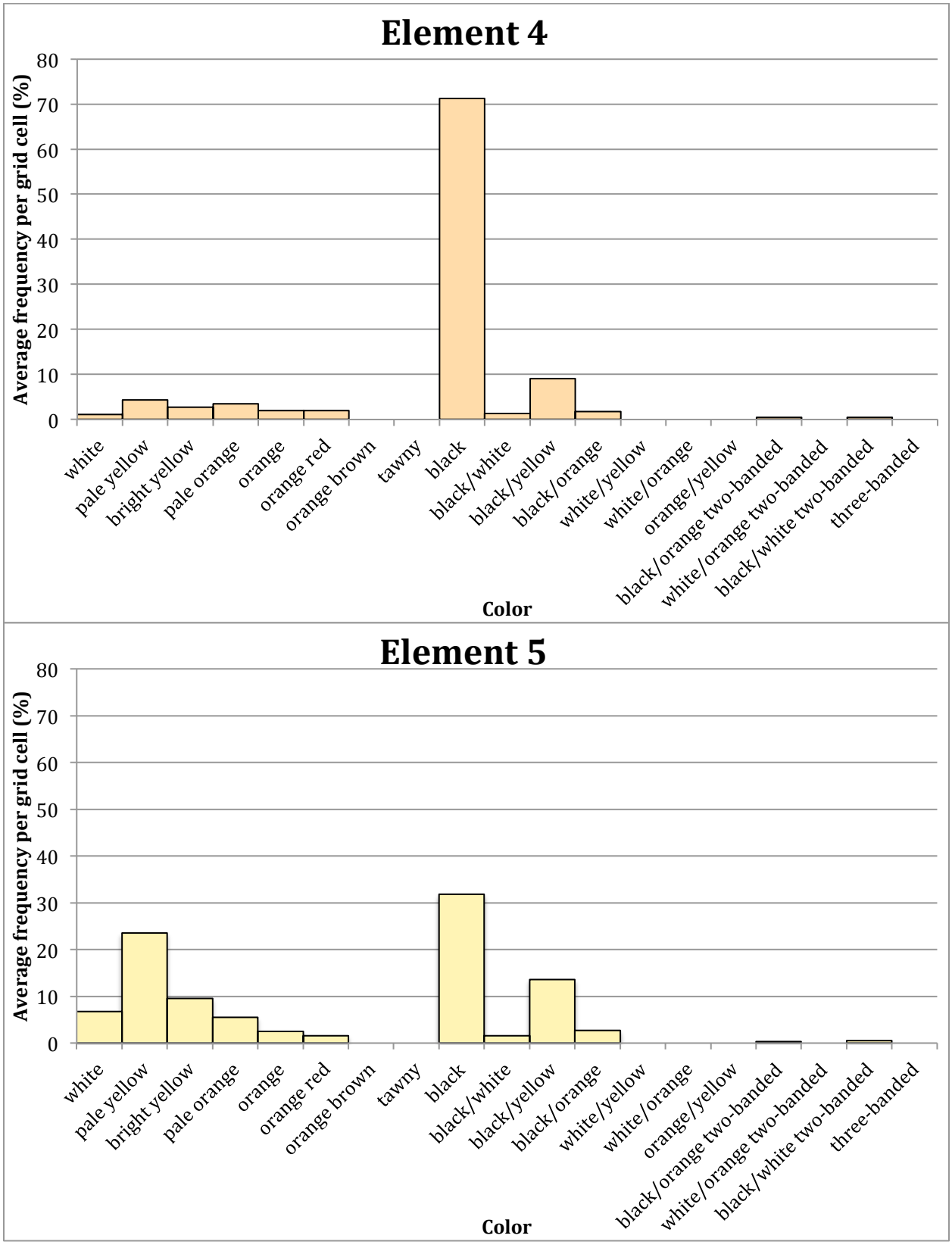

Figure 3.9 (cont.)

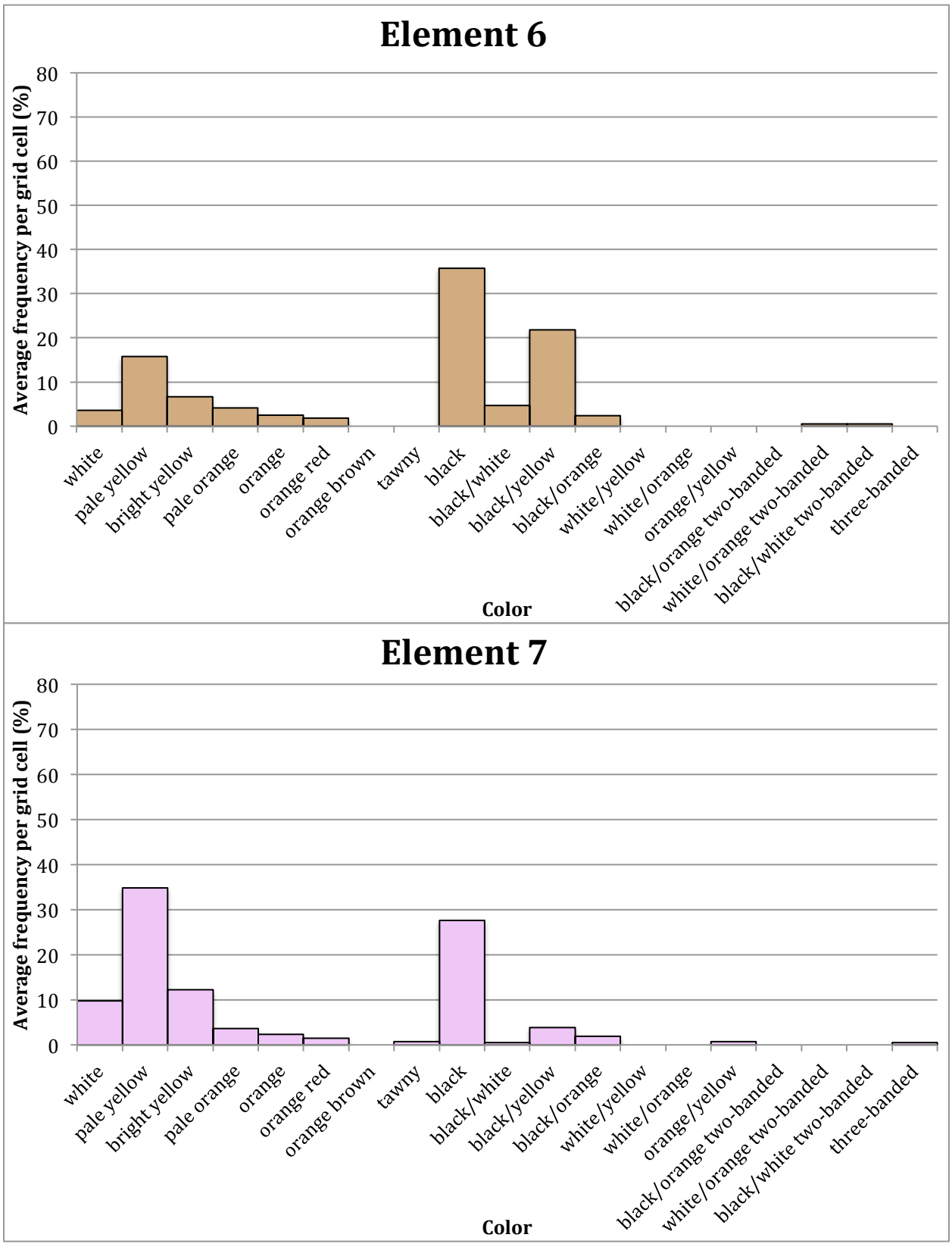

Figure 3.9 (cont.)

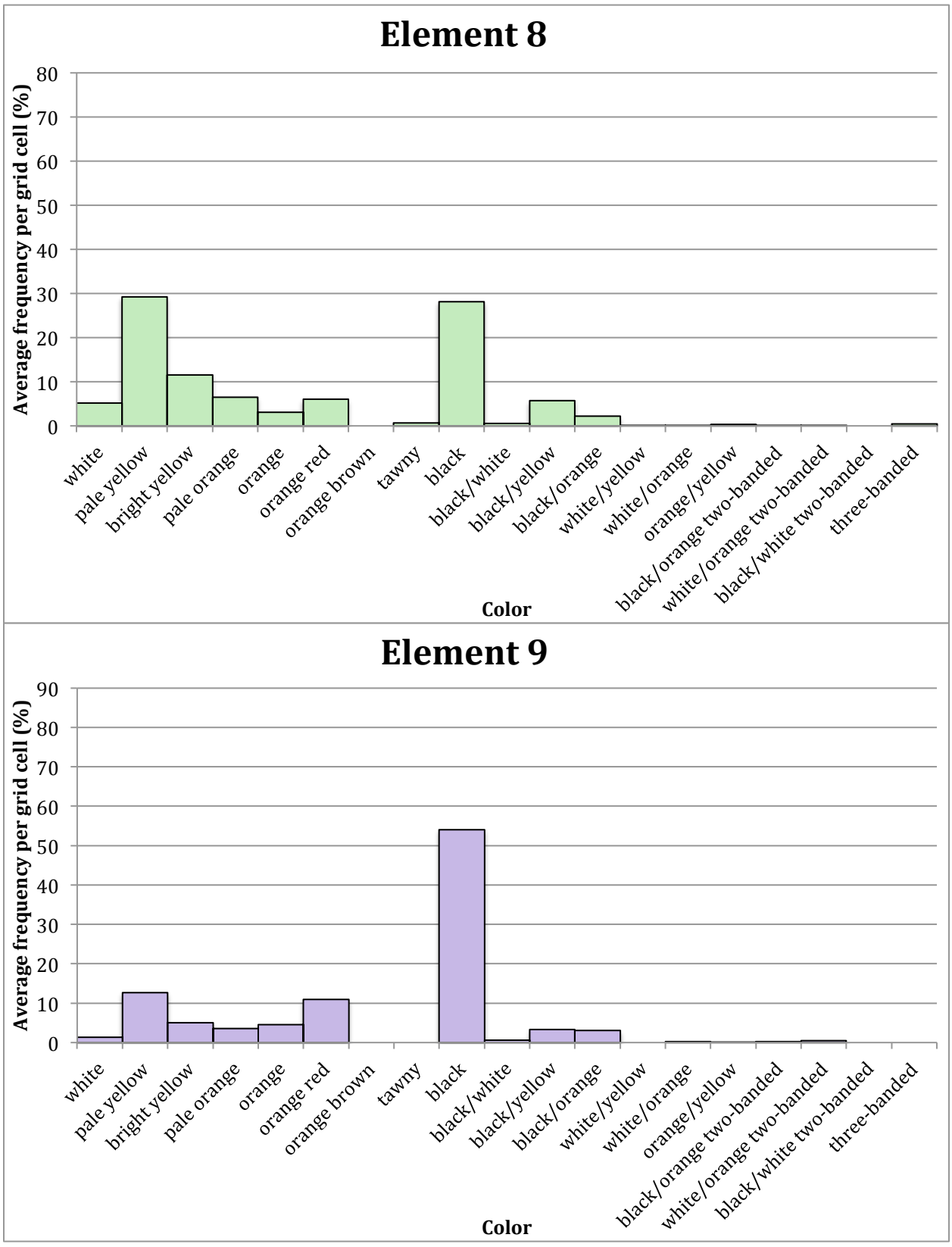

Figure 3.9 (cont.)

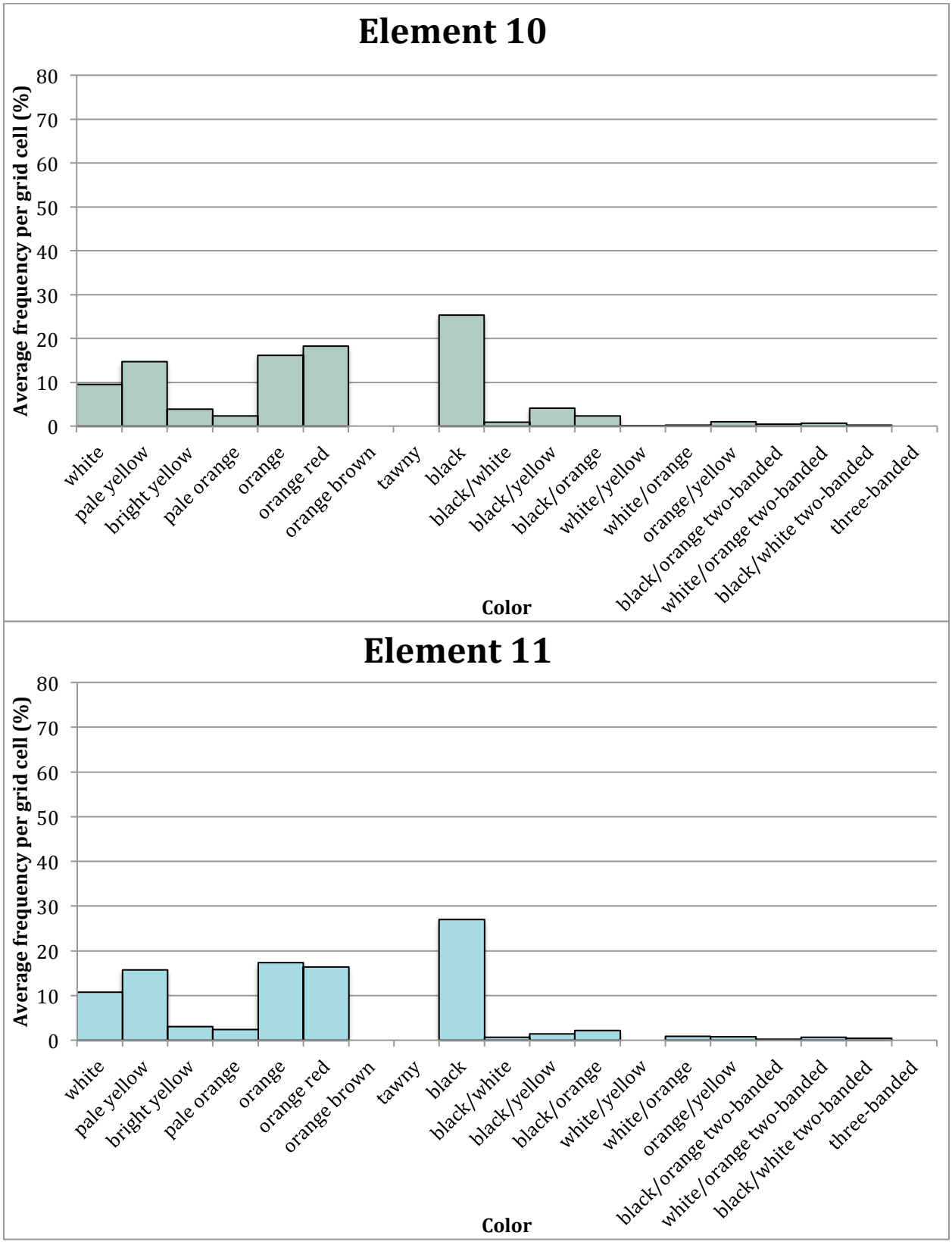

Figure 3.9 (cont.)

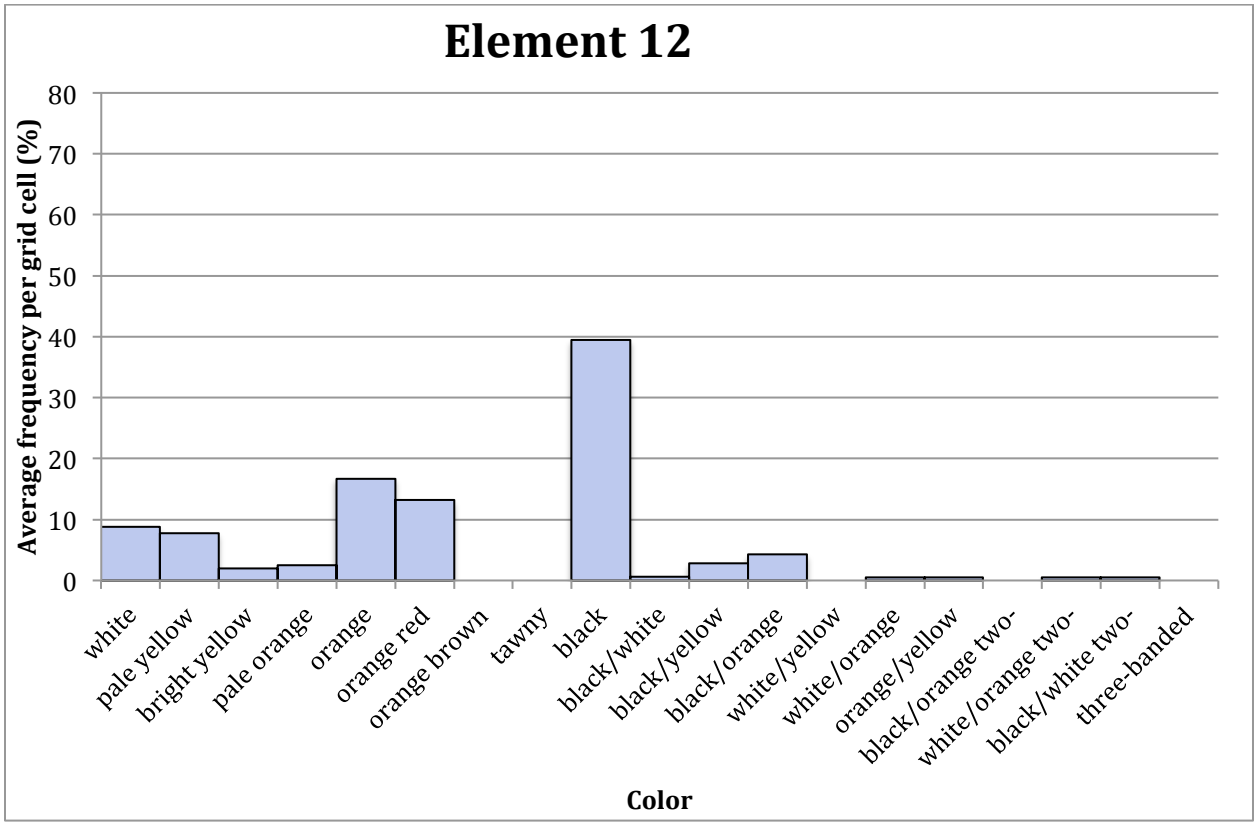

Figure 3.10. (A) Variables factor map showing the superimposition of the 10 colors used in the analysis in PC1 and PC2. Because PC1 and PC2 contain over 70% of the variation in our data, only these two components are shown. **(B)** Plot of elements along component 1 and 2. The elements cluster into four color classes comprising orange pigments (tail elements 10-12), yellows, black and black+yellow mixed.

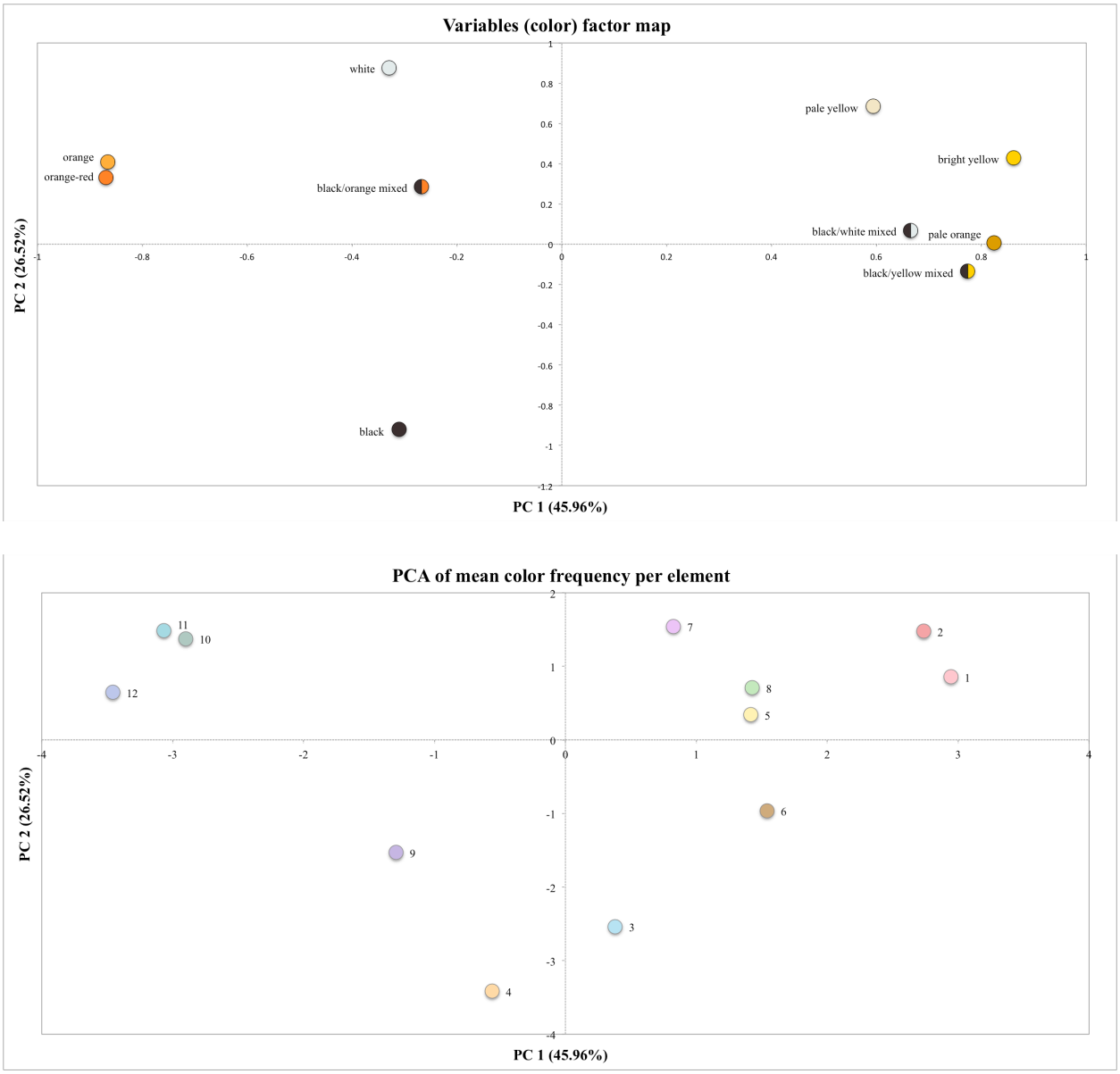

Figure 3.11. Grid cells chosen for comparison to generate the color change matrices (Table 3.3). Pairs of grid cells used for each matrix are highlighted the same color, with arrows indicating the specific comparison. Cells not considered are highlighted in grey and boundary cells are white.

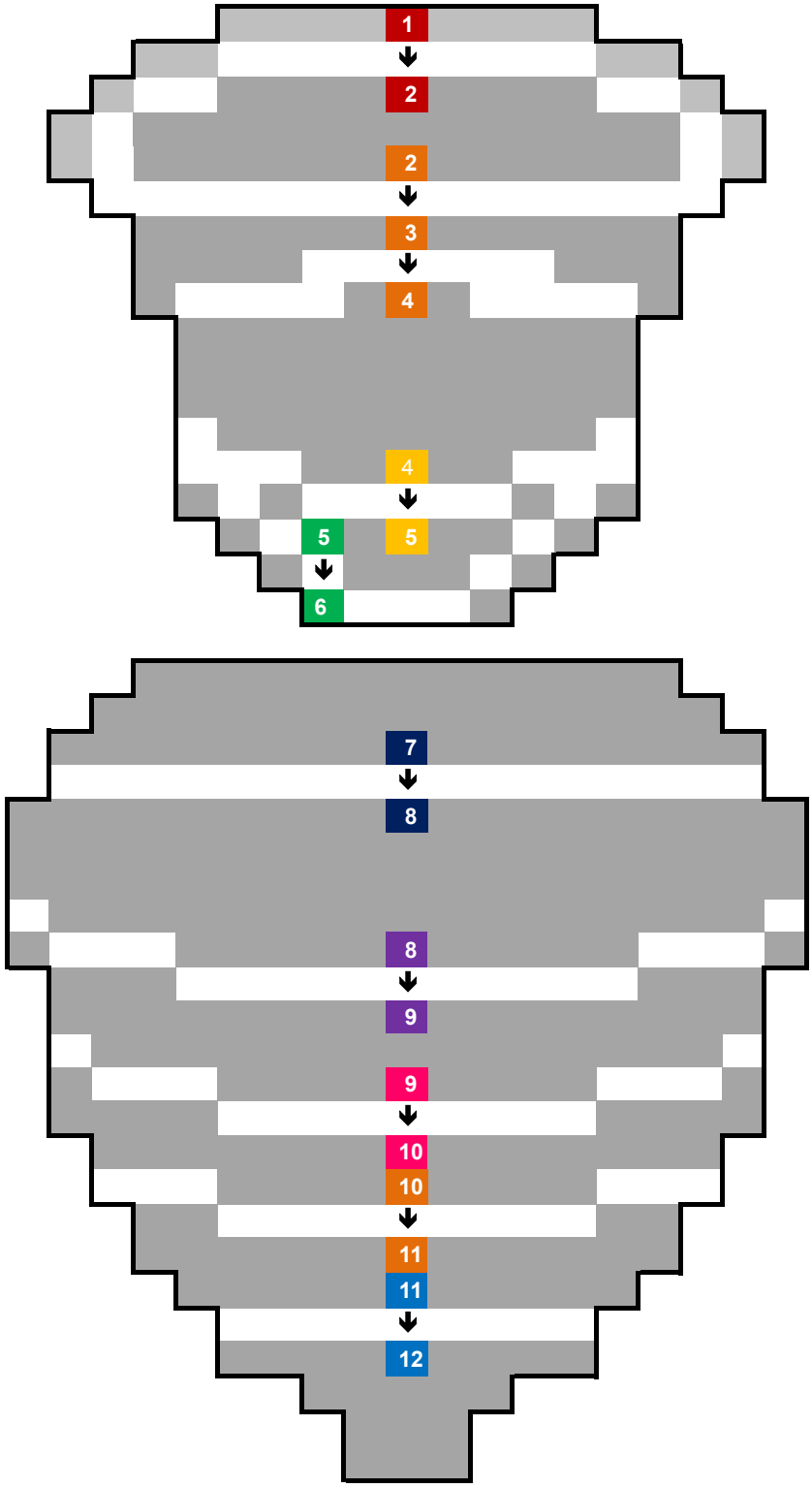

Figure 3.12. Geographic distributions of sample species from two *Bombus* (subgenus *Pyrobombus*) color pattern complexes (black along Pacific coast, red in mountain west and north). Convergent patterns among species within the Pacific west and mountain west, respectively; intraspecific divergence of pattern between the Pacific region (e.g., *B. bifarius* and *B. melanopygus* black forms) and mountain west (*B. bifarius* and *B. melanopygus* orange forms). Sister species (e.g., *B. vosnesenskii and B. huntii*) may also show the same black/red phenotypic divergence between regions.

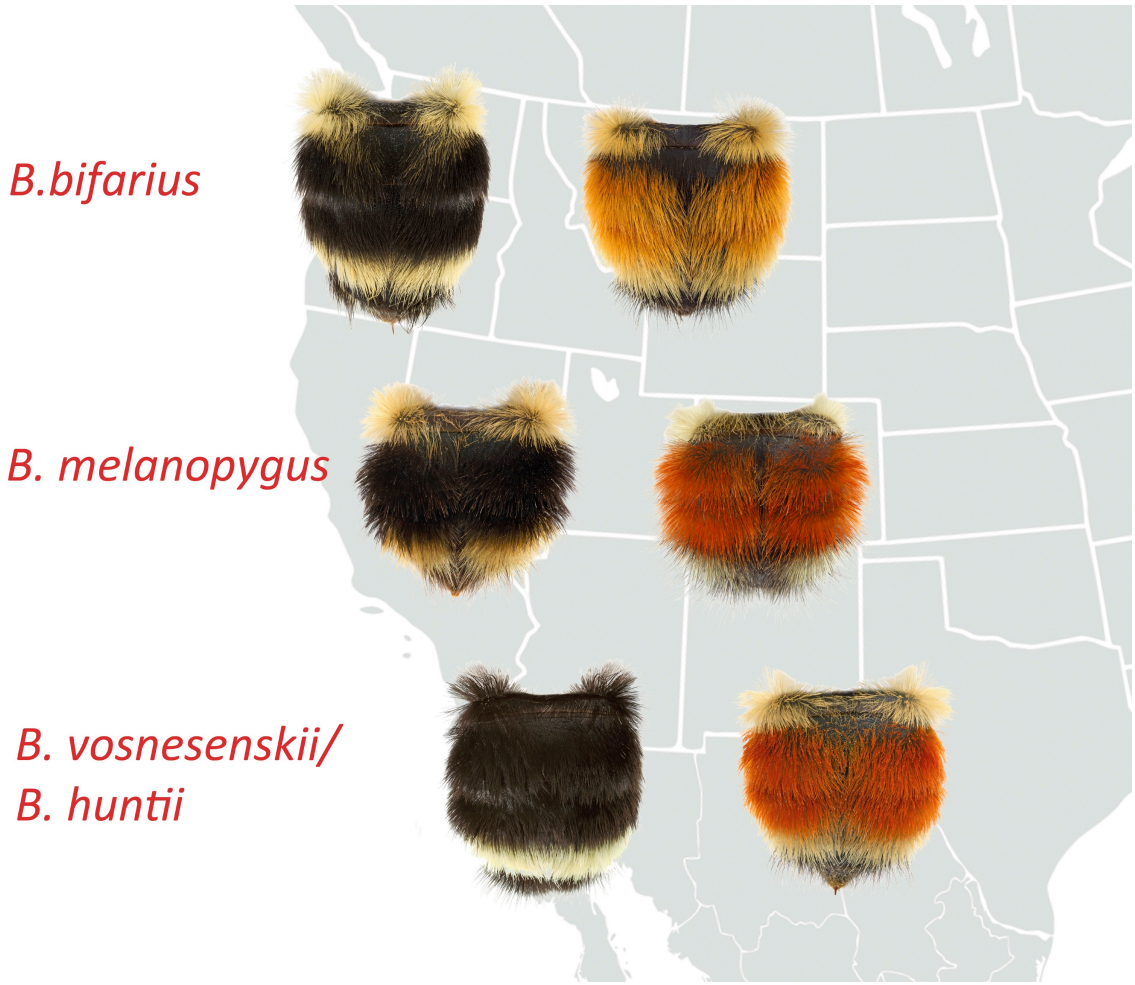

APPENDIX A: SUPPORTING TEXT (SECTIONS 1-4)

1-Perl script for matrix addition

```
print FOUT "\n";
                        }
print FOUT "\n";
print FOUT "bnum=$fnumber;";
print FOUT "\n";
print FOUT "\n";
print FOUT "for i=1:44,";
print FOUT "\n";
print FOUT "for j=1:19,";
for($i=0; $i<$fnumber; $i++){
@modnam[$i]=substr($fname[$i],0,-4);
print FOUT "\n";
$ii=$i+1;
print FOUT "M(i,j,$ii)= $modnam[$i](i,j);";
                        }
print FOUT "\n";
print FOUT "end";
print FOUT "\n";
print FOUT "end";
print FOUT "\n";
```

2-Identification of ground plan pattern elements

Multiple permutation tests (5000 reshuffles) were used to test significance levels for each of the 12 putative elements (Fig. 3.3A) that appear to be discrete based on the relative color transition frequency values observed in the sum matrices (Fig. 3.1E, Fig. 3.5). We calculated the difference between the mean transition frequency within each of 12 putative elements vs the mean frequency of the apparent posterior boundary of each putative element. We tested the null hypothesis that the boundary zones exhibit similar mean transition frequencies as the associated adjacent anterior regions. We performed this analysis on two different datasets to test the effects on the primary color pattern elements of including: 1) only the 204 social bumble bee species, and 2) an additional 18 species of the subgenus *Psithyrus*, which often mimic their social bumble bee hosts (Table 3.1- asterisked species). The combined analysis with *Psithyrus* revealed that the relative transition frequencies of the transition zones (Fig. 3.5B), hence the primary element

boundaries (Table 3.4) were unchanged when the social parasitic taxa were included. All following supplementary information refers to the social bumble bee dataset, except Table 3.4 and Fig. 3.1B, which refer to the combined *Psithyrus* dataset.

The permutation test results presented below for each element are summarized with the distribution summary statistics.

Tabulated means of color transition frequencies that occur within each of 12 elements (Fig. 3.3A), as well as those that fall along the boundaries separating each element. These means are used in the permutation tests that follow.

Ground plan	**Mean transition frequencies**
Element 1	21.47 ± 9.09
Element 2	11.11 ± 6.91
Element 3	11.38 ± 2.7654
Element 4	9.52 ± 8.07
Element 5	29.80 ± 11.04
Element 6	2.75 ± 3.33
Element 7	14.00 ± 5.59
Element 8	21.69 ±9.08
Element 9	19.45 ± 10.59
Element 10	19.88 ±8.25
Element 11	8.82 ± 4.94
Element 12	6.60 ± 5.40
Boundary1&2	44.76 ± 4.3521
Boundary 2&3	81.40 ±6.20
Boundary 3&4	18.94 ± 4.20
Boundary 4&5	93.64 ± 9.54
Boundary 5&6	80.27 ± 2.45
Boundary 7&8	62.35 ± 5.47
Boundary 8&9	99.89 ±3.26
Boundary 9&10	112.76 ± 3.82
Boundary 10&11	43.27 ± 2.66
Boundary 11&12	56.33 ± 2.65

Element permutation tests

Element 1_B1, 2 (Element 1 vs_Boundary between elements 1 and 2)
Permutation distribution summary statistics:
Mean: 0.11069
Std. Error: 4.6222
1st %ile: -10.2508
2.5 %ile: -8.8019
5th %ile: -7.5759
95th %ile: 7.582
97.5 %ile: 9.1424
99th %ile: 10.7028
Difference between Observed Means = -23.3910
***P* < 0.0002**

Element 2_B1, 2
Permutation Distribution Summary statistics:
Mean: 0.04602
Std. Error: 5.0998
1st %ile: -12.8067
2.5 %ile: -10.4034
5th %ile: -8.6555
95th %ile: 8.2118
97.5 %ile: 9.916
99th %ile: 11.358
Difference between Observed Means = -33.6504
***P* < 0.0002**

Element 2_B2, 3
Permutation Distribution Summary statistics:
Mean: -0.0737
Std. Error: 10.1064
1st %ile: -24.0952
2.5 %ile: -20.2857
5th %ile: -16.8571
95th %ile: 16.8571
97.5 %ile: 19.1905
99th %ile: 23.1905
Difference between Observed Means = -70.2857
***P* < 0.0002**

Element 3_B2, 3
Permutation Distribution Summary statistics:
Mean: 0.2427
Std. Error: 11.9652
1st %ile: -28.3619
2.5 %ile: -22.9333
5th %ile: -20.7619

95th %ile: 19.1238
97.5 %ile: 24.6667
99th %ile: 26.8952
Difference between Observed Means = -70.019
***P* < 0.0002**

Element 3_B3, 4
Permutation Distribution Summary statistics:
Mean: -0.0398
Std. Error: 1.7024
1st %ile: -3.9226
2.5 %ile: -3.372
5th %ile: -2.8214
95th %ile: 2.7946
97.5 %ile: 3.2351
99th %ile: 3.7857
Difference between Observed Means = -7.5565
***P* < 0.0002**

Element 4_B3, 4
Permutation Distribution Summary statistics:
Mean: -0.0221
Std. Error: 2.4071
1st %ile: -5.6225
2.5 %ile: -4.715
5th %ile: -4.055
95th %ile: 3.865
97.5 %ile: 4.6075
99th %ile: 5.2675
Difference between Observed Means = -9.4175
***P* < 0.0002**

Element 4_B4, 5
Permutation Distribution Summary statistics:
Mean: -0.0258
Std. Error: 11.3378
1st %ile: -28.9391
2.5 %ile: -22.6727
5th %ile: -20.0109
95th %ile: 18.53
97.5 %ile: 20.4709
99th %ile: 22.0236
Difference between Observed Means = -84.1164
***P* < 0.0002**

Element 5_B4, 5
Permutation Distribution Summary statistics:
Mean: -0.0515
Std. Error: 14.9553
1st %ile: -33.1955
2.5 %ile: -29.3773
5th %ile: -25.0818
95th %ile: 24.3636
97.5 %ile: 28.1818
99th %ile: 34.1
Difference between Observed Means = -63.8364
***P* < 0.0002**

Element 5_B5, 6
Permutation Distribution Summary statistics:
Mean: 0.2400
Std. Error: 11.6071
1st %ile: -26.4182
2.5 %ile: -22.7909
5th %ile: -19.0682
95th %ile: 19.0182
97.5 %ile: 22.2636
99th %ile: 26.8455
Difference between Observed Means = -50.4727
***P* < 0.0002**

Element 6_B5, 6
Permutation Distribution Summary statistics:
Mean: -0.2407
Std. Error: 18.4922
1st %ile: -44.7045
2.5 %ile: -42.3295
5th %ile: -28.5114
95th %ile: 24.6023
97.5 %ile: 39.0682
99th %ile: 40.3636
Difference between Observed Means = -77.5227
***P* < 0.0002**

Element 7_B7, 8
Permutation Distribution Summary statistics:
Mean: -0.0569
Std. Error: 6.471
1st %ile: -15.2052
2.5 %ile: -12.9359
5th %ile: -10.9098

95th %ile: 10.4863
97.5 %ile: 12.1072
99th %ile: 14.5791
Difference between Observed Means = -48.3529
***P* < 0.0002**

Element 8_B7, 8
Permutation Distribution Summary statistics:
Mean: 0.0583
Std. Error: 4.6653
1st %ile: -11.7529
2.5 %ile: -9.7059
5th %ile: -8.0471
95th %ile: 7.4118
97.5 %ile: 8.6471
99th %ile: 10.2
Difference between Observed Means = -40.6588
***P* < 0.0002**

Element 8_B8, 9
Permutation Distribution Summary statistics:
Mean: 0.1760
Std. Error: 7.8154
1st %ile: -19.5034
2.5 %ile: -16.0904
5th %ile: -12.8706
95th %ile: 12.5337
97.5 %ile: 14.53
99th %ile: 16.6873
Difference between Observed Means = -78.2006
***P* < 0.0002**

Element 9_B8, 9
Permutation Distribution Summary statistics:
Mean: 0.0237
Std. Error: 10.1163
1st %ile: -24.1686
2.5 %ile: -19.9689
5th %ile: -16.7551
95th %ile: 16.2589
97.5 %ile: 19.3631
99th %ile: 22.6133
Difference between Observed Means = -80.4458
***P* < 0.0002**

Element 9_B9, 10
Permutation Distribution Summary statistics:
Mean: -0.0153
Std. Error: 11.8132
1st %ile: -27.7911
2.5 %ile: -23.5918
5th %ile: -19.9868
95th %ile: 19.0348
97.5 %ile: 22.2041
99th %ile: 26.8391
Difference between Observed Means = -93.3157
***P* < 0.0002**

Element 10_B9, 10
Permutation Distribution Summary statistics:
Mean: -0.1069
Std. Error: 13.0471
1st %ile: -30.2794
2.5 %ile: -26.4412
5th %ile: -21.0588
95th %ile: 22
97.5 %ile: 24.3824
99th %ile: 29.2353
Difference between Observed Means = -92.8824
***P* < 0.0002**

Element 10_B10, 11
Permutation Distribution Summary statistics:
Mean: -0.0652
Std. Error: 4.0202
1st %ile: -9.549
2.5 %ile: -7.9157
5th %ile: -6.6667
95th %ile: 6.5922
97.5 %ile: 7.7451
99th %ile: 8.898
Difference between Observed Means = -23.3843
***P* < 0.0002**

Element 11_B10, 11
Permutation Distribution Summary statistics:
Mean: 0.1984
Std. Error: 5.4091
1st %ile: -12.6893
2.5 %ile: -10.4881
5th %ile: -8.9524

95th %ile: 8.8619
97.5 %ile: 10.3976
99th %ile: 12.3429
Difference between Observed Means = -34.4452
***P* < 0.0002**

Element 11_B11, 12
Permutation Distribution Summary statistics:
Mean: -0.0368
Std. Error: 8.0921
1st %ile: -20.496
2.5 %ile: -17.5595
5th %ile: -13.7421
95th %ile: 12.3929
97.5 %ile: 15.3294
99th %ile: 17.0913
Difference between Observed Means = -47.5119
***P* < 0.0002**

Element 12_B11, 12
Permutation Distribution Summary statistics:
Mean: -0.2092
Std. Error: 9.6234
1st %ile: -24.2778
2.5 %ile: -19.1222
5th %ile: -17.1889
95th %ile: 15.275
97.5 %ile: 17.1278
99th %ile: 21.8
Difference between Observed Means = -49.7333
***P* < 0.0002**

3-Identification of secondary pattern elements

We tested for any additional (secondary) elements suggested by the sum matrix (Fig. 3.5) using permutation tests of color transition frequencies. We found five secondary elements (a-e, Table 3.4, Fig. 3.3A), with summary statistics presented below.

T1 medial notch (a)
Permutation Distribution Summary statistics:
Mean: -0.0775
Std. Error: 3.2313
1st %ile: -7.0278
2.5 %ile: -6.0556

5th %ile: -5.2778
95th %ile: 5.6111
97.5 %ile: 6.3889
99th %ile: 7.3611
The mean color transition frequency within medial notch (13.39); on boundary (21.00)
Difference between Observed Means = -7.611
***P* = 0. 015**

T2 narrow dorsolateral patch (b)
Permutation Distribution Summary statistics:
Mean: 0.0657
Std. Error: 7.9499
1st %ile: -15.75
2.5 %ile: -15.75
5th %ile: -11.0833
95th %ile: 14.5833
97.5 %ile: 15.1667
99th %ile: 15.1667
The mean color transition frequency within patch (20.00); on boundary (35.75)
Difference between Observed Means = -15.75
***P* = 0.028**

T2 wide dorsolateral patch (c)
Permutation Distribution Summary statistics:
Mean: 0.0460
Std. Error: 3.528
1st %ile: -9.1778
2.5 %ile: -7.6222
5th %ile: -6.2889
95th %ile: 5.2667
97.5 %ile: 5.9333
99th %ile: 6.6
The mean color transition frequency within patch (17.93); on boundary (26.00)
Difference between Observed Means = -8.0667
***P* = 0.019**

T3 dorsolateral patch (d)
Permutation Distribution Summary statistics:
Mean: -0.0137
Std. Error: 4.6102
1st %ile: -11.4535
2.5 %ile: -9.3643
5th %ile: -7.845
95th %ile: 7.3488
97.5 %ile: 8.6783
99th %ile: 10.1977
The mean color transition frequency within patch (16.70); on boundary (39.17)
Difference between Observed Means = -22.47

***P* = 0.00002**

T4 dorsolateral patch (e)
Permutation Distribution Summary statistics:
Mean: -0.0253
Std. Error: 5.8334
1st %ile: -11.9231
2.5 %ile: -11.3846
5th %ile: -9.7692
95th %ile: 9.0769
97.5 %ile: 10.1538
99th %ile: 11.2308
The mean color transition frequency within patch (18.88); on boundary (33.50)
Difference between Observed Means = -14.615
***P* = 0.003**

4-Do ground plan elements correlate with segmentation boundaries?

Perumtation tests of segmentation boundaries

We performed a permutation test to determine whether color transitions occur significantly more frequently on the segmental boundaries (Fig. 3.2B, yellow cells, n = 102 boundary cells) than on the remaining portion of the dorsum (Fig. 3.2B, white cells, n = 448 cells not on boundaries). We performed the following steps for each permutation test:

1. Calculate the difference between the means of all matrix cell transition frequencies corresponding to segment boundaries on the dorsum and those corresponding to non-boundary regions of the dorsum. The mean of all color transitions that occur in cells on segmental boundaries is 72.14 ±27.38 (= 7358/102). The mean of color transitions that occur in cells on the remainder of the dorsum (non-boundary) is 20.43 ± 20.15 (= 9153/448). The observed difference in the means is 51.71 ± 2.87.
2. Permute boundary and non-boundary cells. To do this, we save all values in the color transition matrix that correspond to the yellow cells (Fig. 3.2B) as data set 1 with sample size 102. We save all values in the color transition matrix that correspond to the white cells as data set 2 with sample size 448. We then shuffle these two data sets and randomly pick 102 and 448 values, respectively, and calculate the difference in the means of these two random data sets. We repeat the process a total of 5,000 times (5,000 reshuffles and recalculations of differences between the means). The set of these calculated differences represents the exact distribution of possible differences under the

null hypothesis that group membership (boundary transitions vs non-boundary transitions) does not influence the difference in the means. The *P*-value of the test is calculated as the proportion of sampled permutations in which there are no differences between the means (51.71).

The results of the permutation test are provided in the table below.

Permutation distribution summary statistics for color transitions: boundary vs non-boundary zones.

Mean: 0.0167
Std. Error: 3.2568
1st %ile: -7.3064
2.5 %ile: -6.2352
5th %ile: -5.176
95th %ile: 5.5843
97.5 %ile: 6.7578
99th %ile: 7.9313
Difference between Observed Means = 51.71
***P* < 0.0002**

Permutation tests of scutoscutellar suture boundary

We tested whether the mean of the color transitions along the scutoscutellar suture (Fig. 3.2A, green cells, n = 11 cells) was equal to the mean of the transitions across the scutum (Fig. 3.2A, purple cells, n = 138 cells). Following the above permutation procedure we calculated the total color transitions on the scutoscutellar suture = 967 (mean = 87.91 ± 8.88); total color transition on scutum = 2811 (mean = 20.37 ± 25.25); observed difference between the means is --67.54 ± 3.43.

Summary statistics: scutoscutellar boundary vs scutum
Mean: -0.11542
Std. Error: 9.4268
1st %ile: -24.1548
2.5 %ile: -20.3267
5th %ile: -16.4987
95th %ile: 14.6657
97.5 %ile: 16.4816
99th %ile: 17.7085
Difference between Observed Means = -67.54
***P* < 0.0002**

Finally, we tested whether the mean of the color transitions along the scutoscutellar suture (Fig. 3.2A, green cells, n = 11 cells) was no different than the mean of the transitions across the scutellum (Fig. 3.2A, blue cells, n = 11 cells). Following the above permutation procedure we calculated the total color transitions on the scutoscutellar suture = 967 (mean = 87.91 ± 8.88); total color transitions on scutellum = 382 (mean = 34.73 ± 19.43); observed difference between the means is 53.18 ± 6.44.

Summary statistics: scutoscutellar boundary vs scutellum
Mean: -0.0073
Std. Error: 13.2666
1st %ile: -30.1818
2.5 %ile: -25.5455
5th %ile: -22.0909
95th %ile: 21.3636
97.5 %ile: 25.5455
99th %ile: 31.9091
Difference between Observed Means = 53.18
***P* < 0.0002**

APPENDIX B: THE NOMENCLATURE AND DESCRIPTION OF THE BUMBLE BEE GROUND PLAN ELEMENTS

1. **The *pronotal band*** is the anterior-most element, comprising the first thoracic segment (pronotum), and includes the pronotal lobes (expansions of the posterior margins of the pronotum).
2. The ***anterior scutal band*** lies directly behind the pronotum, comprising the anterior-most band of the thoracic scutum (the largest of the two sclerites of the mesonotum, the second true thoracic segment). The anterior margin conforms to the posterior boundary of the pronotal segment; the posterior margin does not conform to any visible morphological structure.
3. The ***central scutal band*** is a narrow field of color behind the anterior scutal band, which encloses the longitudinal parapsidal lines.
4. The ***posterior scutal band*** occurs behind the central scutal band and encompasses the conspicuous black central spot or bar that extends laterally between the lateral posterior margins of the mesonotal sclerite in many species; the posterior margin is defined by the scuto-scutellar suture.
5. The ***scutellar band*** is defined by the boundaries of the scutellum, the smaller of the two mesonotal sclerites.
6. The ***metanotal band*** is the posterior-most element of the thorax, and comprises the metanotum, the third true thoracic segment.
7. ***Tergal band 1*** comprises tergite 1 of the metasoma (commonly called the abdomen).
8. ***Tergal band 2*** comprises tergite 2 of the metasoma. This is the broadest of the tergal segments, and in some species the segment is divided into bands or arches of contrasting

color, which do not correspond to any visible landmarks on the tergite, such as a suture or punctation pattern.

9. ***Tergal band 3*** comprises termite 3 of the metasoma.
10. ***Tergal band 4*** comprises tergite 4 of the metasoma.
11. ***Tergal band 5*** comprises tergite 5 of the metasoma.
12. ***Tergal band* 6** comprises tergite 6 of the metasoma, also known in bees as the pygidial plate, and is only sparsely covered with setae.